NATURE-INSPIRED META-HEURISTICS FOR POWER SYSTEM OPTIMIZATION

Thesis submitted by Chitralekha Jena

Doctor of Philosophy in Engineering

Department of Electrical Engineering
Faculty Council of Engineering & Technology
Jadavpur University

April 2016

CERTIFICATE

This is to certify that the thesis entitled "**NATURE-INSPIRED META-HEURISTICS FOR POWER SYSTEM OPTIMIZATION"** submitted by Chitralekha Jena who got her name registered on 2013 for the award of Ph. D. (Engineering) degree of Jadavpur University, is absolutely based upon her own work under our joint supervision and neither her thesis nor any part of it has been submitted for any degree or any other academic award anywhere before.

---------- ----------

Dr. M. Basu **Prof. C. K. Panigrahi**

(Signature of Supervisors & Date with Official Seals)

DECLARATION

I, Smt. Chitralekha Jena, hereby certify that the work "**NATURE-INSPIRED META-HEURISTICS FOR POWER SYSTEM OPTIMIZATION**" submitted by me to Jadavpur University, Kolkata, India for the award of Ph.D. **(Engineering)** degree, has not been submitted previously in this university or any other University for the degree of Ph. D./D.Litt./D.Sc.

Chitralekha Jena

List of Papers Published

1. C. Jena, M. Basu, C. K. Panigrahi, "Differential Evolution with Gaussian Mutation for Combined Heat and Power Economic Dispatch**", Soft computing, February 2016,** Volume 20, **Issue-2, pp 681-688, SPRINGER PUBLISHERS.**

2. M. Basu, C. Jena, C. K. Panigrahi, "Differential Evolution with Gaussian Mutation for Economic Dispatch**", The Journal of Institution of Engineers.**December 2016, Volume 97, Issue 4, pp 493–498,**SPRINGER PUBLISHERS**

3. C. Jena, M. Basu, C. K. Panigrahi, "Improved Differential Evolution for Combined Heat and Power Economic Dispatch", **International Journal of emerging electric power system,Volume-17,Issue-2,April, 2016.,DE-GRUYTER PUBLISHERS**

4. C. Jena, M. Basu, , "Group Search Optimization for fixed head hydrothermal power system**",published in The Journal of Institution of Engineers.** February 2017, Volume 98, Issue 1, pp 35–41,**SPRINGER PUBLISHERS**

5. C. Jena, M. Basu, C. K. Panigrahi, "Short Term Hydro-Thermal Scheduling using Artificial Immune System" , **International Journal of Computer Applications. Volume 107 - Number 18, Year of Publication: 2014.**

List of Papers Accepted/Under Review

1. C. Jena, M. Basu, C. K. Panigrahi, "Modified Evolutionary Programming for Short-Term Hydrothermal Scheduling", accepted in **International Journal of Power & Energy Conversion, IDERSCIENCE PUBLISHERS.**

2. C. Jena, M. Basu, C. K. Panigrahi, "Improved Differential Evolution for Multi-area Economic Dispatch", accepted **for publication in the Journal of Institution of Engineers,SPRINGER PUBLISHERS.**

3. C. Jena, M. Basu, C. K. Panigrahi, "Opposition-based Differential Evolution for Fixed Head Hydrothermal Power System", under review in the Journal of Institution of Engineers.

.

4. C. Jena, M. Basu, C. K. Panigrahi, "Group Search Optimization for Short-Term Hydrothermal Scheduling", under review in the Journal of Institution of Engineers.

5. C. Jena, M. Basu, C. K. Panigrahi, "Opposition-based Group Search Optimization for fixed head hydrothermal power system", under review in the International Journal of emerging electric power system.

6. C. Jena, M. Basu, C. K. Panigrahi, "Fuel Constrained Economic Emission Dispatch using Multi-objective Differential Evolution", under review in the International Journal of emerging electric power system.

7. C. Jena, M. Basu, C. K. Panigrahi, "Modified Evolutionary Programming for Short-Term Hydrothermal Scheduling", under review in International Journal of Power & Energy Conversion..

8. C. Jena, M. Basu, C. K. Panigrahi, "Multi-objective differential evolution for multi-area economic environmental dispatch", under review in the Journal of Institution of Engineers.

9. C. Jena, M. Basu, C. K. Panigrahi," Group Search Optimization for Multi-area Economic Dispatch", under review in the Recent Advances in Electrical & Electronic Engineering.

10. C. Jena, M. Basu, C. K. Panigrahi," Quasi-oppositional Particle Swarm Optimization for Economic Dispatch Problem", under review in the Recent Advances in Electrical & Electronic Engineering

Abbreviations and Notations

Symbol	Description
P_i	power output of i th unit
P_i^{min} , P_i^{max}	lower and upper generation limits for i th unit
P_D	load demand
P_L	transmission line losses
B_{ij}	transmission loss coefficient
a_i, b_i, c_i, d_i, e_i	cost coefficients of i th unit
$\alpha_i, \beta_i, \gamma_i, \eta_i, \delta_i$	emission coefficients of i th unit
N	number of generating units
P_{it}	power output of i th unit at time t
P_{Dt}	load demand at time t
P_{Lt}	transmission line losses at time t
B_{ij}	loss formula coefficients
UR_i , DR_i	ramp-up and ramp-down rate limits of i th unit
T	number of hours in the time horizon
a_{si} , b_{si} , c_{si} , d_{si} , e_{si}	cost coefficients of i th thermal unit
$\alpha_{si}, \beta_{si}, \gamma_{si}, \eta_{si}, \delta_{si}$	emission coefficients of i th thermal unit
C_{1j}, C_{2j} , C_{3j} , C_{4j} , C_{5j} , C_{6j}	power generation coefficients of j th hydro unit
I_{hjm}	inflow rate of j th reservoir at time m
P_{Dm}	load demand at time m
P_{Lm}	total transmission line losses at time m
P_{sim}	output power of i th thermal unit at time m
P_{si}^{min} , P_{si}^{max}	lower and upper generation limits for i th thermal unit
P_{hjm}	output power of j th hydro unit at time m
P_{hj}^{min} , P_{hj}^{max}	lower and upper generation limits for j th hydro unit
Q_{hjm}	water discharge rate of j th reservoir at time m
Q_{hj}^{min} , Q_{hj}^{max}	minimum and maximum water discharge rate of j th reservoir

Symbol	Description
R_{uj}	number of upstream units directly above j th hydro plant
S_{hjm}	spillage of j th reservoir at time m
t_{lj}	water transport delay from reservoir l to j
V_{hjm}	storage volume of j th reservoir at time m
$V_{hj}^{\min}, V_{hj}^{\max}$	minimum and maximum storage volume of j th reservoir
V_{hj0}	initial storage volume of j th reservoir
$V_{hj\mathrm{M}}$	final storage volume of j th reservoir
m, M	time index and scheduling period
N_s	number of thermal generating units
N_h	number of hydro generating units
N_{obj}	number of objective functions
N_{P}	number of populations

a_{si}, b_{si}, c_{si}, d_{si}, e_{si}: cost curve coefficients of i th thermal unit

P_{sim}: power output of i th thermal generator during subinterval m

$\mathrm{P}_{si}^{\min}$, $\mathrm{P}_{si}^{\max}$: lower and upper generation limits for i th thermal unit

t_m: duration of subinterval m.

P_{hjm}: power output of j th hydro unit during subinterval m

P_{Dm}: load demand during subinterval m

P_{Lm}: transmission loss during subinterval m

B_{lr}: loss formula coefficients.

a_{0hj}, a_{1hj}, and a_{2hj}: coefficients for water discharge rate function of j th hydro generator

W_{hj}: prespecified volume of water available for generation by j th hydro unit during the scheduling period.

$\mathrm{P}_{hj}^{\min}$, $\mathrm{P}_{hj}^{\max}$: lower and upper generation limits for j th hydro unit

N_s: number of thermal generating units

N_h: number of hydro generating units

F_{im}: Fuel delivered to thermal unit i in interval m

$F_i^{\min}, F_i^{\max}$: Lower and upper fuel delivery limits of thermal unit i

F_{Dm}: Fuel delivered in interval m

F_c: Total fuel cost

F_e: Total fuel emission

P_{im}: Output power of thermal unit i in interval m

$\mathrm{P}_i^{\min}, \mathrm{P}_i^{\max}$: Lower and upper generation limits of thermal unit i

P_{Dm}: Load demand in interval m

t_m : Duration of subinterval m .

V_{im} : Fuel storage of thermal unit i in interval m

$V_i^{\min}, V_i^{\max}$: Lower and upper fuel storage limits of thermal unit i

V_i^0 : Initial fuel storage of thermal unit i

a_i, b_i, c_i, d_i, e_i : Cost coefficients of i th thermal unit

$\alpha_i, \beta_i, \gamma_i, \sigma_i, \theta_i$: Emission coefficients of i th thermal unit

η_i, δ_i, μ_i : Fuel consumption coefficients of thermal unit i

\

Contents

CHAPTER 1

Introduction

1.1 General Introduction

The word ‘‘heuristic” is Greek and means ‘‘to know”, ‘‘to find”, ‘‘to discover” or ‘‘to guide an investigation”. Specifically, ‘‘Heuristics are techniques which seek good (near-optimal) solutions at a reasonable computational cost without being able to guarantee either feasibility or optimality, or even in many cases to state how close to optimality a particular feasible solution is.”

Two common aspects in the population-based heuristic algorithms are exploration and exploitation. The exploration is the ability to expand search space, whereas the exploitation is the ability to find the optima around a good solution. In premier iterations, a heuristic search algorithm explores the search space to find new solutions. To avoid trapping in a local optimum, the algorithm must use the exploration in the first few iterations. Hence, the exploration is an important issue in a population-based heuristic algorithm. By lapse (drop) of iterations, exploration fades out and exploitation fades (weakens) in, so the algorithm tunes itself in semi-optimal points. To have a high performance search, an essential key is a suitable tradeoff between exploration and exploitation. However, all the population-based heuristic algorithms employ the exploration and exploitation aspects but they use different approaches and operators. In other words, all search algorithms have a common framework.

Algorithms with stochastic components were often referred to as heuristic in the past, though the recent literature tends to refer to them as meta-heuristics.

Nature-inspired meta-heuristics can be broadly classified into two categories; evolutionary algorithm and swarm intelligence algorithm.

To tackle complex computational problems, researchers have been looking into nature for years both as model and as metaphor for inspiration. Optimization is at the heart of many natural processes like Darwinian evolution itself. Through millions of years, every one had to adapt physical structure to fit to the environment . A keen observation of the underlying relation between optimization and biological evolution led to the development of an important paradigm of computational intelligence known as evolutionary computing techniques for performing very complex search and optimization. Evolutionary computation uses iterative progress, such as growth or development in a population. This population is then selected in a guided random search using parallel processing to achieve the desired end. The paradigm of evolutionary computing techniques dates back to early 1950s, when the idea to use Darwinian principles for automated problem solving originated. It was not until the sixties that three distinct interpretations of this idea started to be developed in three different places. Evolutionary programming (EP) was introduced by Lawrence J. Fogel in the USA, while almost simultaneously I. Rechenberg and H.-P. Schwefel introduced evolution strategies (ESs) in Germany. Almost a decade later, John Henry Holland from University of Michigan, devised an independent method of simulating the Darwinian evolution to solve practical optimization problems and called it the genetic algorithm (GA). These areas developed separately for about 15 years. From the early 1990s on they are unified as different representatives of one technology, called evolutionary computing.

Swarm Intelligence (SI) introduced by Gerardo Beni and Jing Wang in 1989, is the study of the collective behavior of different natural systems which consist of number of agents working together.

Since the mid-eighties several multi-objective EAs have been developed, capable of searching for multiple pareto-optimal solutions concurrently in a single run. In spite of this variety, it is difficult to determine the appropriate algorithm for a given problem because it lacks extensive, quantitative comparative studies.

After the first studies on evolutionary multi-objective optimization in the mid-eighties, a number of Pareto-based techniques were proposed in 1993 and 1994, e.g., multi-objective genetic algorithm , niched pareto genetic algorithm and

nondominated sorting genetic algorithm , which demonstrated the capability of EMO algorithms to approximate the set of optimal trade-offs in a single optimization run. These approaches did not incorporate elitism explicitly, but a few years later the importance of this concept in multi-objective search was recognized and supported experimentally. A couple of elitist multi-objective evolutionary algorithms were presented at this time, e.g., strength pareto evolutionary algorithm and pareto archived evolution strategy . Strength pareto evolutionary algorithm2 is developed later which outperforms . It provides good performance in terms of convergence and diversity. Nondominated sorting genetic algorithm suffers from high computational complexity of nondominated sorting and lack of elitism. Nondominated sorting genetic algorithm-II overcomes these drawbacks.

Later multi-objective differential evolution , a pareto-based approach, has been developed which also provides a set of solutions in parallel.

Economic dispatch (ED) is one of the important optimization problems in power system operation. ED allocates the load demand among the committed generators most economically while satisfying the physical and operational constraints.

The conversion of fossil fuel into electricity is an inefficient process. Even the most modern combined cycle plants are between 50-60% efficient. Most of the energy wasted in the conversion process is heat. The principle of combined heat and power, known as cogeneration, is to recover and make beneficial use of this heat and as a result the overall efficiency of the conversion process is increased. Combined heat and power generation has higher energy efficiency and less green house gas emission as compared with the other forms of energy supply. Recently, cogeneration units have been extensively used in utility industry. The heat production capacity of cogeneration units depends on the power generation and vice versa. The mutual dependencies of heat and power generation introduce a complication in the integration of cogeneration units into the power economic dispatch.

Differential evolution with Gaussian mutation has been developed and applied to solve economic dispatch problem and combined heat and economic dispatch problem. Thermal generating units with non-smooth/non-convex cost functions due to valve-point loading taking into account transmission losses and nonlinear generator constraints such as prohibited operating zones have been considered here. Differential evolution (DE) is a simple yet powerful global optimization technique. It exploits the differences of randomly sampled pairs of objective vectors for its mutation process.

This mutation process is not suitable for complex multimodal optimization. Here, Gaussian mutation is introduced in DE which improves search efficiency and guarantees a high probability of obtaining the global optimum without significantly impairing the simplicity of the structure of DE. The effectiveness of the proposed method has been verified on different test systems, both small and large.

ED involves allocation of the load demand among the committed generators most economically while satisfying the physical and operational constraints in a single area. Generally, the generators are divided into several generation areas interconnected by tie-lines. Multi-area economic dispatch (MAED) is an extension of economic dispatch. MAED determines the generation levels and interchange powers between areas such that total fuel cost in all the areas is minimized while satisfying power balance constraints, generating limit constraints and tie-line capacity constraints.

Here, improved differential evolution and group search optimization have been applied to solve MAED problem.

The generation of electricity from fossil fuel-based power station releases sulfur oxides (SO_x), nitrogen oxides (NO_x), and carbon dioxide (CO_2) into atmosphere. Atmospheric pollution affects not only human beings but also other life-forms such as animals, birds, fish and plants. It also causes damage to vegetation, acid rain, reducing visibility as well as causing global warming. The increased concern over environmental protection and the passage of the clean air act amendments of 1990 have forced the power utilities to reduce their emissions. So today's concern is to produce electricity not only at the cheapest possible price, but also at the minimum level of pollution.

Several strategies have been proposed to reduce the atmospheric pollution. These include installation of post combustion cleaning equipment, switching to low emission fuels, replacement of the aged fuel burners with cleaner ones, and dispatching with emission considerations. The first three options require installation of new equipment and/or modification of the existing ones that involve considerable capital outlay and hence they can be considered as long-term options. So, the latter option is preferred.

The two objectives i.e. cost and emission are conflicting in nature and they both have to be considered simultaneously to find overall optimal dispatch. Multi-area economic environmental dispatch (MAEED) serves to schedule the committed generator outputs

with the predicted load demand so as to optimize both cost and emission simultaneously while fulfilling the operating constraints.

Here, multi-objective differential evolution (MODE) has been proposed to solve MAEED problem.

Economic emission dispatch involves the allocation of generation among the committed generating units so as to optimize both the fuel cost and emission level simultaneously while satisfying the several operating constraints.

Some power utilities have encountered a new dispatch problem, perhaps more significant than economic emission dispatch problem because of the sudden concern over fuel shortages. Fuel suppliers have imposed increased constraints in their fuel supply contracts to the point that utilities have been forced to reschedule generation on the basis of fuel availability. This came about because certain fuels were no longer available or available only in a limited supply or cut off from certain power plants. Thus, strict economic emission dispatch became impossible. There were no automatic ties between unit fuel availability and desired power production for that unit.

With the ever increasing proportion of the fuel budget in the total operating cost and increasing concern over the environmental consideration, fuel constrained economic emission dispatch problem has been popped up.

Here, multi-objective differential evolution (MODE) has been used for solving fuel constrained economic emission dispatch (FCEED) problem of thermal generating units.

Optimum scheduling of generation in a hydrothermal system is of great importance to electric utility systems. The insignificant marginal cost of hydroelectric operational cost of a hydrothermal system essentially reduces to that of minimizing the fuel cost for thermal plants under the various constraints on the hydraulic, thermal and power system network.

The main constraints include: the time coupling effect of the hydro sub-problem, where the water flow in an earlier time interval affects the discharge capability at a later period of time, the cascaded nature of the hydraulic network, the varying hourly reservoir inflows, the physical limitations on the reservoir storage and turbine flow rate, prohibited operating zones of hydroelectric system, ramp-rate limits of thermal generators, the varying system load demand and the loading limits of both thermal and hydro plants.

The hydrothermal scheduling problem has been the subject of investigation for several decades. Most of the methods that have been used to solve the hydrothermal co-ordination problem make a number of simplifying assumptions in order to make the optimization problem more tractable.

Here, modified evolutionary programming (MEP) has been developed and applied to solve variable head hydrothermal scheduling problem. Group search optimization (GSO) has also been used to solve variable head hydrothermal scheduling problem. Here, Group search optimization (GSO), opposition-based group search optimization (OGSO) and opposition based differential evolution (ODE) have been applied for optimal scheduling of generation in a fixed head hydrothermal system. Here, system with fixed head hydro plants whose water discharge rate curves are modeled as quadratic functions of the hydropower generation and thermal units with nonsmooth fuel cost function. Here, scheduling period is divided into a number of subintervals each having a constant load demand.

1.2 Literature Survey

Evolutionary algorithms (EAs) [1]-[2] are search algorithms based on the simulated evolutionary process of natural selection and genetics. Genetic algorithm (GA) [3] belongs to a class of evolutionary computation techniques [4]-[5] based on models of biological evolution. The main difficulty of GA is its binary representation which arises when dealing with continuous search space with large dimensions. In [6]-[7] real-coded genetic algorithm (RCGA) has been discussed which overcomes the difficulties of GA.

Evolutionary Programming (EP) [4] is a technique in the field of evolutionary computation. It seeks the optimal solution by evolving a population of candidate solutions over a number of generations or iterations

Differential evolution (DE) is a very simple and robust method originally proposed by Price and Stron [8] for optimization problem over a continuous domain. The basic idea of DE [9] is to adapt the search during the evolutionary process.

Particle Swarm Optimization (PSO) [10]-[12] was introduced in 1995 by James Kennedy and Russell Eberhart as a global optimization technique. It is a population-based self-adaptive stochastic search technique with reduced memory requirement.

Group search optimization (GSO) [13]-[14] is a population based optimization algorithm which is inspired by animal searching behavior and group living theory.

Multi-objective evolutionary algorithms (MOEAs) have been discussed very well in [17]-[24]. Zitzler and Thiele [19] have developed strength pareto evolutionary algorithm (SPEA) in 1999. In 2001 they have developed the improved version strength pareto evolutionary algorithm [20] i.e. strength pareto evolutionary algorithm 2 (SPEA2). Deb et al. [21] have proposed nondominatd sorting genetic algorithm-II (NSGA-II) in 2002. Babu and Anbarasu have developed multi-objective differential evolution (MODE) [23] in 2005.

The dynamic programming (DP) approach imposes no restriction on the nature of the cost curves and can solve ED problems with non-smooth and discontinuous cost curves. However, this method suffers from the curse of dimensionality or local optimality.

Meta-heuristic algorithms are successfully applied to solve complex ED problems. Genetic algorithms (GAs) [32]-[34], Hopfield neural network (HNN) [37], simulated annealing (SA) [38]-[39], evolutionary programming (EP) [40]-[41], improved tabu search (ITS) [31], particle swarm optimization (PSO) [30], [42],[43], evolutionary strategy optimization (ESO) [35], ant colony optimization (ACO) [44], differential evolution (DE) [45], self -tuning hybrid differential evolution (SHDE) [46], artificial immune system (AIS) [47], bacterial foraging algorithm (BFA) [48], biogeography-based optimization (BBO) [49], etc. have been developed so far and applied successfully to solve ED problems. Although these methods do not always guarantee global best solutions, they often achieve a fast and near global optimal solution.

The advent of stochastic search algorithms has provided alternative approaches for solving combined heat and economic dispatch (CHPED) [50]-[51] problem. Improved ant colony search algorithm [52], evolutionary programming [53], genetic algorithm [54], harmonic search algorithm [55], multi-objective particle swarm optimization [56], self adaptive real-coded genetic algorithm [57], novel selective particle swarm optimization [58], mesh adaptive direct search algorithm [59], particle swarm optimization with time varying acceleration coefficients [62] and oppositional teaching learning based optimization [63] have been applied to solve CHPED problem.

Doty and McEntire [67] solved a multi-area economic dispatch problem by using spatial dynamic programming and the result obtained was a global optimum. An

application of linear programming to transmission constrained production cost analysis was proposed in Ref. [68]. Helmick [69] solved multi-area economic dispatch with area control error. Ouyang et al [70] proposed heuristic multi-area unit commitment with economic dispatch. Wang and Shahidehpour [71] proposed a decomposition approach for solving multi-area generation scheduling with tie-line constraints using expert systems. Network flow models for solving the multi-area economic dispatch problem with transmission constraints have been proposed by Streiffert [72]. An algorithm for multi-area economic dispatch and calculation of short range margin cost based prices has been presented by Wernerus and Soder [73], where the multi-area economic dispatch problem was solved via Newton–Raphson's method. Yalcinoz and Short [74] solved multi-area economic dispatch problems by using Hopfield neural network approach. Jayabarathi [75] solved multi-area economic dispatch problems with tie line constraints using evolutionary programming. The direct search method for solving economic dispatch problem considering transmission capacity constraints was presented in [76]. Manoharan [77] explored the performance of the various evolutionary algorithms on multi-area economic dispatch (MAED) problems.

Here, evolutionary algorithms such as the Real-coded Genetic Algorithm (RCGA), Particle Swarm Optimization (PSO), Differential Evolution (DE) and Covariance Matrix Adapted Evolution Strategy (CMAES) are considered. Multi-area economic environmental dispatch (MAEED) problem is proposed in [78]. Here, MAEED problem is handled by an improved multi-objective particle swarm optimization (MOPSO) algorithm for searching out the Pareto-optimal solutions. Sharma [79] have presented a close comparison of classic PSO and DE strategies and their variants for solving the reserve constrained multi-area economic dispatch problem with power balance constraint, upper/lower generation limits, ramp rate limits, transmission constraints and other practical constraints. In [80] a discussion of ''Reserve constrained multi-area economic dispatch employing differential evolution with time-varying mutation" has been presented.

The hydrothermal scheduling problem has been the subject of investigation for several decades. Most of the methods that have been used to solve the hydrothermal co-ordination problem make a number of simplifying assumptions in order to make the optimization problem more tractable. Some of these solution methods are mathematical decomposition [98], network flow [99], dynamic programming [100],

deterministic optimization algorithm [101], Lagrangian relaxation [102], and Benders decomposition [103].

Since the mid 1990s, many techniques originated from Darwin's natural evolution theory have emerged. These techniques are usually termed by "evolutionary computation methods" including evolutionary algorithms (EAs), swarm intelligence and artificial immune system.

With the emergence of evolutionary computation methods, attention has been gradually shifted to application of such technology-based approaches to handle the complexity involved in real world problems. Stochastic search algorithms such as simulated annealing technique [104], evolutionary programming technique [105], [108], genetic algorithm [106]-[107], differential evolution [109]-[111], and particle swarm optimization [112], clonal selection algorithm [113] and teaching learning based optimization [114] have been applied for optimal hydrothermal scheduling problem and circumvented the above mentioned weakness.

1.3 Motivation behind the work

The valve-point loading, prohibited operating zones, ramp-rate limits and other constraints turn the decision space into disjoint subsets, transforming the most of the power system problems into difficult non-smooth, non-convex optimization problems.

The calculus-based methods fail to address these types of problems. The dynamic programming method has no restrictions on the shape of the objective function and can solve these types of problems. However, this method suffers from the curse of dimensionality or local optimality. Modern meta-heuristic algorithms are promising alternatives for the solution of complex power system optimization problems.

Keeping this in mind, this work mainly focuses on complex power system optimization by using nature-inspired meta-heuristic techniques.

CHAPTER 2

Nature-inspired Meta-heuristics Techniques

2.1 Introduction

Heuristic algorithms mimic physical or biological processes. Some of the most famous heuristic algorithms are genetic algorithm, simulated annealing, artificial immune systems, ant colony optimization, particle swarm optimization and bacterial foraging algorithm. Genetic algorithm (GA) is inspired from Darwinian evolutionary theory, simulated annealing (SA) is designed by use of thermodynamic effects, artificial immune systems (AIS) simulate biological immune systems, ant colony optimization (ACO) mimics the behavior of ants foraging (searching) for food, bacterial foraging algorithm (BFA) comes from search and optimal foraging of bacteria and particle swarm optimization (PSO) simulates the behavior of flock of birds.

Nowadays, the field of nature-inspired meta-heuristics is mostly constituted by the evolutionary computing (EC) techniques or evolutionary algorithms (EAs) [comprising of genetic algorithm (GA), evolutionary programming (EP), evolutionary strategy (ES), genetic programming (GP), differential evolution (DE), and so on] as well as the swarm intelligence algorithms [e.g., ant colony optimization (ACO), particle swarm optimization (PSO), Bees algorithm, bacterial foraging algorithm, (BFA), and so on]. Also the field extends in a broader sense to include self-organizing systems, artificial life (digital organism), mimetic and cultural algorithms, harmony search, and artificial immune systems.Nature-inspired meta-heuristics deal with a set (i.e. a population) of solutions rather than with a single solution.

2.2. Evolutionary algorithms

Evolutionary algorithms (EAs) are stochastic search methods that mimic evolutionary processes encountered in nature. EAs are inspired by Darwin’s evolutionary theory.

The common conceptual base of these methods is to evolve a population of candidate solutions by simulating the main processes involved in the evolution of genetic material of organism (living being) populations, such as natural selection and biological evolution. EAs can be characterized as global optimization algorithms. Their population-based nature allows them to avoid getting trapped in a local optimum and consequently provides a great chance to find global optimal solutions.

In general, every EA starts by initializing a population of candidate solutions (individuals). The quality of each solution is evaluated using a fitness function. A selection process is applied at each iteration of the EA to produce a new set of solutions (population). The selection process is biased toward the most promising traits of the current population of solutions to increase their chances of being included in the new population. At each iteration (generation), the individuals are evolved through a predefined set of operators, like mutation and recombination. This procedure is repeated until convergence is reached. The best solution found by this procedure is expected to be a near-optimum solution.

Mutation and recombination are the two most frequently used operators and are referred to as evolutionary operators. The role of mutation is to modify an individual by small random changes to generate a new individual. Its main objective is to increase diversity by introducing new genetic material into the population, and thus avoid local optima. The

recombination (or crossover) operator combines two, or more, individuals to generate new promising candidate solutions. The main objective of the recombination operator is to explore new areas of the search space.

Evolutionary computation (EC) is the general term for several optimization algorithms that are inspired by the Darwinian principles of nature’s capability to evolve (develop) living beings well adapted to their environment. EC techniques (also called Evolutionary Algorithms (EAs)) include genetic algorithm, evolution strategy, evolutionary programming and genetic programming. Despite the differences between these techniques, they all share a common underlying idea of simulating the evolution of individual structures via processes of selection, recombination, and mutation, thereby producing better solutions.

Every iteration of the algorithm corresponds to a generation, where a population of candidate solutions to a given optimization problem, called individuals, is capable of reproducing and is subjected to genetic variations followed by the environmental

pressure that causes natural selection (survival of the fittest). New solutions are created by applying recombination, that combines two or more selected individuals (the so-called parents) to produce one or more new individuals (the children or offspring), and mutation, that allows the appearance of new traits (qualities) in the offspring to promote diversity. The fitness (how good the solutions are) values of the resulting solutions are evaluated and a suitable selection strategy is then applied to determine which solutions will be maintained into the next generation. As a termination condition, a predefined number of generations (or function evaluations) of simulated evolutionary process is usually used, or some more complex stopping criteria can be applied.

A main issue in the application of EAs to a given optimization problem is to determine the values of the control parameters of the algorithm that will allow the efficient exploration of the search space, as well as its effective exploitation. Exploration enables the identification of regions of the search space in which good solutions are located. On the other hand, exploitation accelerates the convergence to the optimum solution. Inappropriate choice of the parameter values can cause the algorithm to become greedy or very explorative and consequently the search of the optimum can be hindered. For example, a high mutation rate will result in much of the space being explored, but there is also a high probability of losing promising solutions; the algorithm has difficulty in converging to an optimum due to insufficient exploitation. Several evolutionary computation approaches have been proposed that try to give a satisfactory answer to this exploration/exploitation dilemma (problem).

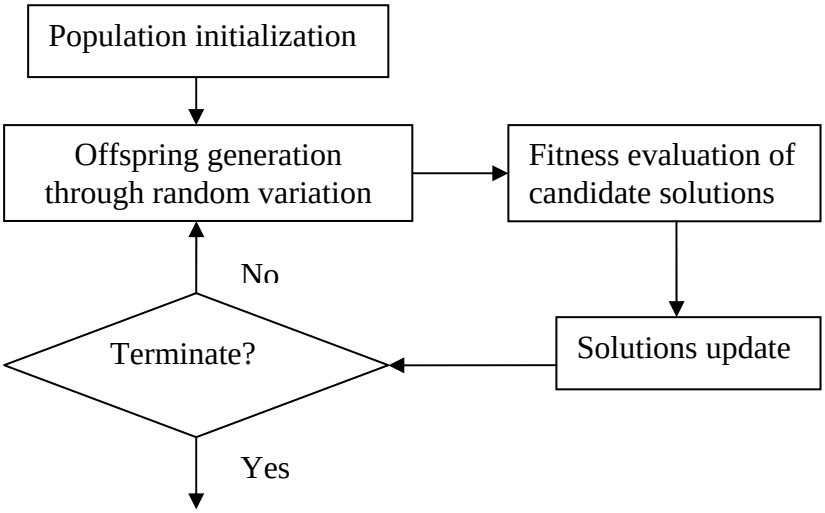

Fig. 1. A general flowchart of typical EAs.

2.2.1 Genetic Algorithm

Genetic algorithm (GA) is a search algorithm based on the mechanics of natural genetics and natural selection. It combines the adaptive nature of the natural genetics or the evolution procedures of organs with functional optimizations. By simulating "the survival of the fittest" of Darwinian evolution among chromosome structures, the optimal chromosome (solution) is searched by randomized information exchange. In every generation, a new set of artificial chromosomes is created by using bits and pieces of the fittest of the old ones. While randomized, GA is not a simple random walk. It efficiently exploits historical information to speculate on new search points with expected improved performance.

GA is essentially derived from a simple model of population genetics. The three prime operators associated with the GA are reproduction, crossover and mutation.

Reproduction is simply an operation whereby an old chromosome is copied into a "mating pool" according to its fitness value. More highly fitted chromosomes (i.e., with better values of the objective function) receive a higher number of copies in the next generation. Coping chromosomes according to their fitness values means that chromosomes with a higher value have higher probability of contributing one or more offsprings in the next generation.

Crossover is an extremely important component of the GA. It is a structured recombination operation. This operation is similar to two scientists exchanging information.

Although reproduction and crossover effectively search and recombine existing chromosomes, they do not create any new genetic material in the population. Mutation is capable of overcoming this shortcoming.

Due to difficulties of binary representation when dealing with continuous search space with large dimensions, real-coded genetic algorithm (RCGA) has been used in this thesis. The Simulated Binary Crossover (SBX) and polynomial mutation have been used. The crossover probability of $p_c = 0.9$ and a mutation probability of $p_m = 1/n$ (where n is the number of decision variables) are used. Here, distribution indices for crossover and mutation operators as $\eta_c = 10$ and $\eta_m = 10$ are used ,respectively.

2.2.1.1 Simulated Binary Crossover (SBX) operator

The procedure of computing child populations c_1 and c_2 from two parent populations y_1 and y_2 under SBX operator is as follows:

1. Create a random number *u* between 0 and 1.
2. Find a parameter γ using a polynomial probability distribution as follows:

$$\gamma = \begin{cases} (u\alpha)^{1/(\eta_c+1)}, & \text{if} \quad u \le \dfrac{1}{\alpha} \\ \left(1/(2-u\alpha)\right)^{1/(\eta_c+)}, & \text{otherwise} \end{cases} \tag{2.1}$$

where $\alpha = 2 - \beta^{-(\eta_c+1)}$ and β is calculated as follows:

$$\beta = 1 + \frac{2}{y_2 - y_1}\min\left[(y_1 - y_l),(y_u - y_2)\right] \tag{2.2}$$

Here, the parameter y is assumed to vary in $[y_l, y_u]$. Here, the parameter η_c is the distribution index for SBX and can take any non-negative value. A small value of η_c allows the creation of child populations far away from parents and a large value restricts only near-parent populations to be created as child populations.

3. The intermediate populations are calculated as follows:

$$c_{p1} = 0.5\left[(y_1 + y_2) - \gamma(|y_2 - y_1|)\right]$$
$$c_{p2} = 0.5\left[(y_1 + y_2) + \gamma(|y_2 - y_1|)\right] \quad (2.3)$$

Each variable is chosen with a probability p_c and the above SBX operator is applied variable-by-variable.

2.2.1.2 Polynomial Mutation operator

A polynomial probability distribution is used to create a child population in the vicinity of a parent population under the mutation operator. The following procedure is used:

1. Create a random number *u* between 0 and 1.
2. Calculate the parameter δ as follows:

$$\delta = \begin{cases} \left[2u + (1-2u)(1-\phi)^{(\eta_m+1)}\right]^{\frac{1}{(\eta_m+1)}} - 1, & \text{if } u \le 0.5 \\ 1 - \left[2(1-u) + 2(u-0.5)(1-\phi)^{(\eta_m+1)}\right]^{\frac{1}{(\eta_m+1)}}, & \text{otherwise} \end{cases} \quad (2.4)$$

where $\varphi = \dfrac{\min\left[(c_p - y_l), (y_u - c_p)\right]}{(y_u - y_l)}$

The parameter η_m is the distribution index for mutation and takes any non-negative value.

3. Calculate the mutated child as follows:

$$c_1 = c_{p1} + \delta(y_u - y_l) \tag{2.5}$$
$$c_2 = c_{p2} + \delta(y_u - y_l)$$

The perturbance in the population can be adjusted by varying η_m and p_m with generations as given below:

$$\eta_m = \eta_{m\min} + gen \tag{2.6}$$

$$p_m = \frac{1}{n} + \frac{gen}{gen_{\max}}\left(1 - \frac{1}{n}\right) \tag{2.7}$$

where $\eta_{m\min}$ is the user defined minimum value for η_m, p_m is the probability of mutation, and n is the number of decision variables.

2.2.2. Evolutionary Programming

Evolutionary Programming (EP) is a technique in the field of evolutionary computation. It seeks the optimal solution by evolving a population of candidate solutions over a number of generations or iterations. During each iteration, a second new population is formed from an existing population through the use of a mutation operator. This operator produces a new solution by perturbing each component of an existing solution by a random amount. The degree of optimality of each of the candidate solutions or individuals is measured by it's fitness, which can be defined as a function of the objective function of the problem. Through the use of a competition scheme, the individuals in each population compete with each other. The winning individuals form a resultant population, which is regarded as the next generation. For optimization to occur, the competition scheme must be such that the more optimal solutions have a greater chance of survival than the poorer solutions. Through this the population evolves towards the global optimal point. The algorithm is described as follows:

2.2.2.1 Initialization

The initial population of control variables is selected randomly from the set of uniformly distributed control variables ranging over their upper and lower limits. The fitness score f_i is obtained according to the objective function and the environment.

2.2.2.2 Statistics

The maximum fitness $f_{\max}$, minimum fitness $f_{\min}$, the sum of fitness $\sum f$, and average fitness f_{avg} of this generation are calculated.

2.2.2.3 Mutation

Each selected parent, for example X_i, is mutated and added to its population with the following rule:

$$\mathrm{X}_{i+m,j} = \mathrm{X}_{ij} + N\left(0, \gamma\left(\overline{x}_j - \underline{x}_j\right)\frac{f_i}{f_{\max}}\right), \qquad j \in D, i \in \mathrm{N_P} \tag{2.8}$$

where D is the number of decision variables in an individual, $\mathrm{N_P}$ is the population size, X_{ij} denotes the jth element of the ith individual; $N\left(\mu, \sigma^2\right)$ represents a Gaussian random variable with mean μ and variance σ^2; $f_{\max}$ is the maximum fitness of the old generation which is obtained in statistics; $\overline{x}_j$ and $\underline{x}_j$ are, respectively, maximum and minimum limits of the jth element; and γ is the mutation scale, $0 < \gamma \le 1$, that could be adaptively decreased during generations. If any mutated value exceeds its limit, it will be given the limit value. The mutation process allows an individual with larger fitness to produce more offspring for the next generation.

2.2.2.4 Competition

Several individuals (k) which have the best fitness values are kept as the parents for the next generation. Other individuals in the combined population of size ($2\mathrm{N_P} - k$)

have to compete with each other to get their chances for the next generation. A weight value w_i of the i th individual is calculated by the following competition:

$$w_i = \sum_{t=1}^{N_t} w_{i,t} \tag{2.9}$$

where N_t is the competition number generated randomly; $w_{i,t}$ is either 0 for loss or 1 for win as the i th individual competes with a randomly selected (r th) individual in the combined population. The value of $w_{i,t}$ is given in the following equation:

$$w_{i,t} = \begin{cases} 1 & \text{if } f_i < f_r \\ 0 & \text{otherwise} \end{cases} \tag{2.10}$$

where f_r is the fitness of randomly selected r th individual, and f_i is the fitness of the i th individual. When all $2N_P$ individuals, get their competition weights, they will be ranked in a descending order according to their corresponding values w_i. The first m individuals are selected along with their corresponding fitness f_i to be the bases for the next generation. The maximum, minimum and the average fitness and the sum of the fitness of the current generation are then calculated in the statistics.

2.2.2.5 Convergence test

If the convergence condition is not met, the mutation and competition will run again. The maximum generation number can be used for convergence condition. Other criteria, such as the ratio of the average and the maximum fitness of the population are computed and generations are repeated until

$$\{f_{avg} / f_{\max}\} \geq \delta \tag{2.11}$$

where δ should be very close to 1, which represents the degree of satisfaction. If the convergence has reached a given accuracy, an optimal solution has been found for an optimization problem.

Figure 2.1 shows the flowchart of evolutionary programming.

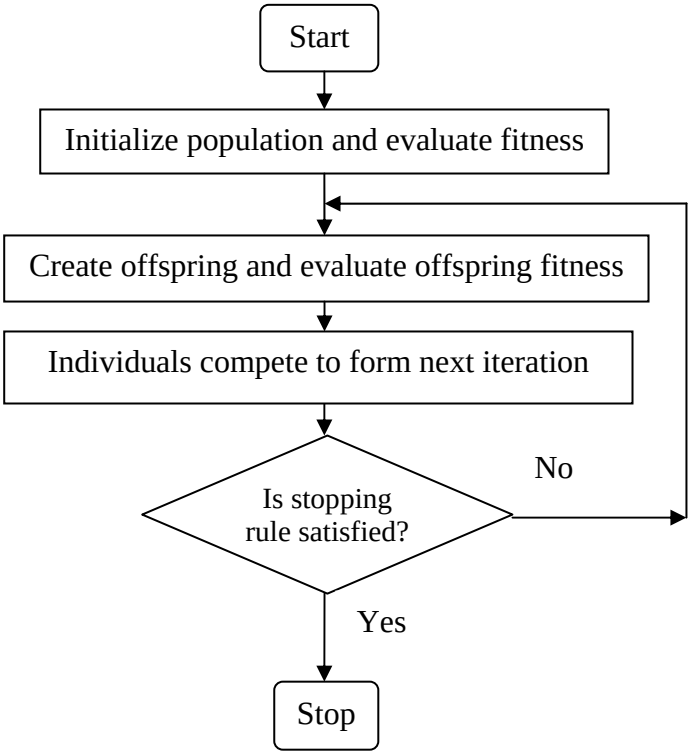

Fig. 2.1. Flowchart of evolutionary programming.

2.2.3. Modified Evolutionary Programming

In modified evolutionary programming (MEP), crossover and one-to-one competition of differential evolution (DE) are introduced in evolutionary programming (EP) to improve the speed of convergence and quality of solution. This one-to-one competition gives rise to faster convergence rate as the fittest offspring competes one-to-one with that of corresponding parent. The main stages are initialization, mutation, crossover and selection. These are listed below:

2.2.3.1. Initialization: The initial population (X_i^0) of control variables is selected randomly as follows:

$$x_{i,j}^0 \sim U\left(x_j^{\min}, x_j^{\max}\right), \quad j \in n, i \in \mathrm{N_P} \tag{2.12}$$

where n is the number of decision variables in an individual ; $\mathrm{N_P}$ is the population size; $x_{i,j}^0$ denotes the initial j th variable of the i th population ; $x_j^{\min}$ and $x_j^{\max}$ are the

lower and upper bounds of the j th decision variable; $U\left(x_j^{\min}, x_j^{\max}\right)$ denotes a uniform random variable ranging over $\left[x_j^{\min}, x_j^{\max}\right]$.

All the populations should satisfy the constraints. Evaluate the objective function f_i of each population according to the objective function. The maximum objective function value $f_{\max}$ is calculated.

2.2.3.2. Mutation: Each selected parent population (X_i^k) is mutated and added to its population to create offspring ($\mathrm{X}_i^{/k}$) with the following rule:

$$x_{i,j}^{/k} = x_{i,j}^k + N\left(0, \beta\left(x_j^{\max} - x_j^{\min}\right)\frac{f_i}{f_{\max}}\right), \qquad j \in n, i \in \mathrm{N_P} \qquad (2.13)$$

where $N\left(\mu, \sigma^2\right)$ represents a Gaussian random variable with mean μ and variance σ^2; $f_{\max}$ is the maximum objective function value of the previous iteration; β is the mutation scale.

2.2.3.3. Crossover

Perform crossover for each parent population X_i^k with its offspring $\mathrm{X}_i^{/k}$ and create a trial population $\mathrm{X}_i^{//k}$ such that

$$\mathrm{X}_i^{//k} = \begin{cases} \mathrm{X}_i^{/k} & \text{, if } \rho \le C_R \\ & \text{, } i \in \mathrm{N_P} \\ \mathrm{X}_i^k & \text{, otherwise} \end{cases} \qquad (2.14)$$

where ρ is an uniformly distributed random number within [0, 1]. Here, binomial crossover is performed. The basic crossover process is a discrete recombination, which employs crossover rate $C_R \in [0,1]$ to determine if the newly generated population is to be recombined.

Each trial population should satisfy the constraints. Evaluate the objective function f_i of each trial population according to the objective function.

2.2.3.4. Selection

Perform selection for each parent population, X_i^k by comparing its objective function value with that of the trial population, $X_i^{//k}$. The population that has lower objective function value of the two would survive for the next iteration.

$$X_i^{k+1} = \begin{cases} X_i^{//k}, \text{ if } f\left(X_i^{//k}\right) \le f\left(X_i^k\right) \\ \qquad\qquad\qquad\qquad , \ i \in N_P \\ X_i^k \ , \text{ otherwise} \end{cases} \tag{2.15}$$

The process is repeated until the maximum number of iterations or no improvement is seen in the best individual after many iterations.

Figure 2.2 shows the flowchart of modified evolutionary programming.

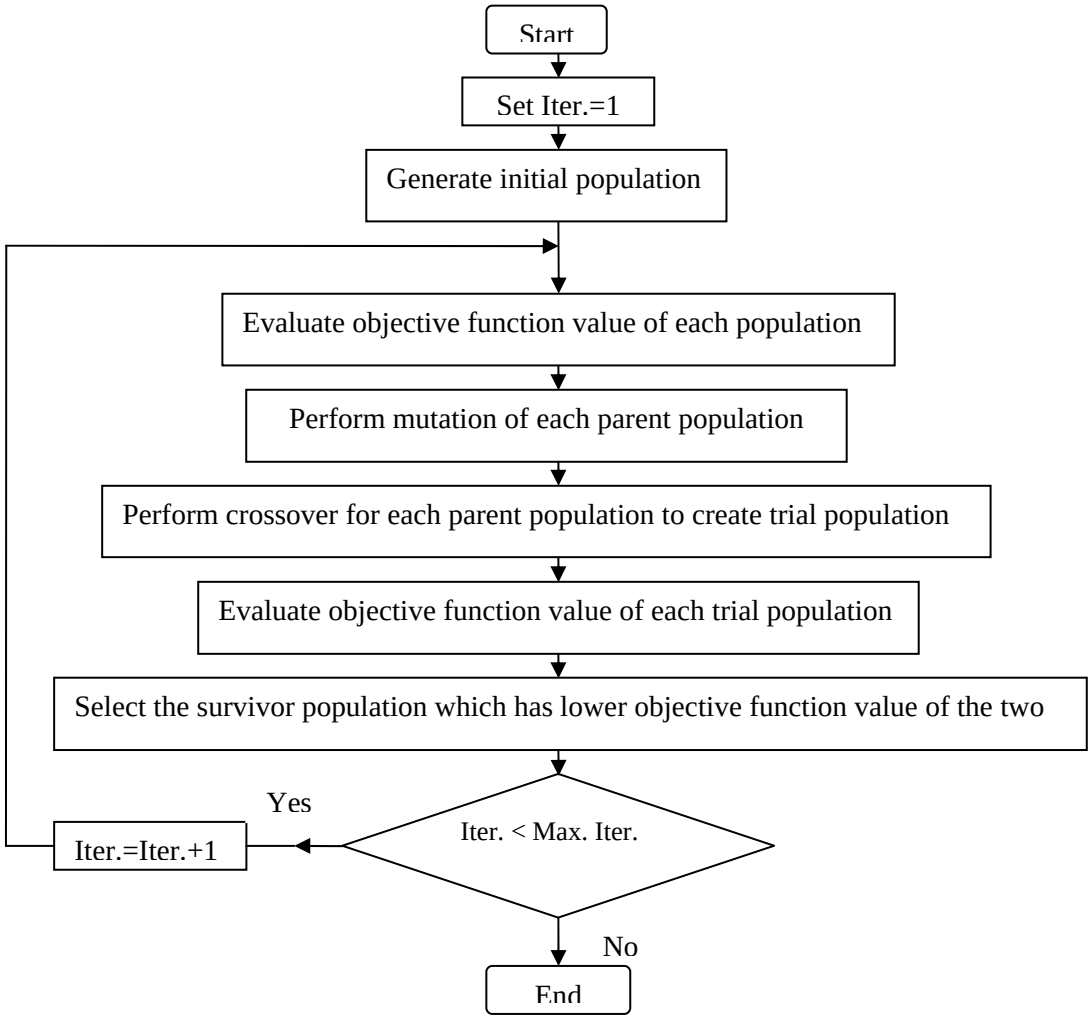

Fig. 2.2. Flowchart of modified evolutionary programming.

2.2.4. Differential Evolution

Differential Evolution (DE), originally proposed by Price and Storn in 1995-1997 at Berkley, is a population-based stochastic parallel direct search method for optimization problems over a continuous domain. DE outperforms other well-known EAs in a plethora of problems and has attracted the interest of the research community. DE is exceptionally simple, significantly faster, precise and robust.

The basic idea of DE is to adapt the search during the evolutionary process. At the start of the evolution, the perturbations are large since parent populations are far away from each other. As the evolutionary process matures, the population converges to a small region and the perturbations adaptively become small. As a result, the evolutionary algorithm performs a global exploratory search during the early stages of the evolutionary process and local exploitation during the mature stage of the search. The optimization process in DE is carried out with three basic operations: mutation, crossover and selection.

Like any evolutionary algorithm, a population of candidate solutions for the optimization problem to be solved is arbitrarily initialized. For each generation of the evolutionary process, new individuals are created by applying crossover and mutation. The fitness values of the resulting solutions are evaluated. Each individual (target individual) of the population competes against a new individual (trial individual) to determine which one will be maintained into the next generation. The trial individual is created by recombining the target individual with another individual created by mutation (called mutant individual). In DE the fittest offspring competes one-to-one with that of corresponding parent which is different from other evolutionary algorithms. This one-to-one competition gives rise to faster convergence rate. Differential evolution exploits the differences of randomly sampled pairs of solution vectors for its mutation process. Consequently the variation between vectors will outfit the objective function toward the optimization process and therefore provides efficient global optimization capability. The key parameters of control in DE are population size, scaling factor and crossover rate. Price and Storn gave the working principle of DE with simple strategy . Later on, they suggested ten different strategies of DE. Strategy-7 (DE/rad/1/bin) is the most successful and widely used strategy.

2.2.4.1. Initialization

The initial population of N_P vectors is randomly selected based on uniform probability distribution for all variables to cover the entire search uniformly. Each individual X_i is a vector that contains as many parameters as the problem decision variables D. Random values are assigned to each decision parameter in every vector according to:

$$X_{ij}^0 \sim U\left(X_j^{\min}, X_j^{\max}\right) \tag{2.16}$$

where i=1,…., N_P and j=1,…., D; $X_j^{\min}$ and $X_j^{\max}$ are the lower and upper bounds of the jth decision variable; $U\left(X_j^{\min}, X_j^{\max}\right)$ denotes a uniform random variable ranging over $\left[X_j^{\min}, X_j^{\max}\right]$; X_{ij}^0 is the initial jth variable of ith population. All the vectors should satisfy the constraints. Evaluate the value of the cost function $f\left(X_i^0\right)$ of each vector.

2.2.4. 2. Mutation

DE generates new parameter vectors by adding the weighted difference vector between two population members to a third member. For each target vector X_i^g at gth generation the noisy vector $X_i^{/g}$ is obtained by

$$X_i^{/g} = X_a^g + F\left(X_b^g - X_c^g\right), \qquad i \in N_P \tag{2.17}$$

where X_a^g, X_b^g and X_c^g are selected randomly from N_P vectors at gth generation and $a \neq b \neq c \neq i$. The scaling factor (F), in the range $0 < F \leq 1.2$, controls the amount of perturbation added to the parent vector. The noisy vectors should satisfy the constraint.

2.2.4. 3. Crossover

Perform crossover for each target vector X_i^g with its noisy vector $X_i^{/g}$ and create a trial vector $X_i^{//g}$ such that

$$X_i^{//g} = \begin{cases} X_i^{/g} \text{ , if } \rho \le C_R \\ \\ X_i^{g} \text{ , otherwise} \end{cases} , \quad i \in N_P \tag{2.18}$$

where ρ is an uniformly distributed random number within [0, 1]. The crossover constant (C_R), in the range $0 \le C_R \le 1$, controls the diversity of the population and aids the algorithm to escape from local optima.

2.2.4. 4. Selection

Perform selection for each target vector, X_i^g by comparing its cost with that of the trial vector, $X_i^{//g}$. The vector that has lesser cost of the two would survive for the next generation.

$$X_i^{g+1} = \begin{cases} X_i^{//g} \text{ , if } f\left(X_i^{//g}\right) \le f\left(X_i^{g}\right) \\ \\ X_i^{g} \text{ , otherwise} \end{cases} , \ i \in N_P \tag{2.19}$$

The process is repeated until the maximum number of generations or no improvement is seen in the best individual after many generations.

Figure 2.3 shows the flowchart of differential evolution.

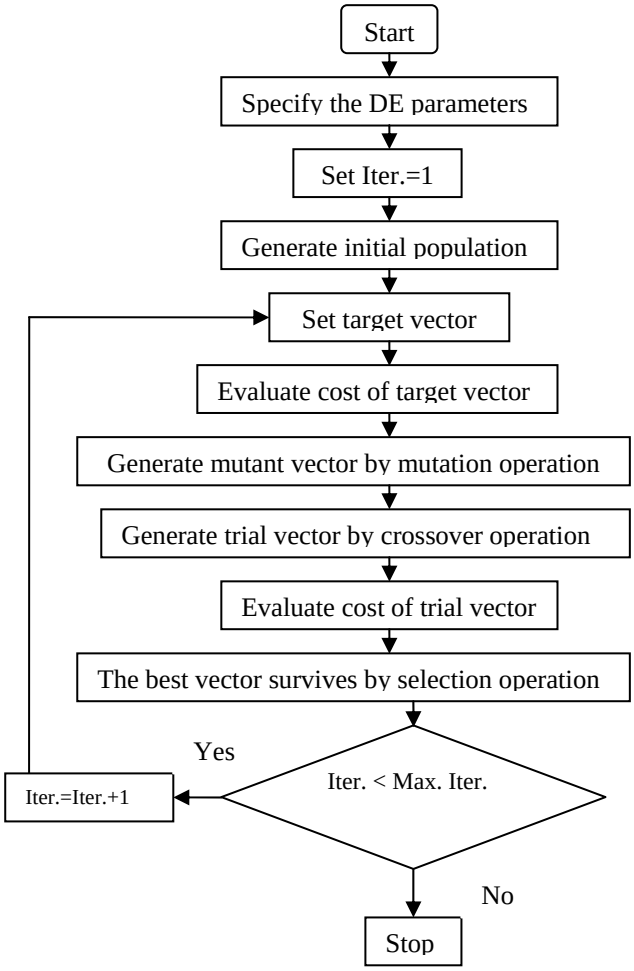

Fig. 2.3. Flowchart of Differential Evolution.

2.2.4.5. Parameter Selection

In differential evolution, scaling factor (S_F), crossover constant (C_R), and population size (N_P) are the three control parameters. Proper selection of control parameters is important for the performance of the algorithm. The scaling factor controls the amount of perturbation in the mutation process. Its value lies in the range of [0, 2]. Lower value of S_F results premature convergence while higher value of S_F tends to slow down convergence speed. The crossover constant whose value is in the range of [0, 1], controls the diversity of the population. The diversity for searching the solution space depends on the population size. However, large population slows down convergence speed.

The optimal control parameters are problem dependent. Generally, parameter tuning is used to select control parameters. By thorough testing, parameter tuning adjusts the control parameters until the best settings are determined.

2.2.5. Improved Differential Evolution

As a relatively new member of EAs, DE is less known outside metaheuristic optimization area. Similar to other EAs, DE relies likewise on the initial population, mutation, crossover and selection to problem search space through iterative progress until the terminate criteria is met. The key parameters of control in DE are population size, scaling factor and crossover rate. In improved differential evolution (IDE), Gaussian random variable is taken instead of scaling factor. The IDE algorithm is described as follows:

2.2.5.1. Initialization

The initial population of $\mathrm{N_P}$ vectors is randomly selected based on uniform probability distribution for all variables to cover the entire search uniformly. Each individual X_i is a vector that contains as many parameters as the problem decision variables D. Random values are assigned to each decision parameter in every vector according to:

$$\mathrm{X}_{ij}^{0} \sim U\left(\mathrm{X}_{j}^{\min}, \mathrm{X}_{j}^{\max}\right) \tag{2.20}$$

where $i = 1,\ldots,\mathrm{N_P}$ and $j = 1,\ldots,D$; $\mathrm{X}_{j}^{\min}$ and $\mathrm{X}_{j}^{\max}$ are the lower and upper bounds of the jth decision variable; $U\left(\mathrm{X}_{j}^{\min}, \mathrm{X}_{j}^{\max}\right)$ denotes a uniform random variable ranging over $\left[\mathrm{X}_{j}^{\min}, \mathrm{X}_{j}^{\max}\right]$; X_{ij}^{0} is the initial jth variable of ith population. All the vectors should satisfy the constraints. Evaluate the value of the cost function $f\left(\mathrm{X}_{i}^{0}\right)$ of each vector.

2.5.2. Mutation

IDE generates new parameter vectors by adding the weighted difference vector between two population members to a third member. For each target vector X_i^g at g th generation the noisy vector $\mathrm{X}_i^{/g}$ is obtained by

$$\mathrm{X}_i^{/g} = \mathrm{X}_a^g + N\left(0,\sigma_i^2\right)\times\left(\mathrm{X}_b^g - \mathrm{X}_c^g\right), \qquad i \in \mathrm{N_P} \tag{2.21}$$

where X_a^g, X_b^g and X_c^g are selected randomly from $\mathrm{N_P}$ vectors at g th generation and $a \neq b \neq c \neq i$. $N\left(0,\sigma_i^2\right)$ represents a Gaussian random variable with mean zero and standard deviation σ_i.

The standard deviation σ_i is given by the expression $\sigma_i = \dfrac{f\left(\mathrm{X}_i\right)}{f_{\min}}$ (2.22)

where $f_{\min}$ is the minimum cost value among $\mathrm{N_P}$ vectors. $f\left(\mathrm{X}_i\right)$ is the value of the objective function associated with i th vector.

This Gaussian random variable controls the amount of perturbation added to the parent vector and aids the algorithm to escape from local optima. This maintains the diversity of the population throughout iterative process which guarantees a high probability of achieving the global optimum.

2.2.5.3. Crossover

Perform crossover for each target vector X_i^g with its noisy vector $\mathrm{X}_i^{/g}$ and create a trial vector $\mathrm{X}_i^{//g}$ such that

$$\mathrm{X}_i^{//g} = \begin{cases} \mathrm{X}_i^{/g} \text{ , if } \rho \le C_R \\ \qquad\qquad , \quad i \in \mathrm{N_P} \\ \mathrm{X}_i^g \text{ , otherwise} \end{cases} \tag{2.23}$$

where ρ is an uniformly distributed random number within [0, 1]. The basic crossover process is a discrete recombination, which employs constant $C_R \in [0,1]$ to determine if the newly generated individual is to be recombined.

2.2.5. 4. Selection

Perform selection for each target vector, X_i^g by comparing its cost with that of the trial vector, $X_i^{//g}$. The vector that has lesser cost of the two would survive for the next generation.

$$X_i^{g+1} = \begin{cases} X_i^{//g}, \text{ if } f\left(X_i^{//g}\right) \leq f\left(X_i^g\right) \\ \qquad\qquad\qquad\qquad , \ i \in N_P \\ X_i^g \ , \text{ otherwise} \end{cases} \tag{2.24}$$

The process is repeated until the maximum number of generations or no improvement is seen in the best individual after many generations.

2.2.6. Differential Evolution with Gaussian Mutation

As a relatively new member of EAs, DE is less known outside metaheuristic optimization area. Similar to other EAs, DE relies likewise on the initial population, mutation, crossover and selection to problem search space through iterative progress until the terminate criteria is met. The key parameters of control in differential evolution with Gaussian mutation (DEGM) are population size and crossover rate. The DEGM algorithm is described as follows:

2.2.6.1. Initialization

The initial population of N_P vectors is randomly selected based on uniform probability distribution for all variables to cover the entire search uniformly. Each individual X_i is a vector that contains as many parameters as the problem decision variables D. Random value is assigned to each decision parameter in every vector according to:

$$X_{ij}^0 \sim U\left(X_j^{\min}, X_j^{\max}\right) \tag{2.25}$$

where $i = 1,\ldots, N_P$ and $j = 1,\ldots, D$; $X_j^{\min}$ and $X_j^{\max}$ are the lower and upper bounds of the jth decision variable; $U\left(X_j^{\min}, X_j^{\max}\right)$ denotes a uniform random variable

ranging over $\left[X_j^{\min}, X_j^{\max}\right]$; X_{ij}^0 is the initial j th variable of i th population. All the vectors should satisfy the constraints. Evaluate the value of the cost function $f\left(X_i^0\right)$ of each vector.

2.2.6. 2. Mutation

DEGM generates new parameter vectors by adding a Gaussian random variable to the parent vector. For each parent vector X_i^g at g th generation the offspring vector $X_i^{/g}$ is obtained by

$$X_i^{/g} = X_i^g + N\left(0, \sigma_i^2\right), \qquad i \in N_P \tag{2.26}$$

where $N\left(0, \sigma_i^2\right)$ represents a Gaussian random variable with mean zero and standard deviation σ_i.

The standard deviation σ_i is given by the expression $\sigma_i = \dfrac{f\left(X_i\right)}{f_{\min}}$, (2.27)

where $f_{\min}$ is the minimum cost value among N_P vectors. $f\left(X_i\right)$ is the value of the objective function associated with the i th vector.

This Gaussian random variable controls the amount of perturbation added to the parent vector and aids the algorithm to escape from local optima. This maintains the diversity of the population throughout iterative process which guarantees a high probability of achieving the global optimum.

2.2.6. 3. Crossover

Perform crossover for each target vector X_i^g with its offspring vector $X_i^{/g}$ and create a trial vector $X_i^{//g}$ such that

$$X_i^{//g} = \begin{cases} X_i^{/g} \text{ , if } \rho \le C_R \\ \qquad\qquad , \quad i \in N_P \\ X_i^{g} \text{ , otherwise} \end{cases} \tag{2.28}$$

where ρ is an uniformly distributed random number within [0, 1]. The basic crossover process is a discrete recombination, which employs constant $C_R \in [0,1]$ to determine if the newly generated individual is to be recombined.

2.2.6. 4. Selection

Perform selection for each target vector, X_i^g by comparing its cost with that of the trial vector, $X_i^{//g}$. The vector that has lesser cost of the two would survive for the next generation.

$$X_i^{g+1} = \begin{cases} X_i^{//g} \text{ , if } f\left(X_i^{//g}\right) \le f\left(X_i^{g}\right) \\ \qquad\qquad , \ i \in N_P \\ X_i^{g} \text{ , otherwise} \end{cases} \tag{2.29}$$

The process is repeated until the maximum number of generations or no improvement is seen in the best individual after many generations.

2.2.7. Opposition-based Differential Evolution

2.2.7.1. Opposition-based learning

Opposition-based learning (OBL) was developed by Tizhoosh [25]-[27] to improve candidate solution by considering current population as well as its opposite population at the same time.

Evolutionary optimization methods start with some initial population and try to improve them toward some optimal solution. The process is started with random guesses. The process can be improved by starting with a closer i.e. fitter solution by simultaneously checking the opposite solution.

2.2.7.2. Definition of opposite point

Let $X = (x_1, x_2, ..., x_n)$ be a point in n - dimensional space where $x_i \in [lb_i, ub_i]$ and $i \in 1,2,...,n$. The opposite point $\overline{X} = (\overline{x_1}, \overline{x_2}, ..., \overline{x_n})$ is completely defined by its components as in (2.30).

$$\overline{x_i} = lb_i + ub_i - x_i \tag{2.30}$$

2.2.7.3. Opposition-based optimization

Let $X = (x_1, x_2, ..., x_n)$ be a point in n - dimensional space i.e. a candidate solution. Assume $f = (\bullet)$ is a fitness function which is used to measure the candidate's fitness. According to the definition of the opposite point, $\overline{X} = (\overline{x_1}, \overline{x_2}, ..., \overline{x_n})$ is the opposite of $X = (x_1, x_2, ..., x_n)$. Now, if $f(\overline{X}) < f(X)$ (for a minimization problem), then point X can be replaced with $\overline{X}$; otherwise, the process is continued with X. Hence, the point and its opposite point are evaluated simultaneously in order to continue with the fitter one.

In the present work, the concept of the opposition-based learning is incorporated in differential evolution. The original DE is chosen as a parent algorithm and the opposition-based ideas are embedded in DE. Figure 2.4 shows the flowchart of opposition-based differential evolution (ODE).

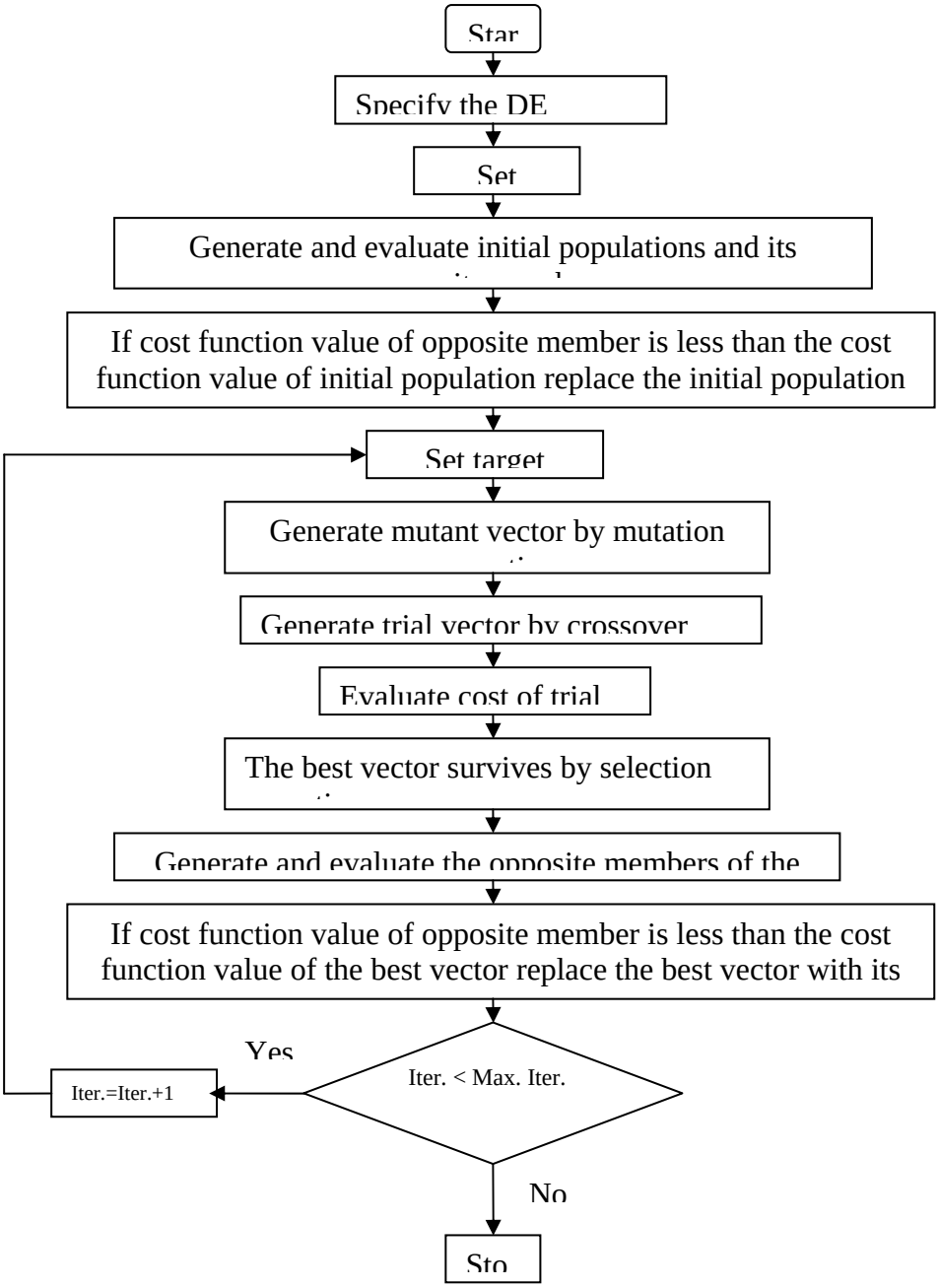

Fig.2.4. Flowchart of ODE.

2.3. Swarm intelligence

Swarm Intelligence (SI) is an innovative (novel or new) distributed intelligent paradigm (model) for solving optimization problems. It takes inspiration from the collective behavior of a group of social insect colonies and of other animal societies. SI is typically made up of a population of simple agents interacting locally with one

another and with their environment. These entities (creatures) with very limited individual capability can jointly (cooperatively) perform many complex tasks necessary for their survival. Although there is normally no centralized control structure dictating how individual agent should behave, local interactions between such agents often lead to the emergence of global and self-organized behavior.

Several optimization algorithms inspired by the metaphors (descriptions) of swarming behavior in nature are proposed. Ant colony optimization, particle swarm optimization, bacterial foraging algorithm, bee colony optimization, firefly algorithm and biogeography-based optimization are examples to this effect.

2.3.1. Particle Swarm optimization

Particle Swarm Optimization (PSO) was introduced in 1995 by James Kennedy and Russell Eberhart as a global optimization technique. It is a population-based self-adaptive stochastic search technique with reduced memory requirement. The PSO method is becoming very popular due to its simplicity of implementation and ability to quickly converge to a reasonably good solution.

The particle swarm optimization starts with the random initialization of a population of individuals called particles in the search space. Each particle is a candidate solution to the problem, and is represented by a velocity, a location in the search space and has a memory which helps it in remembering its previous best position. The PSO algorithm works on the social behavior of particles in the swarm. PSO finds the global best solution by simply adjusting the trajectory of each individual toward its own best location and toward the best particle of the entire swarm at each time step (generation).

PSO is motivated by social behavior of organisms such as fish schooling and bird flocking. In PSO, individuals called particles change their positions or states with time and fly around in a multidimensional search space. During flight, each particle adjusts its position according to its own experience, and the experience of neighboring particles, making use of the best position encountered by itself and its neighbors. The swarm (group or crowd or flock) direction of a particle is defined by the set of particles neighboring the particle and its historical experience.

Each particle moves based on its previous velocity, the particle’s location at which the best fitness so far has been achieved, and the population global location at which the

best fitness so far has been achieved. The particles have tendencies to move toward better search areas over the course of a search process.

In the multidimensional space where the optimal solution is sought, each particle in the swarm is moved toward the optimal point by adding a velocity with its position. The velocity of a particle is influenced by three components, namely, inertial, cognitive and social. The inertial component simulates the inertial behavior of the bird to fly in the previous direction. The cognitive component models the memory of the bird about its previous best position and the social component models the memory of the bird about the best position among the particles. The particles move around the multidimensional search space until they find the food i.e. optimal solution.

After each iteration the new velocity and hence the new position of each particle are updated on the basis of a summated influence of each particle's present velocity, distance of the particle from its own best performance, achieve so far during the search process and the distance of the particle from the leading particle, i.e. the particle which at present is globally the best particle producing till now the best performance.

Let x and v denote a particle's position and its corresponding velocity in a search space, respectively. Therefore, the i th particle is represented as $x_i = (x_{i1}, x_{i2}, ..., x_{id})$ in the d dimensional space. The best previous position of the i th particle is recorded and represented as $pbest_i = (pbest_{i1}, pbest_{i2}, ..., pbest_{id})$. The index for the particle among all the particles in the group is represented by the $gbest_d$. The velocity for the particle i th particle is represented as $v_i = (v_{i1}, v_{i2}, ..., v_{id})$. The modified velocity and position of each particle can be calculated using the current velocity and the distance from $pbest_{id}$ to $gbest_d$ as shown in the following formulae:

$$v_{id}^{(k+1)} = w * v_{id}^{(k)} + c_1 * rand(\ ) * (pbest_{id} - x_{id}^k) + c_2 * rand(\ ) * (gbest_d - x_{id}^k) \qquad (2.31)$$

$$x_{id}^{(k+1)} = x_{id}^k + v_{id}^{(k+1)}\ ,\ i = 1,2,..., \mathrm{N_P},\ d = 1,2,..., \mathrm{N}_g \qquad (2.32)$$

where

$\mathrm{N_P}$: number of particles in the swarm;

N_g : number of members in a particle;

k : pointer of iterations;

w : inertia weight factor;

c_1, c_2 : acceleration constant;

$rand(\ )$: uniform random value in the range [0,1];

$v_i^{(k)}$: velocity of a particle i at iteration k, $v_d^{\min} \le v_{id}^k \le v_d^{\max}$;

x_i^k : current position of a particle i at iteration k;

In the above procedures, the parameter $v^{\max}$ determines the resolution, with which regions are to be searched between the present position and the target position. If $v^{\max}$ is too high, particles might fly past good solutions. If $v^{\max}$ is too small, particles may not explore sufficiently beyond local solutions.

The constants c_1 and c_2 represent the weights of the stochastic acceleration terms. Constant c_1 pulls the particle towards local best position (*pbest*) whereas c_2 pulls it towards the global best position (*gbest*). Low values allow particle to roam far from the target regions before being tugged back. On the other hand, high values result in abrupt movement toward or past target regions. Hence, the acceleration constants c_1 and c_2 are often set to be 2.0 according to past experiences.

Suitable selection of inertia weight w provides a balance between global exploration and local exploitation thus requiring less number of iterations to find a sufficiently optimal solution. A larger inertial weight is used during initial exploration and its value is gradually reduced as the search proceeds. As originally developed, w often decreases linearly from about 0.3 to –0.2 during a run. In general, the inertia weight w is set according to the following equation:

$$w = w_{\max} - \frac{w_{\max} - w_{\min}}{iter_{\max}} \times iter \qquad (2.33)$$

where $iter_{\max}$ is the maximum number of iterations and $iter$ is the current number of iterations.

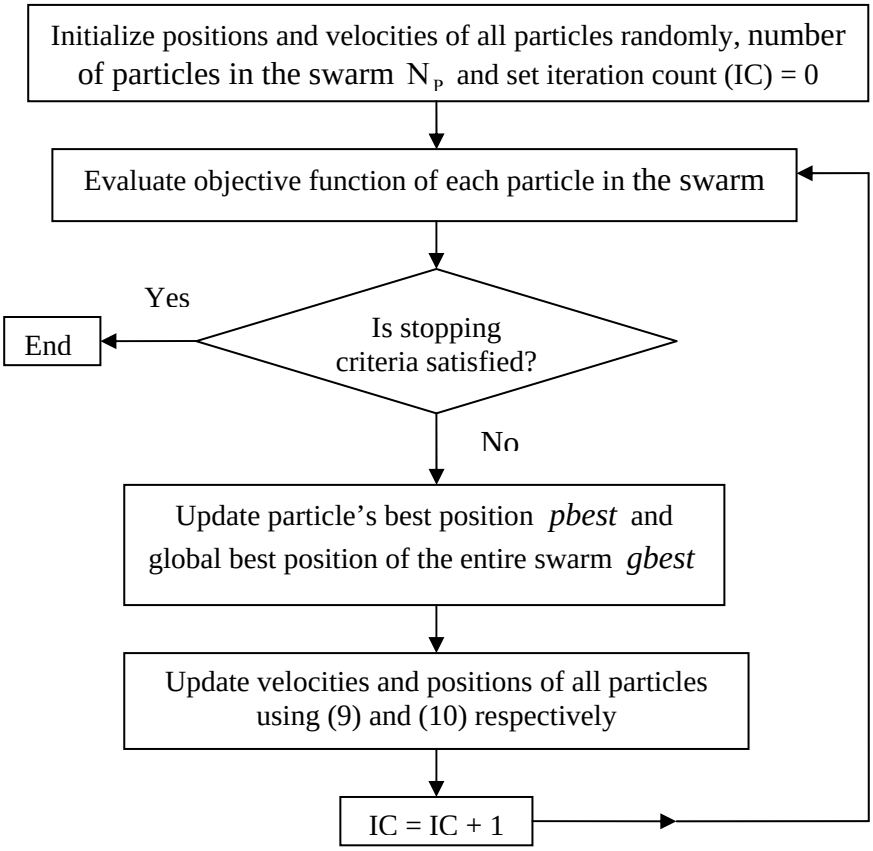

Fig. 2.5. Flowchart of particle swarm optimization.

2.3.2. Group Search Optimization

Group search optimization (GSO) is a population based optimization algorithm which is inspired by animal searching behavior and group living theory. The framework is based on the producer-scrounger (PS) model which assumes that group members search either for 'finding' or for joining opportunities. Based on this framework, concepts from animal scanning mechanisms are employed metaphorically for designing an optimum searching strategy in order to solve continuous optimization problems.

The population of the GSO algorithm is called a group and each individual in the population is called a member. During each iteration, a member is defined by its position and head angle. In n-dimensional search space, the ith member of the GSO at the kth searching iteration has a current position $X_i^k \in R^n$ and a head angle $\phi_i^k = \left(\phi_{i1}^k,...,\phi_{i(n-1)}^k\right) \in R^{n-1}$. The search direction of the ith member, $D_i^k\left(\phi_i^k\right) = \left(d_{i1}^k,....,d_{in}^k\right) \in R^n$ that can be calculated from ϕ_i^k via polar to Cartesian coordinate transformation [15]

$$d_{i1}^{k} = \prod_{q=1}^{n-1} \cos\left(\phi_{iq}^{k}\right)$$

$$d_{ij}^{k} = \sin\left(\phi_{i(j-1)}^{k}\right) \prod_{q=j}^{n-1} \cos\left(\phi_{iq}^{k}\right) \qquad j = 2,....,(n-1) \tag{2.34}$$

$$d_{in}^{k} = \sin\left(\phi_{i(n-1)}^{k}\right)$$

GSO algorithm consists of three kinds of members, i.e., producers and scroungers whose behavior are based on the PS model; and rangers who perform random walk. For convenience of computation, it is assumed that there is only one producer at each iteration and the remaining members are scroungers and rangers. Here, simplest joining policy is used where all scroungers will join the resource found by the producer. In optimization problems, unknown optima can be taken as open patches randomly distributed in a search space. Group members therefore search for the patches by moving over the search space. It is also assumed that the producer and the scroungers do not differ in their relevant phenotypic characteristics. Therefore, they can switch between the two roles [16].

At each iteration, a group member, which is located in the most promising area and adopts animal scanning to seek the optimal resource and conferred the best fitness value, is chosen as the producer. A number of group members except the producer are randomly selected as scroungers and then the rest of members are rangers. Scroungers perform area copying to join the resource found by the producer and do local searching around it. Rangers employ ranging behavior by random walk in the searching space to increase the chance of GSO to escape local optima.

Producer by its vision ability scans the search space for the better states. Vision ability is the ability of testing some points around the producer current position. The producer scans three points around its position in certain distances and head angles.

At the k th iteration, the producer behaves as follows:

1) The producer scans at zero degree and tests three points toward its position using equations (2.35-2.37).

$$\mathrm{X}_z = \mathrm{X}_\mathrm{P}^k + r_1 l_{\max} D_p^k\left(\phi^k\right) \tag{2.35}$$

$$\mathrm{X}_r = \mathrm{X}_\mathrm{P}^k + r_1 l_{\max} D_\mathrm{P}^k\left(\phi^k + \frac{r_2\theta_{\max}}{2}\right) \tag{2.36}$$

$$\mathrm{X}_l = \mathrm{X}_\mathrm{P}^k + r_1 l_{\max} D_\mathrm{P}^k\left(\phi^k - \frac{r_2\theta_{\max}}{2}\right) \tag{2.37}$$

Where X_P is position of the producer, r_1 is a normally distributed random number with mean 0 and standard deviation 1 and r_2 is a uniformly distributed random number in the range of (0, 1), $l_{\max}$ is maximum pursuit distance and $\theta_{\max}$ is maximum pursuit angle.

2) The producer will then find the best point. If the best point has a better value in comparison with its current position.The producer will fly to that point. If not, it will stay in its current position and turn its head using (2.38).

$$\phi^{k+1} = \phi^k + r_2\alpha_{\max} \tag{2.38}$$

where , $\alpha_{\max} \in R^1$ is the maximum turning angle.

3) If the producer cannot find a better area after a iterations, it will turn its head back to zero degree as follows:

$$\phi^{k+a} = \phi^k \tag{2.39}$$

where, $a \in R^1$ is a constant.

During each iteration, some of group members are selected as scroungers. The scroungers will keep searching for opportunities to join the resources found by the producer. At the k th iteration, the area copying behavior of the i th scrounger can be modeled as a random walk toward the producer using (2.40)

$$\mathrm{X}_i^{k+1} = \mathrm{X}_i^k + r_3 \circ \left(\mathrm{X}_\mathrm{P}^k - \mathrm{X}_i^k\right) \tag{2.40}$$

where X_i^k is the position of the i th scrounger at the k th iteration; r_3 is a uniform random number in the range of (0,1). Operator "$\circ$" is the Hadamard product or the Schur product, which calculates the entry-wise product of the two vectors.

At each iteration, some of group members are selected as rangers. Rangers are dispersed from their positions and they randomly walk at search space. At the k th iteration, a ranger generates a random head angle ϕ_i using (2.38), and then it chooses a random distance using (2.41) and move to the new point using (2.42).

$$l_i = br_1 l_{\max} \tag{2.41}$$

$$\mathrm{X}_i^{k+1} = \mathrm{X}_i^k + l_i D_i^k \left(\phi^{k+1}\right) \tag{2.42}$$

where b is a constant and r_1 is a normally distributed random number with mean 0 and standard deviation 1.

Parameter setting

The initial population of GSO is generated uniformly at random in the search space. The initial head angle ϕ^0 of each individual is set to be $(\Pi/4,....,\Pi/4)$. The constant a is given by $round\left(\sqrt{n+1}\right)$ where n is the dimension of the search space. The maximum pursuit angle $\theta_{\max}$ is Π/a^2 . The maximum turning angle $\alpha_{\max}$ is set to be $\theta_{\max}/2$. The maximum pursuit distance $l_{\max}$ is calculated from the following equation.

$$l_{\max} = \sqrt{\sum_{i=1}^{n} (U_i - L_i)^2} \tag{2.43}$$

where L_i and U_i are the lower and upper bounds for the i th dimension.

The most important control parameter that affects the search performance of GSO is the percentage of scroungers and rangers. In this paper scroungers are taken as 70% and rangers are taken as 30% of the total population.

Figure 2.6 shows the flowchart of GSO algorithm.

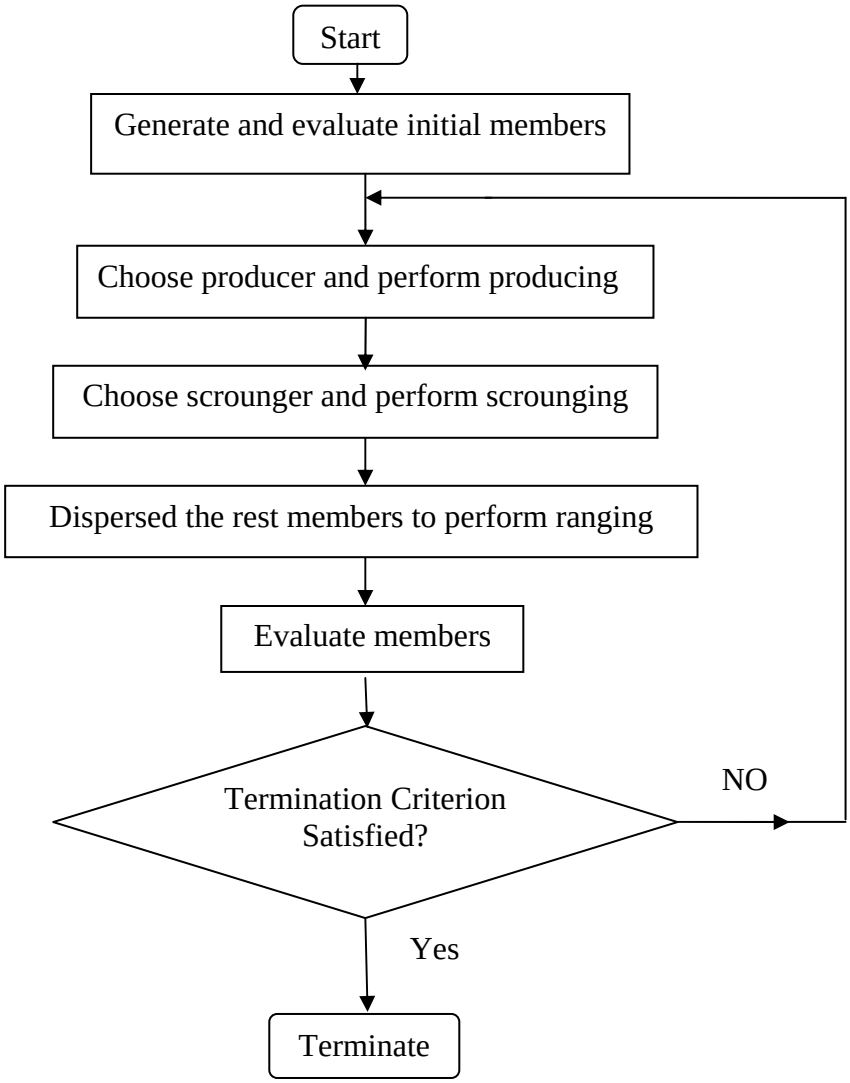

Fig. 2.6. Flowchart of the GSO algorithm

2.3.3. Opposition-based Group Search Optimization

2.3.3.1. Opposition-based learning

Opposition-based learning (OBL) was developed by Tizhoosh to improve candidate solution by considering current population as well as its opposite population at the same time.

Evolutionary optimization methods start with some initial population and try to improve them toward some optimal solution. The process of searching terminates when some predefined criteria are satisfied. The process is started with random guesses in the absence of a priori information about the solution. The process can be improved by starting with a closer i.e. fitter solution by simultaneously checking the

opposite solution. By doing this, the fitter one (guess or opposite guess) may be chosen as an initial solution. According to the theory of probability, 50% of the time, a guess is further from the solution than its opposite guess. Therefore, process starts with the closer of the two guesses. The same approach can be applied not only to the initial solution but also continuously to each solution in the current population.

2.3.3. 2. Definition of opposite number

If x be a real number between $[lb, ub]$, its opposite number is defined as

$$\bar{x} = lb + lu - x \tag{2.44}$$

Similarly, this definition can be extended to higher dimensions as stated in the next sub-section.

2.3.3. 3. Definition of opposite point

Let $X = (x_1, x_2, ..., x_n)$ be a point in n- dimensional space where $x_i \in [lb_i, ub_i]$ and $i \in 1,2,..., n$. The opposite point $\overline{X} = (\overline{x_1}, \overline{x_2}, ..., \overline{x_n})$ is completely defined by its components as in (2.45).

$$\overline{x_i} = lb_i + ub_i - x_i \tag{2.45}$$

By employing the definition of opposite point, the opposition-based optimization is defined in the following sub-section.

2.3.3.4. Opposition-based optimization

Let $X = (x_1, x_2, ..., x_n)$ be a point in n- dimensional space i.e. a candidate solution. Assume $f = (\bullet)$ is a fitness function which is used to measure the candidate's fitness. According to the definition of the opposite point, $\overline{X} = (\overline{x_1}, \overline{x_2}, ..., \overline{x_n})$ is the opposite of $X = (x_1, x_2, ..., x_n)$. Now, if $f(\overline{X}) < f(X)$ (for a minimization problem), then point X can be replaced with $\overline{X}$; otherwise, the process is continued with X.

Hence, the point and its opposite point are evaluated simultaneously in order to continue with the fitter one.

2.3.3.5. Opposition-based Group Search Optimization

In the present work, the concept of the opposition-based learning is incorporated in group search optimization method. The original GSO is chosen as a parent algorithm and the opposition-based ideas are embedded in GSO. Figure 2.7 shows the flowchart of opposition-based group search optimization (OGSO).

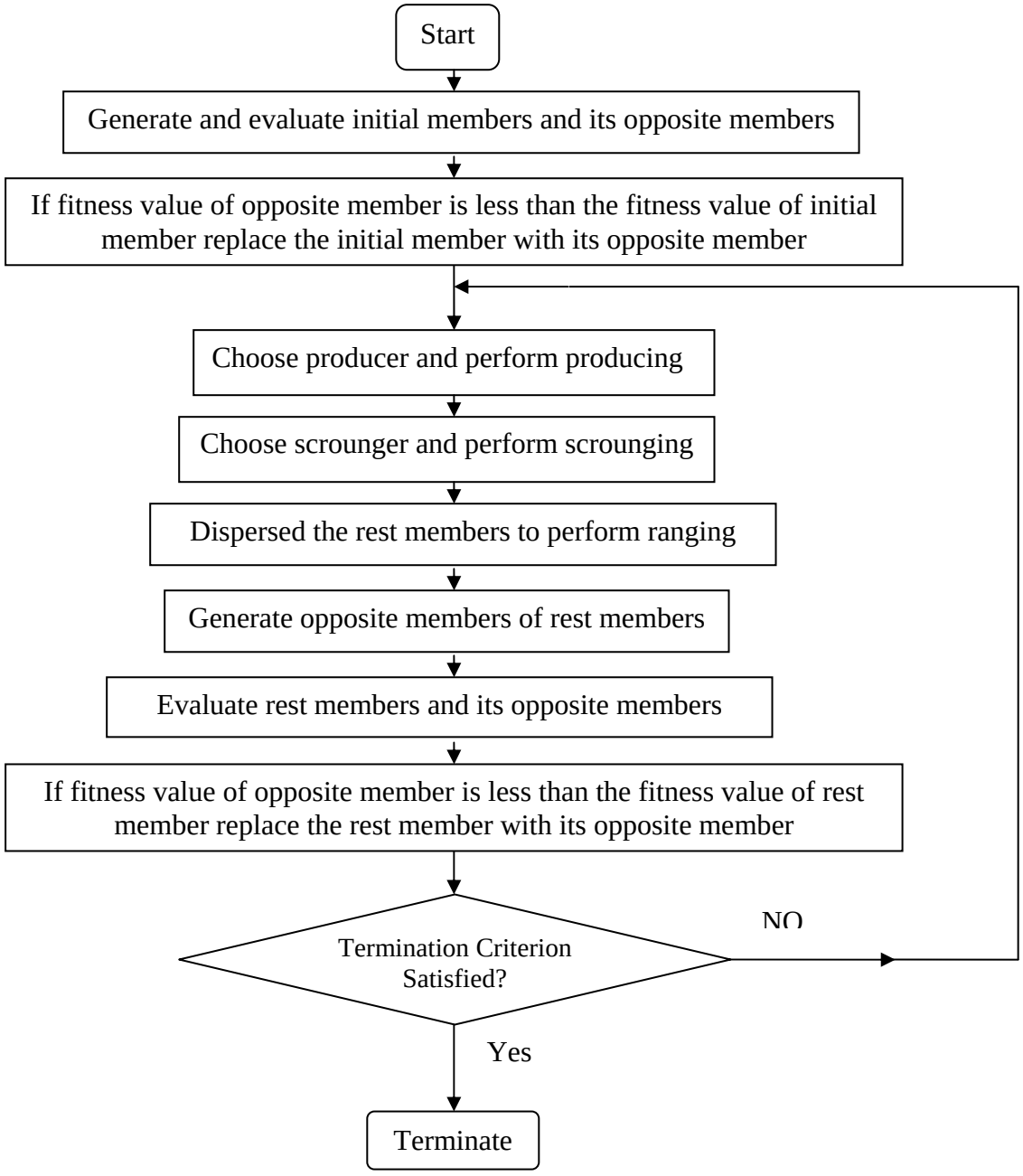

Fig. 2.7. Flowchart of the OGSO algorithm.

2.4. Principle of Multi-objective Optimization

Most of the real-world problems involve simultaneous optimization of several objective functions which are not commensurable and often competing and conflicting. Multi-objective optimization having such objective functions gives rise to a set of optimal solutions, instead of one optimal solution because no solution can be considered to be better than any other with respect to all objectives. These optimal solutions are known as pareto-optimal solutions.

Generally, multi-objective optimization problem consisting of a number of objectives and several equality and inequality constraints can be formulated as follows:

$$\text{Minimize} \quad f_i(x) \quad i = 1,\ldots..,\ \mathrm{N_{obj}} \tag{2.46}$$

$$\text{Subject to} \quad \begin{cases} g_k(x) = 0 & k = 1,....,\mathrm{K} \\ h_l(x) \le 0 & l = 1,....,L \end{cases} \tag{2.47}$$

where f_i is the ith objective function; x is a decision vector that represents a solution ; and $\mathrm{N_{obj}}$ is the number of objectives.

2.4.1. Multi-objective Differential Evolution

Differential Evolution (DE) is a type of evolutionary algorithm for optimization problems over a continuous domain. DE is exceptionally simple, significantly faster and robust. The basic idea of DE is to adapt the search during the evolutionary process. At the start of the evolution, the perturbations are large since parent populations are far away from each other. As the evolutionary process matures, the population converges to a small region and the perturbations adaptively become small. As a result, the evolutionary algorithm performs a global exploratory search during the early stages of the evolutionary process and local exploitation during the mature stage of the search. In DE, the fittest offspring competes one-to-one with the corresponding parent which is different from other evolutionary algorithms. This one-to-one competition gives rise to faster convergence rate. In multi-objective differential

evolution (MODE), a pareto-based approach is introduced to implement the selection of the best individuals. Firstly, a population of size, N, is generated randomly and objective functions are evaluated. At a given generation of the evolutionary search, the population is sorted into several ranks based on non-domination. Secondly, DE operations are carried out over the individuals of the population. Trial vectors of size N are generated and objective functions are evaluated. Both the parent vectors and trial vectors are combined to form a population of size $2N$. Then, the ranking of the combined population is carried out followed by the crowding distance calculation. The best N individuals are selected based on their ranking and crowding distances. These individuals act as the parent vectors for the next generation. The algorithm of MODE can be described in the following steps:

Step1. Generate box, R, of size N. Parent vectors of size N is randomly generated and kept in R.

Step 2. Classify these vectors into fronts based on nondomination as follows:

a) Create new empty box $R^{/}$ of size N.
b) Compare each vector with all other vectors in R.
c) Start with $i = 1$.
d) If i th vector is not dominated by any other vector in R, keep i th vector in $R^{/}$ and go to (f).
e) If i th vector is dominated by any other vector in R, go to (f).
f) Increment i by one. If $i \leq N$, go to (d) otherwise go to (g).
g) $R^{/}$ now contains a sub-box (of size $\leq N$) of nondominated vectors, referred to as the first front or sub-box. Assign it a rank number equal to one ($I_{rank} = 1$).
h) Create subsequent fronts or sub-boxes of $R^{/}$ with the vectors remaining in R and assign these $I_{rank} = 2,3,....$ Finally, all N vectors are in $R^{/}$ into one or more fronts.

Step 3. To calculate the crowding distance, $I_{i,dist}$, for the i th vector in any front, F, of $R^{/}$, sort all the vectors in front, F, according to each objective function value in ascending order of magnitude. The crowding distance of the $_i$ th vector in its front F is the average side-length of the cuboid formed by using the nearest neighbors as the

vertices. Assign large values of crowding distance I_{dist} to the boundary vectors (vectors with smallest and largest function values).

The following procedure is adopted to identify the better of the two vectors. Vector i is better than vector j (i) if $I_{i,rank} < I_{j,rank}$ or (ii) if $I_{i,rank} = I_{j,rank}$ and $I_{i,dist} > I_{j,dist}$.

Step 4. Take a new empty box $R^{//}$ of size N. Perform DE operations over N vectors in $R^{/}$ to generate N trial vectors and store these vectors in $R^{//}$.

a) Select a target vector, i in $R^{/}$.

b) Start with $i = 1$.

c) Choose two vectors, r_1 and r_2 at random from the N vectors in $R^{/}$. Find the vector difference between these two vectors and multiply this difference with the scaling factor F_s to get the weighted difference.

d) Choose a third random vector r_3 from the N vectors in $R^{/}$ and add this vector to the weighted difference to obtain the noisy random vector.

e) Perform crossover between the target vector and noisy random vector to find the trial vector. This is carried out by generating a random number and if random number $> C_R$ (crossover factor), copy the target vector into the trial vector else copy the noisy random vector into the trial vector and put it in box $R^{//}$.

f) Increment i by one. If $i \leq N$, go to (c) otherwise go to Step 5.

Step 5. Copy all N parent vectors from $R^{/}$ and all N trial vectors from $R^{//}$ into box $R^{///}$. Box $R^{///}$ has $2N$ vectors.

a) Classify these $2N$ vectors into fronts based on non-domination and calculate the crowding distance of each vector. Take the best N vectors from Box $R^{///}$ and put into Box $R^{////}$.

This completes one generation. Stop if generation number is equal to maximum number of generations, else copy N vectors from Box $R^{////}$ to the starting box R and go to Step2.

Figure 2.8 shows the flowchart of multi-objective differential evolution.

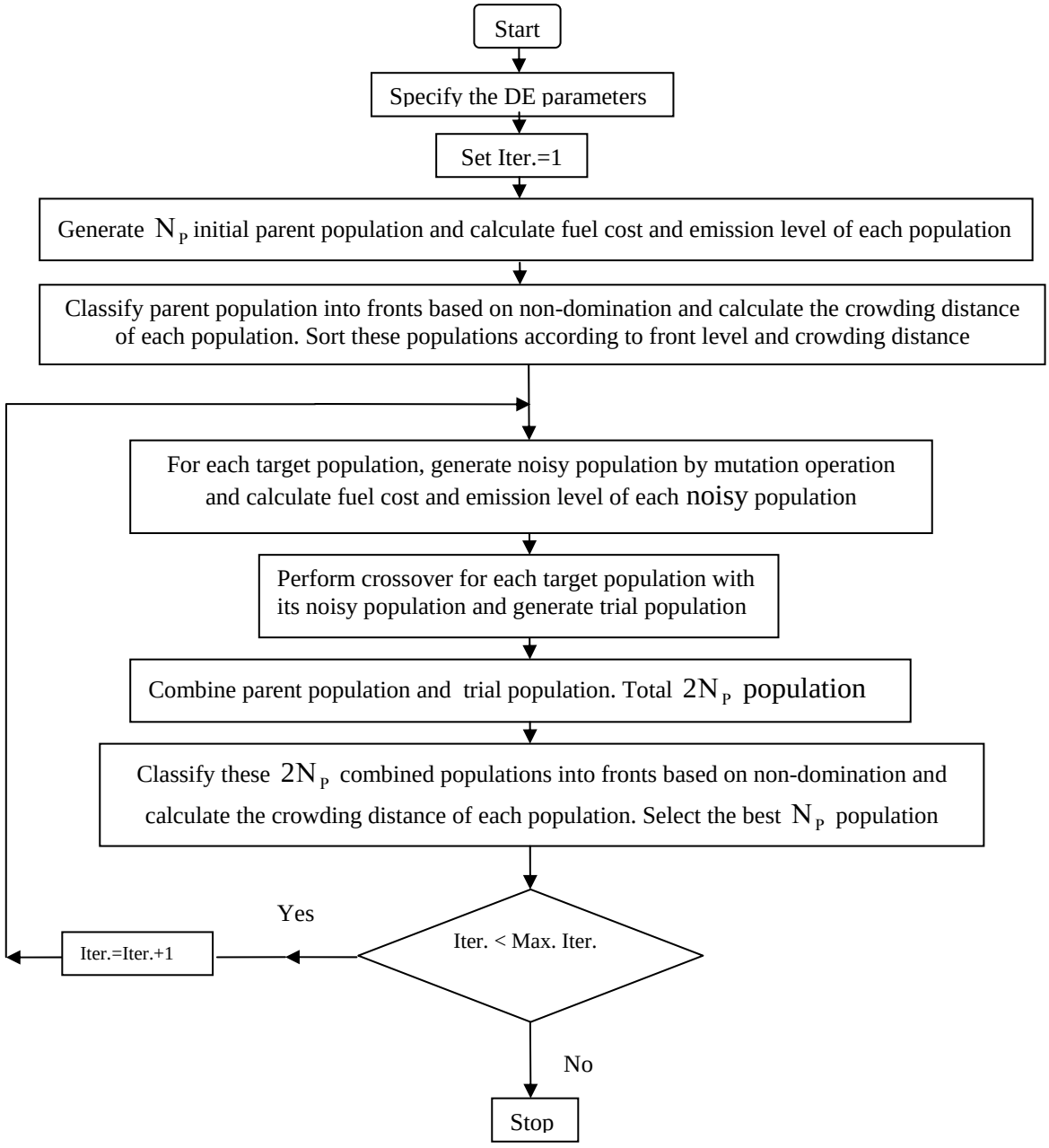

Fig. 2.8. Flowchart of Multi-objective Differential Evolution

2.4.2. Opposition-based Group Search Optimization

2.4.3. Best Compromise Solution

The best compromise solution is seen under an acceptability criterion, although an idea based on some kind of optimality should be more appropriate. The best solution is a good compromise which is accepted by the Decision Maker(DM) as the final solution. According to this definition, the concept of best compromise is relative to the set of solutions which is generated by the algorithm and depends on the effort dedicated by the DM to compare compromise solutions. Coello state the need of

selecting a compromise solution satisfying the objectives as ‘‘best” possible. Hakanan identify the best compromise as the compromise solution which is the most preferred one.

2.4.4. Fuzzy Sets

Fuzzy sets were first introduced by Zadeh as an effective means of solving nonprobabilistic problems. The different objectives are easily integrated because all the membership function values of these objectives are in the same range [0, 1]. It is assumed that the decision maker (DM) has imprecise or fuzzy goals for each of objective functions. The fuzzy goals are quantified by defining their corresponding membership functions. The DM then specifies the reference membership values for each of the objective functions and the corresponding optimal noninferior solution can be obtained. Through the interaction the DM’s reference membership values are updated by considering the current values of the membership functions as well as the objectives until a satisfactory solution for the DM is obtained.

2.4.4.1 Fuzzy Satisfying method

Considering the imprecise nature of the decision-maker’s judgment, it is natural to assume that the decision-maker may have fuzzy or imprecise goals for each of the objectives. The fuzzy sets are defined by equations called membership functions. The higher the value of the membership function implies a greater satisfaction with the solution. The membership function consists of lower and upper boundary values together with a strictly monotonically decreasing and continuous function. Fig. 2.9 illustrates the graph of the possible shape of a strictly monotonically decreasing membership function. The lower and upper bounds, $f_q^{\min}(\overline{X})$, $f_q^{\max}(\overline{X})$ of each of the

objective functions $f_q(\overline{X})$, $q = 1,2,....,n$ under given constraints are established to elicit a membership

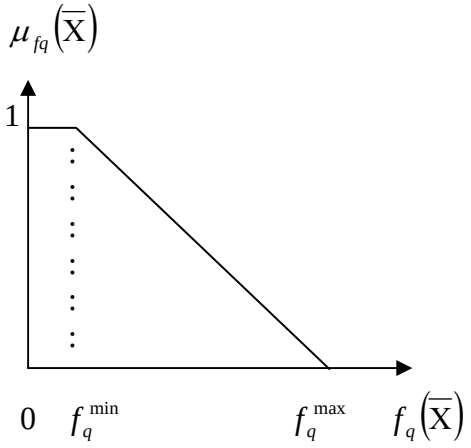

Fig. 2.9 The membership function.

function $\mu_{fq}(\overline{X})$ for each objective function $f_q(\overline{X})$. The DM is fully satisfied with the objective value $f_q(\overline{X})$ if $\mu_{fq}(\overline{X}) = 1$, and not satisfied at all if $\mu_{fq}(\overline{X}) = 0$. The qth membership function is now defined as:

$$\mu_{fq}(\overline{X}) = \begin{cases} 0, & \text{if } f_q(\overline{X}) \geq f_q^{\max} \\ \dfrac{f_q^{\max} - f_q(\overline{X})}{f_q^{\max} - f_q^{\min}} & \text{if } f_q^{\min} < f_q(\overline{X}) < f_q^{\max} \\ 1, & \text{if } f_q(\overline{X}) \leq f_q^{\min} \end{cases} \tag{2.48}$$

After defining the membership functions, the DM is asked to specify the reference (desirable) levels of achievement of the membership functions, called the reference membership values μ_{rq}, $q = 1,2,....,n$. Then to obtain the satisfying solution, the following minimax problem is solved.

$$\min_{X \in \Omega} \left\{ \max_{q=1,2,\ldots,n} \left| \mu_{rq} - \mu_{fq}(\overline{X}) \right| \right\} \tag{2.49}$$

where Ω : the set of noninferior solutions.

In this thesis the minimax problem is solved by using simulated annealing technique. If the DM is not satisfied with the current solution, then through the interaction, the reference membership values can be updated and the updating is done by considering the current values of the membership functions as well as the objectives. This interactive updating process is continued until the satisfactory solution for the DM is obtained.

CHAPTER 3

Economic Dispatch of Thermal Power Plants

3.1. Introduction

Economic dispatch (ED) is an important optimization task in power system operation for allocating generation among the committed generating units in the most economical manner while satisfying various physical constraints. The input-output characteristics or cost functions of a generator are approximated by using quadratic or piecewise quadratic functions, under the assumption that the incremental cost curves of the units are monotonically increasing piecewise-linear functions. However, real input-output characteristics show higher-order nonlinearities and discontinuities due to valve-point loading in fossil fuel fired generating plants. The valve-point loading effect has been modeled in as a recurring rectified sinusoidal function, such as the one shown in Fig. 3.1.

The discontinuous prohibited operating zones in the input-output performance curve for a typical thermal unit can be due to vibration in a shaft bearing caused by a steam valve or can be due to faults in the machines themselves or the associated auxiliary equipment, such as boilers, feed pumps etc. In practice, the shape of the input-output curve in the neighborhood of a prohibited zone is difficult to determine by actual performance testing. In actual operation, the best economy is achieved by avoiding operation in these areas. Cost function that takes into account prohibited operating zones, can be represented as in Fig. 3.2.

The valve-point loading, prohibited operating zones and other constraints turn the decision space into disjoint subsets, transforming the ED problem into a difficult non-smooth, non-convex optimization problem.

The calculus-based methods fail to address these types of problems. The dynamic programming (DP) approach imposes no restriction on the nature of the cost curves and can solve ED problems with non-smooth and discontinuous cost curves. However, this method suffers from the curse of dimensionality or local optimality.

Meta-heuristic algorithms are successfully applied to solve complex ED problems. Although these methods do not always guarantee global best solutions, they often achieve a fast and near global optimal solution.

Since the mid 1990s, many techniques originated from Darwin's natural evolution theory have emerged. These techniques are usually termed by "evolutionary computation methods" including evolutionary algorithms (EAs), swarm intelligence and artificial immune system. Differential evolution (DE), first proposed over 1995-1997 by Storn and Price at Berkeley is a novel approach to numerical optimization. It is a population-based stochastic parallel search evolutionary algorithm which is very simple yet powerful. DE modifies individuals by using differences of randomly sampled pairs of individual vectors from the population during its mutation process. But this mutation process is not appropriate for complex multimodal optimization. To overcome this drawback, this thesis proposes Gaussian mutation which maintains the diversity of the population, and guarantees a high probability of obtaining the global optimum.

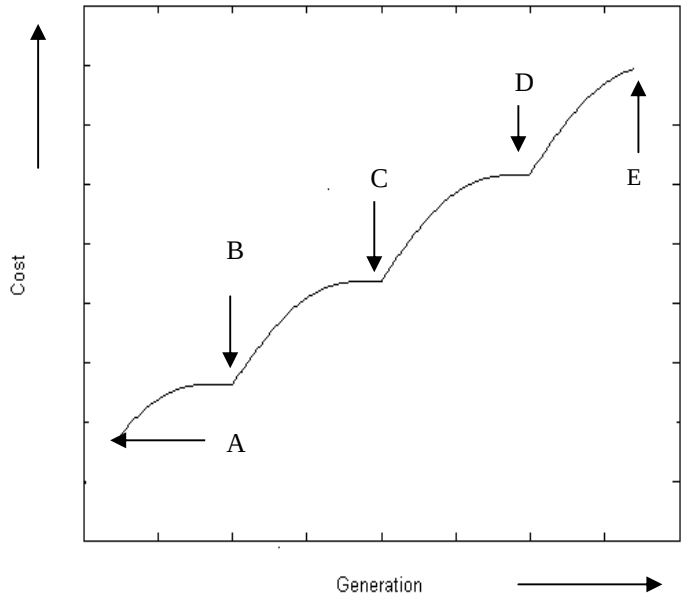

Fig. 3.1. Example of valve-point cost function with 5 valves;
A - Primary Valve, B - Secondary Valve, C - Tertiary Valve, D - Quaternary Valve, E - Quandary Valve

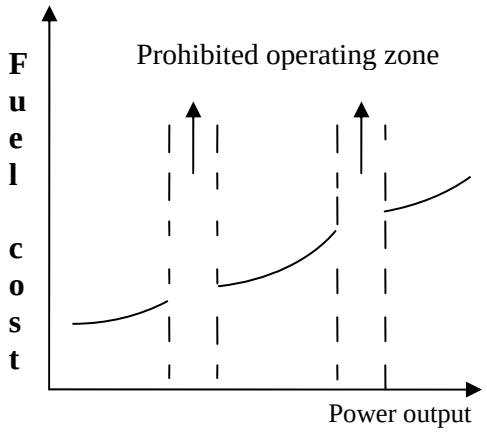

Fig. 3.2. Input-output curve with prohibited operating zones.

In this study, the differential evolution with Gaussian mutation (DEGM) is applied to solve the non-smooth/non-convex complex ED problems considering the various physical constraints. This thesis considers three types of non-smooth/non-convex ED problems. These are 1) ED with prohibited operating zones and transmission loss: 6-generator system, 2) ED with valve-point loading effect, prohibited operating zones and transmission loss: 40-generator system and 3) ED with valve-point loading effect and multi-fuel options without transmission loss: 10-generator systems. The performance of the proposed method has been compared with other previously developed stochastic optimization methods.

3.2. Problem Formulation

The objective of the ED is to minimize the total generation cost of a power system over some appropriate period while satisfying various constraints. The practical non-smooth/non-convex ED problem considers generator nonlinearities such as valve-point loading effects, prohibited operating zones and multi-fuel options along with system power demand, transmission loss and operational limit constraints.

3.2.1. Economic dispatch with prohibited operating zones and transmission loss

The ED problem can be described as a minimization problem with the objective:

$$\text{Min} \sum_{i=1}^{N} F_i(\mathrm{P}_i) = \sum_{i=1}^{N} a_i + b_i \mathrm{P}_i + c_i \mathrm{P}_i^2 \tag{3.1}$$

where $F_i(\mathrm{P}_i)$ is the fuel cost function of i th unit; a_i, b_i and c_i are the fuel cost coefficients of i th unit; N is the number of committed units; P_i is the power output of i th unit.

Subject to the following constraints

(i) Power balance constraint:

$$\sum_{i=1}^{\mathrm{N}} \mathrm{P}_i - \mathrm{P}_D - \mathrm{P}_L = 0 \tag{3.2}$$

The transmission loss P_L may be expressed by using B -coefficients as

$$\mathrm{P}_L = \sum_{i=1}^{\mathrm{N}} \sum_{j=1}^{\mathrm{N}} \mathrm{P}_i \mathrm{B}_{ij} \mathrm{P}_j + \sum_{i=1}^{\mathrm{N}} \mathrm{B}_{0i} \mathrm{P}_i + \mathrm{B}_{00} \tag{3.3}$$

where P_D is the system load demand. B_{ij}, B_{0i} and B_{00} are B -coefficients.

(ii) Generation capacity constraints

The power generated by each unit should be within its lower limit $\mathrm{P}_i^{\min}$ and upper limit $\mathrm{P}_i^{\max}$, so that

$$\mathrm{P}_i^{\min} \le \mathrm{P}_i \le \mathrm{P}_i^{\max} \qquad i \in \mathrm{N} \tag{3.4}$$

(iii) Prohibited operating zone

The feasible operating zones of a unit with prohibited operating zones can be described as follows:

$$\begin{aligned} &\mathrm{P}_i^{\min} \le \mathrm{P}_i \le \mathrm{P}_{i,1}^{l} \\ &\mathrm{P}_{i,j-1}^{u} \le \mathrm{P}_i \le \mathrm{P}_{i,j}^{l}, \quad j = 2,3,...,n_i \\ &\mathrm{P}_{i,n_i}^{u} \le \mathrm{P}_i \le \mathrm{P}_i^{\max}, \qquad i \in \mathrm{N} \end{aligned} \tag{3.5}$$

where j represents the number of prohibited operating zones of i th unit. $\mathrm{P}_{i,j-1}^{u}$ is the upper limit of $(j-1)$th prohibited operating zone of i th unit. $\mathrm{P}_{i,j}^{l}$ is the lower limit of

j th prohibited operating zone of i th unit. Total number of prohibited operating zone of i the unit is n_i.

3.2.2. Economic dispatch with valve-point loading effect, prohibited operating zones and transmission loss

The ED problem can be described as a minimization process with the objective:

$$\text{Min} \sum_{i=1}^{\text{N}} F_i(\text{P}_i) = \sum_{i=1}^{\text{N}} a_i + b_i \text{P}_i + c_i \text{P}_i^2 + \left| d_i \times \sin\left\{ e_i \times \left(\text{P}_i^{\min} - \text{P}_i \right) \right\} \right| \tag{3.6}$$

where d_i and e_i are the fuel cost coefficients of i th unit with valve-point effects.

The above objective function is to be minimized subject to constraints as mentioned in (3.2) - (3.5).

2.3. Economic dispatch with valve-point loading effect and multi-fuel options

Since generators are practically supplied with multi-fuel sources, each generator should be represented with several piecewise quadratic functions superimposed sine terms reflecting the valve-point effect and fuel type changes and the generator must identify the most economical fuel to burn. The fuel cost function of the i th generator with N_F fuel types is expressed as

$$F_i(\text{P}_i) = \alpha_{ij} + \beta_{ij} \text{P}_i + \gamma_{ij} \text{P}_i^2 + \left| \eta_{ij} \times \sin\left\{ \delta_{ij} \times \left(\text{P}_{ij}^{\min} - \text{P}_i \right) \right\} \right| \tag{3.7}$$

if $\text{P}_{ij}^{\min} \le \text{P}_i \le \text{P}_{ij}^{\max}$ for fuel type j and $j = 1,2,...,\text{N}_F$

where $\text{P}_{ij}^{\min}$ and $\text{P}_{ij}^{\max}$ are the minimum and maximum power generation limits of the i th unit with fuel type j ,respectively. α_{ij}, β_{ij}, γ_{ij}, η_{ij} and δ_{ij} are the fuel-cost coefficients of unit i for fuel j.

The problem can be described as minimization process with the objective:

$$\text{Min} \sum_{i=1}^{\text{N}} F_i(\text{P}_i) \tag{3.8}$$

The above objective function is to be minimized subject to constraints as mentioned in (3.2) and (3.4). Here transmission loss (P_L) is not considered.

3.3. Numerical Results

This section presents the computational results on three test systems which have been performed to evaluate the performance of the proposed DEGM method. ED problems for 6-, 10-, 40-unit power systems from the literature have been investigated. In order to simulate the valve-point effect of any generating unit, a recurring sinusoid component is added with the objective function of fuel cost. However, many practical constraints of generators, such as ramp rate limits, prohibited operating zones and power loss are considered in the optimization process. To verify the performance of the proposed method, these three test systems are repeatedly tested by the DEGM. The software has been written in MATLAB 7 on a PC (Pentium – IV, 80 GB, 3.0 GHZ).

Test System 1: A 6-generator system with prohibited operating zones, ramp rate limits and transmission loss is considered here. The input data are taken from [30]. The total load demand of the system is 1263 MW. The ED problem is solved by using DEGM. Here, the population size (N_P), crossover constant (C_R) and maximum iteration number have been selected 10, 1 and 50 ,respectively. The computational results of the best fuel cost, unit generations and power loss corresponding to the best fuel cost, average and the worst fuel cost, and average CPU time among 100 runs of solutions obtained from the proposed DEGM are summarized in Table 3.1. The results obtained from different PSO techniques i.e. SOH_PSO [43], NPSO-LRS [42], NPSO [42] and PSO [30] have also been shown in Table 3.1. The convergence characteristic of the 6-generator system in case of DEGM is shown in Fig. 3.3. The fuel cost found in this thesis by using DEGM is lower than those of all other methods reported in the literature.

Table 3.1: Results of 6-generator system

Unit Power (MW)	DEGM	SOH_PSO	NPSO-LRS	NPSO	PSO
P_1	447.1284	438.21	446.9600	447.4734	447.4970
P_2	173.0964	172.58	173.3944	173.1012	173.3221
P_3	263.1827	257.42	262.3436	262.6804	263.4745
P_4	139.5016	141.09	139.5120	139.4156	139.0594
P_5	165.7462	179.37	164.7089	165.3002	165.4761
P_6	86.7842	86.88	89.0162	87.9761	87.1280
Power Loss (MW)	12.4395	12.55	12.9361	12.9470	12.9584
Total generation (MW)	1275.4395	1275.55	1275.94	1275.95	1276.01
Best cost ($/h)	15443.08	15446.02	15450	15450	15450
Average cost ($/h)	15443.09	-	-	-	-
Worst cost ($/h)	15443.10	-	-	-	-
Average CPU time (s)	0.3281	0.0633	-	-	-

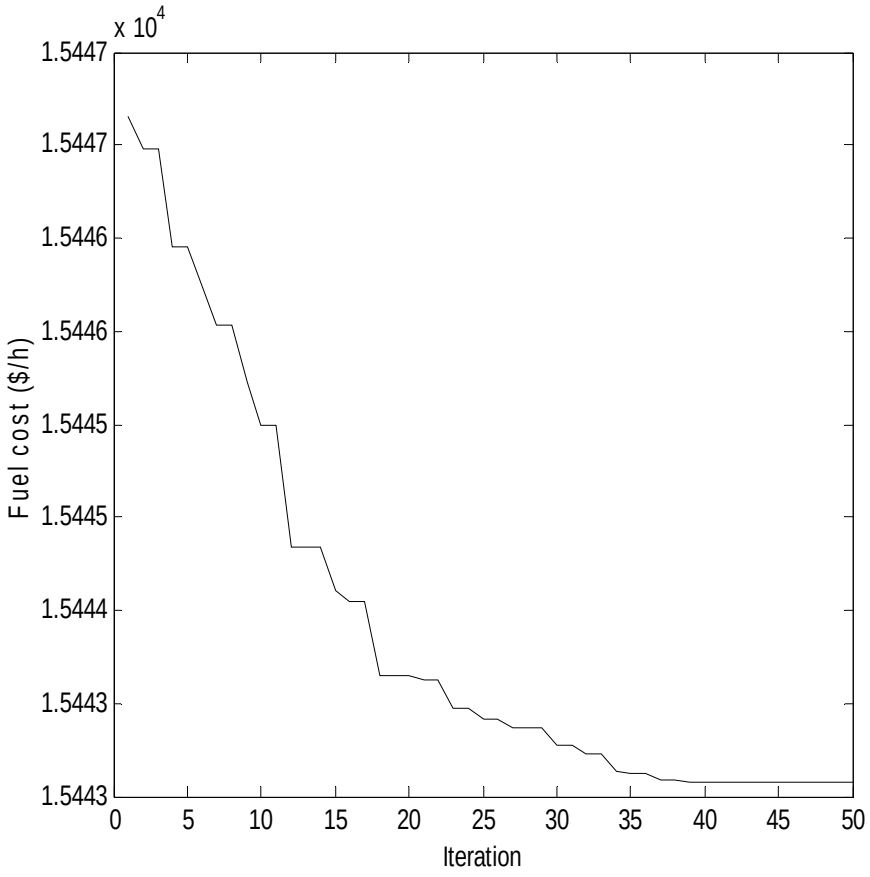

Fig. 3.3. Convergence characteristic of DEGM for the 6-generator system

Test System 2: This system consists of ten generating units with valve-point loading and multi-fuel sources. The input data are taken from [6]. The load demand is 2700

MW. Transmission loss, prohibited operating zones and ramp rate limits have not been considered here. The ED problem is solved by using DEGM. Here, the population size (N_P), crossover constant (C_R) and maximum iteration number have been selected 20, 1 and 300, respectively. The computational results of the best fuel cost, unit generations and power loss corresponding to the best fuel cost, average and worst fuel costs, and average CPU time among 100 runs of solutions obtained from proposed IPSO is shown in Table II. The results obtained from different PSO techniques [42] and different GA [34] methods are also summarized in Table 3.2. The convergence characteristic of the ten generator system in case of DEGM is depicted in Fig. 3.4. It is seen from Table 3.2 that the fuel cost found in this paper by using DEGM is the lowest among all other methods.

Table 3.2: Results of 10-generator system

Unit Power Output (MW)	DEGM		NPSO-LRS		NPSO		IGA_MU		CGA_MU	
				Fuel		Fuel		Fuel		Fuel
P_1	233.9161	2	223.33	2	220.657	2	219.126	2	222.0108	2
P_2	215.1414	1	212.19	1	211.785	1	211.164	1	211.6352	1
P_3	299.3166	1	276.21	1	280.402	1	280.657	1	283.9455	1
P_4	137.9084	1	239.41	3	238.601	3	238.477	3	237.8052	3
P_5	295.9636	1	274.64	1	277.562	1	276.417	1	280.4480	1
P_6	240.3314	3	239.79	3	239.120	3	240.467	3	236.0330	3
P_7	309.7218	1	285.53	1	292.139	1	287.739	1	292.0499	1
P_8	241.1571	3	240.63	3	239.153	3	240.761	3	241.9708	3
P_9	428.9392	3	429.26	3	426.114	3	429.337	3	424.2011	3
P_{10}	297.6044	1	278.95	1	274.463	1	275.851	1	269.9005	1
Best cost ($/h)	608.7234		624.1273		624.1624		624.5178		624.7193	
Average cost ($/h)	609.4653		-		-		-		-	
Worst cost ($/h)	610.8972		-		-		-		-	
Average CPU time (s)	2.8281		0.52		0.35		7.25		26.17	

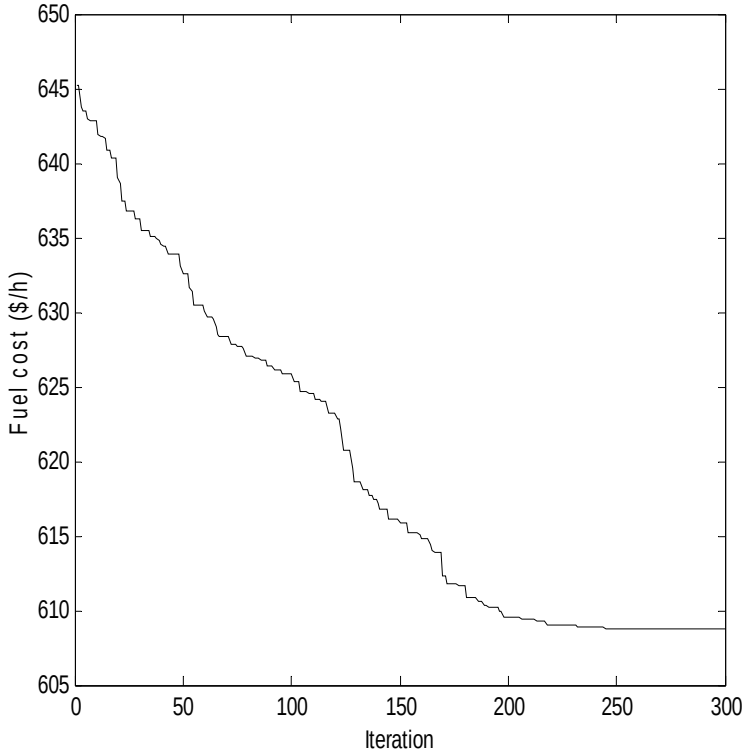

Fig. 3.4. Convergence characteristic of 10- generator system.

Test System 3: This system consists of a practical 40- units Taiwan power system [33], with modification to incorporate the valve-point effect [40]. The total load demand of the system is 10500 MW. Generator constraints including ramp rate limits of all the generators and prohibited operating zones from unit number 10 to 14 are taken from [45]. These prohibited zones result in four disjoint feasible sub-regions for each of the units. Hence, those zones result in a non-convex decision space which consists of 1024 convex sub-spaces for this system. The ED problem is solved by using DEGM. Here, the population size (N_P), crossover constant (C_R) and maximum iteration number have been selected 50, 1 and 500, respectively. The computational results of the best fuel cost, unit generations and power loss corresponding to best fuel cost, average and worst fuel cost, and average CPU time among 100 runs of solutions obtained from proposed DEGM, SHDE [45], HDE [45] and DE [45] are shown in Table 3.3. The convergence characteristic of the forty generator system in case of DEGM is shown in Fig. 3.5. The fuel cost found in this paper by using DEGM is lower than those of other methods reported in the literature.

Table 3.3: Results of 40-generator system

Output (MW)	DEGM	SHDE	HDE	DE	Output (MW)	DEGM	SHDE	HDE	DE
P_1	110.8507	110.8469	113.9783	113.5764	P_{21}	523.2803	523.1869	524.4637	523.2794
P_2	110.8252	112.1565	114.0000	113.7926	P_{22}	523.2797	530.5903	526.8726	523.9855
P_3	119.9993	120.0000	98.53020	97.4058	P_{23}	523.2815	523.1463	524.7330	523.7207
P_4	179.7335	179.4657	182.8223	180.0051	P_{24}	523.2798	522.9946	523.2879	523.2843
P_5	88.0155	93.1712	91.9957	89.6192	P_{25}	523.2805	523.6739	524.1151	523.3065
P_6	139.9991	139.6558	139.1252	139.9999	P_{26}	523.2816	525.2442	523.2267	523.2793
P_7	299.9991	299.9904	299.2042	299.9999	P_{27}	10.0006	10.0000	10.1714	10.0000
P_8	284.6021	292.9315	285.6743	284.7046	P_{28}	10.0001	10.0271	10.0000	10.1671
P_9	284.6030	284.5741	296.1914	284.6111	P_{29}	10.0000	10.0000	10.6397	10.0000
P_{10}	130.0015	130.000	200.0000	130.0000	P_{30}	96.9977	89.0125	91.9425	91.1653
P_{11}	168.7995	94.0099	94.6673	94.2149	P_{31}	189.9990	188.8546	190.0000	189.9883
P_{12}	94.0003	94.000	169.3861	168.7940	P_{32}	189.9990	189.9981	187.2378	189.9996
P_{13}	214.7597	125.0000	125.0000	304.4362	P_{33}	189.9994	189.6139	190.0000	189.9956
P_{14}	394.2795	393.6505	394.5668	394.2793	P_{34}	164.8177	200.0000	165.6872	199.9996
P_{15}	394.2798	478.7679	484.7173	394.2793	P_{35}	199.9998	199.9993	200.0000	199.9997
P_{16}	394.2802	393.1025	304.5127	304.5195	P_{36}	164.8230	199.9172	174.8976	165.8468
P_{17}	489.2797	489.1105	491.3617	489.2794	P_{37}	109.9995	108.4430	110.0000	109.9999
P_{18}	489.2822	489.0735	489.4712	489.2793	P_{38}	109.9993	110.0000	109.9254	99.3086
P_{19}	511.2824	511.2153	511.4723	511.2793	P_{39}	109.9990	110.0000	109.8258	105.9249
P_{20}	511.2804	511.0469	511.5457	511.2982	P_{40}	511.2799	511.2681	512.1575	511.2793
Power Loss (MW)						117.7500	117.7404	117.4074	119.9064
Total generation (MW)						10617.75	10617.740	10617.407	10619.906
Best cost ($/h)						123100.00	123496.02	123598.76	125074.40
Average cost ($/h)						123126.50	124007.10	124210.34	127399.36
Worst cost ($/h						123175.90	124570.74	124855.80	129639.79
Average CPU time (s)						57.4632	16.86025	17.94273	29.31566

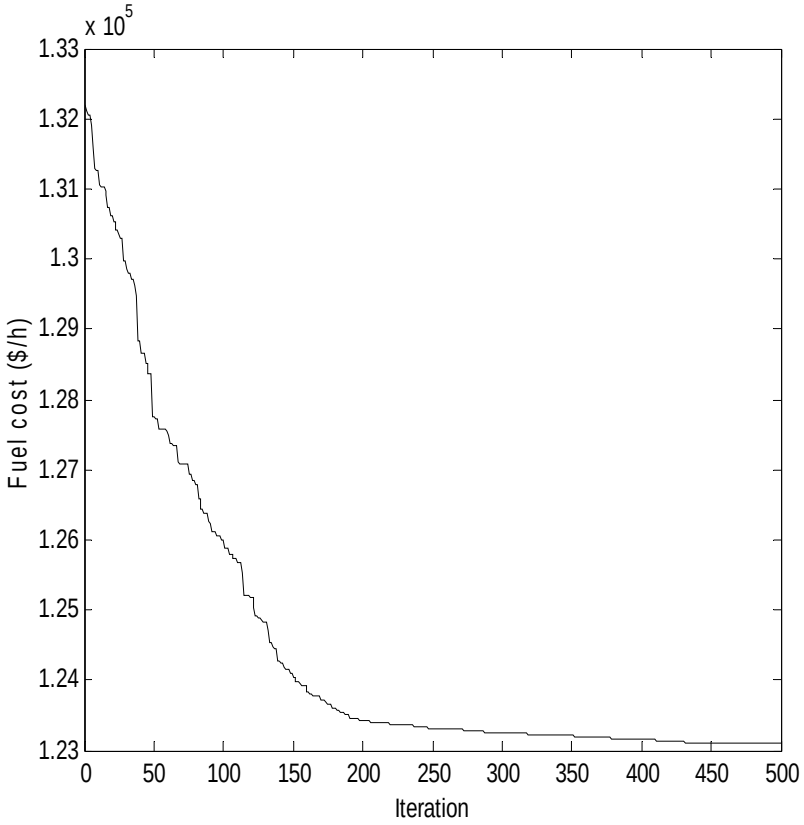

Fig. 3.5. Convergence characteristic of 40- generator system.

3.4. Conclusion

Here, the DEGM method has been developed and successfully implemented to solve the non-smooth /non-convex economic dispatch problem with the generator constraints. It has been observed that DEGM method has the ability to converge to a better quality solution and possesses good convergence characteristics and robustness. Many nonlinear characteristics of the generator such as prohibited operating zones, valve-point loadings, multi-fuel options, etc have been considered. It is clear from the results obtained by different trials that the proposed DEGM method can avoid the shortcoming of premature convergence exhibited by other optimization techniques. Due to these properties, the DEGM method in future can be tried for the solution of complex power system optimization problems.

CHAPTER 4

Combined Heat and Power Economic Dispatch

4.1. Introduction

The conversion of fossil fuel into electricity is not an efficient process. Even the energy efficiency of the most modern combined cycle plants is less than 60%. Most of the energy wasted in the conversion process is heat. But the fuel efficiency of combined heat and power generation unit can be as much as 90%. Also combined heat and power generation unit has less green house gas emission as compared with the other forms of energy supply. The principle of combined heat and power, known as cogeneration, is to recover and make beneficial use of this heat and as a result the overall efficiency of the conversion process is increased. Cogeneration units play an increasingly important role in the utility industry. For most cogeneration units, the heat production capacity depends on the power generation and vice versa. This introduces complexity due to the non-separable nature of electrical power and heat in the combined heat and power unit. The mutual dependencies of heat and power generation initiate a complication in the incorporation of cogeneration units into the power economic dispatch.

Non-linear optimization methods, such as dual and quadratic programming and gradient descent approaches, such as Lagrangian relaxation, have been applied for solving combined heat and power economic dispatch (CHPED). However, these methods cannot handle non-convex fuel cost functions of the generating units.

The advent of stochastic search algorithms has provided alternative approaches for solving CHPED problem. Since the mid 1990s, many techniques originated from Darwin's natural evolution theory have emerged. These techniques are usually termed by "evolutionary computation methods". Differential evolution (DE), a relatively new member in the family of evolutionary algorithms, first proposed over 1995-1997 by Storn and Price at Berkeley is a novel approach to numerical optimization. It is a population-based stochastic parallel search evolutionary algorithm which is very simple yet powerful. DE modifies individuals by using

differences of randomly sampled pairs of individual vectors from the population during its mutation process. But this mutation process is not appropriate for complex multimodal optimization. To overcome this drawback, this paper proposes Gaussian mutation which maintains the diversity of the population, and guarantees a high probability of obtaining the global optimum.

In this study, differential evolution with Gaussian mutation (DEGM) is applied to solve the complex non-smooth/non-convex combined heat and power economic dispatch (CHPED) problem considering the various constraints. Valve-point loading and prohibited zones of conventional thermal generators have been considered. Transmission loss is accounted through the use of loss coefficients. To illustrate the performance of the proposed method, four test systems are used. The test results are compared with those obtained by other evolutionary methods reported in the literature. It is found that the proposed DEGM based approach provides better solution.

4.2. Problem Formulation

The system under consideration has conventional thermal generating units, cogeneration units, and heat-only units. The feasible heat-power operation region i.e. heat-power dependency characteristics of a combined cycle co-generation unit is depicted in Fig.1. For the co-generation unit, the heat and power outputs are non-separable and one output will affect the other.

The heat-power feasible operation is enclosed by the boundary curve ABCDEF. Along the boundary curve BC, the heat capacity increases as the electric power generation decreases and the heat capacity declines along the curve CD. Along the boundary there is a trade-off between power generation and heat production from the unit. It can be seen that along the curve AB the unit reaches maximum output power. In contrast, the unit reaches maximum heat production along the curve CD. Therefore, power generation limits of the co-generation unit are the combined functions of the unit heat production and vice versa.

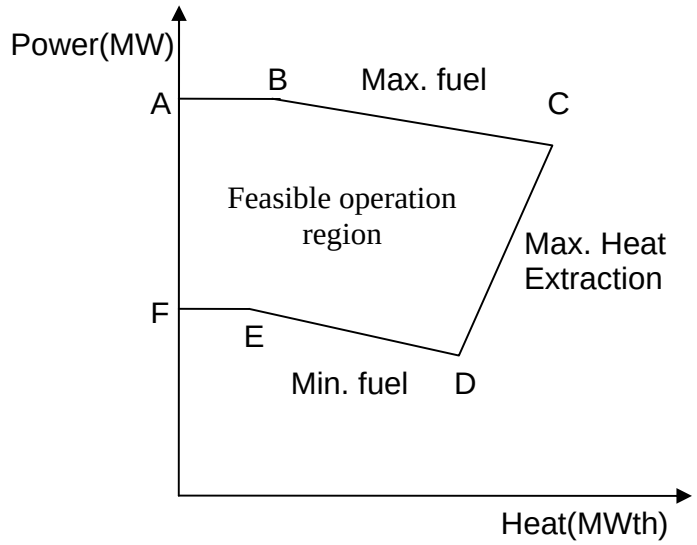

Fig. 4.1. Heat-Power Feasible Operation Region for a Cogeneration unit.

The power outputs of the conventional thermal generating units and the heat outputs of heat units are restricted by their own upper and lower limits. The power is generated by conventional thermal generating units and cogeneration units while the heat is generated by cogeneration units and heat-only units. The CHPED problem is to determine the unit power and heat production so that the system's production cost is minimized while the power demand and heat demand and other constraints are met. The objective function and constraints of CHPED problem are described as follows:

4.2.1. Objective

The cost function of conventional thermal generating unit is obtained from data points taken during "heat run" tests, when input and output data are measured as the unit is slowly run through its operating region. Wire drawing effects, occurring as each steam admission valve in a turbine starts to open, produce a rippling effect on the unit curve. In reality, a sharp increase in fuel loss is added to the fuel cost curve due to wire drawing effects when steam admission valve starts to open. This procedure is named as valve point effect. To model the effect of valve-points, a recurring rectified sinusoid contribution is added to the quadratic function such as the one shown in Fig. 3.1.

The total heat and power production cost can be expressed as

$$
\begin{aligned}
C_{\mathrm{T}} &= \sum_{i=1}^{\mathrm{N}_t} C_{ti}\left(\mathrm{P}_{ti}\right) + \sum_{i=1}^{\mathrm{N}_c} C_{ci}\left(\mathrm{P}_{ci}, \mathrm{H}_{ci}\right) + \sum_{i=1}^{\mathrm{N}_h} C_{hi}\left(\mathrm{H}_{hi}\right) \\
&= \sum_{i=1}^{\mathrm{N}_t} \left[a_i + b_i \mathrm{P}_{ti} + d_i \mathrm{P}_{ti}^2 + \left| e_i \sin\left\{ f_i \left(\mathrm{P}_{ti}^{\min} - \mathrm{P}_{ti} \right) \right\} \right| \right] \\
&+ \sum_{i=1}^{\mathrm{N}_c} \left[\alpha_i + \beta_i \mathrm{P}_{ci} + \gamma_i \mathrm{P}_{ci}^2 + \delta_i \mathrm{H}_{ci} + \varepsilon_i \mathrm{H}_{ci}^2 + \xi_i \mathrm{P}_{ci} \mathrm{H}_{ci} \right] + \sum_{i=1}^{\mathrm{N}_h} \left[\varphi_i + \eta_i \mathrm{H}_{hi} + \lambda_i \mathrm{H}_{hi}^2 \right]
\end{aligned}
\tag{4.1}
$$

where C_{T} is the total production cost; C_{ti}, C_{ci}, C_{hi} are the respective fuel characteristics of the conventional thermal generating units, cogeneration units and heat-only units. P_{ti} is the power output of ith conventional thermal generating unit. $\mathrm{P}_{ti}^{\min}$ and $\mathrm{P}_{ti}^{\max}$ are the ith conventional thermal generating unit power capacity limits. P_{ci} and H_{ci} are ,respectively, the power output and heat output of ith cogeneration unit. H_{hi} is the heat output of ith heat-only unit. N_t, N_c and N_h are the numbers of conventional thermal generating units, cogeneration units and heat-only units respectively, a_i, b_i, d_i, e_i, f_i are the cost coefficients of ith conventional thermal generating unit. $\alpha_i, \beta_i, \gamma_i, \delta_i, \varepsilon_i, \xi_i$ are the cost coefficients of ith cogeneration unit. $\varphi_i, \eta_i, \lambda_i$ are the cost coefficients of ith heat-only unit.

4.2.2. Constraints:

Two types of constraints i.e. equality and inequality constraints are considered. Equality constraints are the power and heat balance constraints that cover the total heat and power demands including power losses in the transmission lines. Inequality constraints are the capacity limits on heat and power generated by each unit and the prohibited operating zones of conventional thermal generating unit.

4.2.2.1. Power balance constraint

$$\sum_{i=1}^{N_t} P_{ti} + \sum_{i=1}^{N_c} P_{ci} = P_D + P_L \tag{4.2}$$

where P_D is the system power demand and P_L is the transmission loss.

Transmission loss is a function of power productions of all units. There are two approaches to calculate transmission loss, i.e. load flow approach and Kron's loss formula which is known as B-coefficient loss formula. Kron's loss formula is used in this work. The transmission loss P_L can be stated as follows

$$P_L = \sum_{i=1}^{N_t}\sum_{j=1}^{N_t} P_{ti} B_{ij} P_{tj} + \sum_{i=1}^{N_t}\sum_{j=1}^{N_c} P_{ti} B_{ij} P_{cj} + \sum_{i=1}^{N_c}\sum_{j=1}^{N_c} P_{ci} B_{ij} P_{cj} \tag{4.3}$$

4.2.2.2. Heat balance constraint

$$\sum_{i=1}^{N_c} H_{ci} + \sum_{i=1}^{N_h} H_{hi} = H_D \tag{4.4}$$

where H_D is the system heat demand. The heat demands are used within a short distance of cogeneration units and so the heat losses are negligible.

4.2.2.3. Capacity limits of conventional thermal generating units

$$P_{ti}^{\min} \le P_{ti} \le P_{ti}^{\max} \qquad i \in 1,2,...,N_t \tag{4.5}$$

4.2.2.4. Capacity limits of cogeneration units

The heat and power outputs of the cogeneration units are non-separable and one output will affect the other. $P_c^{\min}(H_c), P_c^{\max}(H_c)$, $H_c^{\min}(P_c)$ and $H_c^{\max}(P_c)$ are the linear inequalities that define the feasible operating region of the cogeneration units

$$P_{ci}^{\min}(H_{ci}) \le P_{ci} \le P_{ci}^{\max}(H_{ci}) \qquad i \in 1,2,...,N_c \tag{4.6}$$

$$H_{ci}^{\min}(P_{ci}) \le H_{ci} \le H_{ci}^{\max}(P_{ci}) \qquad i \in 1,2,...,N_c \tag{4.7}$$

4.2.2.5. Production limits of heat-only units

$$\mathrm{H}_{hi}^{\min} \le \mathrm{H}_{hi} \le \mathrm{H}_{hi}^{\max} \qquad i \in 1,2,...,\mathrm{N}_h \tag{4.8}$$

where $\mathrm{H}_{hi}^{\min}$ and $\mathrm{H}_{hi}^{\max}$ are heat production limits of the i th heat-only unit.

4.2.2.6. Prohibited operating zone

The prohibited operating zones in the input-output performance curve for a typical conventional thermal generating unit can be due to vibration in a shaft bearing caused by a steam valve or can be due to faults in the machines themselves or the associated auxiliary equipment, such as boilers, feed pumps etc. In practice, the shape of the input-output curve in the neighborhood of a prohibited zone is difficult to determine by actual performance testing. In actual operation, the best economy is achieved by avoiding operation in these areas. Cost function that takes into account prohibited operating zones, can be represented as in Fig. 3.2. Prohibited zones generate disjoint feasible sub-regions for each of the conventional thermal generating units. These zones make a non-convex decision space.

The feasible operating zones of a conventional thermal generating unit with prohibited operating zones can be described as follows:

$$\begin{aligned}
&\mathrm{P}_{ti}^{\min} \le \mathrm{P}_{ti} \le \mathrm{P}_{ti,1}^{l} \\
&\mathrm{P}_{ti,j-1}^{u} \le \mathrm{P}_{ti} \le \mathrm{P}_{ti,j}^{l}, \quad j = 2,3,...,n_i \\
&\mathrm{P}_{ti,n_i}^{u} \le \mathrm{P}_{ti} \le \mathrm{P}_{ti}^{\max}, \qquad i \in \mathrm{N}_t
\end{aligned} \tag{4.9}$$

where j represents the number of prohibited operating zones of i th conventional thermal generating unit. $\mathrm{P}_{ti,j-1}^{u}$ is the upper limit of $(j-1)$th prohibited operating zone of i th conventional thermal generating unit. $\mathrm{P}_{ti,j}^{l}$ is the lower limit of j th prohibited operating zone of i th conventional thermal generating unit. Total number of prohibited operating zones of i th conventional thermal generating unit is n_i.

4.2.3. Calculation of Slack Generator

In order to meet exactly the power balance constraint, a dependent unit should be selected. Due to the complex mutual dependencies of cogeneration units, the dependent unit is usually selected from the conventional thermal generating units. $(N_t + N_c)$ committed units deliver their power outputs subject to the power balance constraint (4.2) and the respective capacity constraints (4.5) and (4.6). Assuming the power loading of N_c cogeneration units and first $(N_t - 1)$ conventional thermal generating units are known, the power level of the N_t th conventional thermal generating unit (i.e. the slack generator) is given by

$$P_{tN_t} = P_D + P_L - \sum_{i=1}^{N_c} P_{ci} - \sum_{i=1}^{N_t-1} P_{ti} \qquad (4.1.0)$$

The transmission loss P_L is a function of all generator outputs including the slack generator and it is given by

$$P_L = \sum_{i=1}^{N_t}\sum_{j=1}^{N_t} P_{ti} B_{ij} P_{tj} + \sum_{i=1}^{N_t}\sum_{j=1}^{N_c} P_{ti} B_{ij} P_{cj} + \sum_{i=1}^{N_c}\sum_{j=1}^{N_c} P_{ci} B_{ij} P_{cj} \qquad (4.11)$$

Expanding and rearranging, (4.10) becomes

$$B_{N_tN_t} P_{tN_t}^2 + \left(2\sum_{i=1}^{N_t-1} B_{N_ti} P_{ti} + \sum_{i=1}^{N_c} B_{N_ti} P_{ci} - 1 \right) P_{tN_t} + \left(P_D + \sum_{i=1}^{N_t-1}\sum_{j=1}^{N_t-1} P_{ti} B_{ij} P_{tj} + \sum_{i=1}^{N_t-1}\sum_{j=1}^{N_c} P_{ti} B_{ij} P_{cj} \right.$$
$$\left. + \sum_{i=1}^{N_c}\sum_{j=1}^{N_c} P_{ci} B_{ij} P_{cj} - \sum_{i=1}^{N_t-1} P_{ti} - \sum_{i=1}^{N_c} P_{ci} \right) = 0 \qquad (4.12)$$

The loading of the slack generator (i.e. N_t th conventional thermal generating unit) can then be found by solving (4.12) using standard algebraic method.

4.3. Application of DEGM Method

The proposed DEGM is applied to four test systems. The computational results are used to compare the performance of the proposed DEGM based approach with that of other evolutionary

methods. The proposed DEGM and DE used in this paper are implemented by using MATLAB 7.0 on a PC (Pentium-IV, 80 GB, 3.0 GHz).

4.3.1. Test System 1

This **t**est system consists of one conventional thermal generator and two cogeneration units and a heat-only unit. Unit data have been taken from [62]. The power and heat demands of the test system are 250 MW and 115 MWth, respectively. Here, two cases are considered.

Case 1

Here, only valve point loading of conventional thermal generator has been considered. The problem is solved by using both DEGM and DE. Here, the population size (N_P), crossover rate (C_R) and the maximum iteration number (N_{max}) have been selected as 50, 1.0 and 100, respectively, for the test system under consideration.

The power and heat generations corresponding to the best cost obtained from the proposed DEGM and DE are shown in Table 4.1. The best, average and the worst costs and average CPU time among 100 runs of solutions obtained from the proposed DEGM and DE are summarized in Table 4.2. The cost obtained from classical PSO (CPSO) [62] and time varying acceleration coefficients PSO (TVAC-PSO) [13] are also shown in Table 4.2. The cost convergence characteristic obtained from the proposed DEGM and DE is shown in Fig. 4.1. It is seen from Table 4.2 that the cost found by using DEGM is the lowest among all other methods.

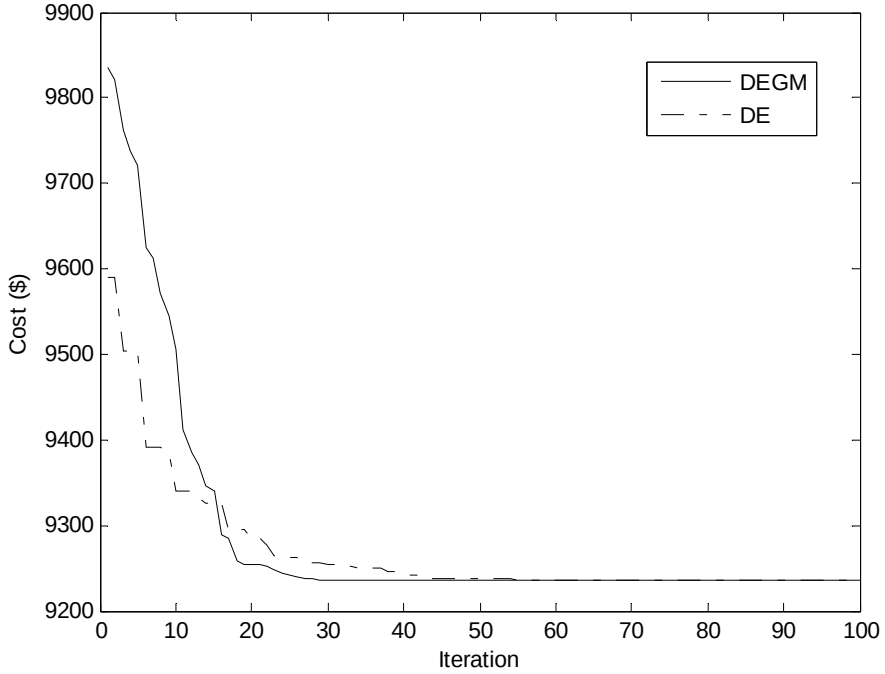

Fig. 4.1. Cost convergence characteristics for case 1 of test system 1.

Table 4.1: Power generation (MW) and heat generation (MWth) for Case 1 of Test System 1

	DEGM	DE
P_1	113.4014	113.3946
P_2	92.5986	92.5982
P_3	44.0000	44.0072
H_2	36.5216	36.5716
H_3	78.4784	78.3954
H_4	0	0.0330

Table 4.2: Comparison of performance for Case 1 of Test System 1

Techniques	DEGM	DE	TVAC-PSO	CPSO
Best cost ($)	9235.1032	9236.1437	9257.07	9257.08
Average cost ($)	9235.1110	9236.7422	-	-
Worst cost ($)	9235.1145	9237.0886	-	-
CPU time (s)	1.0827	1.0674	-	-

Case 2

Here, valve point loading of conventional thermal generator and prohibited operating zones of conventional thermal generator have been considered. The data of conventional thermal generator are same as in [62] except the following modifications in Table A.1. Table A.1 lists the prohibited zones of conventional thermal generator. These prohibited zones result in four disjoint feasible sub-regions for the conventional thermal generator. Hence, those zones result in a non-convex decision space which consists of four convex sub-spaces for this system.

The problem is solved by using both DEGM and DE. Here, the population size (N_P), crossover rate (C_R) and the maximum iteration number (N_{max}) have been selected as 50, 1.0 and 100, respectively, for the test system under consideration.

The power and heat generations corresponding to the best cost obtained from proposed DEGM and DE is summarized in Table 4.3. The best, average and the worst cost and average CPU time among 100 runs of solutions obtained from the proposed DEGM and DE are shown in Table 4.4. The cost convergence characteristic obtained from the proposed DEGM and DE is depicted in Fig. 4.2. It is seen from Table 4.4 that the cost found by using DEGM is the lower than that obtained from DE.

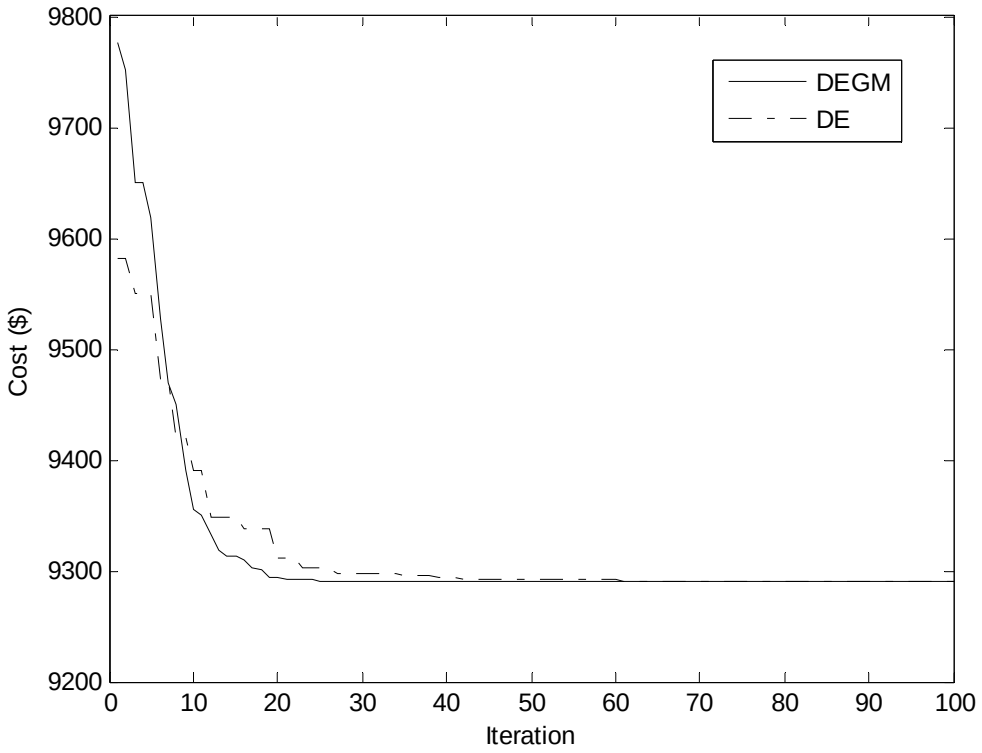

Fig. 4.2. Cost convergence characteristics for Case 2 of Test system 1

Table 4.3: Power generation (MW) and heat generation (MWth) for case 2 of Test System 1

	DEGM	DE
P_1	109.9997	109.9766
P_2	96.0003	96.0202
P_3	44.0000	44.0032
H_2	36.5188	36.5172
H_3	78.4812	78.4698
H_4	0	0.0130

Table 4.4: Comparison of performances of DE & DEGM for Case 2 of Test System 1

Techniques	DEGM	DE
Best cost ($)	9290.4804	9291.1375
Average cost ($)	9290.5331	9291.6290
Worst cost ($)	9290.5810	9292.4286
CPU time (s)	1.2403	1.2173

4.3.2. Test System 2

This system consists of four conventional thermal generators, two cogeneration units and a heat-only unit. Here, transmission loss is considered. Unit data are taken from [62]. The power and heat demands of this test system are 600 MW and 150 MWth, respectively. Here, two cases are considered.

Case 1

In this case , only valve point loading of conventional thermal generators has been considered. The problem is solved by using both DEGM and DE. Here, the population size (N_P), crossover rate (C_R) and the maximum iteration number (N_{max}) have been selected as 50, 1.0 and 100, respectively, for the test system under consideration.

The power and heat generations corresponding to the best cost obtained from the proposed DEGM and DE are shown in Table 4.5. The best, average and the worst costs and average CPU time among 100 runs of solutions obtained from proposed DEGM and DE are summarized in Table 4.6. The cost obtained from classical PSO (CPSO) [62], time varying acceleration coefficients PSO (TVAC-PSO) [13], teaching learning based optimization (TLBO) [63] and oppositional teaching learning based optimization (OBTLBO) [63] are also shown in Table 4.6. The cost convergence characteristics obtained from the proposed DEGM and DE are depicted in Fig. 4.3. It is seen from Table 11 that the cost found by using DEGM is the lowest among all other methods.

Table 4.6: Comparison of performances of the algorithms for Case 1 of Test System 2

Techniques	DEGM	DE	TVAC-PSO	CPSO	OBTLBO	TLBO
Best cost ($)	10094.2497	10094.3330	10100.3124	10325.3339	10094.3529	10094.8384
Average cost ($)	10094.2515	10094.3884	-	-	10099.4057	10114.1539
Worst cost ($)	10094.2612	10094.4545	-	-	10106.8314	10133.6130
CPU time (s)	2.1836	2.1795	-	-	3.06	2.86

Table 4.5: Power generation (MW) and heat generation (MWth) for Case 1 of Test System 2

	DEGM	DE
P_1	45.6710	45.6493
P_2	98.5403	98.5412
P_3	112.6738	112.6756
P_4	209.8170	209.8143
P_5	94.0477	94.0681
P_6	40.0000	40.0013
H_5	27.9800	27.8638
H_6	75.0000	74.9902
H_7	47.0200	47.1460
Ploss	0.7498	0.7498

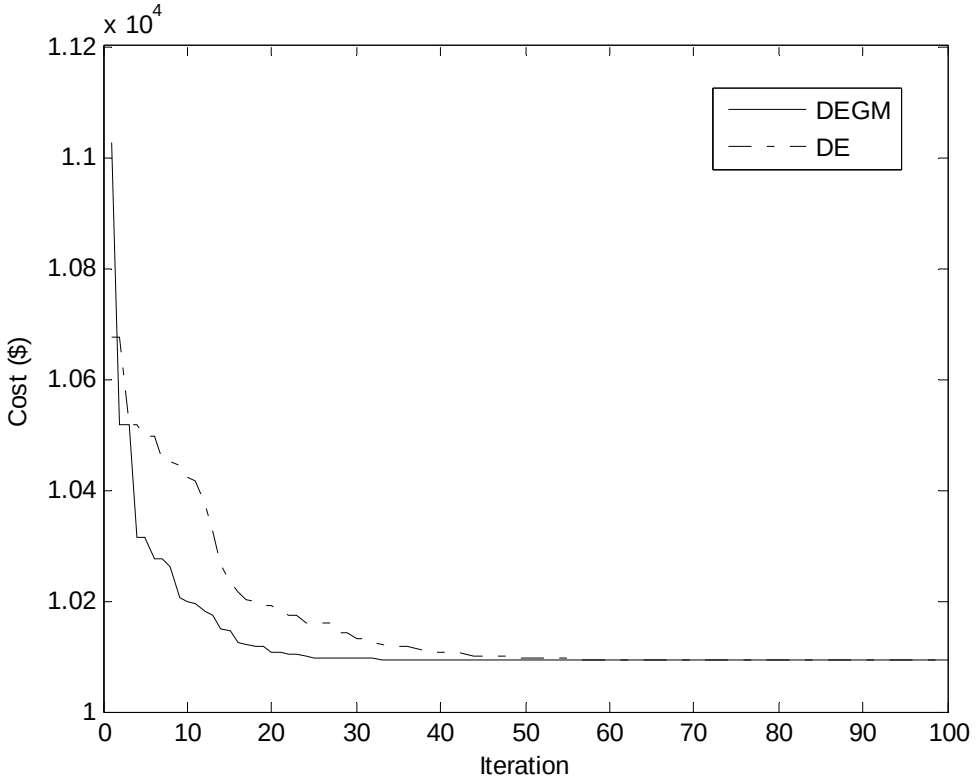

Fig. 4.3. Cost convergence characteristics of DE & DEGM for Case 1 of Test system 2

Case 2

Here, valve point loading of conventional thermal generators and prohibited operating zones of conventional thermal generators are considered. The data of conventional thermal generator are same as in [62] except the following modifications in Table A.2. Table A.2 lists the prohibited zones of conventional thermal generating units. These prohibited zones result in three disjoint feasible sub-regions for each of the conventional thermal generators. Hence, those zones result in a non-convex decision space which consists of 81 convex sub-spaces for this system.

The problem is solved by using both the DEGM and DE. Here, the population size (N_P), crossover rate (C_R) and the maximum iteration number (N_{max}) have been selected as 50, 1.0 and 100 ,respectively, for the test system under consideration.

The power and heat generations corresponding to the best cost obtained from proposed DEGM and DE is summarized in Table 4.7. The best, average and worst costs and average CPU time among 100 runs of solutions obtained from the proposed DEGM and DE are shown in Table 4.8. The cost convergence characteristics obtained from the proposed DEGM and DE are shown in Fig. 4.4.

Table 4.7: Power generation (MW) and heat generation (MWth) for Case 2 of Test System 2

	DEGM	DE
P_1	44.1139	44.1797
P_2	100.0001	100.0029
P_3	112.6736	112.6755
P_4	209.8159	209.8103
P_5	94.1462	94.0812
P_6	40.0001	40.0000
H_5	27.4001	27.7867
H_6	74.9998	74.9999
H_7	47.6001	47.2134
Ploss	0.7497	0.7496

Table 4.8: Comparison of performances of DE & DEGM for Case 2 of Test System 2

Techniques	DEGM	DE
Best cost ($)	10101.2995	10101.3772

Average cost ($)	10101.3487	10101.4128
Worst cost ($)	10101.3902	10101.4624
CPU time (s)	2.3176	2.2681

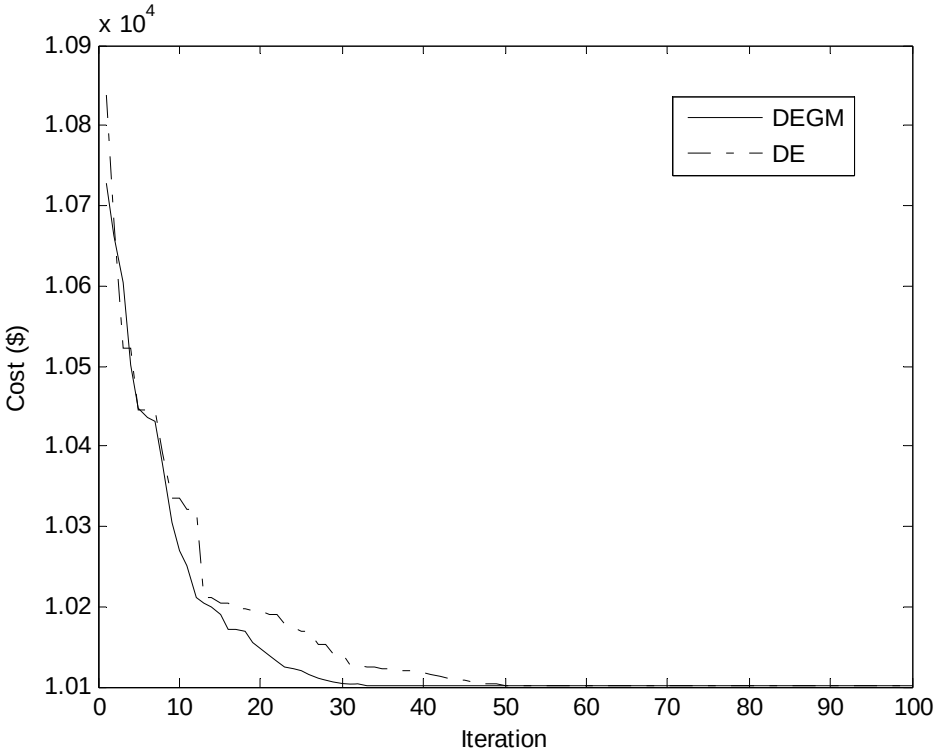

Fig. 4.4. Cost convergence characteristics of DE & DEGM for Case 2 of Test system 2

4.3.3. Test System 3

This system consists of thirteen conventional thermal generators, six cogeneration units and five heat-only units. Unit data are taken from [62]. The power and heat demands of the test system are 2350 MW and 1250 MWth, respectively. Here, two cases are considered.

Case 1

Here, only valve point loading of conventional thermal generators has been considered. The problem is solved by using both the DEGM and DE. Here, the population size (N_P), crossover rate (C_R) and the maximum iteration number (N_{max}) have been selected as 100, 1.0 and 200, respectively, for the test system under consideration.

The power and heat generations corresponding to best cost obtained from proposed DEGM and DE is shown in Table 4.9. The best, average and worst costs and average CPU time among 100 runs of solutions obtained from proposed DEGM and DE are summarized in Table 4.10. The cost obtained from classical PSO (CPSO) [62], time varying acceleration coefficients PSO (TVAC-PSO) [13], teaching learning based optimization (TLBO) [63] and oppositional teaching learning based optimization (OBTLBO) [63] are also shown in Table 4.10. The cost convergence characteristics obtained from the proposed DEGM and DE are shown in Fig. 4.5. It is seen from Table 4.10 that the cost found by using DEGM is the lowest among all other methods.

Table 4.9: Power generation (MW) and heat generation (MWth) for Case 1 of Test System 3

	DEGM	DE		DEGM	DE
P_1	405.8240	538.5518	P_{16}	91.9008	81.2732
P_2	228.3453	298.6687	P_{17}	49.5467	40.0017
P_3	232.2610	298.9085	P_{18}	14.3991	10.0002
P_4	82.1304	110.0920	P_{19}	35.0000	35.0001
P_5	180.0000	110.1545	H_{14}	145.4696	105.2221
P_6	146.6926	110.0381	H_{15}	80.4921	76.5203
P_7	60.0000	110.1044	H_{16}	104.8984	105.5137
P_8	103.6535	110.2453	H_{17}	81.7680	75.4838
P_9	141.2192	109.8992	H_{18}	37.1367	39.9997
P_{10}	57.3959	77.3995	H_{19}	18.7811	18.3946
P_{11}	107.4889	77.8361	H_{20}	154.8362	468.9049
P_{12}	113.7753	55.0021	H_{21}	155.7581	59.9997
P_{13}	90.2413	55.0107	H_{22}	155.1761	59.9996
P_{14}	158.0832	81.0524	H_{23}	158.3652	119.9861
P_{15}	52.0430	40.7615	H_{24}	157.3184	119.9755

Table 4.10: Comparison of performancesof E & DEGM for Case 1 of Test System 3

Techniques	DEGM	DE	TVAC-PSO	CPSO	OBTLBO	TLBO
Best cost ($)	57435.1423	57847.8251	58122.7460	59736.2635	57856.2676	58006.9992
Average cost ($)	57445.4357	57858.5731	58198.3106	59853.478	57883.2105	58014.3685
Worst cost ($)	57457.3845	57872.6723	58359.5520	60076.6903	57913.7731	58038.5273
CPU time (s)	5. 1374	5.0187	7.84	8.00	5.82	5.67

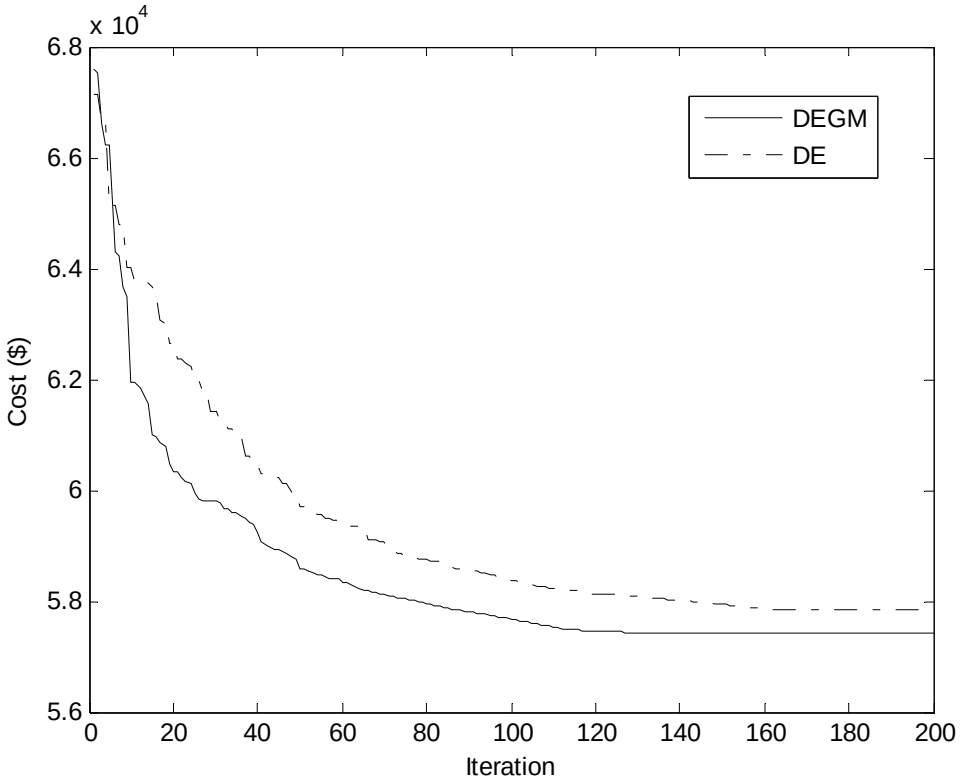

Fig. 4.5. Cost convergence characteristics of DE & DEGM for Case 1 of Test system 3.

Case 2

Here, valve point loading of conventional thermal generators and prohibited operating zones of conventional thermal generators are considered. The data of conventional thermal generator is same as in [62] except the following modifications in Table A.3. Table A.3 lists the prohibited zones of conventional thermal generating units 1, 2, 3, 10 and 11. These prohibited zones result in four disjoint feasible sub-regions for each of conventional thermal generating units 1, 2, and 3 and three disjoint feasible sub-regions for each of the conventional thermal generating units 10 and 11. Hence, those zones result in a non-convex decision space which consists of 576 convex sub-spaces for this system.

The problem is solved by using both the DEGM and DE. Here, the population size (N_P), crossover rate (C_R) and the maximum iteration number (N_{max}) have been selected as 100, 1.0 and 200, respectively, for the test system under consideration.

The power and heat generations corresponding to the best cost obtained from the proposed DEGM and DE are summarized in Table 4.11. The best, average and worst costs and average CPU time among 100 runs of solutions obtained from the proposed DEGM and DE are given in Table 4.12. The cost convergence characteristics obtained from the proposed DEGM and DE are depicted in Fig. 4.6.

Table 4.11: Power generation (MW) and heat generation (MWth) for Case 2 of Test System 3

	DEGM	DE		DEGM	DE
P_1	352.6891	538.5583	P_{16}	85.5662	98.5144
P_2	236.8071	299.2039	P_{17}	45.8052	45.5971
P_3	304.6099	149.6013	P_{18}	14.9670	10.0001
P_4	65.4600	159.7337	P_{19}	44.9197	40.1097
P_5	164.1774	159.7336	H_{14}	120.1593	115.0561
P_6	158.5786	60.0009	H_{15}	74.4085	79.6944
P_7	164.1946	60.0000	H_{16}	91.9492	114.6300
P_8	103.3653	159.7327	H_{17}	60.0778	79.8603
P_9	61.2580	159.7336	H_{18}	40.7192	40.0003
P_{10}	85.6485	40.0011	H_{19}	11.8679	22.3225
P_{11}	57.9012	114.8002	H_{20}	238.9227	438.4368
P_{12}	86.4798	55.0000	H_{21}	82.5488	59.9998
P_{13}	114.0153	55.0005	H_{22}	150.3922	60.0000
P_{14}	156.2659	99.2738	H_{23}	191.9765	119.9999
P_{15}	47.2913	45.4050	H_{24}	186.9779	120.0000

Table 4.12: Comparison of performance of DE & DEGM for Case 2 of Test System 3

Techniques	DEGM	DE
Best cost ($)	57818.3785	58075.9543
Average cost ($)	57830.5122	58084.9919
Worst cost ($)	57841.9561	58095.7992
CPU time (s)	5.2148	5.1974

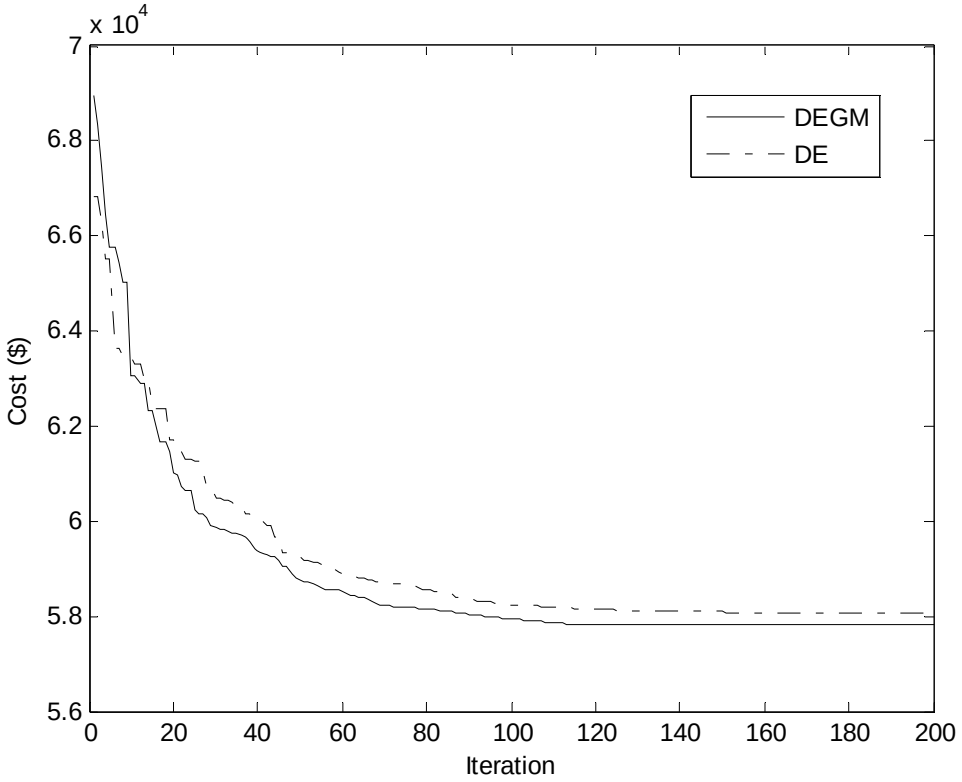

Fig. 4.6. Cost convergence characteristics of DE & DEGM for Case 2 of Test system 3

4.3.4. Test System 4

This system consists of twenty six conventional thermal generators, twelve cogeneration units and ten heat-only units. Data of this test system are obtained by duplicating data of test system 3. Characteristics of conventional thermal generating units 1-13 and 14-26 in this test system are same as units 1-13 in test system 3. Characteristics of cogeneration units 27-32 and 33-38 are

same as units 14-19 in case of test system 3. Also characteristics of heat-only units 39-43 and 44-48 are same as units 19-24 in case of test system 3. The power and heat demands of this test system are 4700 MW and 2500 MWth, respectively. Total number of decision variables is sixty. Here, two cases are considered.

Case 1

In this case ,only valve point loading of conventional thermal generators has been considered. The problem is solved by using the proposed DEGM. The problem is solved by using both the DEGM and DE. Here, the population size (N_P), crossover rate (C_R) and the maximum iteration number (N_{max}) have been selected as 200, 1.0 and 300 ,respectively for the test system under consideration.

The power and heat generations corresponding to best cost obtained from proposed DEGM is shown in Table 4.13. The best, average and worst costs and average CPU time among 100 runs of solutions obtained from proposed DEGM are summarized in Table 4.14. The cost obtained from classical PSO (CPSO) [62], time varying acceleration coefficients PSO (TVAC-PSO) [62], teaching learning based optimization (TLBO) [63] and oppositional teaching learning based optimization (OBTLBO) [63] are also shown in Table 4.14. The cost convergence characteristics obtained from the proposed DEGM & DE are depicted in Fig. 4.7. It is seen from Table 4.14 that the cost found by using DEGM is the lowest among all other methods.

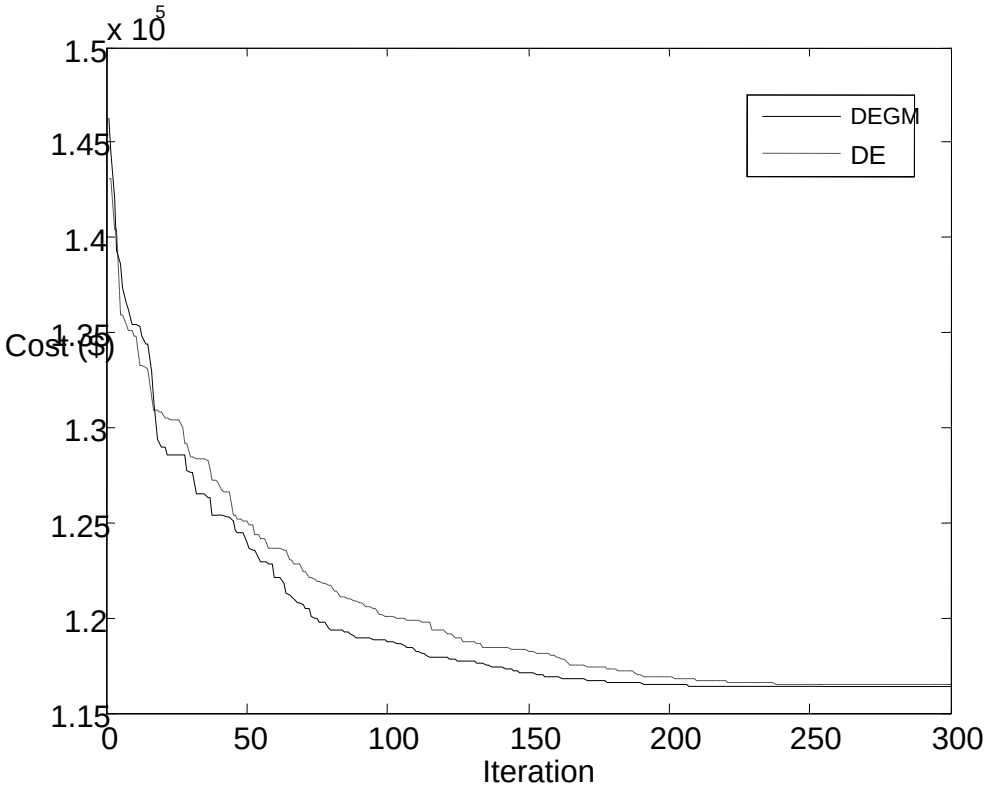

Fig. 4.7. Cost convergence characteristics of DE & DEGM for Case 1 of Test system4

Table 4.13: Power generation (MW) and heat generation (MWth) for Case 1 of Test System 4

	ODE	DE		ODE	DE
P_1	628.3929	448.9126	P_{31}	10.0067	10.0212
P_2	152.5706	150.5151	P_{32}	35.2229	37.7288
P_3	225.0390	80.7660	P_{33}	84.3443	92.0380
P_4	159.7318	160.0923	P_{34}	52.4982	50.4524
P_5	60.1085	109.9592	P_{35}	88.3203	95.2834
P_6	159.8778	159.8520	P_{36}	52.6043	52.3657
P_7	159.8202	160.1104	P_{37}	10.0031	10.0683
P_8	60.2052	159.8453	P_{38}	41.3405	45.7741
P_9	159.7669	160.0219	H_{27}	110.0733	109.8046
P_{10}	114.9815	114.9957	H_{28}	80.5513	83.3599
P_{11}	114.8295	115.1906	H_{29}	105.4872	104.9610
P_{12}	55.0982	92.6482	H_{30}	88.2216	80.8014
P_{13}	55.4608	55.0420	H_{31}	40.0032	39.9976
P_{14}	269.2848	269.4783	H_{32}	20.0959	21.2295
P_{15}	299.7439	299.4636	H_{33}	106.6740	110.9901
P_{16}	299.5403	299.7175	H_{34}	85.8196	84.0301
P_{17}	60.0000	159.9635	H_{35}	108.9010	112.7913
P_{18}	109.9347	159.8998	H_{36}	85.9112	85.6985
P_{19}	60.0133	159.7568	H_{37}	39.9970	40.0211
P_{20}	159.7334	60.0218	H_{38}	22.8801	24.8763
P_{21}	159.7326	160.0075	H_{39}	461.4785	458.7095
P_{22}	159.8841	159.9142	H_{40}	59.9991	59.9975
P_{23}	40.0244	114.9146	H_{41}	59.9991	60.0000
P_{24}	114.8484	40.1116	H_{42}	119.9983	119.9632
P_{25}	92.7310	93.8700	H_{43}	119.9995	119.9990
P_{26}	119.9937	93.6315	H_{44}	423.9159	422.7929
P_{27}	90.3997	89.9223	H_{45}	59.9989	59.9792
P_{28}	46.4014	49.6516	H_{46}	59.9998	59.9974
P_{29}	82.2287	81.2954	H_{47}	119.9997	120.0000
P_{30}	55.2821	46.6966	H_{48}	119.9958	120.0000

Table 4.14: Comparison of performance of DE & DEGM for Case 1 of Test System 4

Techniques	DEGM	DE	TVAC-PSO	CPSO	OBTLBO	TLBO
Best cost ($)	116406.2452	116457.9578	117824.8956	119708.8818	116579.2390	116739.3640
Average cost ($)	116411.4248	116464.2643	-	-	116613.6505	116756.0057
Worst cost ($)	116417.0139	116472.3293	-	-	116649.4473	116825.8223
CPU time (s)	9.4681	9.1073	-	-	10.93	10.38

Case 2

In this case, valve point loading of conventional thermal generators and prohibited operating zones of conventional thermal generators are considered. The data of conventional thermal generator are same as in case 1 except the following modifications in Table A.4. Table A.4 lists the prohibited zones of conventional thermal generating units 1, 2, 3, 10, 11, 14, 15, 16, 23 and 24. These prohibited zones result in four disjoint feasible sub-regions for each of conventional thermal generating units 1, 2, 3, 14, 15 and 16 and three disjoint feasible sub-regions for each of the conventional thermal generating units 10, 11, 23 and 24. Hence, those zones result in a non-convex decision space which consists of 331776 convex sub-spaces for this system.

The problem is solved by using the proposed MPSO. The problem is solved by using both the DEGM and DE. Here, the population size (N_P), crossover rate (C_R) and the maximum iteration number (N_{max}) have been selected as 200, 1.0 and 200, respectively for the test system under consideration.

The power and heat generations corresponding to the best cost obtained from proposed DEGM is summarized in Table 4.15. The best, average and worst costs and average CPU time among 100 runs of solutions obtained from the proposed DEGM are shown in Table 4.16.

Table 4.16: Comparison of performance of DE & DEGM for Case 2 of Test System 4

Techniques	DEGM	DE
Best cost ($)	116681.5578	116977.2048
Average cost ($)	116689.4748	116988.8263
Worst cost ($)	116699.8950	116996.4316
CPU time (s)	10.5638	10.2793

Table 4.15: Power generation (MW) and heat generation (MWth) for Case 2 of Test System 4

	ODE	DE		ODE	DE
P_1	628.3352	0.0471	P_{31}	10.1295	10.9795
P_2	0.0153	360.0000	P_{32}	35.7065	43.1498
P_3	359.9893	359.1999	P_{33}	91.9319	82.6940
P_4	159.8018	160.0293	P_{34}	57.5933	47.7510
P_5	60.1367	160.3777	P_{35}	81.0980	85.2154
P_6	60.0099	161.0244	P_{36}	47.3499	45.2857
P_7	60.0770	159.7844	P_{37}	10.0254	10.1040
P_8	159.7174	61.5254	P_{38}	35.0302	35.4258
P_9	159.7489	160.0464	H_{27}	118.8178	105.2132
P_{10}	114.6906	40.0234	H_{28}	78.9442	87.4681
P_{11}	114.7044	117.2796	H_{29}	110.6110	105.1607
P_{12}	55.0000	55.0000	H_{30}	82.5351	80.2841
P_{13}	55.0009	96.0207	H_{31}	40.0419	39.7728
P_{14}	179.4172	627.4600	H_{32}	20.3118	22.9621
P_{15}	299.3710	150.4142	H_{33}	110.7778	104.4973
P_{16}	359.9722	359.5863	H_{34}	90.2101	80.9460
P_{17}	60.0213	162.4424	H_{35}	104.7815	106.6665
P_{18}	159.8378	60.0000	H_{36}	81.3584	79.5110
P_{19}	109.9424	161.8982	H_{37}	40.0036	39.7946
P_{20}	159.7331	60.1077	H_{38}	20.0126	20.1340
P_{21}	159.9230	162.0103	H_{39}	433.6195	441.6983
P_{22}	159.7265	60.6194	H_{40}	59.9453	59.9941
P_{23}	114.8838	115.6517	H_{41}	59.9982	59.8580
P_{24}	115.3210	114.0506	H_{42}	120.0000	119.8318
P_{25}	55.0122	56.3107	H_{43}	119.9627	119.8444
P_{26}	119.9559	92.1742	H_{44}	448.0942	467.1149
P_{27}	106.0168	81.8378	H_{45}	59.9968	60.0000
P_{28}	44.6073	54.7657	H_{46}	60.0000	59.7449
P_{29}	91.4706	83.4146	H_{47}	119.9959	119.9997
P_{30}	48.6959	46.2928	H_{48}	119.9814	119.5034

4.4. Conclusion

Here, DEGM method has been successfully implemented to solve the five test problems and four complex non-smooth /non-convex combined heat and power economic dispatch problem. The results have been compared with those obtained by other evolutionary algorithms reported in the literature. It is seen from the comparisons that the proposed DEGM performs better than other evolutionary algorithms in the literature. It is clear from the results obtained by different trials that the proposed DEGM can avoid the shortcoming of premature convergence. Due to these properties, in future DEGM can be tried for solution of complex power system optimization problems.

4. 5. Application of IDE Method

The proposed improved differential evolution (IDE) is applied to four test systems. The computational results have been used to compare the performance of the proposed IDE based approach with those evolutionary methods. The proposed IDE and DE used in this paper are implemented by using MATLAB 7.0 on a PC (Pentium-IV, 80 GB, 3.0 GHz).

4.5.1. Test System 1

This test system consists of one conventional thermal generator and two cogeneration units and a heat-only unit. Unit data are taken from [62]. The power and heat demands of the test system are 250 MW and 115 MWth, respectively. Here, two cases are considered.

Case 1

In this case, only valve point loading of conventional thermal generator has been considered. The problem is solved by using both the proposed IDE and DE. In case of IDE and DE, the population size (N_P), crossover rate (C_R) and the maximum iteration number (N_{max}) have been selected as 50, 1.0 and 100, respectively, for this test system under consideration. In case of DE, scaling factor (F) has been selected 1.0.

The power and heat generations corresponding to the best cost obtained from the proposed IDE and DE are shown in Table 4.17. The best, average and the worst costs and average CPU time among 100 runs of solutions obtained from the proposed IDE and DE are summarized in Table 4.18. The cost obtained from classical PSO (CPSO) [62] and time varying acceleration coefficients PSO (TVAC-PSO) [62] are also shown in Table 4.18. The

cost convergence characteristics obtained from the proposed IDE and DE are shown in Fig. 4.8. It is seen from Table 4.18 that the total production cost found by using IDE is the lowest among all other methods.

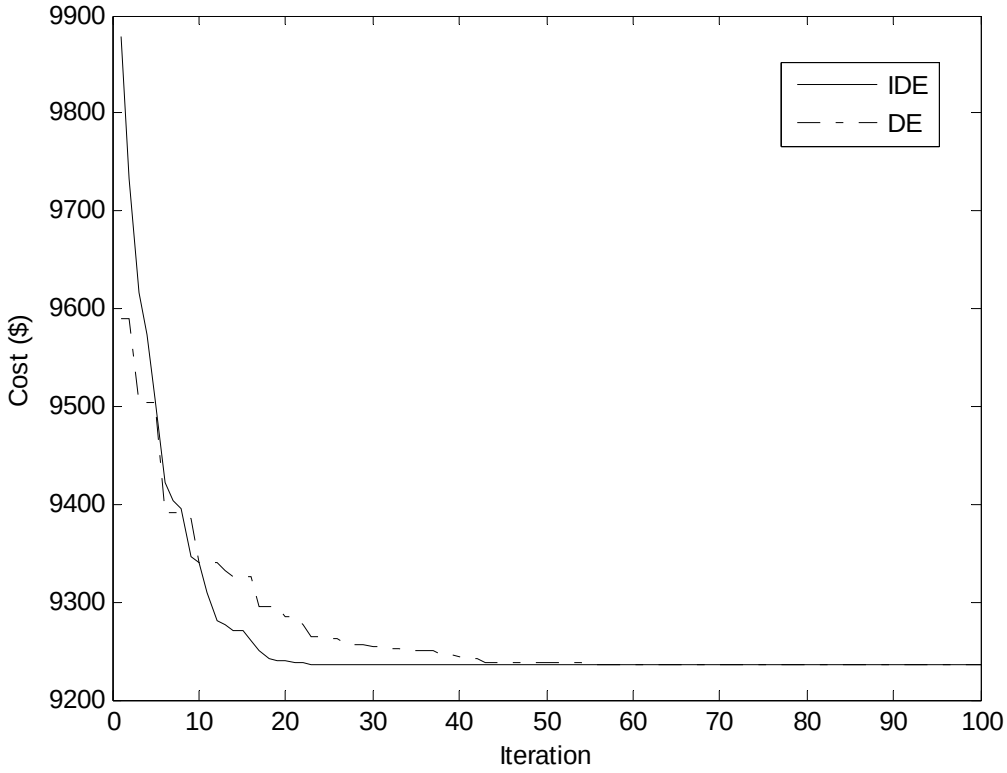

Fig. 4.8. Cost convergence characteristics of DE & IDE for Case 1 of Test system 1

Table 4.17: Power generation (MW) and heat generation (MWth) for Case 1 of Test System 1

	IDE	DE
P_1	113.4009	113.3946
P_2	92.5991	92.5982
P_3	44.0000	44.0072
H_2	36.5188	36.5716
H_3	78.4812	78.3954
H_4	0	0.0330

Table 4.18: Comparison of performance for Case 1 of Test System 1

Techniques	IDE	DE	TVAC-PSO	CPSO
Best cost ($)	9235.0999	9236.1437	9257.07	9257.08
Average cost ($)	9235.1011	9236.7422	-	-
Worst cost ($)	9235.1127	9237.0886	-	-
CPU time (s)	1.0716	1.0674	-	-

Case 2

In this case, the valve point loading of conventional thermal generator and prohibited operating zones of conventional thermal generator are considered. The data of conventional thermal generator is same as in [62] except the following modifications in Table A.1. Table A.1 lists the prohibited zones of conventional thermal generator. These prohibited zones result in four disjoint feasible sub-regions for the conventional thermal generator. Hence, those zones result in a non-convex decision space which consists of four convex sub-spaces for this system.

The problem is solved by using both the proposed IDE and DE. In case of IDE and DE, the population size (N_P), crossover rate (C_R) and the maximum iteration number (N_{max}) have been selected as 50, 1.0 and 100, respectively, for this test system under consideration. The scaling factor (F) has been selected 1.0 in case of DE.

The power and heat generations corresponding to best cost obtained from the proposed IDE and DE is summarized in Table 4.19. The best, average and the worst costs and average CPU time among 100 runs of solutions obtained from the proposed IDE and DE are shown in Table 4.20. The cost convergence characteristics obtained from the proposed IDE and DE is depicted in Fig. 4.9. It is seen from Table 4.20 that the total production cost found by using IDE is the lower than that found by DE.

Table 4.19: Power generation (MW) and heat generation (MWth) for Case 2 of Test System 1

	IDE	DE
P_1	109.9935	109.9766
P_2	96.0065	96.0202
P_3	44.0000	44.0032
H_2	36.5188	36.5172
H_3	78.4812	78.4698
H_4	0	0.0130

Table 4.20: Comparison of performance for Case 2 of Test System 1

Techniques	IDE	DE
Best cost ($)	9290.5796	9291.1375
Average cost ($)	9290.5800	9291.6290
Worst cost ($)	9290.5815	9292.4286
CPU time (s)	1.2308	1.2173

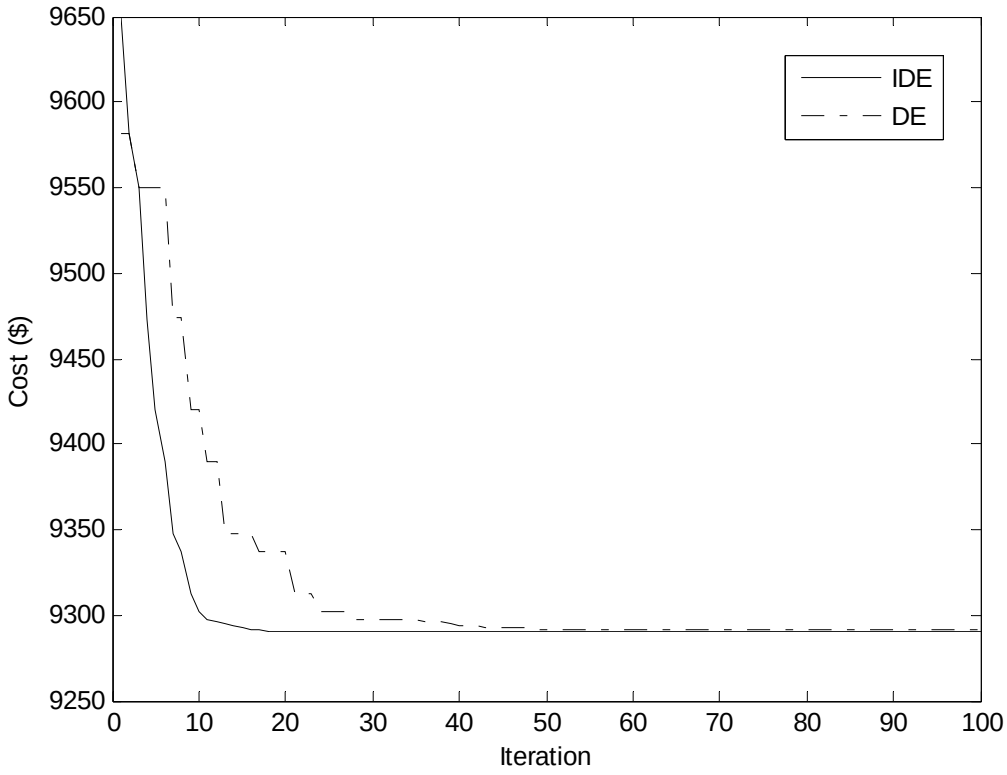

Fig. 4.9. Cost convergence characteristics of DE & IDE for Case 2 of Test system 1

4.5.2. Test System 2

This system consists of four conventional thermal generators, two cogeneration units and a heat-only unit. Here, transmission loss is considered. Unit data are taken from [62]. The power and heat demands of this test system are 600 MW and 150 MWth respectively. Here, two cases are considered.

Case 1

In this case , only valve point loading of conventional thermal generators has been considered.

The problem is solved by using both the proposed IDE and DE. In case of IDE and DE, the population size (N_P), crossover rate (C_R) and the maximum iteration number (N_{max}) have been selected as 50, 1.0 and 100, respectively, for this test system under consideration. In case of DE, scaling factor (F) has been selected 1.0.

The power and heat generations corresponding to best cost obtained from the proposed IDE and DE are shown in Table 4.21. The best, average and the worst costs and average CPU time among 100 runs of solutions obtained from proposed IDE and DE are summarized in Table 4.22. The cost obtained from classical PSO (CPSO) [62], time varying acceleration coefficients PSO (TVAC-PSO) [13], teaching learning based optimization (TLBO) [63] and oppositional teaching learning based optimization (OBTLBO) [63] are also shown in Table 4.22. The cost convergence characteristics obtained from the proposed IDE and DE is depicted in Fig. 4.10. It is seen from Table 4.22 that the total production cost found by using IDE is the lowest among all other methods.

Table 4.21: Power generation (MW) and heat generation (MWth) for Case 1 of Test System 2

	IDE	DE
P_1	45.6583	45.6493
P_2	98.5398	98.5412
P_3	112.6735	112.6756
P_4	209.8158	209.8143
P_5	94.0624	94.0681
P_6	40.0000	40.0013
H_5	27.8933	27.8638
H_6	75.0000	74.9902
H_7	47.1067	47.1460
Ploss	0.7499	0.7498

Table 4.22: Comparison of performanceof the algorithms for Case 1 of Test System 2

Techniques	IDE	DE	TVAC-PSO	CPSO	OBTLBO	TLBO
Best cost ($)	10094.2370	10094.3330	10100.3124	10325.3339	10094.3529	10094.8384
Average cost ($)	10094.3226	10094.3884	-	-	10099.4057	10114.1539
Worst cost ($)	10094.3852	10094.4545	-	-	10106.8314	10133.6130
CPU time (s)	2.1914	2.1795	-	-	3.06	2.86

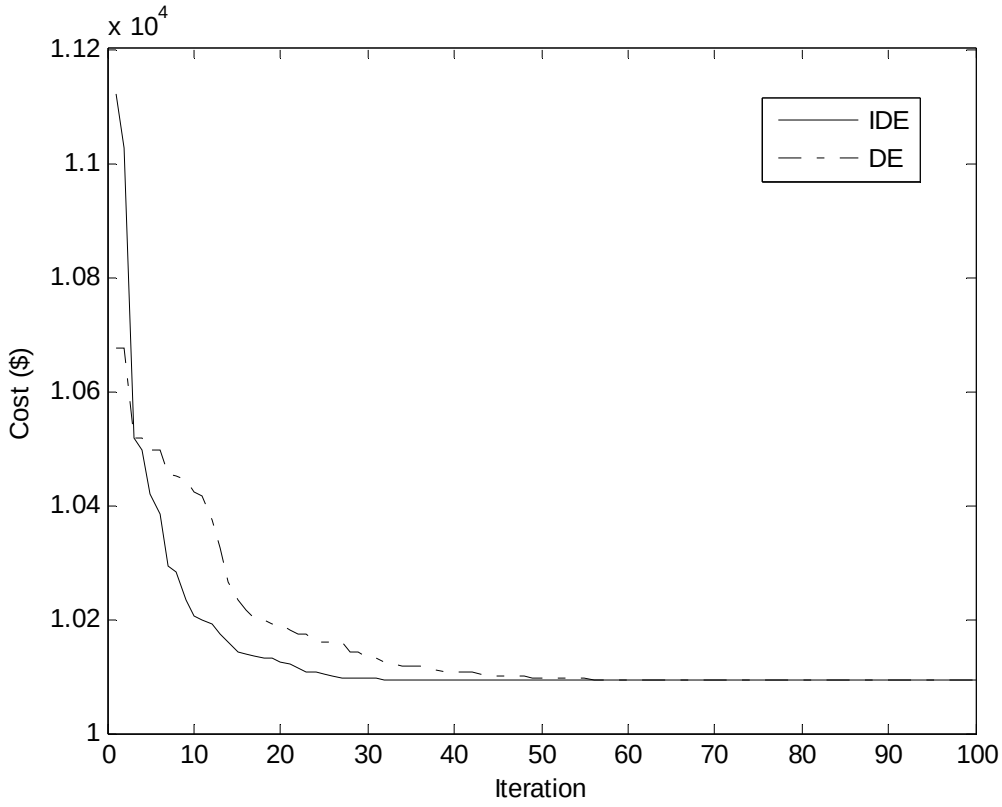

Fig. 4.10. Cost convergence characteristics of DE & IDE for Case 1 of Test system 2

Case 2

In this case , valve point loading of conventional thermal generators and prohibited operating zones of conventional thermal generators have been considered. The data of conventional thermal generator is same as in [62] except the following modifications in Table A.2. Table A.2 lists the prohibited zones of conventional thermal generating units. These prohibited zones result in three disjoint feasible sub-regions for each of the conventional thermal generators. Hence, those zones result in a non-convex decision space which consists of 81 convex sub-spaces for this system.

The problem is solved by using both the proposed IDE and DE. In case of IDE and DE, the population size (N_P), crossover rate (C_R) and the maximum iteration number (N_{max}) have been selected as 50, 1.0 and 100, respectively, for this test system under consideration. The scaling factor (F) has been selected 1.0 in case of DE.

The power and heat generations corresponding to the best cost obtained from proposed IDE and DE is summarized in Table 4.23. The best, average and the worst costs and average CPU time among 100 runs of solutions obtained from proposed IDE and DE are shown in Table

4.24. The cost convergence characteristics obtained from the proposed IDE and DE is shown in Fig. 4.11. It is seen from Table 4.24 that the total production cost obtained from IDE is the lower than that obtained from DE.

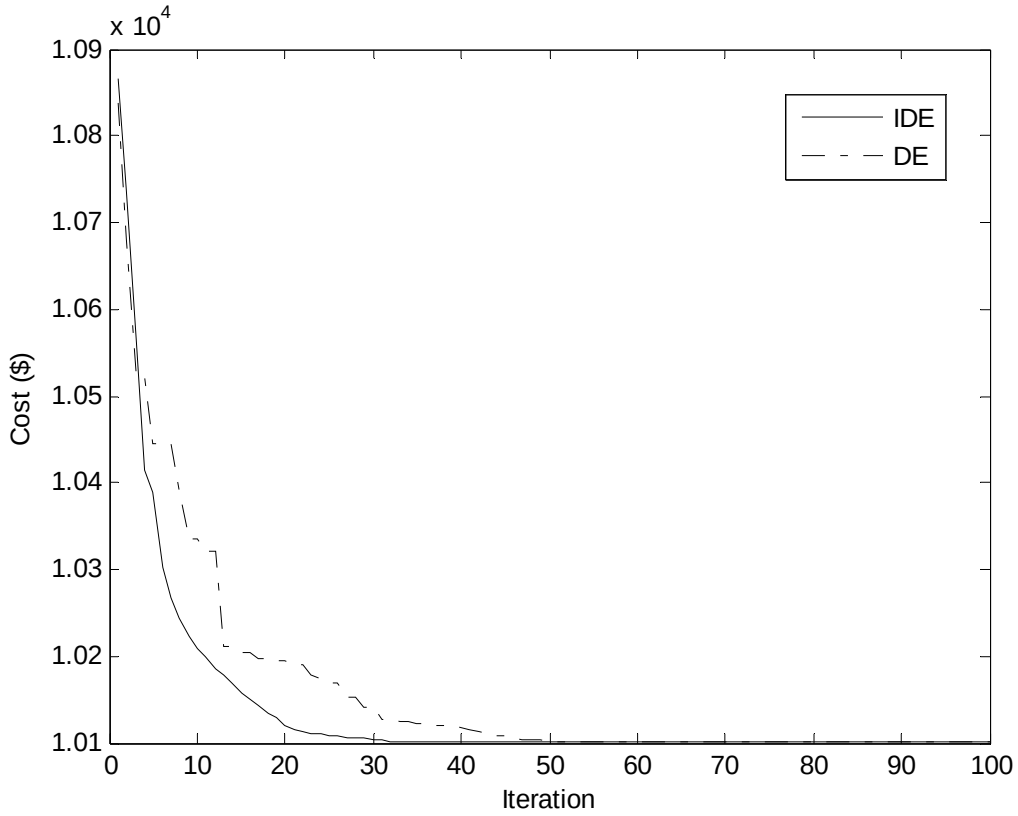

Fig. 4.11. Cost convergence characteristics of DE & IDE for Case 2 of Test system 2

Table 4.24: Comparison of performance of algorithms for Case 2 of Test System 2

Techniques	IDE	DE
Best cost ($)	10101.2941	10101.3772
Average cost ($)	10101.3598	10101.4128
Worst cost ($)	10101.4165	10101.4624
CPU time (s)	2.2751	2.2681

Table 4.23: Power generation (MW) and heat generation (MWth) for Case 2 of Test System 2

	IDE	DE
P_1	44.1425	44.1797
P_2	100.0000	100.0029
P_3	112.6735	112.6755
P_4	209.8158	209.8103
P_5	94.1178	94.0812
P_6	40.0000	40.0000
H_5	27.5673	27.7867
H_6	75.0000	74.9999
H_7	47.4327	47.2134
Ploss	0.7496	0.7496

4.5.3. Test System 3

This system consists of thirteen conventional thermal generators, six cogeneration units and five heat-only units. Unit data has been taken from [62]. The power and heat demands of the test system are 2350 MW and 1250 MWth respectively. Here, two cases are considered.

Case 1

Here, only valve point loading of conventional thermal generators has been considered.

The problem is solved by using both the proposed IDE and DE. In case of IDE and DE, the population size (N_P), crossover rate (C_R) and the maximum iteration number (N_{max}) have been selected as 100, 1.0 and 200 respectively for this test system under consideration. The scaling factor (F) has been selected 1.0 in case of DE.

The power and heat generations corresponding to best cost obtained from proposed IDE and DE is shown in Table 4.25. The best, average and worst cost and average CPU time among 100 runs of solutions obtained from proposed IDE and DE are summarized in Table 4.26. The cost obtained from classical PSO (CPSO) [62], time varying acceleration coefficients PSO (TVAC-PSO) [62], teaching learning based optimization (TLBO) [63] and oppositional teaching learning based optimization (OBTLBO) [63] are also shown in Table 4.26. The cost convergence characteristic obtained from proposed IDE and DE is shown in Fig. 4.12. It is seen from Table 4.26 that the total production cost found by using IDE is the lowest among all other methods.

Table 4.25: Power generation (MW) and heat generation (MWth) for Case 1 of Test System 3

	IDE	DE		IDE	DE
P_1	535.7328	538.5518	P_{16}	147.1269	81.2732
P_2	87.9941	298.6687	P_{17}	45.4364	40.0017
P_3	88.4237	298.9085	P_{18}	18.5330	10.0002
P_4	166.7972	110.0920	P_{19}	48.4332	35.0001
P_5	155.0323	110.1545	H_{14}	115.5126	105.2221
P_6	167.5964	110.0381	H_{15}	84.4229	76.5203
P_7	101.1912	110.1044	H_{16}	73.4368	105.5137
P_8	90.1035	110.2453	H_{17}	79.3906	75.4838
P_9	179.0407	109.8992	H_{18}	43.2269	39.9997
P_{10}	85.1536	77.3995	H_{19}	25.8061	18.3946
P_{11}	109.1897	77.8361	H_{20}	255.7989	468.9049
P_{12}	96.7976	55.0021	H_{21}	159.0120	59.9997
P_{13}	69.3873	55.0107	H_{22}	152.9706	59.9996
P_{14}	102.9362	81.0524	H_{23}	105.1496	119.9861
P_{15}	55.0940	40.7615	H_{24}	155.2730	119.9755

Table 4.26: Comparison of performance of Case 1 of Test System 3

Techniques	IDE	DE	TVAC-PSO	CPSO]	OBTLBO	TLBO
Best cost ($)	57500.1658	57847.8251	58122.7460	59736.2635	57856.2676	58006.9992
Average cost ($)	57512.3457	57858.5731	58198.3106	59853.478	57883.2105	58014.3685
Worst cost ($)	57526.8475	57872.6723	58359.5520	60076.6903	57913.7731	58038.5273
CPU time (s)	5.0217	5.0187	7.84	8.00	5.82	5.67

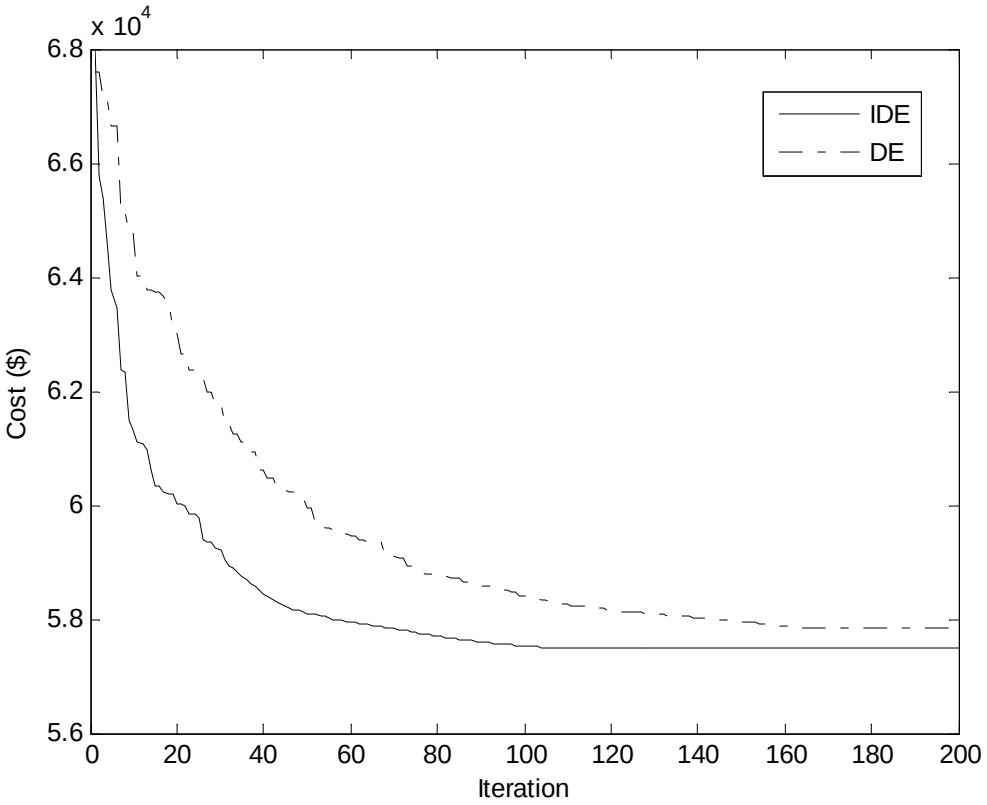

Fig. 4.12. Cost convergence characteristics of DE & IDE for Case 1 of Test system 3

Case 2

Here, valve point loading of conventional thermal generators and prohibited operating zones of conventional thermal generators have been considered. The data of conventional thermal generator is same as in [62] except the following modifications in Table A.3. Table A.3 lists the prohibited zones of conventional thermal generating units 1, 2, 3, 10 and 11. These prohibited zones result in four disjoint feasible sub-regions for each of conventional thermal generating units 1, 2, and 3 and three disjoint feasible sub-regions for each of the conventional thermal generating units 10 and 11. Hence, those zones result in a non-convex decision space which consists of 576 convex sub-spaces for this system.

The problem is solved by using both the proposed IDE and DE. In case of IDE and DE, the population size (N_P), crossover rate (C_R) and the maximum iteration number (N_{max}) have been selected as 100, 1.0 and 200 respectively for this test system under consideration. In case of DE, the scaling factor (F) has been selected 1.0.

The power and heat generations corresponding to best cost obtained from proposed IDE and DE is summarized in Table 4.27. The best, average and worst cost and average CPU time among 100 runs of solutions obtained from proposed IDE and DE are given in Table 4.28. The cost convergence characteristic obtained from proposed IDE and DE is depicted in Fig. 4.13. It is seen from Table 4.28 that the total production cost found by using IDE is the lower than that obtained from DE.

Table 4.27: Power generation (MW) and heat generation (MWth) for Case 2 of Test System 3

	IDE	DE		IDE	DE
P_1	149.4434	538.5583	P_{16}	95.8221	98.5144
P_2	304.6058	299.2039	P_{17}	58.0163	45.5971
P_3	258.0091	149.6013	P_{18}	11.4125	10.0001
P_4	72.0967	159.7337	P_{19}	71.9769	40.1097
P_5	107.7057	159.7336	H_{14}	125.2448	115.0561
P_6	118.1354	60.0009	H_{15}	77.7217	79.6944
P_7	177.6320	60.0000	H_{16}	100.2979	114.6300
P_8	180.0000	159.7327	H_{17}	89.3979	79.8603
P_9	156.5191	159.7336	H_{18}	39.5096	40.0003
P_{10}	117.1895	40.0011	H_{19}	33.0278	22.3225
P_{11}	62.8599	114.8002	H_{20}	205.3785	438.4368
P_{12}	116.9323	55.0000	H_{21}	167.3824	59.9998
P_{13}	114.3197	55.0005	H_{22}	158.5770	60.0000
P_{14}	127.7132	99.2738	H_{23}	163.3474	119.9999
P_{15}	49.6102	45.4050	H_{24}	90.1151	120.0000

Table 4.28: Comparison of performance of DE & IDE for Case 2 of Test System 3

Techniques	IDE	DE
Best cost ($)	57626.8083	58075.9543
Average cost ($)	57641.0265	58084.9919
Worst cost ($)	57655.6638	58095.7992
CPU time (s)	5.2028	5.1974

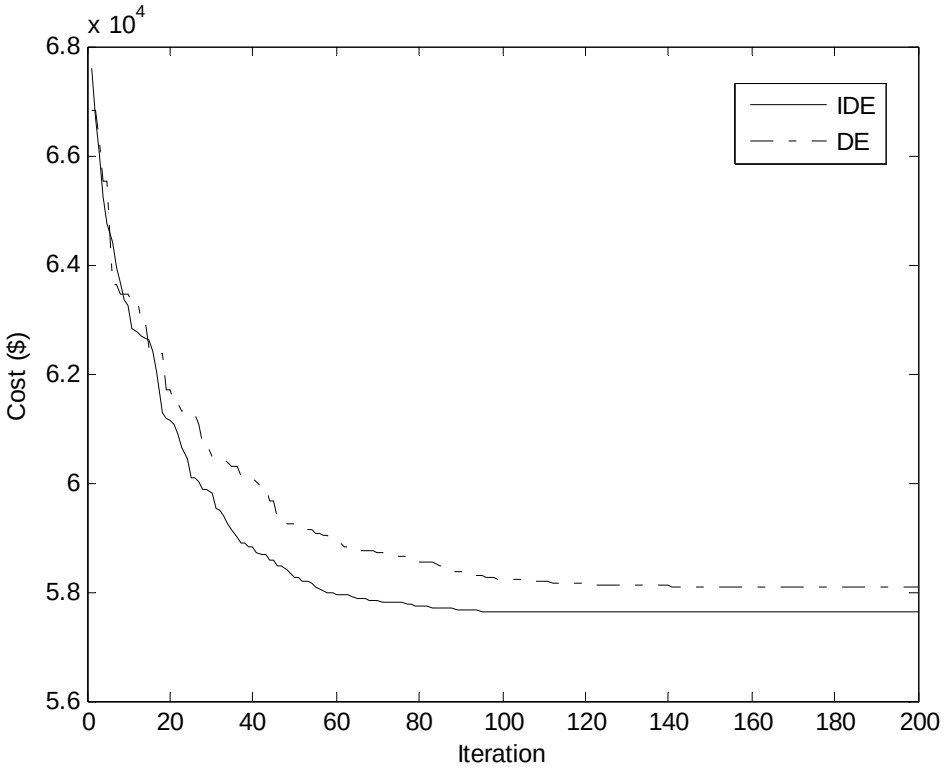

Fig. 4.13. Cost convergence characteristics of DE & IDE for Case 2 of Test system 3

4.5.4. Test System 4

This system consists of twenty six conventional thermal generators, twelve cogeneration units and ten heat-only units. Data of this test system is obtained by duplicating data of test system 3. Characteristics of conventional thermal generating units 1-13 and 14-26 in this test system are same as units 1-13 in test system 3. Characteristics of cogeneration units 27-32 and 33-38 are same as units 14-19 in case of test system 3. Also characteristics of heat-only units 39-43 and 44-48 are same as units 19-24 in case of test system 3. The power and heat demands of this test system are 4700 MW and 2500 MWth respectively. Total number of decision variables is sixty. Here, two cases are considered.

Case 1

Here, only valve point loading of conventional thermal generators has been considered.

The problem is solved by using both the proposed IDE and DE. In case of IDE and DE, the population size (N_P), crossover rate (C_R) and the maximum iteration number (N_{max}) have been selected as 200, 1.0 and 300 respectively for this test system under consideration. The scaling factor (F) has been selected 1.0 in case of DE.

The power and heat generations corresponding to best cost obtained from proposed IDE and DE is shown in Table 4.29. The best, average and worst cost and average CPU time among 100 runs of solutions obtained from proposed IDE and DE are summarized in Table 4.30. The cost obtained from classical PSO (CPSO) [62], time varying acceleration coefficients PSO (TVAC-PSO) [62], teaching learning based optimization (TLBO) [63] and oppositional teaching learning based optimization (OBTLBO) [63] are also shown in Table 4.30. The cost convergence characteristic obtained from proposed IDE and DE is depicted in Fig. 4.14.

Table 4.30: Comparison of performance for Case 1 of Test System 4

Techniques	IDE	DE	TVAC-PSO	CPSO	OBTLBO	TLBO
Best cost ($)	116395.7388	116553.8786	117824.8956	119708.8818	116579.2390	116739.3640
Average cost ($)	116404.4248	116566.2643	-	-	116613.6505	116756.0057
Worst cost ($)	116417.0139	116581.3293	-	-	116649.4473	116825.8223
CPU time (s)	9.1204	9.1073	-	-	10.93	10.38

Table 4.29: Power generation (MW) and heat generation (MWth) for Case 1 of Test System 4

	IDE	DE		IDE	DE
P_1	448.7989	628.3788	P_{31}	10.0013	10.0000
P_2	306.3151	300.7263	P_{32}	37.4216	42.9297
P_3	149.8257	69.5038	P_{33}	81.6484	86.9998
P_4	159.7516	159.8836	P_{34}	44.3481	44.2322
P_5	110.3379	111.0085	P_{35}	84.8291	93.0621
P_6	159.7393	161.3487	P_{36}	45.8490	44.1610
P_7	160.1196	159.7830	P_{37}	10.0001	10.0000
P_8	159.7383	60.1759	P_{38}	36.7439	35.3042
P_9	161.2440	111.0732	H_{27}	105.7972	115.9058
P_{10}	78.4224	40.5821	H_{28}	83.2074	78.7522
P_{11}	114.8455	115.4596	H_{29}	107.9138	105.1800
P_{12}	119.9998	93.1656	H_{30}	83.5528	78.5260
P_{13}	92.4058	94.1436	H_{31}	40.0011	40.0006
P_{14}	269.2796	449.8255	H_{32}	21.1007	23.6042
P_{15}	300.1488	224.8231	H_{33}	105.1644	108.1677
P_{16}	299.2742	82.6100	H_{34}	78.7817	78.6816
P_{17}	159.7625	159.7870	H_{35}	106.9498	111.5700
P_{18}	109.8995	160.0493	H_{36}	80.0776	78.6202
P_{19}	60.0141	64.9357	H_{37}	40.0004	40.0005
P_{20}	109.0102	162.3119	H_{38}	20.7926	20.1380
P_{21}	64.0415	110.5421	H_{39}	480.0298	484.5378
P_{22}	110.4698	161.2920	H_{40}	60.0000	60.0000
P_{23}	77.4349	114.8351	H_{41}	59.9999	60.0000
P_{24}	114.8022	77.7608	H_{42}	120.0000	120.0000
P_{25}	92.4082	96.0141	H_{43}	119.9999	119.9999
P_{26}	92.4006	92.4619	H_{44}	426.6309	416.3160
P_{27}	82.7754	100.7881	H_{45}	60.0000	59.9995
P_{28}	49.4732	44.3139	H_{46}	60.0000	60.0000
P_{29}	86.5469	81.6757	H_{47}	120.0000	120.0000
P_{30}	49.8731	44.0520	H_{48}	120.0000	119.9998

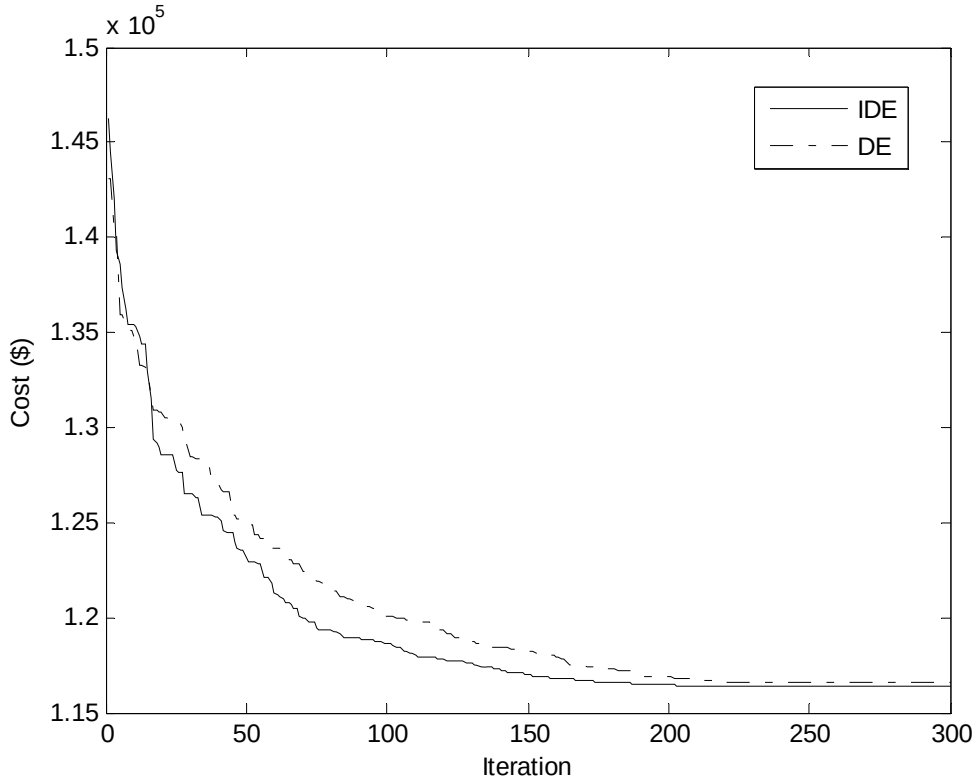

Fig. 4.14. Cost convergence characteristics of DE & IDE for Case 1 of Test system 4

Case 2

Here, valve point loading of conventional thermal generators and prohibited operating zones of conventional thermal generators have been considered. The data of conventional thermal generator is same as in case 1 except the following modifications in Table A.4. Table A.4 lists the prohibited zones of conventional thermal generating units 1, 2, 3, 10, 11, 14, 15, 16, 23 and 24. These prohibited zones result in four disjoint feasible sub-regions for each of conventional thermal generating units 1, 2, 3, 14, 15 and 16 and three disjoint feasible sub-regions for each of the conventional thermal generating units 10, 11, 23 and 24. Hence, those zones result in a non-convex decision space which consists of 331776 convex sub-spaces for this system.

The problem is solved by using both the proposed IDE and DE. In case of IDE and DE, the population size (N_P), crossover rate (C_R) and the maximum iteration number (N_{max})

have been selected as 200, 1.0 and 300 respectively for this test system under consideration. In case of DE, the scaling factor (F) has been selected 1.0.

The power and heat generations corresponding to best cost obtained from proposed IDE and DE is summarized in Table 4.31. The best, average and worst cost and average CPU time among 100 runs of solutions obtained from proposed IDE and DE are shown in Table 4.32. The cost convergence characteristic obtained from proposed IDE and DE is shown in Fig. 4.15. . It is seen from Table 4.32 that the total production cost found by using IDE is the lower than that obtained from DE.

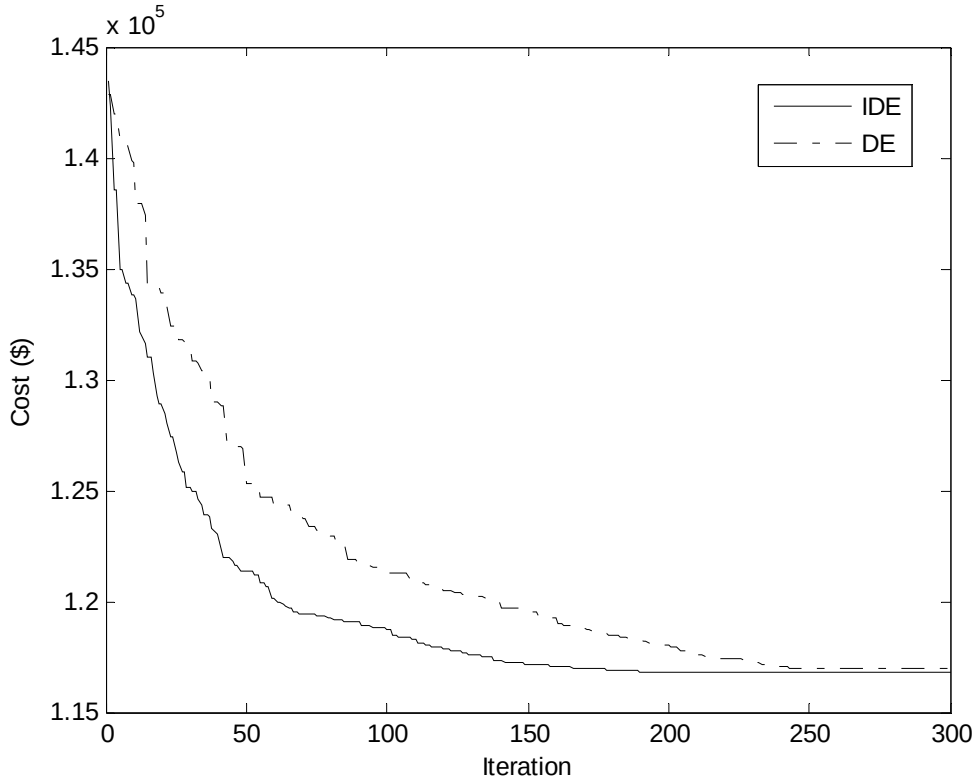

Fig. 15. Cost convergence characteristics of DE & IDE for Case 2 of Test system 4

Table 4.32: Comparison of performance for Case 2 of Test System 4

Techniques	IDE	DE
Best cost ($)	116781.0812	116977.2048
Average cost ($)	116789.4748	116988.8263
Worst cost ($)	116799.8950	116996.4316
CPU time (s)	10.2856	10.2793

Table 4.31: Power generation (MW) and heat generation (MWth) for Case 2 of Test System 4

	IDE	DE		IDE	DE
P_1	89.7716	0.0471	P_{31}	10.0000	10.9795
P_2	299.6422	360.0000	P_{32}	35.6009	43.1498
P_3	299.2076	359.1999	P_{33}	82.5980	82.6940
P_4	159.7589	160.0293	P_{34}	44.0334	47.7510
P_5	60.0910	160.3777	P_{35}	81.2598	85.2154
P_6	159.7752	161.0244	P_{36}	45.0500	45.2857
P_7	159.9963	159.7844	P_{37}	10.0004	10.1040
P_8	159.8186	61.5254	P_{38}	35.1071	35.4258
P_9	167.7682	160.0464	H_{27}	106.4146	105.2132
P_{10}	114.8354	40.0234	H_{28}	80.3886	87.4681
P_{11}	115.2708	117.2796	H_{29}	110.4245	105.1607
P_{12}	92.5386	55.0000	H_{30}	79.2001	80.2841
P_{13}	92.4524	96.0207	H_{31}	40.0005	39.7728
P_{14}	259.9997	627.4600	H_{32}	20.2731	22.9621
P_{15}	299.2173	150.4142	H_{33}	105.6974	104.4973
P_{16}	299.4302	359.5863	H_{34}	78.5099	80.9460
P_{17}	159.7344	162.4424	H_{35}	104.9466	106.6665
P_{18}	109.9216	60.0000	H_{36}	79.3876	79.5110
P_{19}	159.7389	161.8982	H_{37}	40.0002	39.7946
P_{20}	155.5700	60.1077	H_{38}	20.0485	20.1340
P_{21}	109.8835	162.0103	H_{39}	520.7487	441.6983
P_{22}	159.8539	60.6194	H_{40}	60.0000	59.9941
P_{23}	115.5359	115.6517	H_{41}	59.9999	59.8580
P_{24}	78.1970	114.0506	H_{42}	120.0000	119.8318
P_{25}	120.0000	56.3107	H_{43}	119.9996	119.8444
P_{26}	92.4022	92.1742	H_{44}	393.9605	467.1149
P_{27}	83.8763	81.8378	H_{45}	59.9998	60.0000
P_{28}	46.2093	54.7657	H_{46}	59.9999	59.7449
P_{29}	91.0207	83.4146	H_{47}	119.9997	119.9997
P_{30}	44.8326	46.2928	H_{48}	120.0000	119.5034

4.6. Conclusion

Here, IDE algorithm has been successfully implemented to solve two test problems and four non-smooth/non-convex combined heat and power economic dispatch problems. It has been observed that IDE algorithm has the ability to converge to a better quality solution and exhibit more robustness. It is clear from the results obtained by different trials that the proposed IDE algorithm can avoid the shortcoming of premature convergence. Due to these properties, the IDE algorithm in future can be tried for solution of complex power system optimization problems.

CHAPTER 5

Multi-area Economic Dispatch

5.1. Introduction

Economic dispatch (ED) is one of the important optimization problems in power system operation. ED allocates the load demand among the committed generators most economically while satisfying the physical and operational constraints in a single area. Generally, the generators are divided into several generation areas interconnected by tie-lines. Multi-area economic dispatch (MAED) is an extension of economic dispatch. MAED determines the generation levels and interchange powers between areas such that total fuel cost for all the areas is minimized while satisfying power balance constraints, generating limits constraints and tie-line capacity constraints.

Here, improved differential evolution (IDE) and group search optimization (GSO) have been applied to solve MAED problem. Here, three types of MAED problems have been considered. These are A) multi-area economic dispatch with quadratic cost function, prohibited operating zones and transmission losses B) multi-area economic dispatch with valve point loading C) multi-area economic dispatch with valve point loading, multiple fuel sources and transmission losses.

The proposed methods have been validated by application to three different test systems. The performance of the proposed methods in terms of solution quality has been compared with differential evolution (DE), evolutionary programming (EP) and real coded genetic algorithm (RCGA).

5.2. Problem Formulation

The objective of MAED is to minimize the total production cost of supplying loads to all areas while satisfying power balance constraints, generating limits constraints and tie-line capacity constraints.

Three different types of MAED problems have been considered.

5.2.1. Multi area economic dispatch with quadratic cost function, prohibited operating zones and transmission losses

The objective function F_t, total cost of committed generators of all areas, of MAED problem may be written as

$$F_t = \sum_{i=1}^{N}\sum_{j=1}^{M_i} F_{ij}\left(P_{ij}\right) = \sum_{i=1}^{N}\sum_{j=1}^{M_i}\left(a_{ij} + b_{ij}P_{ij} + c_{ij}P_{ij}^2\right) \quad (1)$$

where $F_{ij}\left(P_{ij}\right)$ is the cost function of j th generator in area i and is usually expressed as a quadratic polynomial; a_{ij}, b_{ij} and c_{ij} are the cost coefficients of j th generator in area i; N is the number of areas, M_i is the number of committed generators in area i; P_{ij} is the real power output of j th generator in area i. The MAED problem minimizes F_t subject to the following constraints.

5.2.1.1. Real power balance constraint:

$$\sum_{j=1}^{M_i} P_{ij} = P_{Di} + P_{Li} + \sum_{k,k\neq i} T_{ik} \qquad i \in N \quad (2)$$

The transmission loss P_{Li} of area i may be expressed by using B -coefficients as

$$P_{Li} = \sum_{l=1}^{M_i}\sum_{j=1}^{M_i} P_{ij}B_{ilj}P_{il} + \sum_{j=1}^{M_i} B_{0ij}P_{ij} + B_{00i} \quad (3)$$

where P_{Di} real power demand of area i; T_{ik} is the tie line real power transfer from area i to area k. T_{ik} is positive when power flows from area i to area k and T_{ik} is negative when power flows from area k to area i.

5.2.1.2. Tie line capacity constraints

The tie line real power transfer T_{ik} from area i to area k should not exceed the tie line transfer capacity for security consideration.

$$-T_{ik}^{max} \le T_{ik} \le T_{ik}^{max} \quad (4)$$

where T_{ik}^{max} is the power flow limit from area i to area k and $-T_{ik}^{max}$ is the power flow limit from area k to area i.

5.2.1.3. Real power generation capacity constraints

The real power generated by each generator should be within its lower limit P_{ij}^{min} and upper limit P_{ij}^{max}, so that

$$P_{ij}^{min} \le P_{ij} \le P_{ij}^{max} \qquad i \in N \text{ and } j \in M_i \tag{5}$$

5.2.1.4. Prohibited Operating Zones

The prohibited operating zones are the ranges of power outputs of a generator where the operation causes undue vibration of the turbine shaft bearing caused by opening or closing of the steam valve. This undue vibration might cause damage to the shaft and bearings. Normally operation is avoided in such regions. The feasible operating zones of unit can be described as follows:

$$\begin{aligned} &P_{ij}^{min} \le P_{ij} \le P_{ij,1}^{l} \\ &P_{ij,m-1}^{u} \le P_{ij} \le P_{ij,m}^{l} \;\; ; \quad m = 2,3,...,n_{ij} \\ &P_{ij,n_{ij}}^{u} \le P_{ij} \le P_{ij}^{max} \end{aligned} \tag{6}$$

where m represents the number of prohibited operating zones of j the generator in area i; $P_{ij,m-1}^{u}$ is the upper limit of $(m-1)$th prohibited operating zone of j the generator in area i, $P_{ij,m}^{l}$ is the lower limit of mth prohibited operating zone of j the generator in area i. Total number of prohibited operating zone of j the generator in area i is n_{ij}.

5.2.2. Multi-area economic dispatch with valve point loading

The generator cost function is obtained from data points taken during "heat run" tests, when input and output data are measured as the unit is slowly run through its operating region. Wire drawing effects, occurring as each steam admission valve in a turbine starts to open, produce a rippling effect on the unit curve. To model the effect of valve-points, a recurring rectified sinusoid contribution is added to the quadratic function [22]. The fuel cost function considering valve-point loading of the generator is given as

$$F_t = \sum_{i=1}^{N}\sum_{j=1}^{M_i} F_{ij}\left(P_{ij}\right) = \sum_{i=1}^{N}\sum_{j=1}^{M_i}\left[a_{ij} + b_{ij}P_{ij} + c_{ij}P_{ij}^2 + \left|d_{ij} \times \sin\left\{e_{ij} \times \left(P_{ij}^{\min} - P_{ij}\right)\right\}\right|\right] \quad (7)$$

where d_{ij} and e_{ij} are cost coefficients of ith generator in area i due to valve-point effect. The objective of MAEDVPL is to minimize F_t subject to the constraints given in (5.2), (5.4) and (5.5). Here transmission loss (P_L) is not considered.

5.2.3. Multi-area economic dispatch with valve point loading multiple fuel sources and transmission losses

Since generators are practically supplied with multi-fuel sources, each generator should be represented with several piecewise quadratic functions superimposed sine terms reflecting the effect of fuel type changes and the generator must identify the most economical fuel to burn. The fuel cost function of the ith generator with N_F fuel types, considering valve-point loading, is expressed as:

$$F_{ij}\left(P_{ij}\right) = a_{ijm} + b_{ijm}P_{ij} + c_{ijm}P_{ij}^2 + \left|d_{ijm} \times \sin\left\{e_{ijm} \times \left(P_{ijm}^{\min} - P_{ij}\right)\right\}\right| \quad (8)$$

if $P_{ijm}^{\min} \le P_{ij} \le P_{ijm}^{\max}$ for fuel type m and $m = 1,2,...,N_F$

The objective function F_t is given by

$$F_t = \sum_{i=1}^{N}\sum_{j=1}^{M_i} F_{ij}\left(P_{ij}\right) \quad (9)$$

The objective function F_t is to be minimized subject to the constraints given in (2), (4) and (5).

5.3. Determination of Generation Level of slack generator

M_i committed generators in area i deliver their power output subject to the power balance constraint (5.2), tie line capacity constraints (5.4) and the respective generation capacity constraints (5.5). Assuming the power loading of first $(M_i - 1)$ generators are known, the power level of the M_i th generator (i.e. the slack generator) is given by

$$P_{iM_i} = P_{Di} + P_{Li} + \sum_{k,k\neq i} T_{ik} - \sum_{j=1}^{M_i-1} P_{ij} \tag{10}$$

The transmission loss P_{Li} is a function of all generator outputs including the slack generator and it is given by

$$P_{Li} = \left[\sum_{l=1}^{M_i-1} \sum_{j=1}^{M_i-1} \left(P_{ij} B_{ilj} P_{il}\right) + 2P_{iM_i} \left(\sum_{j=1}^{M_i-1} B_{iM_i j} P_{ij} \right) + B_{iM_iM_i} P_{iM_i}^2 + \sum_{j=1}^{M_i-1} \left(B_{0ij} P_{ij}\right) + B_{0iM_i} P_{iM_i} + B_{00i} \right] \tag{11}$$

Expanding and rearranging, (5.10) becomes

$$B_{iM_iM_i} P_{iM_i}^2 + \left(2\sum_{j=1}^{M_i-1} B_{iM_i j} P_{ij} + B_{0iM_i} - 1 \right) P_{iM_i} + \left(P_{Di} + \sum_{k,k\neq i} T_{ik} + \sum_{j=1}^{M_i-1} \sum_{l=1}^{M_i-1} P_{ij} B_{ilj} P_{il} + \sum_{j=1}^{M_i-1} B_{0ij} P_{ij} \right.$$
$$\left. - \sum_{j=1}^{M_i-1} P_{ij} + B_{00i} \right) = 0 \tag{12}$$

The loading of the slack generator (i.e. M_i th) can then be found by solving equation (5.12) using standard algebraic method.

5. 4. Application of IDE Algorithm

Here, the performance of the proposed improved differential evolution (IDE) algorithm has been evaluated by using three test systems. In order to show the effectiveness of the proposed IDE algorithm, differential evolution (DE), evolutionary programming (EP) and real coded genetic algorithm (RCGA) have been applied to the same three test systems. All the algorithms i.e. IDE, DE, EP, and RCGA used in this paper for solving multi-area economic dispatch (MAED) problem are implemented by using MATLAB 7.0 on a PC (Pentium-IV, 80 GB, 3.0 GHz).

5.4.1. Test System 1: This system consists of two areas. Each area consists of three generators with prohibited operating zones. Transmission loss is considered here. The generator data have modified from [30]. The generator data and B-coefficients are given in the Appendix-1. The percentage of the total load demand in area 1 is 60% and 40% in area 2. The total load demand is 1263 MW and power flow limit of the system is 100 MW.

The problem is solved by using IDE algorithm. For this test system, Here, the population size (N_P), crossover constant (C_R) and maximum iteration number have been selected 100, 1 and 50, respectively.

To validate the proposed IDE based approach, the same test system is solved using differential evolution (DE), evolutionary programming (EP) and real coded genetic algorithm (RCGA). The population size, scaling factor and crossover constant have been selected as 100, 1.0 and 1.0 ,respectively ,in case of DE. In case of EP, the population size and scaling factor have been selected 100 and 0.1 ,respectively. In RCGA, the population size, crossover and mutation probabilities have been selected as 100, 0.9 and 0.2 ,respectively. Maximum number of iterations has been selected as 50 for DE, EP and RCGA.

Results obtained from the proposed IDE, DE, EP and RCGA have been summarized in Table 5.1. The cost convergence characteristics of this test system obtained from IDE, DE, EP and RCGA are shown in Fig. 5.1.

Table 5.1: Simulation results for Test system 1

	IDE	DE	EP	RCGA
$P_{1,1}$ (MW)	500.0000	500.0000	500.0000	500.0000
$P_{1,2}$ (MW)	200.0000	200.0000	200.0000	200.0000
$P_{1,3}$ (MW)	149.9999	150.0000	149.9919	149.6328
$P_{2,1}$ (MW)	204.3352	204.3341	206.4493	205.9398
$P_{2,2}$ (MW)	154.7092	154.7048	154.8892	155.8322
$P_{2,3}$ (MW)	67.5716	67.5770	65.2717	65.2209
T_{12} (MW)	82.7731	82.7731	82.7652	82.4135
P_{L1} (MW)	9.4268	9.4269	9.4267	9.4193
P_{L2} (MW)	4.1981	4.1890	4.1754	4.2064
Cost ($/h)	12255.38	12255.42	12255.43	12256.23
CPU time (second)	5.9012	5.9219	8.8906	9.6094

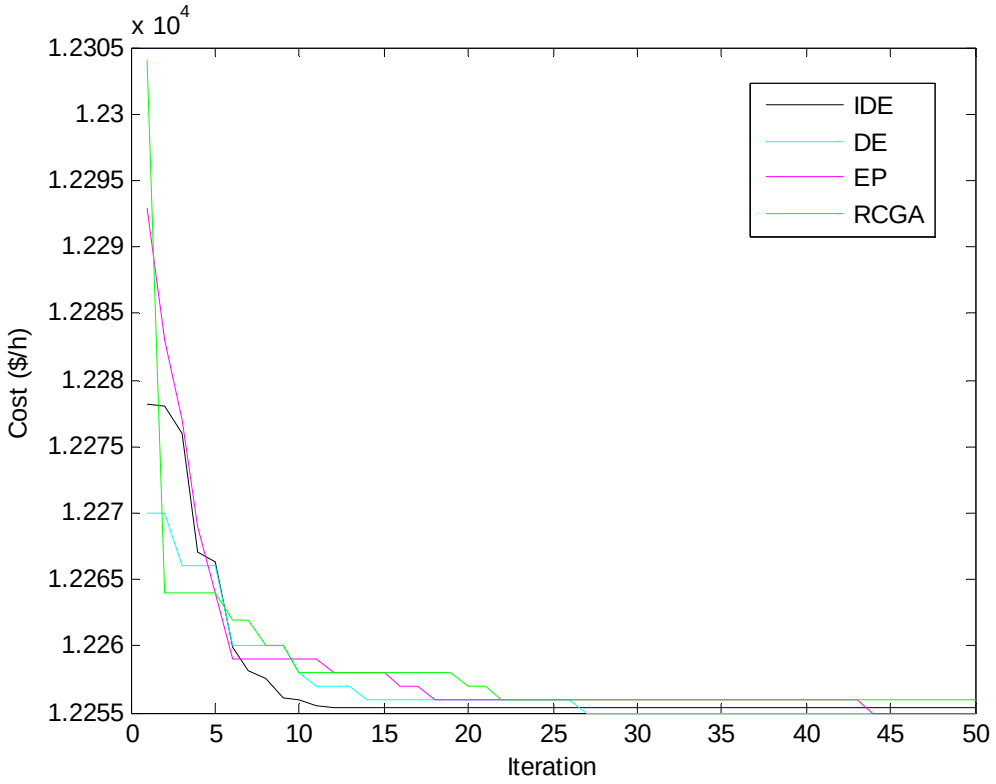

Fig. 5.1. Cost convergence characteristics of IDE,DE,EP,RCGA of Test system 1

5.4.2.Test System 2: This system comprises ten generators with valve-point loading and multi-fuel sources having three fuel options. Transmission loss is considered here. The generator data are taken from [34]. The total load demand is 2700 MW. The 10-generators are divided into three areas. Area 1 consists of the first four units; area 2 includes the next three units and area 3 includes the last three units. The load demand in area 1 is assumed as 50 % of the total demand. The load demand in area 2 is assumed as 25 % and in area 3 is taken as 25 % of the total demand. The power flow limit from area 1 to area 2 or from area 2 to area 1 is 100 MW. The power flow limit from area 1 to area 3 or from area 3 to area 1 is 100 MW. Also the power flow limit from area 2 to area 3 or from area 3 to area 2 is 100 MW. The B-coefficients are given in the appendix.

IDE algorithm is used to solve the problem. Here, the population size (N_P), crossover constant (C_R) and maximum iteration number have been selected 100, 1 and 100 respectively for this test system under consideration.

In order to validate the proposed IDE based approach, the same test system is solved using DE, EP and RCGA. In DE, the population size, scaling factor and crossover constant have been selected as 100, 1.0 and 1.0, respectively. The population size and scaling factor have been selected 100 and 0.1, respectively in case of EP. In RCGA, the population size, crossover and mutation probabilities have been selected as 100, 0.9 and 0.2, respectively. Maximum number of iterations has been selected as 100 for DE, EP and RCGA.

Results obtained from the proposed IDE, DE, EP and RCGA have been presented in Table 5.2. The cost convergence characteristics of this test system obtained from IDE, DE, EP and RCGA are shown in Fig. 5.2.

Table 5.2: Simulation results for Test system 2

	IDE		DE		EP		RCGA	
		Fuel		Fuel		Fuel		Fuel
$P_{1,1}$ (MW)	225.2091	2	225.4448	2	223.8491	2	239.0958	2
$P_{1,2}$ (MW)	212.6498	1	210.1667	1	209.5759	1	216.1166	1
$P_{1,3}$ (MW)	488.0654	2	491.2844	2	496.0680	2	484.1506	2
$P_{1,4}$ (MW)	241.2988	3	240.8956	3	237.9954	3	240.6228	3
$P_{2,1}$ (MW)	247.7606	1	251.0049	1	259.4299	1	259.6639	1
$P_{2,2}$ (MW)	236.4360	3	238.8603	3	228.9422	3	219.9107	3
$P_{2,3}$ (MW)	266.3883	1	264.0906	1	264.1133	1	254.5140	1
$P_{3,1}$ (MW)	236.1927	3	236.9982	3	238.2280	3	231.3565	3
$P_{3,2}$ (MW)	330.9512	1	326.5394	1	331.2982	1	341.9624	1
$P_{3,3}$ (MW)	250.5790	1	250.3339	1	246.6025	1	248.2782	1
T_{21} (MW)	99.9665		99.4680		100		93.1700	
T_{31} (MW)	99.9696		100		100		93.8739	
T_{32} (MW)	34.0383		30.2810		32.5231		43.7824	
P_{L1} (MW)	17.2000		17.2680		17.4884		17.0297	
P_{L2} (MW)	9.6567		9.7688		10.0085		9.7010	
P_{L3} (MW)	8.7150		8.5905		8.6056		8.9408	
Cost ($/h)	653.8516		654.0184		655.1716		657.3325	
CPU time (second)	64.9987		65.0351		78.0625		83.8438	

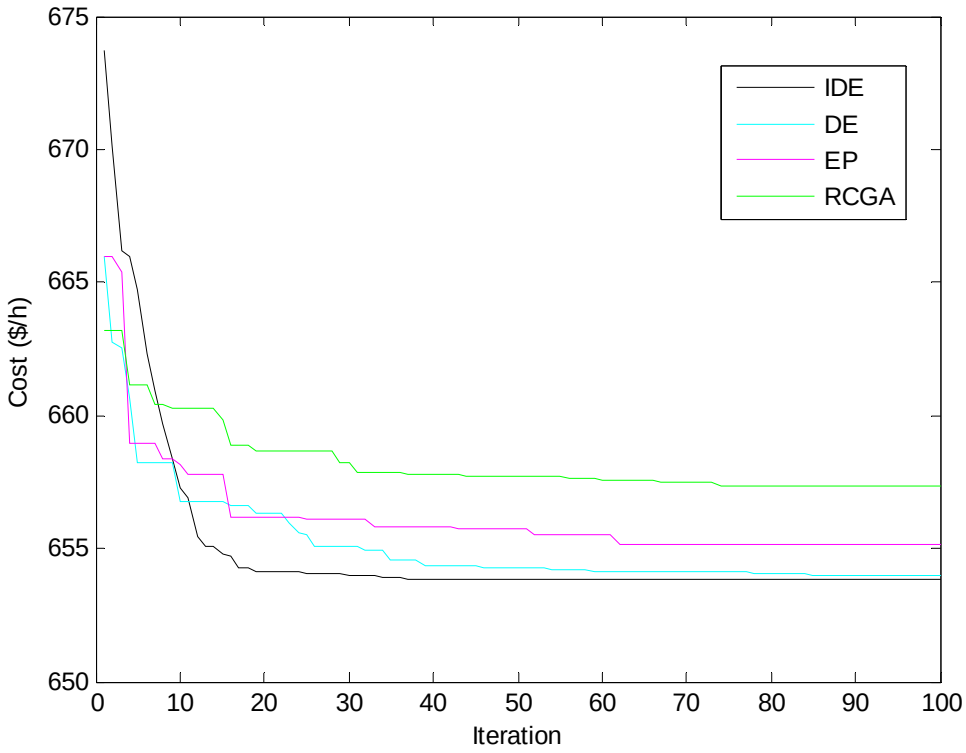

Fig. 5.2. Cost convergence characteristic of IDE ,DE,EP,RCGA of Test system 2

5.4.3. Test System 3: This system comprises forty generators with valve-point loading. The generator data have been taken from [41]. The total load demand is 10500 MW. The forty generators are divided into four areas. Area 1 includes first ten units and 15 % of the total load demand. Area 2 has second ten generators and 40 % of the total load demand. Area 3 consists of third ten generators and 30 % of the total load demand. Area four includes last ten generators and 15 % of the total load demand. The power flow limit from area 1 to area 2 or from area 2 to area 1 is 200 MW. The power flow limit from area 1 to area 3 or from area 3 to area 1 is 200 MW. The power flow limit from area 2 to area 3 or from area 3 to area 2 is 200 MW. The power flow limit from area 4 to area 1 or from area 1 to area 4 is 100 MW. The power flow limit from area 4 to area 2 or from area 2 to area 4 is 100 MW. The power flow limit from area 4 to area 3 or from area 3 to area 4 is 100 MW. Transmission loss is neglected here.

The problem is solved by using IDE algorithm. . For this test system, the population size (N_P), crossover constant (C_R) and maximum iteration number have been selected 200, 1 and 500, respectively.

To validate the proposed IDE based approach, the same test system is solved using DE, EP and RCGA. The population size, scaling factor and crossover constant have been selected as 200, 1.0 and 1.0, respectively in case of DE. In EP, the population size and scaling factor have been selected 200 and 0.1, respectively. In case of RCGA, the population size, crossover and mutation probabilities have been selected as 200, 0.9 and 0.2, respectively. Maximum number of iterations has been selected as 500 for DE, EP and RCGA.

Results obtained from the proposed IDE, DE, EP and RCGA have been depicted in Table 5.3. The cost convergence characteristics of this test system obtained from IDE, DE, EP and RCGA are shown in Fig. 5.3.

Table 5.3: Simulation results for Test system 3

Power (MW)	IDE	DE	EP	RCGA	Power (MW)	IDE	DE	EP	RCGA
$P_{1,1}$	111.0210	111.5448	107.6644	95.7552	$P_{3,4}$	523.3661	523.4073	525.7752	518.1120
$P_{1,2}$	111.2493	111.7092	112.0673	88.5828	$P_{3,5}$	523.3068	523.7703	531.2092	538.1994
$P_{1,3}$	97.4051	98.2429	91.8132	97.6063	$P_{3,6}$	523.3044	523.5424	513.5659	527.4775
$P_{1,4}$	179.7467	179.8834	175.3171	126.4966	$P_{3,7}$	10.0000	10.1621	11.3612	24.4133
$P_{1,5}$	92.2492	95.9500	92.4242	71.0127	$P_{3,8}$	10.0267	10.1326	10.0000	28.9856
$P_{1,6}$	139.9723	139.3533	112.5634	116.3866	$P_{3,9}$	10.0188	10.6366	10.0000	28.8571
$P_{1,7}$	259.6164	259.3395	257.5370	244.5857	$P_{3,10}$	88.9325	88.1189	78.3523	87.9016
$P_{1,8}$	284.6065	285.3569	297.3619	210.6920	$P_{4,1}$	189.9994	161.2220	162.4480	159.7482
$P_{1,9}$	284.6489	284.9627	285.2035	236.1685	$P_{4,2}$	190.0000	189.5668	166.3508	153.6255
$P_{1,10}$	130.0838	130.2217	134.5862	130.1286	$P_{4,3}$	189.9957	189.9240	190.0000	160.4706
$P_{2,1}$	94.00477	243.6005	162.4313	367.4862	$P_{4,4}$	165.1003	165.6621	178.4541	169.9359
$P_{2,2}$	243.6037	95.3890	217.8387	297.9501	$P_{4,5}$	165.0921	165.4321	168.0752	168.5220
$P_{2,3}$	214.7675	214.5171	125.0000	394.9246	$P_{4,6}$	165.0804	164.9868	174.4529	172.2638
$P_{2,4}$	394.3151	394.0808	384.0187	370.3473	$P_{4,7}$	89.2760	109.8137	77.3875	91.2423
$P_{2,5}$	394.2897	394.2481	397.6902	455.7123	$P_{4,8}$	109.99459	109.7935	90.1059	86.4778
$P_{2,6}$	394.2725	394.4360	407.4993	393.9673	$P_{4,9}$	90.76587	90.1543	109.5654	88.3627
$P_{2,7}$	489.2777	489.9552	500.0000	424.1994	$P_{4,10}$	458.7993	459.1140	549.0335	279.2691
$P_{2,8}$	489.2944	488.8885	480.8874	484.5498	T_{12}	181.4527	172.0652	200	- 71.7855
$P_{2,9}$	511.2936	511.4713	524.8487	528.4148	T_{31}	20.2524	-36.3060	17.5885	161.9336
$P_{2,10}$	511.3452	511.4125	499.7857	511.3403	T_{32}	188.1426	191.1128	200	95.2833
$P_{3,1}$	523.2950	523.2896	523.4522	525.4497	T_{41}	45.6004	86.8070	90.8733	-76.1340
$P_{3,2}$	523.2812	523.2950	526.5051	510.7391	T_{42}	93.9398	98.8231	100	-52.3900
$P_{3,3}$	523.2996	523.4129	537.3675	533.6399	T_{43}	99.5636	45.0391	100	83.4418
Cost ($)						121682.59	121794.8	123591.9	128046.5

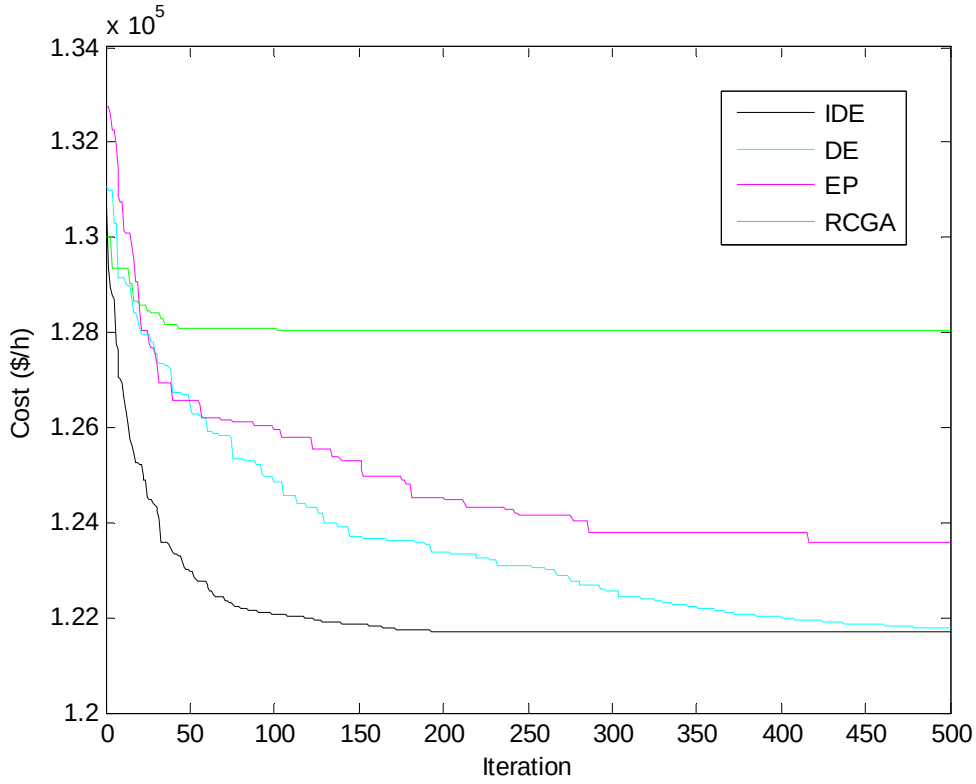

Fig. 5.3. Cost convergence characteristic of IDE ,DE,EP,RCGA of Test system 3

5.5. Conclusion

Here, IDE algorithm has been successfully implemented to solve MAED problems. The effectiveness of the proposed method is illustrated by using three different test systems and the test results are compared with those obtained from DE, EP and RCGA. It has been observed from the comparison that the proposed IDE has the ability to converge to a better quality solution and exhibit more robustness than DE, EP and RCGA. It is also clear from the results obtained by different trials that the proposed IDE algorithm can avoid the shortcoming of premature convergence. Due to these properties, the IDE algorithm in future can be tried for the solution of complex power system optimization problems.

5.6. Application of GSO method

Here, the performance of the proposed group search optimization (GSO) method has been evaluated by using three test systems. In order to show the effectiveness of the proposed GSO method, differential evolution (DE), evolutionary programming (EP) and real coded genetic algorithm (RCGA) have been applied to the same three test systems. All the algorithms i.e. GSO, DE, EP, and RCGA used in this paper for solving multi-area economic dispatch (MAED) problem are implemented by using MATLAB 7.0 on a PC (Pentium-IV, 80 GB, 3.0 GHz).

5.6.1. Test System 1: This system consists of two areas. Each area consists of three generators with prohibited operating zones. Transmission loss is considered here. The generator data has modified from [30]. The generator data and B-coefficients are given in the Appendix-1. The percentage of the total load demand in area 1 is 60% and 40% in area 2. The total load demand is 1263 MW and power flow limit of the system is 100 MW.

The problem is solved by using GSO. For this test system, Here, the population size (N_P) and maximum iteration number have been selected 100 and 50, respectively.

To validate the proposed GSO based approach, the same test system is solved using differential evolution (DE), evolutionary programming (EP) and real coded genetic algorithm (RCGA). The population size, scaling factor and crossover constant have been selected as 100, 1.0 and 1.0 ,respectively, in case of DE. In case of EP, the population size and scaling factor have been selected 100 and 0.1 respectively. In RCGA, the population size, crossover and mutation probabilities have been selected as 100, 0.9 and 0.2 respectively. Maximum number of iterations has been selected 50 for DE, EP and RCGA.

Results obtained from proposed GSO, DE, EP and RCGA have been summarized in Table 5.4. The cost convergence characteristics of this test system obtained from GSO, DE, EP and RCGA are shown in Fig. 5.4.

Table 5.4: Simulation results for Test system 1

	GSO	DE	EP	RCGA
$P_{1,1}$ (MW)	500.0000	500.0000	500.0000	500.0000
$P_{1,2}$ (MW)	200.0000	200.0000	200.0000	200.0000
$P_{1,3}$ (MW)	150.0000	150.0000	149.9919	149.6328
$P_{2,1}$ (MW)	204.3345	204.3341	206.4493	205.9398
$P_{2,2}$ (MW)	154.7030	154.7048	154.8892	155.8322
$P_{2,3}$ (MW)	67.5784	67.5770	65.2717	65.2209
T_{12} (MW)	82.7731	82.7731	82.7652	82.4135
P_{L1} (MW)	9.4269	9.4269	9.4267	9.4193
P_{L2} (MW)	4.1890	4.1890	4.1754	4.2064
Cost ($/h)	12255.38	12255.42	12255.43	12256.23
CPU time (second)	5.0324	**5.9219**	8.8906	**9.6094**

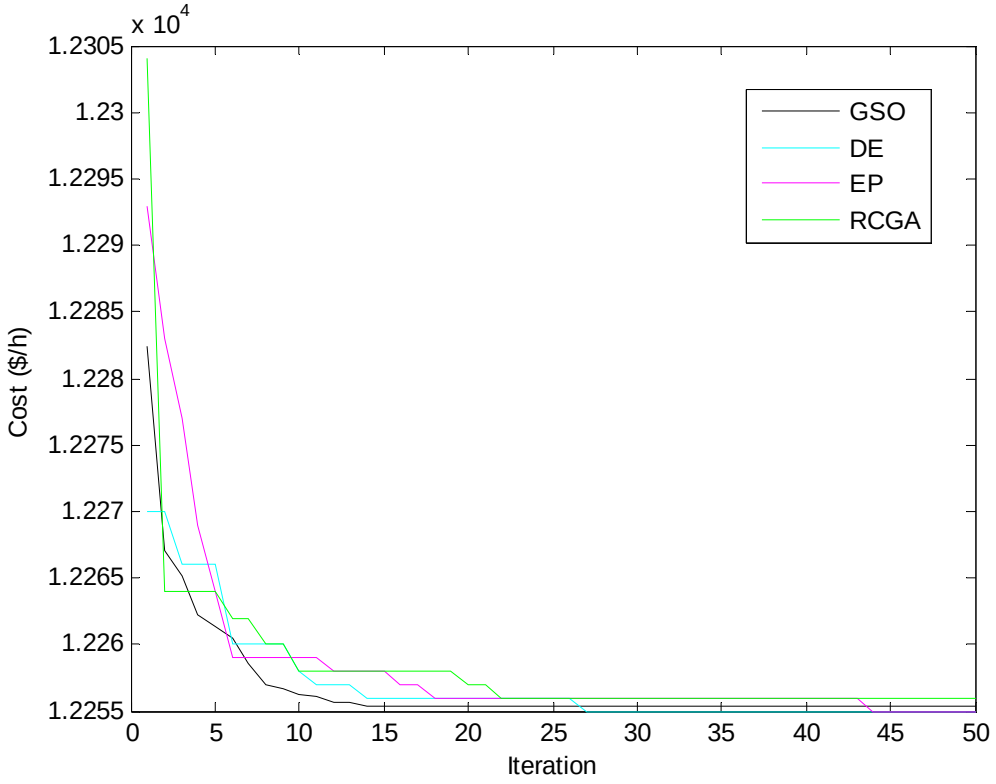

Fig. 5.4. Cost convergence characteristic of GSO ,DE,EP,RCGA Test system 1

5.6.2. Test System 2: This system comprises ten generators with valve-point loading and multi-fuel sources having three fuel options. Transmission loss is considered here. The generator data have been taken from [34]. The total load demand is 2700 MW. The ten generators are divided into three areas. Area 1 consists of the first four units; area 2 includes the next three units and area 3 includes the last three units. The load demand in area 1 is assumed as 50 % of the total demand. The load demand in area 2 is assumed as 25 % and in area 3 is taken as 25 % of the total demand. The power flow limit from area 1 to area 2 or from area 2 to area 1 is 100 MW. The power flow limit from area 1 to area 3 or from area 3 to area 1 is 100 MW. Also the power flow limit from area 2 to area 3 or from area 3 to area 2 is 100 MW. The B-coefficients are given in the appendix.

GSO method is used to solve the problem. Here, the population size (N_P) and maximum iteration number have been selected 100 and 100, respectively, for this test system under consideration.

In order to validate the proposed GSO based approach, the same test system is solved using DE, EP and RCGA. In DE, the population size, scaling factor and crossover constant have been selected as 100, 1.0 and 1.0, respectively. The population size and scaling factor have been selected 100 and 0.1 respectively in case of EP. In RCGA, the population size, crossover and mutation probabilities have been selected as 100, 0.9 and 0.2, respectively. Maximum number of iterations has been selected 100 for DE, EP and RCGA.

Results obtained from proposed GSO, DE, EP and RCGA have been presented in Table 5.5. The cost convergence characteristic of this test system obtained from GSO, DE, EP and RCGA is shown in Fig. 5.5.

Table 5.5: Simulation results for Test system 2

	GSO		DE		EP		RCGA	
		Fuel		Fuel		Fuel		Fuel
$P_{1,1}$ (MW)	225.7002		220.2200	2	223.8491	2	239.0958	2
$P_{1,2}$ (MW)	212.1994		212.1510	1	209.5759	1	216.1166	1
$P_{1,3}$ (MW)	487.3917		493.2287	2	496.0680	2	484.1506	2
$P_{1,4}$ (MW)	242.1126		242.3742	3	237.9954	3	240.6228	3
$P_{2,1}$ (MW)	250.8376		251.5901	1	259.4299	1	259.6639	1
$P_{2,2}$ (MW)	234.9589		234.5500	3	228.9422	3	219.9107	3
$P_{2,3}$ (MW)	264.0710		268.1343	1	264.1133	1	254.5140	1
$P_{3,1}$ (MW)	236.7312		234.9833	3	238.2280	3	231.3565	3
$P_{3,2}$ (MW)	332.0932		328.5371	1	331.2982	1	341.9624	1
$P_{3,3}$ (MW)	249.4448		250.1525	1	246.6025	1	248.2782	1
T_{21} (MW)	99.7121		99.4945		100		93.1700	
T_{31} (MW)	100		99.9849		100		93.8739	
T_{32} (MW)	34.5573		30.0535		32.5231		43.7824	
P_{L1} (MW)	17.1160		17.5000		17.4884		17.0297	
P_{L2} (MW)	9.7127		9.8334		10.0085		9.7010	
P_{L3} (MW)	8.7118		8.6345		8.6056		8.9408	
Cost ($/h)	654.0572		654.0811		655.1716		657.3325	
CPU time (second)	64.0387		65.0351		78.0625		83.8438	

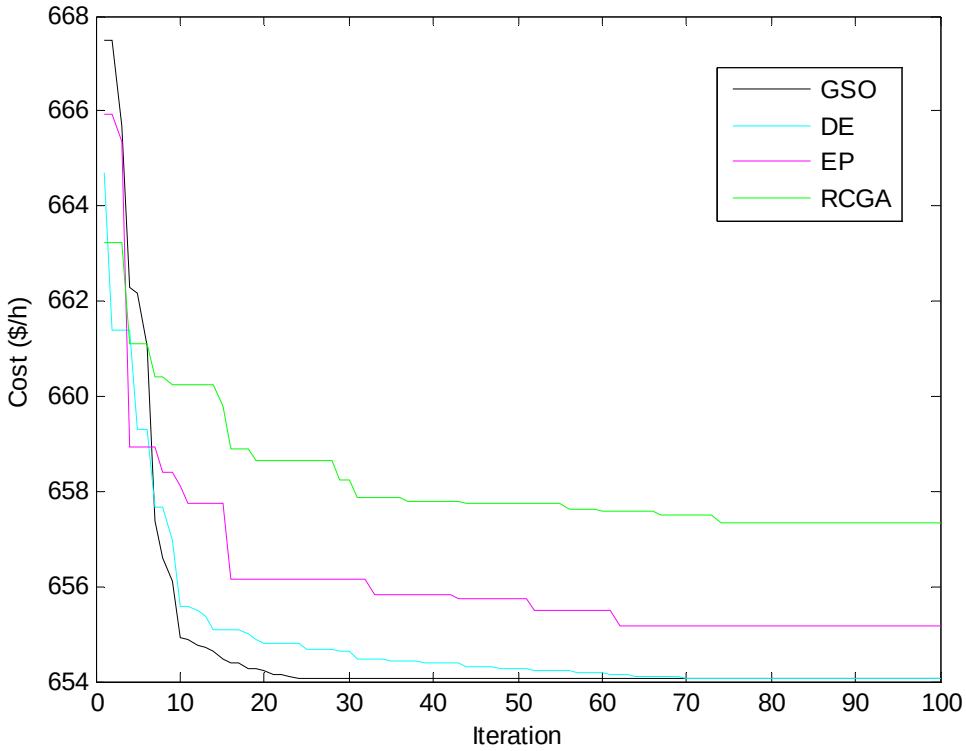

Fig. 5.5. Cost convergence characteristic of ,GSO ,DE,EP,RCGA for Test system 2

Test System 3: This system comprises forty generators with valve-point loading. The generator data have been taken from [41]. The total load demand is 10500 MW. The forty generators are divided into four areas. Area 1 includes first ten units and 15 % of the total load demand. Area 2 has second ten generators and 40 % of the total load demand. Area 3 consists of third ten generators and 30 % of the total load demand. Area four includes last ten generators and 15 % of the total load demand. The power flow limit from area 1 to area 2 or from area 2 to area 1 is 200 MW. The power flow limit from area 1 to area 3 or from area 3 to area 1 is 200 MW. The power flow limit from area 2 to area 3 or from area 3 to area 2 is 200 MW. The power flow limit from area 4 to area 1 or from area 1 to area 4 is 100 MW. The power flow limit from area 4 to area 2 or from area 2 to area 4 is 100 MW. The power flow limit from area 4 to area 3 or from area 3 to area 4 is 100 MW. Transmission loss is neglected here.

The problem is solved by using GSO. For this test system, the population size (N_P) and maximum iteration number have been selected 200 and 500, respectively.

To validate the proposed GSO based approach, the same test system is solved using DE, EP and RCGA. The population size, scaling factor and crossover constant have been selected as 200, 1.0 and 1.0, respectively, in case of DE. In EP, the population size and scaling factor have been selected 200 and 0.1, respectively. In case of RCGA, the population size, crossover and mutation probabilities have been selected as 200, 0.9 and 0.2, respectively. Maximum number of iterations has been selected 500 for DE, EP and RCGA.

Results obtained from the proposed GSO, DE, EP and RCGA have been depicted in Table 5.6. The cost convergence characteristic of this test system obtained from GSO, DE, EP and RCGA is shown in Fig. 5.6.

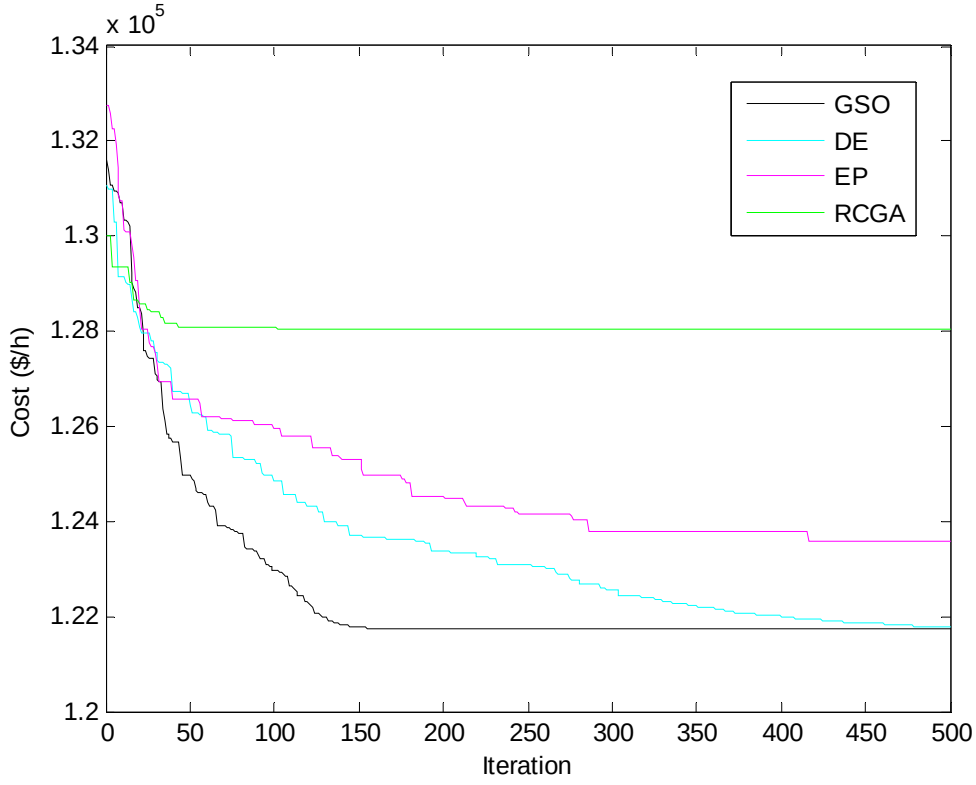

Fig. 5.6. Cost convergence characteristic of GSO,DE,EP,RCGA for Test system 3

Table 5.6: Simulation results for Test system 3

Power (MW)	GSO	DE	EP	RCGA	Power (MW)	GSO	DE	EP	RCGA
$P_{1,1}$	113.1055	111.5448	107.6644	95.7552	$P_{3,4}$	523.2764	523.4073	525.7752	518.1120
$P_{1,2}$	111.4605	111.7092	112.0673	88.5828	$P_{3,5}$	523.2811	523.7703	531.2092	538.1994
$P_{1,3}$	97.4011	98.2429	91.8132	97.6063	$P_{3,6}$	523.2820	523.5424	513.5659	527.4775
$P_{1,4}$	179.7327	179.8834	175.3171	126.4966	$P_{3,7}$	10.0021	10.1621	11.3612	24.4133
$P_{1,5}$	88.0580	95.9500	92.4242	71.0127	$P_{3,8}$	10.0001	10.1326	10.0000	28.9856
$P_{1,6}$	139.9988	139.3533	112.5634	116.3866	$P_{3,9}$	10.0006	10.6366	10.0000	28.8571
$P_{1,7}$	259.6082	259.3395	257.5370	244.5857	$P_{3,10}$	96.9950	88.1189	78.3523	87.9016
$P_{1,8}$	284.6292	285.3569	297.3619	210.6920	$P_{4,1}$	189.9978	161.2220	162.4480	159.7482
$P_{1,9}$	284.6025	284.9627	285.2035	236.1685	$P_{4,2}$	160.5677	189.5668	166.3508	153.6255
$P_{1,10}$	130.0060	130.2217	134.5862	130.1286	$P_{4,3}$	189.9996	189.9240	190.0000	160.4706
$P_{2,1}$	168.8025	243.6005	162.4313	367.4862	$P_{4,4}$	164.8009	165.6621	178.4541	169.9359
$P_{2,2}$	168.7990	95.3890	217.8387	297.9501	$P_{4,5}$	164.8567	165.4321	168.0752	168.5220
$P_{2,3}$	304.5216	214.5171	125.0000	394.9246	$P_{4,6}$	164.8847	164.9868	174.4529	172.2638
$P_{2,4}$	394.2822	394.0808	384.0187	370.3473	$P_{4,7}$	109.9983	109.8137	77.3875	91.2423
$P_{2,5}$	394.2821	394.2481	397.6902	455.7123	$P_{4,8}$	94.4214	109.7935	90.1059	86.4778
$P_{2,6}$	304.5222	394.4360	407.4993	393.9673	$P_{4,9}$	109.9990	90.1543	109.5654	88.3627
$P_{2,7}$	489.2911	489.9552	500.0000	424.1994	$P_{4,10}$	458.8241	459.1140	549.0335	279.2691
$P_{2,8}$	489.2790	488.8885	480.8874	484.5498	T_{12}	164.2681	172.0652	200	- 71.7855
$P_{2,9}$	511.2789	511.4713	524.8487	528.4148	T_{31}	6.9173	-36.3060	17.5885	161.9336
$P_{2,10}$	511.2980	511.4125	499.7857	511.3403	T_{32}	199.3783	191.1128	200	95.2833
$P_{3,1}$	523.2852	523.2896	523.4522	525.4497	T_{41}	43.7481	86.8070	90.8733	-76.1340
$P_{3,2}$	523.2845	523.2950	526.5051	510.7391	T_{42}	99.9969	98.8231	100	-52.3900
$P_{3,3}$	523.2835	523.4129	537.3675	533.6399	T_{43}	89.6051	45.0391	100	83.4418
Coat ($)						121722.35	121794.8	123591.9	128046.5

5.7. Conclusion

Here, GSO has been successfully implemented to solve MAED problems. The effectiveness of the proposed method is illustrated by using three different test systems and the test results are compared with those obtained from DE, EP and RCGA. It has been observed from the comparison that the proposed GSO has the ability to converge to a better quality solution than DE, EP and RCGA. Due to this property, the GSO method in future can be tried for the solution of complex power system optimization problems.

CHAPTER 6

Multi-area Economic Environmental Dispatch

1. Introduction

The generation of electricity from fossil fuel releases sulfur oxides (SO_x), nitrogen oxides (NO_x), and carbon dioxide (CO_2) into atmosphere. Atmospheric pollution affects not only human beings but also other life-forms such as animals, birds, fish and plants. It also causes damage to vegetation, acid rain, reducing visibility as well as causing global warming. The increased concern over environmental protection and the passage of the clean air act amendments of 1990 have forced the power utilities to reduce their emissions. So today's concern is to produce electricity not only at the cheapest possible price, but also at minimum level of pollution.

Several strategies have been proposed to reduce the atmospheric pollution. These include installation of post combustion cleaning equipment, switching to low emission fuels, replacement of the aged fuel burners with cleaner ones, and dispatching with emission considerations. The first three options require installation of new equipment and/or modification of the existing ones that involve considerable capital outlay and hence they can be considered as long-term options. So,the latter option is preferred.

The two objectives i.e. cost and emission are conflicting in nature and both of them have to be considered simultaneously to find overall optimal dispatch. Economic environmental dispatch (EED) shows how to schedule the committed generator outputs with the predicted load demand in a single area so as to optimize both cost and emission simultaneously while fulfilling the operating constraints. Different techniques have been reported in the literature pertaining to EED problem.

Generally, the generators are divided into several generation areas interconnected by tie-lines. Multi-area economic dispatch (MAED) determines the generation levels and interchange powers between areas such that total fuel cost considering all the areas minimized while satisfying power balance constraints, generating limits constraints and tie-line capacity constraints. Several researches have been conducted to deal with MAED.

Multi-area economic environmental dispatch (MAEED) is an extension of economic environmental dispatch. MAEED determines the generation levels and interchange power between areas such that total fuel cost and emission levels in all areas are optimized simultaneously while satisfying power balance constraints, generating limit constraints and tie-line capacity constraints.

Here, multiobjective differential evolution (MODE) is proposed for multi-area economic environmental dispatch (MAEED) problem. This problem is formulated as a nonlinear constrained multiobjective optimization problem. In order to show the effectiveness of the proposed approach, a 4-area test system is used in this thesis. Results obtained from the proposed approach have been compared with those obtained from strength pareto evolutionary algorithm 2 (SPEA 2).

6.2. Problem Formulation

The objective of MAEED is to optimize the total cost and emission level simultaneously of supplying loads to all areas while satisfying power balance constraints, generating limits constraints and tie-line capacity constraints. The following objectives and constraints are taken into account in the formulation of MAEED problem.

Objectives:

(i) Cost

The fuel cost function of each fossil fuel fired generator, considering the valve-point effect, is expressed as the sum of a quadratic and a sinusoidal function. The total fuel cost of committed generators of all areas can be expressed as

$$F_c = \sum_{i=1}^{\mathrm{N}} \sum_{j=1}^{\mathrm{M}_i} F_{cij}\left(\mathrm{P}_{ij}\right) = \sum_{i=1}^{\mathrm{N}} \sum_{j=1}^{\mathrm{M}_i} a_{ij} + b_{ij}\mathrm{P}_{ij} + c_{ij}\mathrm{P}_{ij}^2 + \left| d_{ij} \times \sin\left\{ e_{ij} \times \left(\mathrm{P}_{ij}^{\min} - \mathrm{P}_{ij}\right)\right\}\right| \tag{6.1}$$

where $F_{cij}\left(\mathrm{P}_{ij}\right)$ is the cost function of j th generator in area i; a_{ij}, b_{ij}, c_{ij}, d_{ij} and e_{ij} are the cost coefficients of j th generator in area i; N is the number of areas, M_i is the

number of committed generators in area i; P_{ij} is the real power output of j th generator in area i.

(ii) Emission

The atmospheric pollutants such as sulfur oxides (SO_x), nitrogen oxides (NO_x) and carbon dioxide (CO_2) caused by fossil fuel fired generator can be modeled separately. However, for comparison purposes, the total emission of these pollutants is expressed as the sum of a quadratic and an exponential function. The total emission of committed generators of all areas can be expressed as

$$F_e = \sum_{i=1}^{N}\sum_{j=1}^{M_i} F_{eij}\left(P_{ij}\right) = \sum_{i=1}^{N}\sum_{j=1}^{M_i} \alpha_{ij} + \beta_{ij}P_{ij} + \gamma_{ij}P_{ij}^2 + \eta_{ij}\exp\left(\delta_{ij}P_{ij}\right) \tag{6.2}$$

where $F_{eij}\left(P_{ij}\right)$ is the emission function of j th generator in area i; α_{ij}, β_{ij}, γ_{ij}, η_{ij} and δ_{ij} are the emission coefficients of j th generator in area i.

Constraints:

(i) Real power balance constraint

$$\sum_{j=1}^{M_i} P_{ij} = P_{Di} + P_{Li} + \sum_{k,k\neq i} T_{ik} \qquad i \in N \tag{6.3}$$

where P_{Di} is the real power demand of area i; T_{ik} is the tie line real power transfer from area i to area k. T_{ik} is positive when power flows from area i to area k and T_{ik} is negative when power flows from area k to area i.

(ii) Tie line capacity constraints

The tie line real power transfer T_{ik} from area i to area k should not exceed the tie line transfer capacity for security consideration.

$$-T_{ik}^{max} \le T_{ik} \le T_{ik}^{max} \tag{6.4}$$

where T_{ik}^{max} is the power flow limit from area i to area k and $-T_{ik}^{max}$ is the power flow limit from area k to area i.

(iii) Real power generation capacity constraints

The real power generated by each generator should be within its lower limit P_{ij}^{min} and upper limit P_{ij}^{max}, so that

$$P_{ij}^{min} \le P_{ij} \le P_{ij}^{max} \qquad i \in N \text{ and } j \in M_i \tag{6.5}$$

6.3. Simulation Results

A 4-area test system consisting of four generators in each area with nonsmooth fuel cost and emission level functions is used in this paper to demonstrate the performance of the proposed MODE method. The generator data and tie line transfer limits are given in Table A-1 and Table A-2 in the Appendices. Load demands in area 1, area 2, area 3 and area 4 are 30 MW, 50 MW, 40 MW and 60 MW ,respectively. The software has been written in MATLAB 7 on a PC (Pentium – IV, 80 GB, 3.0 GHZ).

Total fuel cost and emission objectives are minimized individually by using differential evolution (DE) in order to explore the extreme points of the trade-off surface.

The population size, maximum number of generations, scaling factor and crossover constant have been selected as 100, 500, 1.0 and 0.7, respectively,for this test system under consideration. It is seen that under the cost minimization criterion, fuel cost is 1521.94 $/hr and emission is 277.1573 $lb/$ hr. But cost increases to 2855.31 $/hr and emission decreases to 250.6933 $lb/$ hr for the case of emission minimization. Fig. 6.1 shows convergence of cost and emission.

MODE has been applied to optimize both cost and emission objectives simultaneously. In this case the population size, maximum number of generations, scaling factor and crossover constant have been selected as 20, 50, 1.0 and 0.7, respectively for this test system. It is seen that cost is 2132.72 $/hr which is more than 1521.94 $/hr and less than

2855.31 $/hr and emission is 261.4986 lb / hr which is less than 277.1573 lb / hr and more than 250.6933 lb / hr.

In order to show the effectiveness of the proposed MODE, SPEA 2 has been applied to solve MAEED problem. The population size, crossover and mutation probabilities and the maximum number of generations have been selected as 20, 0.9, 0.2 and 50 respectively.

Results obtained from proposed MODE and SPEA 2 corresponding to the best compromise solution of the last generation are summarized in Table 6.1. Minimum cost and minimum emission obtained by using DE are also given in Table 6.1.

The distribution of 20 nondominated solutions obtained in the last generation of proposed MODE and SPEA 2 is shown in Fig.6.2.

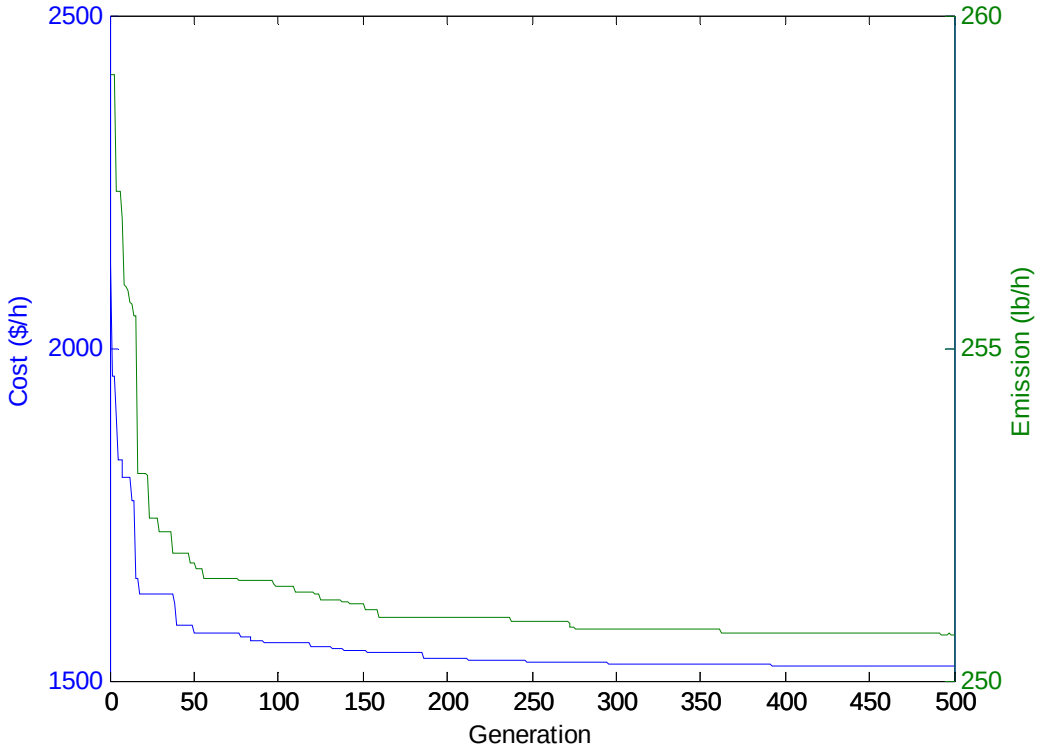

Fig. 6.1. Cost and emission convergence characteristics of MODE & SPEA2

Table 6.1: Simulation results for MODE & SPEA-2 Test system

	Minimum cost	Minimum emission	MODE	SPEA 2
$P_{1,1}$ (MW)	6.4086	0.0500	0.0500	3.7801
$P_{1,2}$ (MW)	0.0889	0.0500	0.0500	1.9565
$P_{1,3}$ (MW)	0.0500	13.0000	13.0000	9.0004
$P_{1,4}$ (MW)	11.4642	11.9042	11.3288	9.0604
$P_{2,1}$ (MW)	8.4984	25.0000	4.8129	13.9816
$P_{2,2}$ (MW)	0.5204	11.9068	12.0000	8.0030
$P_{2,3}$ (MW)	20.0000	9.3987	19.8703	17.5303
$P_{2,4}$ (MW)	17.9927	11.4347	15.5994	15.6876
$P_{3,1}$ (MW)	0.0500	12.4807	8.2807	14.2898
$P_{3,2}$ (MW)	22.2896	9.7328	6.3315	6.8935
$P_{3,3}$ (MW)	10.5197	10.9974	7.8585	3.3478
$P_{3,4}$ (MW)	15.5179	10.4942	17.0962	18.2130
$P_{4,1}$ (MW)	4.8804	11.0000	7.4932	7.1157
$P_{4,2}$ (MW)	13.3469	16.9329	19.3730	13.0403
$P_{4,3}$ (MW)	29.7653	13.8588	16.4536	18.8948
$P_{4,4}$ (MW)	18.6070	11.7588	20.4019	19.2051
T_{21} (MW)	5.9952	5.7402	6.0000	4.3529
T_{13} (MW)	-3.9935	0.6949	1.7021	-1.5756
T_{14} (MW)	-1.9997	0.0495	-1.2733	-0.2741
T_{32} (MW)	3.4837	3.5000	1.1060	1.0910
T_{24} (MW)	-5.5000	5.5000	-2.6114	1.9407
T_{34} (MW)	0.9000	0.9000	0.1629	0.0775
Cost ($/hr)	1521.94	2855.31	2132.72	2294.82
Emission (lb / hr)	277.1573	250.6933	261.4986	263.5606
CPU Time (Sec)	30.2435	32.3674	2.0254	2.8543

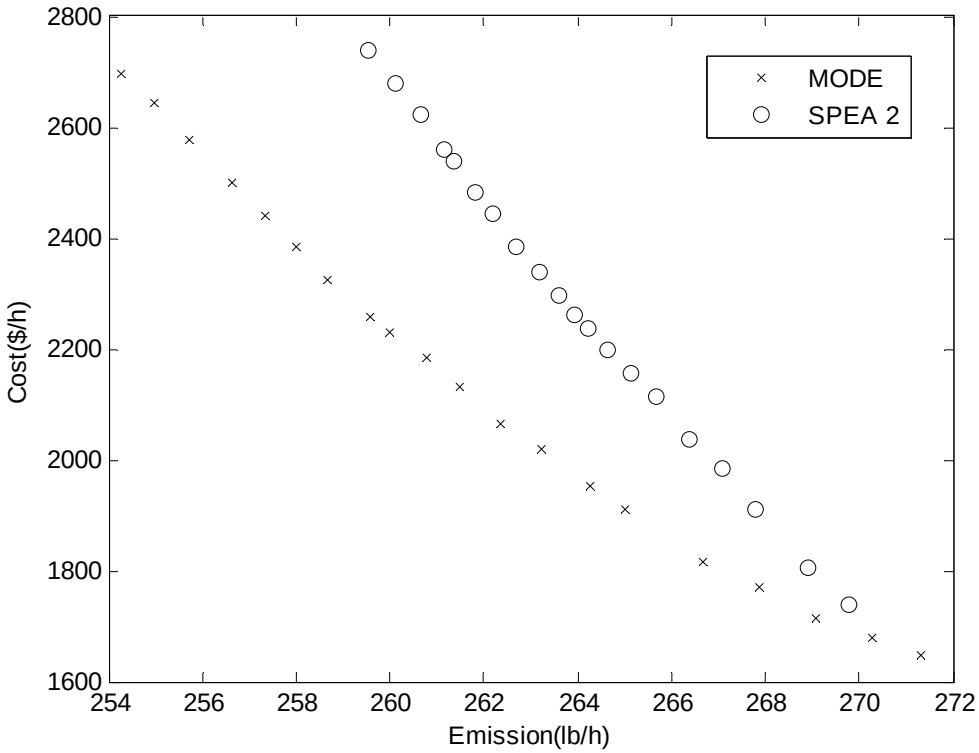

Fig.6.2. Pareto-optimal front obtained from proposed MODE and SPEA 2 in the last generation

6.4. Conclusion

Here, multi-objective differential evolution has been implemented to solve multi-area economic environmental dispatch problem. Results obtained from the proposed approach have been compared to those obtained from strength pareto evolutionary algorithm 2. The proposed multi-objective differential evolution is simple, robust and efficient. It does not impose any limitation on the number of objectives and can be extended to include more objectives.

CHAPTER 7

Fuel Constrained Economic Emission Dispatch

1. INTRODUCTION

Economic emission dispatch involves the allocation of generations among the committed generating units so as to optimize both the fuel cost and emission level simultaneously while satisfying the several operating constraints.

Some power utilities have encountered a new dispatch problem, perhaps more significant than economic emission dispatch problem because of the sudden concern over fuel shortages. Fuel suppliers have imposed increased constraints in their fuel supply contracts to the point that utilities have been forced to reschedule generation on the basis of fuel availability. This has occurred about because certain fuels are no longer available or available only in a limited supply or cut off from certain power plants. Thus, strict economic emission dispatch has become impossible. There are no automatic ties between unit fuel availability and desired power production for that unit.

With the ever increasing proportion of the fuel budget in the total operating cost and increasing concern over the environmental consideration, fuel constrained economic emission dispatch problem has popped up.

Several papers have been published in the area of fuel scheduling of thermal units [94]-[97]. The fuel constrained economic emission dispatch problem is a multi-objective mathematical programming problem which is concerned with the attempt to optimize both the fuel cost and emission level simultaneously while satisfying the standard load constraints and fuel constraints. The fuel constrained economic emission dispatch problem may be solved by dividing the total time period involved into discrete time increments. Each of the objectives is a function of one or more variables from only one time step. Some constraints are made up of variables drawn from one time step whereas others span two or more time steps.

Over the past few years, several researches have been done on the development of multi-objective evolutionary search strategies. Non-dominating sorting genetic algorithm II

(NSGA II), multi-objective evolutionary algorithm (MOEA), multi-objective particle swarm optimization, fuzzy clustering-based particle swarm optimization (FCPSO) etc., constitute the pioneering multi-objective approaches that have been applied to solve the economic emission dispatch (EED) problem. These methods are population-based techniques and multiple pareto-optimal solutions can be found in one single run.

Here, multi-objective differential evolution (MODE) is proposed for solving fuel constrained economic emission dispatch (FCEED) problem of thermal generating units. This problem is formulated as a nonlinear constrained multi-objective optimization problem. The proposed method is validated by applying it to a test system. Results obtained from the proposed method are compared with those obtained from strength pareto evolutionary algorithm 2 (SPEA 2).

7.2. PROBLEN FORMULATION

For convenience the entire scheduling period is divided into a number of sub intervals each having a constant load demand. The system has N thermal generating units over M time intervals. The following objectives and constraints are taken into account in the formulation of fuel constrained economic emission dispatch (FCEED) problem.

7.2.1. Objectives

7.2.1.1. Economy

The total fuel cost in terms of power output considering the valve-point effect, can be expressed as

$$F_c = \sum_{m=1}^{M}\sum_{i=1}^{N} t_m \left[a_i + b_i \mathrm{P}_{im} + c_i \mathrm{P}_{im}^2 + \left| d_i \sin\left\{ e_i \left(\mathrm{P}_i^{\min} - \mathrm{P}_{im} \right) \right\} \right| \right] \tag{7.1}$$

7.2.1.2. Emission

The fossil-based generating stations are the primary sources of nitrogen oxides. The total NO_x emission level from all the units in the system can be expressed as

$$F_e = \sum_{m=1}^{\mathrm{M}} \sum_{i=1}^{\mathrm{N}} t_m \left[\alpha_i + \beta_i \mathrm{P}_{im} + \gamma_i \mathrm{P}_{im}^2 + \sigma_i \exp\left(\theta_i \mathrm{P}_{im}\right) \right] \tag{7.2}$$

7.2.2. Constraints

7.2.2.1. Power balance constraints

At each interval, the total active power generation must balance the predicted power demand.

$$\sum_{i=1}^{\mathrm{N}} \mathrm{P}_{im} - \mathrm{P}_{Dm} = 0 \text{ , } m \in \mathrm{M} \tag{7.3}$$

7.2.2.2 Fuel delivery constraints

At each interval, summation of fuel delivered to all units must be equal to fuel supplied by the supplier.

$$\sum_{i=1}^{\mathrm{N}} F_{im} - F_{Dm} = 0 \text{ , } m \in \mathrm{M} \tag{7.4}$$

7.2.2.3. Fuel storage constraints

The volume of fuel at each unit at the beginning of each interval plus delivery of fuel to that unit minus the fuel burned at that unit gives the fuel remaining at the beginning of the next interval.

$$V_{im} = V_{i(m-1)} + F_{im} - t_m \left(\eta_i + \delta_i \mathrm{P}_{im} + \mu_i \mathrm{P}_{im}^2 \right), \; i \in \mathrm{N} \text{ , } m \in \mathrm{M} \tag{7.5}$$

7.2.2.4. Generation limits

The power generated by each unit at each interval should be within its lower limit $\mathrm{P}^{\min}$ and upper limit $\mathrm{P}^{\max}$. So that

$$\mathrm{P}_i^{\min} \le \mathrm{P}_{im} \le \mathrm{P}_i^{\max} \text{ , } i \in \mathrm{N} \text{ , } m \in \mathrm{M} \tag{7.6}$$

7.2.2.5. Fuel delivery limits

The fuel delivered to each unit at each interval should be within its lower limit $F^{\min}$ and upper limit $F^{\max}$. So that

$$F_i^{\min} \le F_{im} \le F_i^{\max} \ , \ i \in \mathrm{N} \ , \ m \in \mathrm{M} \tag{7.7}$$

7.2.2.6. Fuel storage limits

The fuel storage limit of each unit at each interval should be within its lower limit $V^{\min}$ and upper limit $V^{\max}$. So that

$$V_i^{\min} \le V_{im} \le V_i^{\max} \ , \ i \in \mathrm{N} \ , \ m \in \mathrm{M} \tag{7.8}$$

7.3. SIMULATION RESULTS

The proposed multi-objective differential evolution (MODE) method has been applied to a test system with five coal-burning generating units which remain on line for a 3-week period. All the generator data containing coefficients of cost, emission and coal consumption, fuel delivery limits, fuel storage limits, load demand and fuel delivered during the scheduling period are given in the Appendix.

In order to show the effectiveness of the proposed MODE approach, strength pareto evolutionary algorithm 2 (SPEA 2) has been applied to solve the problem. All the algorithms i.e. MODE, SPEA 2, and DE, used in this paper for solving fuel constrained economic emission dispatch problem are implemented by using MATLAB 7.0 on a PC (Pentium-IV, 80 GB, 3.0 GHz).

Here, four cases are considered. In Case 1 economic dispatch, emission dispatch and economic emission dispatch are done without considering fuel constraints. In Case 2 economic fuel dispatch, emission fuel dispatch and economic emission fuel dispatch are done considering fuel constraints when all the units have sufficient coal. Case 3 and case 4 are purposely structured to show the interaction of the fuel deliveries and different types of dispatch of the generating units when there is fuel shortage. In Case 3 there is fuel shortage at unit 4 and in case 4 there is fuel shortage at unit 5. Table 7.1 shows description of all cases.

In order to explore the extreme points of the trade-off surface, fuel cost and emission objectives are minimized individually by using differential evolution (DE) for all the four cases. In case of DE, the population size, maximum number of iteration, scaling factor and crossover factor have been selected as 100, 100, 0.75 and 1.0, respectively for all the four cases of the test system.

MODE has been applied to optimize both cost and emission objectives simultaneously for all the four cases. The population size, maximum number of iteration, scaling factor and crossover factor have been selected as 20, 50, 0.75 and 1.0, respectively in the proposed MODE for all the four cases of the test system.

For comparison, SPEA 2 has been applied to solve the problem. In case of SPEA 2, the population size, maximum number of iteration, crossover and mutation probabilities have been selected as 20, 50, 0.9 and 0.2 respectively for all the four cases of the test system.

Table 7.1 shows the dispatch solutions for Case 1. Fig. 7.1 depicts cost and emission convergence obtained from case 1 using DE. The distribution of 20 non-dominated solutions obtained in the last generation of proposed MODE and SPEA 2 for Case 1 is shown in Fig. 7.2.

The dispatch solutions for Case 2 are summarized in Table 7.2. Cost and emission convergence obtained from Case 2 using DE are shown in Fig. 7.3. The distribution of 20 non-dominated solutions obtained in the last generation of proposed MODE and SPEA 2 for Case 2 is depicted in Fig. 7.4.

The dispatch solutions for Case 3 are shown in Table 7.3. Fig. 7.5 depicts cost and emission convergence obtained from Case 3 using DE. The distribution of 20 non-dominated solutions obtained in the last generation of proposed MODE and SPEA 2 for Case 3 is depicted in Fig. 7.6.

Table 7.4 summarizes the dispatch solutions for case 4. Fig. 7.7 depicts cost and emission convergence obtained from Case 4 using DE. The distribution of 20 non-dominated solutions obtained in the last generation of proposed MODE and SPEA 2 for Case 4 is shown in Fig. 7.8.

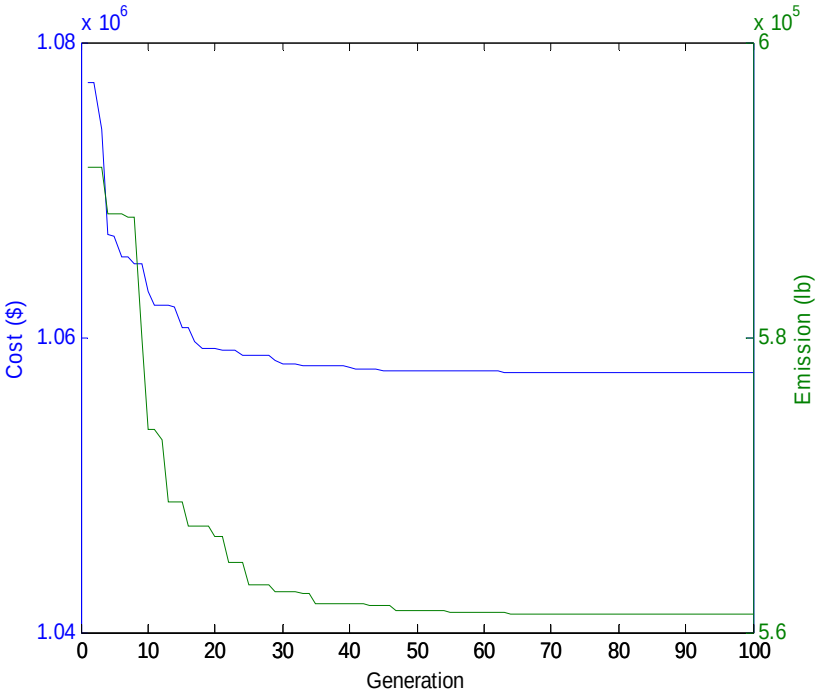

Fig. 7.1. Cost and emission convergence for Case 1

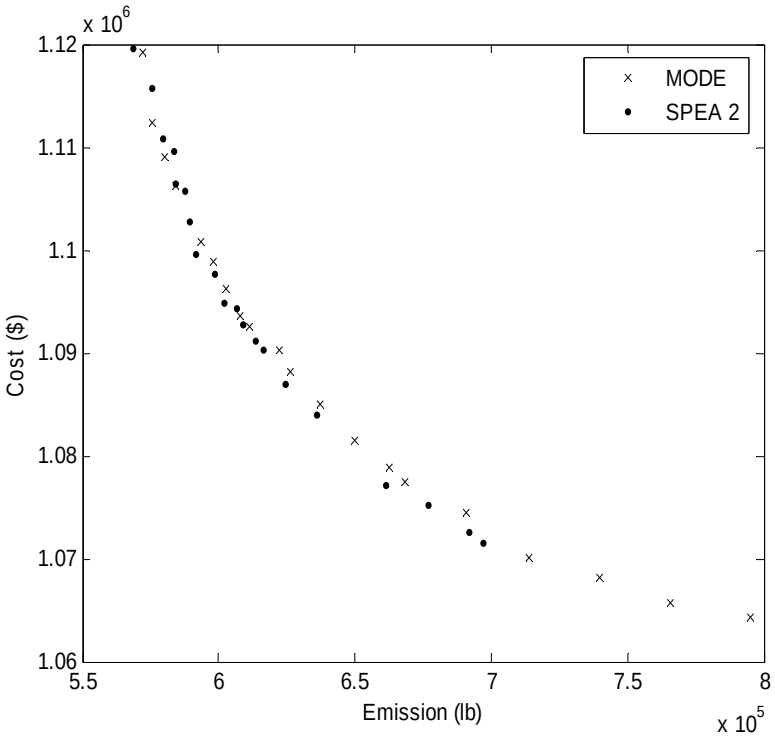

Fig. 7.2. Pareto-optimal front of the last generation for Case 1

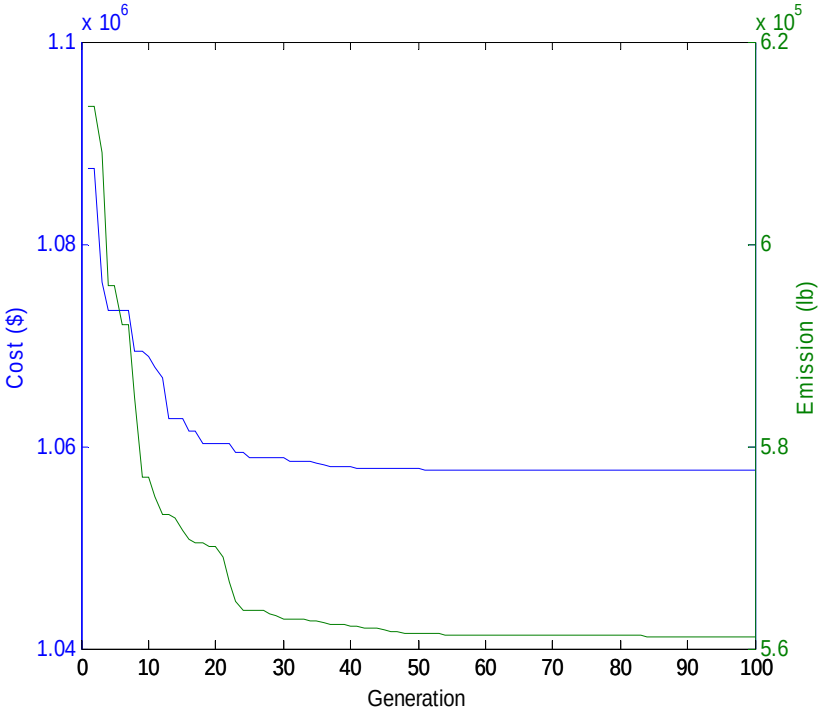

Fig. 7.3. Cost and emission convergence for Case 2

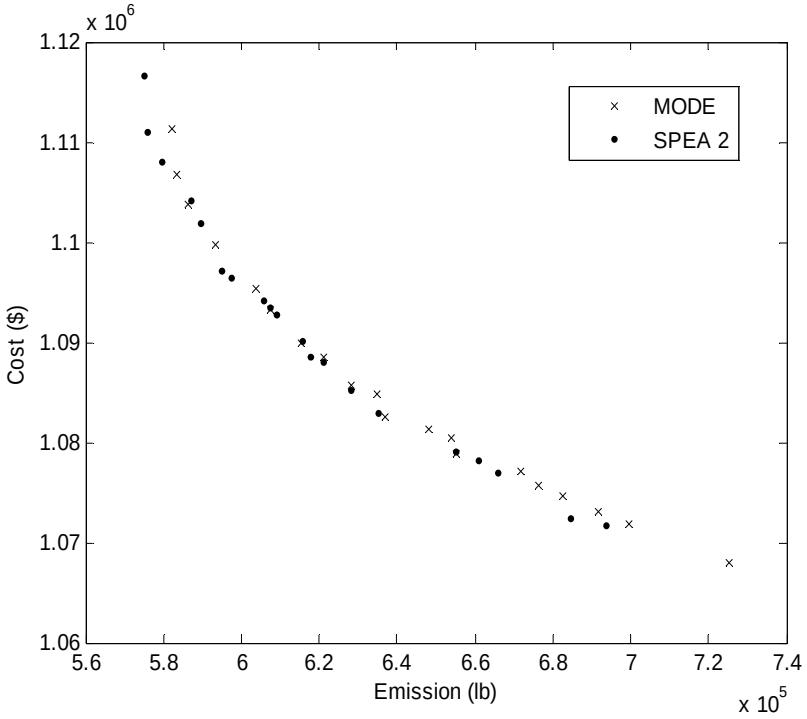

Fig. 7.4: Pareto-optimal front of the last generation for Case 2

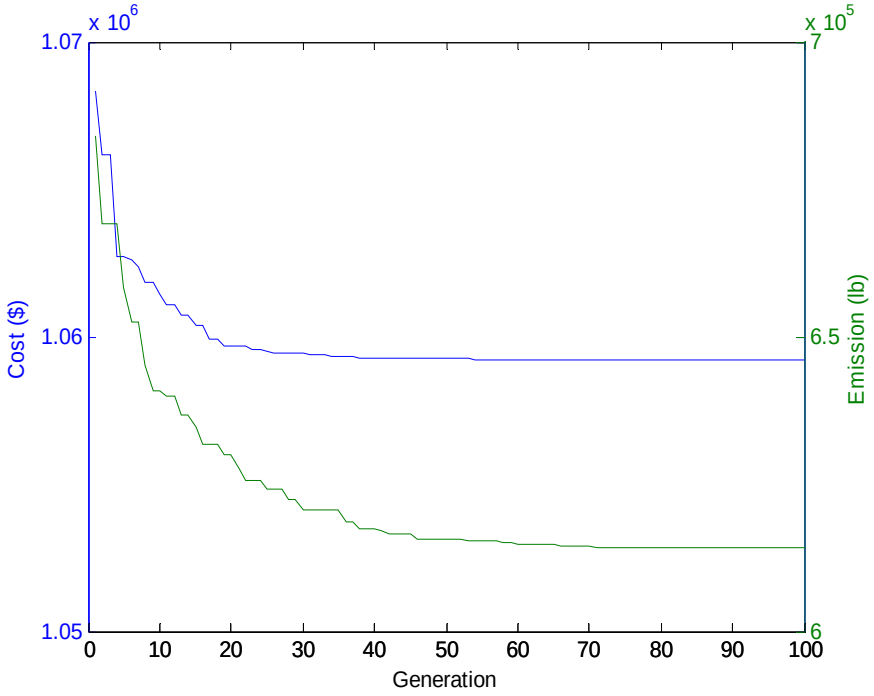

Fig. 7.5. Cost and emission convergence for Case 3

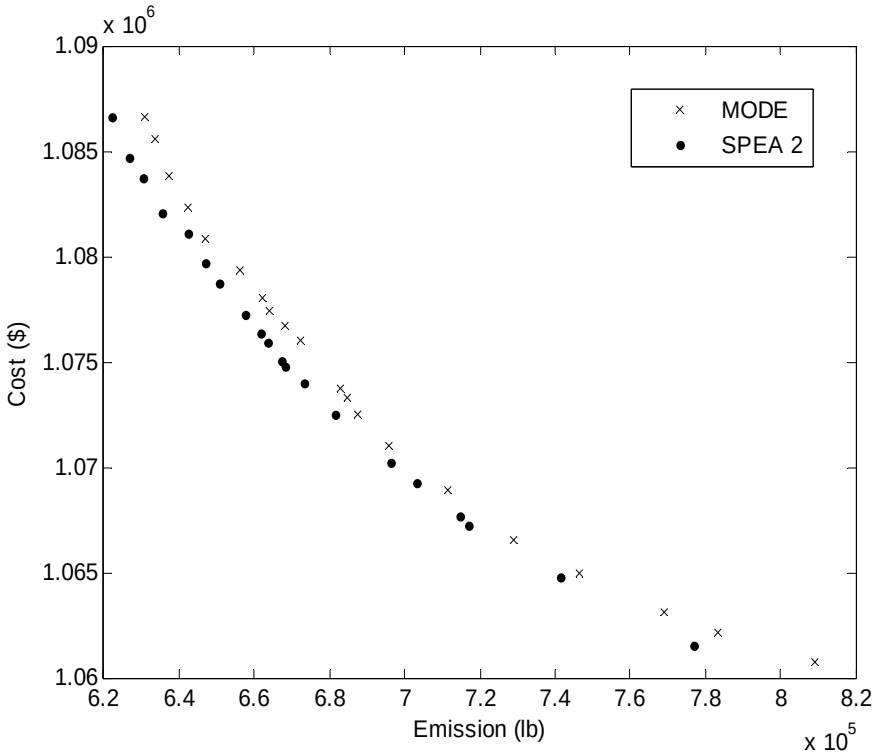

Fig. 7.6.. Pareto-optimal front of the last generation for Case 3

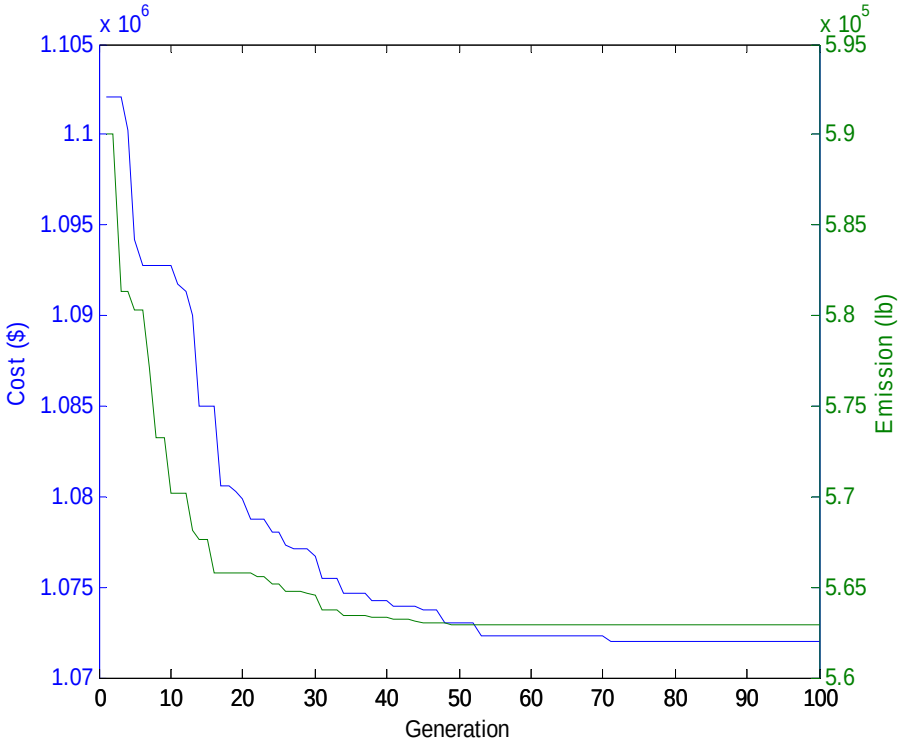

Fig. 7.7. Cost and emission convergence for Case 4

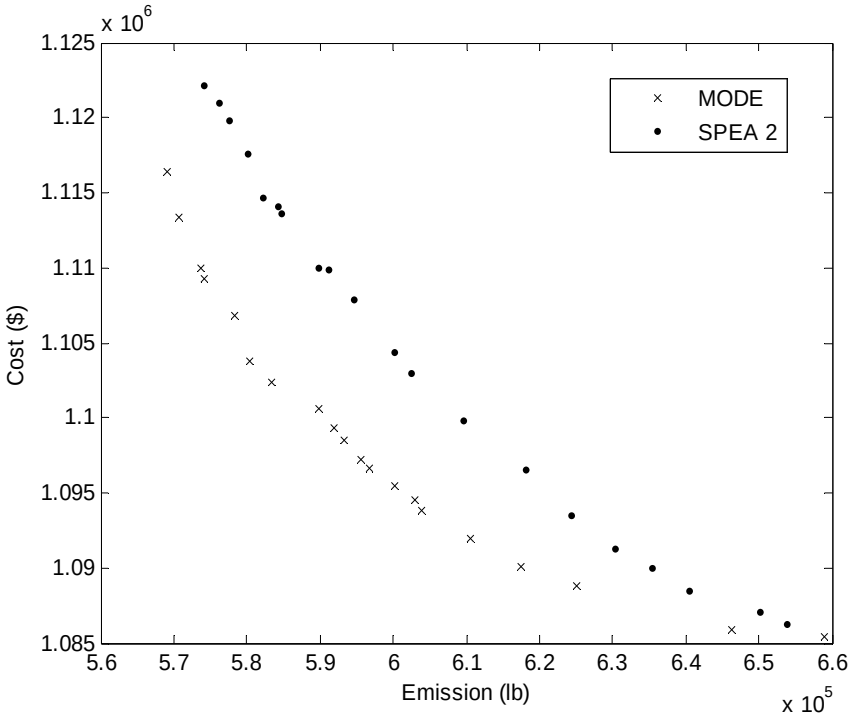

Fig. 7.8. Pareto-optimal front of the last generation for Case 4

Table 7.1. DISPATCH SOLUTION FOR CASE 1 WITHOUT CONSIDERING FUEL CONSTRAINTS

Interval	Economic dispatch (DE) Generation (MW) Objective	Emission dispatch (DE) Generation (MW) Objective	Economic emission dispatch (MODE) Generation (MW) Objective	Economic emission dispatch (SPEA2) Generation (MW) Objective
1	P_1 = 50.3045 Cost=	P_1 = 75.0000 Cost=	P_1 = 70.3819 Cost=	P_1 = 62.7705 Cost=
	P_2 =125.000 1057633 $	P_2 =107.5394 1127536 $	P_2 =121.5701 1085076 $	P_2 =110.6314 1086926 $
	P_3 =175.000 Emission=	P_3 = 148.3539 Emission=	P_3 = 151.2118 Emission=	P_3 =158.9422 Emission=
	P_4 = 49.6955 854052 *lb*	P_4 = 208.4844 561219 *lb*	P_4 = 145.6957 637173 *lb*	P_4 =139.9314 624523 *lb*
	P_5 = 300.000	P_5 =160.6224	P_5 = 211.1404	P_5 =227.7245
2	P_1 = 75.0000	P_1 = 75.0000	P_1 = 69.6273	P_1 = 74.8493
	P_2 =125.0000	P_2 =120.3204	P_2 = 117.1540	P_2 =121.2990
	P_3 =175.0000	P_3 =162.6283	P_3 = 160.8912	P_3 =174.0485
	P_4 =125.0000	P_4 =234.2381	P_4 = 170.3515	P_4 =174.1388
	P_5 = 300.0000	P_5 =207.8132	P_5 = 281.9759	P_5 =255.6644
3	P_1 = 31.8215	P_1 = 75.0000	P_1 = 63.7779	P_1 = 53.9416
	P_2 =120.0214	P_2 =100.0806	P_2 = 110.764	P_2 =119.1979
	P_3 =175.0000	P_3 =140.2288	P_3 = 142.2972	P_3 =153.1367
	P_4 = 40.0000	P_4 =193.4620	P_4 =118.8558	P_4 =139.2248
	P_5 = 283.1571	P_5 = 141.2286	P_5 = 214.3050	P_5 =184.4991

Table 7.2. FUEL CONSTRAINED DISPATCH SOLUTION FOR CASE 2 WITH INITIAL FUEL STORAGE (tons) V_1^0 = 2000, V_2^0 =5000, V_3^0 =5000, V_4^0 =8000, V_5^0 =8000

Inter-val	Economic dispatch (DE) Generation (MW)	Fuel delivered (tons)	Objective	Emission dispatch (DE) Generation (MW)	Fuel delivered (tons)	Objective	Economic emission dispatch (MODE) Generation (MW)	Fuel delivered (tons)	Objective	Economic emission dispatch (SPEA2) Generation (MW)	Fuel delivered (tons)	Objective
1	P_1 = 50.3298	F_1 = 803.3	Cost=	P_1 = 75.0000	F_1 = 971.1	Cost=	P_1 = 65.0870	F_1 = 374.9	Cost=	P_1 = 64.6209	F_1 = 976.7	Cost=
	P_2 =125.0000	F_2 = 400.4	1057633 $	P_2 =107.5394	F_2 = 183.5	1133665 $	P_2 =118.3058	F_2 = 821.3	1085760 $	P_2 =115.2044	F_2 = 914.4	1086487 $
	P_3 = 175.0000	F_3 =1925.5	Emission=	P_3 =148.3558	F_3 =1935.3	Emission=	P_3 =161.9117	F_3 =2000.0	Emission=	P_3 =159.0814	F_3 =1621.1	Emission=
	P_4 = 49.6707	F_4 =1190.2	854047 *lb*	P_4 =208.4572	F_4 =2775.5	561219 *lb*	P_4 =137.7627	F_4 =1045.6	628291 *lb*	P_4 =160.1219	F_4 =2952.3	627198
	P_5 = 299.9995	F_5 =2680.6		P_5 =160.6476	F_5 =1134.5		P_5 =216.9328	F_5 =2758.1		P_5 =200.9714	F_5 = 535.5	
2	P_1 = 74.9996	F_1 = 170.0		P_1 = 75.0000	F_1 = 149.6		P_1 = 72.4646	F_1 = 63.2		P_1 = 74.5789	F_1 = 891.6	
	P_2 =125.0000	F_2 = 20.1		P_2 =120.3054	F_2 = 996.2		P_2 =122.3103	F_2 = 603.9		P_2 =120.9823	F_2 = 602.7	
	P_3 =175.0000	F_3 =2000.0		P_3 =162.5958	F_3 =2000.0		P_3 = 175.0000	F_3 =1674.1		P_3 =170.2571	F_3 = 1257.0	
	P_4 =125.0005	F_4 =3000.0		P_4 =234.2259	F_4 =2043.9		P_4 =186.1858	F_4 =2067.3		P_4 =162.5534	F_4 =2708.3	
	P_5 =299.9999	F_5 = 1810.0		P_5 =207.8730	F_5 =1810.2		P_5 =244.0392	F_5 =2591.4		P_5 =271.6283	F_5 =1540.4	
3	P_1 = 31.8285	F_1 = 191.6		P_1 = 75.0000	F_1 = 996.7		P_1 = 61.1643	F_1 = 963.3		P_1 = 62.7666	F_1 = 936.4	
	P_2 =120.0186	F_2 = 646.3		P_2 =100.0379	F_2 = 96.3		P_2 =123.2043	F_2 =1000.0		P_2 =105.5265	F_2 = 762.7	
	P_3 =174.9998	F_3 =1978.8		P_3 =140.2360	F_3 = 796.8		P_3 =138.9994	F_3 =1867.7		P_3 =169.4441	F_3 = 956.4	
	P_4 = 40.0000	F_4 =1961.0		P_4 =193.4661	F_4 =2166.8		P_4 =114.3206	F_4 =2016.5		P_4 =122.2385	F_4 =2175.0	
	P_5 =283.1530	F_5 =2222.4		P_5 =141.2599	F_5 = 2943.4		P_5 =212.3115	F_5 =1152.6		P_5 =190.0243	F_5 =2169.5	

Table 7.3. FUEL CONSTRAINED DISPATCH SOLUTION FOR CASE 3 WITH INITIAL FUEL STORAGE (tons) V_1^0 = 2000, V_2^0 =5000, V_3^0 =5000, V_4^0 =500, V_5^0 =8000

Inter-val	Economic dispatch (DE) Generation (MW)	Fuel delivered (tons)	Objective	Emission dispatch (DE) Generation (MW)	Fuel delivered (tons)	Objective	Economic emission dispatch (MODE) Generation (MW)	Fuel delivered (tons)	Objective	Economic emission dispatch (SPEA2) Generation (MW)	Fuel delivered (tons)	Objective
1	P_1 = 39.8274	F_1 = 86.5	Cost=	P_1 = 75.0000	F_1 =1000.0	Cost=	P_1 = 59.4445	F_1 = 549.7	Cost=	P_1 = 73.0084	F_1 = 844.6	Cost=
	P_2 =118.4045	F_2 = 160.6	1059205 $	P_2 =113.6015	F_2 = 2.3	1093126 $	P_2 =125.0000	F_2 = 351.9	1073303 $	P_2 =122.6514	F_2 = 801.8	1074008 $
	P_3 =165.2075	F_3 =1570.2	Emission=	P_3 =155.6017	F_3 =1990.5	Emission=	P_3 = 174.8987	F_3 = 638.0	Emission=	P_3 =168.2436	F_3 = 1702.3	Emission=
	P_4 = 78.0233	F_4 =2372.5	837673 *lb*	P_4 =173.5134	F_4 =2999.5	614091 *lb*	P_4 =103.5303	F_4 =2626.5	684693 *lb*	P_4 =118.2999	F_4 =1972.3	673024 *lb*
	P_5 =298.5374	F_5 =2810.2		P_5 =182.2834	F_5 =1007.7		P_5 =237.1265	F_5 =2833.9		P_5 =217.7967	F_5 = 1679.1	
2	P_1 = 75.0000	F_1 = 981.9		P_1 =74.9805	F_1 = 633.0		P_1 = 69.9770	F_1 = 68.1		P_1 = 74.7721	F_1 = 432.3	
	P_2 =125.0000	F_2 = 217..9		P_2 =124.9818	F_2 = 949.5		P_2 =119.0024	F_2 = 344.3		P_2 =124.6438	F_2 = 848.4	
	P_3 =175.0000	F_3 =1998.9		P_3 =170.4118	F_3 =2000.0		P_3 =175.0000	F_3 =1307.3		P_3 =174.6266	F_3 =1980.4	
	P_4 =125.0001	F_4 =2059.5		P_4 =148.1378	F_4 =2997.7		P_4 =153.0358	F_4 =2697.4		P_4 =146.2138	F_4 =2976.6	
	P_5 =300.0000	F_5 =1741.8		P_5 =281.4881	F_5 = 419.8		P_5 =282.9848	F_5 =2583.0		P_5 =279.7437	F_5 = 762.5	
3	P_1 = 31.9035	F_1 = 813.9		P_1 = 74.9942	F_1 = 535.3		P_1 = 59.0161	F_1 = 859.9		P_1 = 72.7733	F_1 = 491.8	
	P_2 =119.9734	F_2 = 216.8		P_2 =108.2428	F_2 = 999.6		P_2 =116.8183	F_2 = 133.0		P_2 =118.0090	F_2 = 795.5	
	P_3 =174.9968	F_3 =1998.1		P_3 =149.5267	F_3 =1850.7		P_3 =143.8090	F_3 =1223.1		P_3 =162.5505	F_3 =1888.8	
	P_4 = 40.0005	F_4 =1516.3		P_4 =147.9900	F_4 =2997.2		P_4 =109.3848	F_4 =2712.6		P_4 = 80.7817	F_4 =2696.7	
	P_5 =283.1257	F_5 =2454.9		P_5 =169.2462	F_5 = 617.2		P_5 =220.9717	F_5 =2071.3		P_5 =215.8855	F_5 =1127.3	

Table 7.4. FUEL CONSTRAINED DISPATCH SOLUTION FOR CASE 4 WITH INITIAL FUEL STORAGE (tons) V_1^0 = 2000, V_2^0 =5000, V_3^0 =5000, V_4^0 =8000, V_5^0 =500

Inter-val	Economic dispatch (DE) Generation (MW)	Fuel delivered (tons)	Objective	Emission dispatch (DE) Generation (MW)	Fuel delivered (tons)	Objective	Economic emission dispatch (MODE) Generation (MW)	Fuel delivered (tons)	Objective	Economic emission dispatch (SPEA2) Generation (MW)	Fuel delivered (tons)	Objective
1	P_1= 64.6327	F_1= 959.6	Cost=	P_1= 73.6410	F_1= 370.03	Cost=	P_1= 68.8702	F_1= 625.8	Cost=	P_1= 56.4094	F_1= 302.1	Cost=
	P_2 =121.5749	F_2 = 897.1	1072011 $	P_2 =112.3754	F_2 = 321.7	1126446 $	P_2 =114.7729	F_2 = 236.3	1096650 $	P_2 =116.0625	F_2 = 330.4	1096509 $
	P_3 =174.5428	F_3 =1994.6	Emission=	P_3 =150.7188	F_3 =1395.2	Emission=	P_3 =166.3807	F_3 = 738.3	Emission=	P_3 =159.7154	F_3 =1606.5	Emission=
	P_4 =101.2611	F_4 = 151.3	694273 *lb*	P_4 =201.5249	F_4 =2188.4	562921 *lb*	P_4 =143.4241	F_4 =2497.8	596646 *lb*	P_4 =160.5276	F_4 =1826.7	618125 *lb*
	P_5 =237.9886	F_5 =2997.5		P_5 =161.7399	F_5 =2724.7		P_5 =206.5521	F_5 =2901.9		P_5 =207.2852	F_5 =2934.3	
2	P_1 = 74.8386	F_1= 982.8		P_1= 74.9254	F_1= 994.9		P_1= 74.2855	F_1= 659.7		P_1= 73.4619	F_1= 999.1	
	P_2 =124.9129	F_2 = 17.5		P_2 =120.1896	F_2 = 8.2		P_2 =121.4536	F_2 = 928.1		P_2 =110.6655	F_2 = 377.9	
	P_3 =174.7765	F_3 = 0.1		P_3 =161.1406	F_3 = 51.7		P_3 =170.0481	F_3 =1477.8		P_3 = 174.4181	F_3 = 717.7	
	P_4 =168.3754	F_4 =2999.9		P_4 =236.1880	F_4 =2991.8		P_4 =208.1990	F_4 =1294.0		P_4 =219.8668	F_4 =2663.9	
	P_5 = 257.0966	F_5 = 2999.7		P_5 =207.5564	F_5 =2953.3		P_5 =226.0138	F_5 =2640.5		P_5 =221.5877	F_5 =2241.5	
3	P_1= 57.4434	F_1= 499.9		P_1= 72.2428	F_1= 288.2		P_1= 62.6368	F_1= 952.5		P_1= 59.0782	F_1= 808.5	
	P_2 =124.7904	F_2 = 935.6		P_2 = 98.6504	F_2 = 701.4		P_2 =104.5039	F_2 = 193.1		P_2 = 84.7793	F_2 = 556.8	
	P_3 =175.0000	F_3 = 1818.7		P_3 =131.3219	F_3 =1227.1		P_3 =158.7797	F_3 =1916.9		P_3 =170.6290	F_3 =1323.7	
	P_4 = 63.5782	F_4 = 756.5		P_4 =196.2013	F_4 =2994.2		P_4 =144.5260	F_4 =1164.5		P_4 =114.8903	F_4 =1459.2	
	P_5 =229.1879	F_5 =2989.2		P_5 =151.5836	F_5 =1789.1		P_5 =179.5516	F_5 =2773.1		P_5 =220.6232	F_5 =2851.9	

Table 7.4. FUEL CONSTRAINED DISPATCH SOLUTION FOR CASE 4 WITH INITIAL FUEL STORAGE (tons) V_1^0 **= 2000,** V_2^0 **=5000,** V_3^0 **=5000,** V_4^0 **=8000,** V_5^0 **=500**

Inter-val	Economic dispatch (DE) Generation (MW)	Fuel delivered (tons)	Objective	Emission dispatch (DE) Generation (MW)	Fuel delivered (tons)	Objective	Economic emission dispatch (MODE) Generation (MW)	Fuel delivered (tons)	Objective	Economic emission dispatch (SPEA2) Generation (MW)	Fuel delivered (tons)	Objective
1	P_1 = 64.6327	F_1 = 959.6	Cost=	P_1 = 73.6410	F_1 = 370.03	Cost=	P_1 = 68.8702	F_1 = 625.8	Cost=	P_1 = 56.4094	F_1 = 302.1	Cost=
	P_2 =121.5749	F_2 = 897.1	1072011 $	P_2 =112.3754	F_2 = 321.7	1126446 $	P_2 =114.7729	F_2 = 236.3	1096650 $	P_2 =116.0625	F_2 = 330.4	1096509 $
	P_3 =174.5428	F_3 =1994.6	Emission=	P_3 =150.7188	F_3 =1395.2	Emission=	P_3 =166.3807	F_3 = 738.3	Emission=	P_3 =159.7154	F_3 =1606.5	Emission=
	P_4 =101.2611	F_4 = 151.3	694273 *lb*	P_4 =201.5249	F_4 =2188.4	562921 *lb*	P_4 =143.4241	F_4 =2497.8	596646 *lb*	P_4 =160.5276	F_4 =1826.7	618125 *lb*
	P_5 =237.9886	F_5 =2997.5		P_5 =161.7399	F_5 =2724.7		P_5 =206.5521	F_5 =2901.9		P_5 =207.2852	F_5 =2934.3	
2	P_1 = 74.8386	F_1 = 982.8		P_1 = 74.9254	F_1 = 994.9		P_1 = 74.2855	F_1 = 659.7		P_1 = 73.4619	F_1 = 999.1	
	P_2 =124.9129	F_2 = 17.5		P_2 =120.1896	F_2 = 8.2		P_2 =121.4536	F_2 = 928.1		P_2 =110.6655	F_2 = 377.9	
	P_3 =174.7765	F_3 = 0.1		P_3 =161.1406	F_3 = 51.7		P_3 =170.0481	F_3 =1477.8		P_3 = 174.4181	F_3 = 717.7	
	P_4 =168.3754	F_4 =2999.9		P_4 =236.1880	F_4 =2991.8		P_4 =208.1990	F_4 =1294.0		P_4 =219.8668	F_4 =2663.9	
	P_5 = 257.0966	F_5 = 2999.7		P_5 =207.5564	F_5 =2953.3		P_5 =226.0138	F_5 =2640.5		P_5 =221.5877	F_5 =2241.5	
3	P_1 = 57.4434	F_1 = 499.9		P_1 = 72.2428	F_1 = 288.2		P_1 = 62.6368	F_1 = 952.5		P_1 = 59.0782	F_1 = 808.5	
	P_2 =124.7904	F_2 = 935.6		P_2 = 98.6504	F_2 = 701.4		P_2 =104.5039	F_2 = 193.1		P_2 = 84.7793	F_2 = 556.8	
	P_3 =175.0000	F_3 = 1818.7		P_3 =131.3219	F_3 =1227.1		P_3 =158.7797	F_3 =1916.9		P_3 =170.6290	F_3 =1323.7	
	P_4 = 63.5782	F_4 = 756.5		P_4 =196.2013	F_4 =2994.2		P_4 =144.5260	F_4 =1164.5		P_4 =114.8903	F_4 =1459.2	
	P_5 =229.1879	F_5 =2989.2		P_5 =151.5836	F_5 =1789.1		P_5 =179.5516	F_5 =2773.1		P_5 =220.6232	F_5 =2851.9	

7.4. CONCLUSION

Here, the usefulness of the multi-objective differential evolution is examined for solving fuel constrained economic emission dispatch problem of thermal generating units. The results show that fuel consumption can be adequately controlled to satisfy constraints imposed by suppliers using the proposed method. Optimum economic emission dispatch is not achieved always, but this is generally much less than the penalty that could be imposed for violating the fuel system constraints.

CHAPTER 8

Short-term Scheduling of Variable Head Hydrothermal Power system

8.1. Introduction

The hydro thermal generation scheduling problem is a nonlinear constrained dynamic optimization problem which plays an important role to electric utility systems. With the insignificant marginal cost of hydroelectric power, operational cost of a hydrothermal system essentially reduces to that of minimizing the fuel cost for thermal plants under the various constraints on the hydraulic, thermal and power system network.

The main constraints include: the time coupling effect of the hydro sub problem, where the water flow in an earlier time interval affects the discharge capability at a later period of time, the cascaded nature of the hydraulic network, the varying hourly reservoir inflows, the physical limitations on the reservoir storage and turbine flow rate, the varying system load demand and the loading limits of both thermal and hydro plants.

Modified evolutionary programming (MEP) and group search optimization (GSO) have been applied to solve the short-term optimal scheduling of generation in a hydrothermal system which involves the allocation of generations among the multi-reservoir cascaded hydro plants having prohibited operating zones and thermal units with valve point loading so as to minimize the fuel cost of thermal plants while satisfying the various constraints on the hydraulic, thermal and power system. The ramp-rate limits of thermal generators are taken into consideration. The transmission losses are also accounted for through the use of loss coefficients. To illustrate the performance of the proposed MEP method, two test problems and two hydrothermal test systems reported in the literature are used. Test results are compared with those obtained by other evolutionary methods. From numerical results, it is found that the proposed MEP based approach provides better solution.

8.2. Problem Formulation

The hydrothermal scheduling problem is aimed to minimize the fuel cost of thermal plants, while making use of the availability of hydro power as much as possible. The objective function and associated constraints of the hydrothermal scheduling problem are formulated as follows.

8.2.1. Objective function

$$\text{Minimize } F = \sum_{t=1}^{\mathrm{T}} \sum_{i=1}^{\mathrm{N_s}} \left[a_{si} + b_{si} \mathrm{P}_{sit} + c_{si} \mathrm{P}_{sit}^2 + \left| d_{si} \times \sin\left\{ e_{si} \times \left(\mathrm{P}_{si}^{\min} - \mathrm{P}_{sit} \right) \right\} \right| \right] \tag{8.1}$$

8.2.2. Constraints

(i) Power balance constraints:

The total active power generation must balance the predicted power demand and transmission loss, at each time interval over the scheduling horizon

$$\sum_{i=1}^{\mathrm{N}_s} \mathrm{P}_{sit} + \sum_{j=1}^{\mathrm{N}_h} \mathrm{P}_{hjt} - \mathrm{P}_{Dt} - \mathrm{P}_{Lt} = 0 \quad t \in \mathrm{T} \tag{8.2}$$

The hydroelectric generation is a function of water discharge rate and reservoir water head, which in turn, is a function of storage

$$\mathrm{P}_{hjt} = C_{1j} V_{hjt}^2 + C_{2j} Q_{hjt}^2 + C_{3j} V_{hjt} Q_{hjt} + C_4 V_{hjt} + C_{5j} Q_{hjt} + C_{6j}, \qquad j \in \mathrm{N}_h \;\; t \in \mathrm{T} \tag{8.3}$$

The transmission loss P_{Lt} is given by

$$\mathrm{P}_{Lt} = \sum_{i=1}^{\mathrm{N}_t} \sum_{j=1}^{\mathrm{N}_t} \mathrm{P}_{sit} \mathrm{B}_{ij} \mathrm{P}_{sjt} + \sum_{i=1}^{\mathrm{N}_t} \sum_{j=1}^{\mathrm{N}_h} \mathrm{P}_{sit} \mathrm{B}_{ij} \mathrm{P}_{hjt} + \sum_{i=1}^{\mathrm{N}_h} \sum_{j=1}^{\mathrm{N}_h} \mathrm{P}_{hit} \mathrm{B}_{ij} \mathrm{P}_{hjt} + \sum_{i=1}^{\mathrm{N}_t} \mathrm{B}_{0i} \mathrm{P}_{sit} + \sum_{j=1}^{\mathrm{N}_h} \mathrm{B}_{0j} \mathrm{P}_{hjt} + \mathrm{B}_{00} \tag{8.4}$$

(ii) Generation limits:

$$\mathrm{P}_{hj}^{\min} \le \mathrm{P}_{hjt} \le \mathrm{P}_{hj}^{\max}, \;\; j \in \mathrm{N}_h \;\; t \in \mathrm{T} \tag{8.5}$$

and

$$P_{si}^{\min} \le P_{sit} \le P_{si}^{\max},\ i \in N_s,\ t \in T \tag{8.6}$$

(iii) Ramp rate limits of thermal generating unit

The power generated, P_i, by the ith thermal unit in certain interval may not exceed that of previous interval by more than a certain amount UR_i, the up-ramp limit and neither may it be less than that of the previous interval by more than some amount DR_i the down-ramp limit of the unit. These give rise to the following constraints.

$$P_{sit} - P_{si(t-1)} \le UR_i,\quad i \in N_s,\ t \in T \tag{8.7}$$

$$P_{si(t-1)} - P_{sit} \le DR_i,\ i \in N_s\quad t \in T \tag{8.8}$$

(iv) Hydraulic network constraints

The hydraulic operational constraints comprise the water balance equations for each hydro unit as well as the bounds on reservoir storage and release targets. These bounds are determined by the physical reservoir and plant limitations as well as the multipurpose requirements of the hydro system. These constraints include:

(a) Physical limitations on reservoir storage volumes and discharge rates,are given by

$$V_{hj}^{\min} \le V_{hjt} \le V_{hj}^{\max}\ ,\quad j \in N_h,\ t \in T \tag{8.9}$$

$$Q_{hj}^{\min} \le Q_{hjt} \le Q_{hj}^{\max}\quad j \in N_h,\ t \in T \tag{8.10}$$

b) The continuity equation for the hydro reservoir network is given by

$$V_{hj(t+1)} = V_{hjt} + I_{hjt} - Q_{hjt} - S_{hjt} + \sum_{l=1}^{R_{uj}} \left(Q_{hl(t-\tau_{lj})} + S_{hl(t-\tau_{lj})}\right),\quad j \in N_h,\ t \in T \tag{8.11}$$

c) Initial and final reservoir storage volume are as follows :

$$V_{hj}^{0} = V_{hj}^{begin},\quad j \in N_h \tag{8.12}$$

$$V_{hj}^{T} = V_{hj}^{end},\quad j \in N_h \tag{8.13}$$

(v) Prohibited operating regions of water discharge rates are as follows :

$$Q_{hj} \in \begin{cases} Q_{hj}^{\min} \le Q_{hj} \le Q_{hj,1}^{L} \\ Q_{hj,k-1}^{U} \le Q_{hj} \le Q_{hj,k}^{L}, \quad k = 2,..,n_j \\ Q_{hj,n_j}^{U} \le Q_{hj} \le Q_{hj}^{\max} \end{cases} \tag{8.14}$$

8.3. Application of MEP Method

The proposed modified evolutionary programming (MEP) has been applied to solve two hydrothermal multi-reservoir cascaded hydroelectric test systems having prohibited operating zones and thermal units with valve point loading. For each case 100 runs are conducted to compare the solution quality. The computational results have been used to compare the performance of the proposed MEP approach with that of other evolutionary methods reported in the literature. The proposed MEP used in this paper is implemented by using MATLAB 7.0 on a PC (Pentium-IV, 80 GB, 3.0 GHz).

Two hydrothermal test systems are considered to inspect and verify the proposed MEP method.

8.3.1. Test System 1

The system considers a multi-chain cascade of four reservoir hydro plants and three thermal plants. The entire scheduling period is 1 day and divided into 24 intervals. The valve point loading effect and transmission loss are taken into account. For this test system, two cases are considered. In the first case prohibited operating zones of hydro plants and ramp rate limits of thermal generators are not taken into consideration but in the second case both are taken into account. The detailed parameters are given in the Appendix.

Case 1: The problem is solved by using MEP. Here, parameters are taken as $N_P = 100$, $\beta = 0.5$, $C_R = 1$ and $iter_{\max} = 300$.

The optimal hourly discharges and hydrothermal generation obtained by the proposed MEP method are provided in Table 8.1 and Table 8.2 respectively. Figure 8.1 shows the reservoir storage volumes of four hydro plants obtained from MEP. The best, average and the worst costs and average CPU time among 100 runs of solutions obtained from proposed MEP are shown in Table 8.3. The costs obtained from clonal selection algorithm (CSA) [113] and teaching learning

based optimization (TLBO) [114] is also shown in Table 8.3. The cost convergence characteristic in case of MEP is depicted in Fig. 8.2. Results show that the best cost for this test system as obtained by MEP is less compared to those obtained from CSA [113] and TLBO [114]. Moreover, the best, the worst, average costs obtained by MEP out of certain number of trials are quite close to each other. It establishes better robustness of the algorithm.

Table 8.1: Optimal Hydro Discharge ($\times 10^4 m^3$) for Case 1 of Test system 1

1	8.3137	9.4629	22.5907	11.0102
2	12.0381	10.7128	24.2330	7.8830
3	10.2607	8.2215	18.4826	8.3539
4	6.9790	7.2737	24.2664	11.3111
5	5.6008	7.3567	24.6145	13.7302
6	5.8274	6.7404	14.6097	14.7870
7	8.7252	7.2394	14.8602	17.9333
8	5.6972	6.8517	29.2682	10.0631
9	6.8871	7.8676	11.5319	13.2347
10	11.5933	6.6753	16.1021	6.0494
11	11.4489	10.3040	15.3343	16.7608
12	5.4383	10.4748	25.4544	17.3946
13	5.0471	8.5465	17.4615	16.8455
14	10.3692	10.1086	21.2560	20.0000
15	12.7068	9.2567	12.0091	19.3661
16	5.8504	7.5990	10.6866	10.8001
17	7.6697	6.6162	12.5960	17.6331
18	5.8233	6.1733	12.2395	14.7619
19	9.0188	13.6679	15.5357	19.3778
20	5.1454	7.1701	15.7034	18.1969
21	7.2424	6.9259	19.4917	19.2632
22	14.2528	9.1624	14.1855	10.7292
23	6.0377	7.8139	10.0000	13.2968
24	7.0265	9.7785	16.9681	16.8537

Table 8.2: Optimal Hydrothermal generation (MW) for Case 1 of Test system 1

Hour	P_{h1}	P_{h2}	P_{h3}	P_{h4}	P_{s1}	P_{s2}	P_{s3}
1	77.0487	69.9893	32.1728	191.8366	104.2184	55.0345	229.6572
2	94.3289	74.8225	16.7056	148.3780	103.6019	209.9259	139.8579
3	86.6656	60.6198	40.8487	148.4766	104.7717	125.5186	139.4297
4	67.2427	55.4408	6.9818	172.7214	174.6274	42.7177	139.4118
5	56.7620	57.0493	4.0827	180.2028	54.9352	182.7057	139.6454
6	58.7012	53.4707	48.0078	199.5433	102.3673	118.7307	229.5069
7	78.7864	56.8691	49.1421	232.3317	103.0065	212.5113	229.1587
8	57.7659	53.6031	0	168.4012	20.0000	124.9980	243.4758
9	67.7585	60.0509	46.9654	214.8638	20.0000	125.2033	307.6816
10	93.7034	52.6100	43.9487	143.2654	102.3089	106.5135	492.4429
11	92.9852	74.3911	44.8133	265.0220	108.1098	213.0840	320.2285
12	57.0308	74.2981	0	267.5719	20.1121	195.9729	498.3319
13	54.3633	63.0963	37.5156	275.7953	173.3571	209.7612	318.1784
14	92.0493	70.6222	22.8742	291.0220	30.0043	220.4909	319.5045
15	101.2885	65.7579	47.1504	283.1017	138.4388	72.9871	319.6155
16	62.1615	56.3550	48.4995	206.8452	83.7333	40.0875	228.7123
17	76.8908	50.3619	52.1451	283.0372	89.6146	198.2788	317.0089
18	62.4432	47.5945	55.2213	259.6838	20.1566	120.0839	312.2452
19	86.2813	82.5634	54.2511	301.1373	33.7892	126.9923	409.1162
20	56.3641	49.6264	54.1656	285.9255	97.2084	122.9434	408.9512
21	74.0465	48.6592	42.6745	284.7750	117.3128	125.1093	228.9323
22	106.1392	62.9251	54.9258	205.5468	101.1637	293.4938	50.1541
23	63.7403	55.4195	54.5068	233.3604	100.1694	123.5292	229.7527
24	72.0016	65.9572	53.5398	265.6134	172.8562	40.0000	139.5193

Table 8.3: Comparison of performance for Case 1 of Test system 1

Techniques	Best cost ($)	Average cost ($)	Worst cost ($)	CPU time (S)
MEP	41704.98	41742.14	41771.12	101.52
CSA	42440.57	-	-	-
TLBO	42385.88	42407.23	42441.36	-

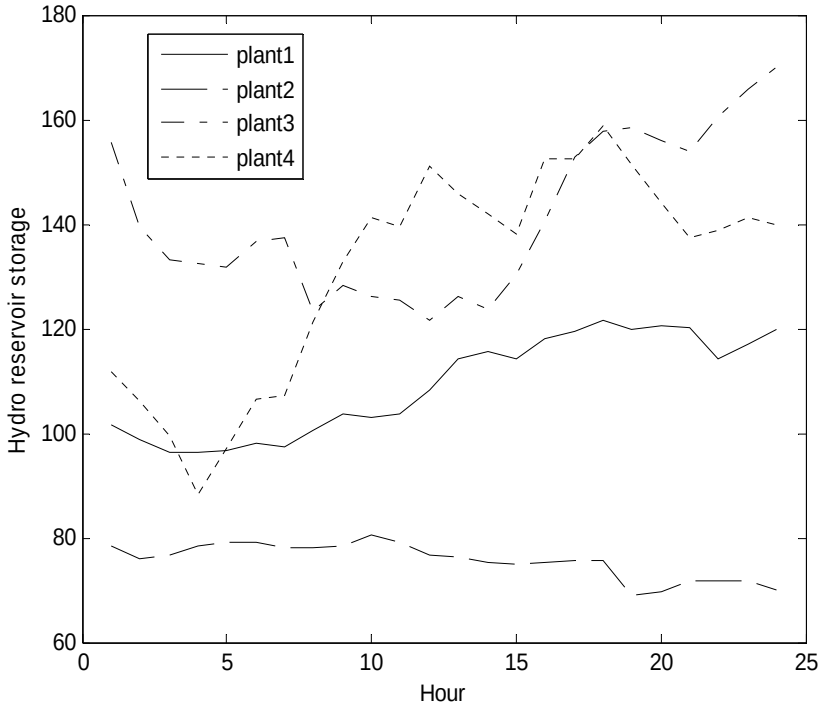

Fig. 8.1. Hydro reservoir storage volumes for Case 1 of Test system 1

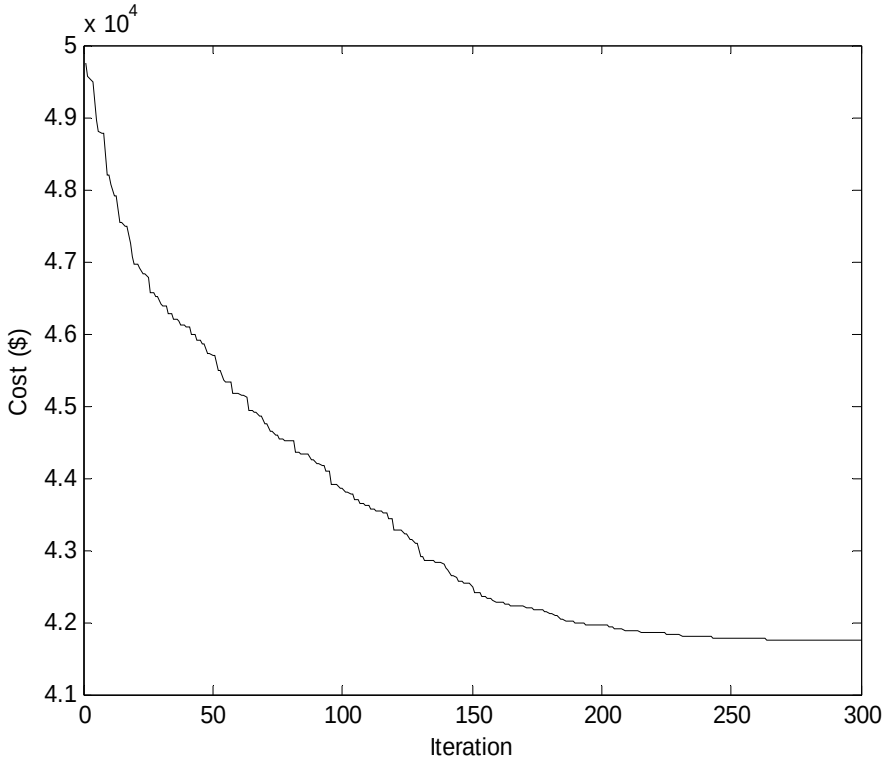

Fig. 8.2. Cost convergence characteristics for Case 1 of Test system 1

Case 2: The problem is solved by using MEP. Here, parameters are taken as $N_P = 100$, $\beta = 0.5$, $C_R = 1$ and $iter_{max} = 300$.

The optimal hourly discharges and hydrothermal generation obtained by the proposed MEP method are provided in Table 8.4 and Table 8.5 respectively. Figure 8.3 shows the reservoir storage volumes of four hydro plants obtained from MEP. The best, average and worst cost and average CPU time among 100 runs of solutions obtained from proposed MEP are shown in Table 8.6. The cost convergence characteristic in case of MEP is depicted in Fig. 8.4.

Table 8.4: Optimal Hydro Discharge ($\times 10^4 m^3$) for Case 2 of Test system 1

Hour	Q_{h1}	Q_{h2}	Q_{h3}	Q_{h4}
1	11.7012	8.3383	29.9999	13.2560
2	7.6046	6.0001	13.4436	8.9722
3	11.1345	6.8522	19.1919	8.5532
4	13.4743	9.2913	16.4968	19.6001
5	6.8706	11.0735	29.6399	14.2180
6	11.2900	9.0272	15.8359	10.3870
7	12.3397	8.0459	21.3733	10.5360
8	5.3016	6.0003	21.1498	6.3047
9	5.1180	8.6659	13.4586	8.7915
10	7.9769	9.0539	28.3579	15.4097
11	5.4565	6.0001	14.0775	18.2466
12	10.2535	6.7587	17.1459	15.1010
13	7.8906	13.9984	17.7219	19.8992
14	7.7823	6.0000	16.6551	15.5421
15	5.8835	6.1088	17.1686	18.7010
16	7.7244	6.0000	12.2951	15.9921
17	5.0029	8.0445	19.8803	18.0055
18	7.0031	6.0011	10.0610	14.1998
19	5.2009	12.4074	14.6564	8.8970
20	6.1788	8.1388	10.6560	14.1843
21	7.8476	6.9769	13.1601	15.9596
22	9.5373	11.8528	11.8787	15.3522
23	6.5095	8.3099	12.3214	19.9802
24	9.9177	13.0540	13.0304	19.9765

Table 8.5: Optimal Hydrothermal generation (MW) for Case 2 of Test system 1

Hour	P_{h1}	P_{h2}	P_{h3}	P_{h4}	P_{s1}	P_{s2}	P_{s3}
1	92.6100	63.9615	0	213.6601	122.1689	125.2868	139.7785
2	72.0690	48.8005	53.9559	158.9365	102.1068	124.9066	229.5288
3	90.5573	55.8236	39.3585	147.3153	22.3948	209.8356	139.7956
4	95.2653	71.4961	46.8511	226.7319	37.4826	124.9118	50.3266
5	64.4403	79.5934	0	168.2443	103.4868	209.7797	50.0244
6	86.4464	68.0254	45.6081	155.0956	102.6608	209.8791	139.7594
7	87.0237	61.2782	27.9579	160.1385	102.5044	294.8457	229.5773
8	49.2803	46.8086	28.2529	120.8731	174.9965	294.7645	319.2813
9	49.1387	64.1123	51.9322	161.4573	175.0000	209.8045	409.0575
10	71.2390	65.7464	0	247.9682	102.8565	209.7914	409.1246
11	54.4256	46.9804	49.8889	268.9013	174.9520	124.9140	408.9994
12	86.6665	54.0037	43.1493	249.0915	101.1599	233.6258	409.1566
13	73.9668	87.2270	41.9211	288.9727	21.3038	294.7193	319.2980
14	74.1884	45.8833	45.3111	252.3226	101.2632	209.7447	319.2779
15	61.1788	48.5052	44.8146	288.6069	54.3860	209.8203	319.3000
16	76.0425	49.4609	51.7633	264.2455	102.5348	300.0000	229.5336
17	54.5668	63.9598	39.2267	280.3727	101.6611	294.2266	229.5039
18	71.8442	50.0229	51.4094	249.6692	102.6795	294.6845	319.2968
19	56.7906	83.3577	53.5455	194.2653	174.9987	209.8079	319.2752
20	65.5160	60.4779	52.9102	259.2640	100.7737	209.7701	319.2732
21	78.3576	53.2899	55.3335	273.3419	20.8830	124.9627	319.0909
22	88.8353	79.0570	55.1741	271.7308	20.0101	124.8635	229.5576
23	67.9998	60.8176	57.2467	300.3369	20.0000	209.8037	139.7718
24	91.0733	80.6164	58.3263	294.6325	20.0000	209.6778	50.0052

Table 8.6: Cost and CPU time for Case 2 of Test system 1

Techniques	MEP
Best cost ($)	43719.08
Average cost ($)	43748.13
Worst cost ($)	43788.21
CPU time (s)	136.45

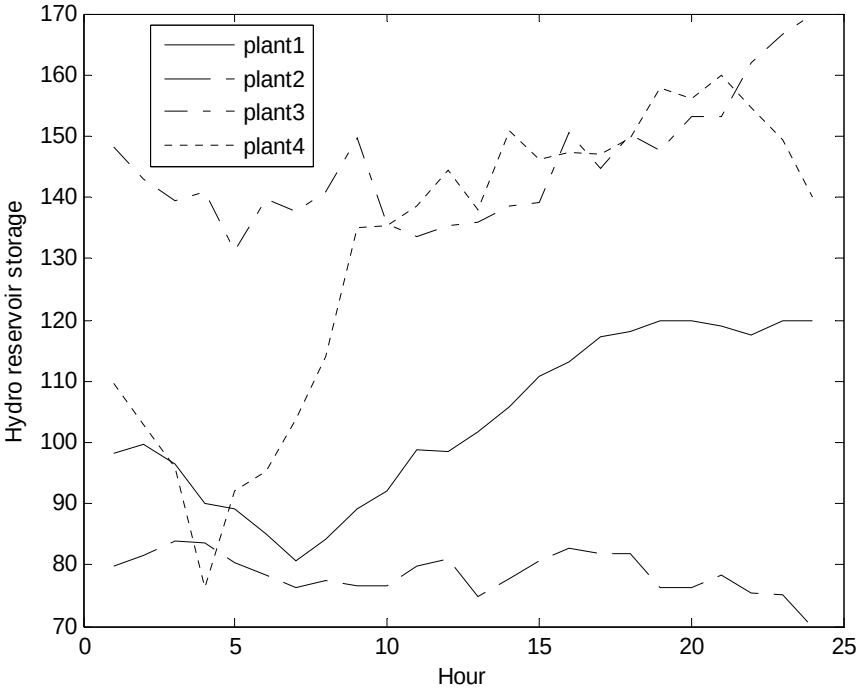

Fig. 8.3. Hydro reservoir storage volumes for Case 2 of Test system 1

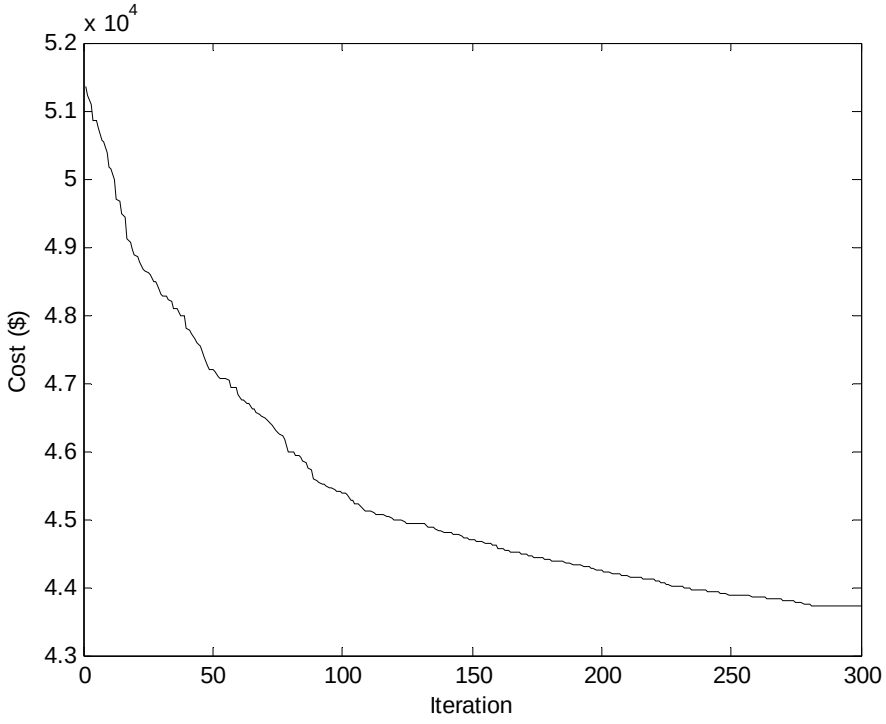

Fig. 8.4. Cost convergence characteristics for Case 2 of Test system 1

8.3.2. Test System 2

The system considers a multi-chain cascade of four reservoir hydro plants and ten thermal plants. The entire scheduling period is 1 day and divided into 24 intervals. The effect of valve point loading is taken into account. The hydro plant data is same as in test system 1 and the thermal plant data is given in the appendix.

The problem is solved by using MEP. Here, parameters are taken as $N_P = 100$, $\beta = 0.5$, $C_R = 1$ and $iter_{max} = 600$.

The optimal hourly discharges and hydrothermal generation obtained by the proposed MEP method are provided in Table 8.7 and Table 8.8 respectively, Figure 8.5 shows the reservoir storage volumes of four hydro plants obtained from MEP. The best, average and worst cost and average CPU time among 100 runs of solutions obtained from proposed FCEP are summarized in Table 8.9. The cost obtained from differential evolution (DE) [110] method is also shown in Table 8.9. The cost convergence characteristic in case of MEP is depicted in Fig. 8.6. Results show that the best cost for this test system as obtained by MEP is less than those obtained from DE [110]. Moreover, the best, worst, average costs obtained by MEP out of certain number of trials are quite close to each other. It establishes the improved robustness of the algorithm.

Table 8.7: Optimal Hydro Discharge ($\times 10^4 m^3$) for Test system 2

Hour	Q_{h1}	Q_{h2}	Q_{h3}	Q_{h4}
1	7.8833	6.6397	30.000	8.285
2	12.904	6.7961	19.013	11.707
3	5.3944	7.4013	15.646	10.551
4	6.1076	6.5282	21.477	9.478
5	5.9737	6.8022	30.000	8.144
6	6.9325	6.0589	12.761	15.093
7	8.8653	8.0255	15.560	6.682
8	5.0001	6.0093	27.122	10.452
9	10.1801	10.0930	10.063	13.289
10	11.7320	6.0008	10.002	11.807
11	7.8904	12.3461	16.155	14.939
12	7.7506	9.5169	18.092	18.056
13	9.9329	6.0557	20.684	11.143
14	8.6058	11.0472	10.977	13.675
15	5.0061	10.0483	15.431	14.983
16	9.6209	8.2951	24.294	19.223
17	11.4310	11.9580	10.014	17.666
18	9.7916	6.8591	17.201	13.939
19	6.0958	9.5813	15.938	19.970
20	8.4204	6.1953	12.360	18.201
21	5.0000	8.2018	10.137	19.932
22	8.2182	12.9871	14.437	12.583
23	10.7490	10.2610	20.011	20.000
24	5.5137	8.2937	14.131	19.778

Table 8.8: Optimal Hydrothermal generation (MW) for Test system 2

Hour	P_{h1}	P_{h2}	P_{h3}	P_{h4}	P_{s1}	P_{s2}	P_{s3}	P_{s4}	P_{s5}	P_{s6}	P_{s7}	P_{s8}	P_{s9}	P_{s10}
1	74.3811	53.4191	0	161.1561	229.4918	199.3606	94.9902	119.6121	274.3415	189.2577	45.0098	84.8895	98.2500	125.8405
2	96.7439	55.2736	41.9161	193.1701	139.8012	349.1918	20.2030	20.0022	174.4235	239.4293	163.5059	84.7458	25.0000	176.5935
3	55.4954	59.9003	48.0375	171.4724	229.2625	124.6643	95.5600	119.9075	324.3470	139.6317	45.0267	84.9201	25.0730	176.7015
4	61.9277	55.0861	24.8062	150.2950	319.0316	50.0001	20.0004	119.8904	124.7640	239.2678	104.2990	178.9790	25.0558	176.5970
5	61.0675	58.3209	0	124.9159	139.7358	273.6890	94.2244	119.7487	174.6065	40.0449	223.3538	85.0589	98.4727	176.7610
6	68.3906	53.7998	45.3094	215.9834	229.4193	125.1702	20.0000	120.2536	124.7198	289.1639	222.1683	134.2248	25.0000	126.3967
7	80.8140	67.2851	43.3817	134.0935	319.2095	274.4587	94.2960	119.6850	173.8420	189.0789	104.2134	134.6693	97.8724	117.1004
8	52.6940	52.8663	0	187.4420	229.7633	349.2578	94.6387	69.7966	324.1460	287.1512	104.1468	84.6620	98.1583	75.2771
9	88.5164	77.8345	42.3013	227.0123	318.9880	348.6034	20.0000	69.8373	124.7022	189.6397	222.7823	134.9166	98.5611	126.3049
10	94.5742	52.2096	44.1260	227.7515	229.2607	347.6756	20.1319	69.9257	224.2217	239.2966	222.9305	35.0367	98.4181	174.4411
11	75.5537	87.5986	41.4255	259.1608	319.4205	199.4831	94.8218	119.7352	323.0090	40.0006	281.7792	84.8624	98.1757	74.9741
12	75.6297	73.5535	35.9179	284.1861	229.4701	124.5714	20.0058	119.6885	373.3563	239.2792	104.1592	183.7503	159.9221	126.5099
13	88.9545	51.5721	26.9853	229.1679	139.6887	423.1678	94.6534	69.6805	423.9153	139.5681	163.5473	35.0051	97.4705	126.6236
14	81.8635	80.8717	47.4727	255.1393	229.2460	348.7871	94.8599	20.0255	274.1660	139.6729	222.7474	84.0564	25.0013	126.0903
15	54.7486	75.1676	48.7010	264.1232	139.9014	423.6967	94.6401	119.7889	174.8115	40.0294	103.9937	184.3588	159.9997	126.0392
16	89.6371	65.3307	12.0227	297.4801	229.8796	124.8048	94.7917	119.7629	25.0400	189.4061	341.1465	134.6513	160.0000	176.0465
17	98.3834	82.2172	49.6345	285.8024	140.0193	199.3870	20.4951	20.1612	124.7868	339.3083	282.0454	234.4866	98.2815	74.9913
18	90.1868	53.2709	47.0367	257.1652	229.4313	423.9930	94.7168	69.9551	323.7187	139.9808	104.1276	135.3306	25.0005	126.0858
19	64.5535	68.2912	51.4123	300.8917	409.0538	199.8691	20.0001	69.5723	74.5428	239.4277	163.5398	234.6874	98.1449	76.0135
20	81.9364	46.6343	55.7243	285.0431	50.0000	200.0078	94.3709	119.8313	324.0908	40.0000	281.1232	134.4220	159.9998	176.8164
21	54.7444	60.4544	55.5549	302.2867	229.7679	274.3812	94.8104	20.0633	274.5393	89.9110	45.0000	184.5704	98.1656	125.7504
22	80.5452	81.5119	58.4872	233.7478	319.2161	349.1525	20.0583	69.7106	25.0000	40.0004	223.1170	134.7023	98.4035	126.3471
23	94.5605	68.7179	46.3529	297.0912	139.8009	199.6968	94.3613	20.1141	74.6949	415.5009	163.1718	35.0003	25.0000	175.9365
24	59.3956	57.2693	58.2317	291.4354	319.2163	274.2234	91.0358	69.5051	124.7541	139.4959	45.0011	35.0009	159.9996	75.4360

Table 8.9: Comparison of performance for Test system 2

Techniques	MEP	DE
Best cost ($)	170344.24	170964.15
Average cost ($)	170403.51	-
Worst cost ($)	170578.40	-
CPU time (s)	157.06	-

Table 8.8: Optimal Hydrothermal generation (MW) for Test system 2

Hour	P_{h1}	P_{h2}	P_{h3}	P_{h4}	P_{s1}	P_{s2}	P_{s3}	P_{s4}	P_{s5}	P_{s6}	P_{s7}	P_{s8}	P_{s9}	P_{s10}
1	74.3811	53.4191	0	161.1561	229.4918	199.3606	94.9902	119.6121	274.3415	189.2577	45.0098	84.8895	98.2500	125.8405
2	96.7439	55.2736	41.9161	193.1701	139.8012	349.1918	20.2030	20.0022	174.4235	239.4293	163.5059	84.7458	25.0000	176.5935
3	55.4954	59.9003	48.0375	171.4724	229.2625	124.6643	95.5600	119.9075	324.3470	139.6317	45.0267	84.9201	25.0730	176.7015
4	61.9277	55.0861	24.8062	150.2950	319.0316	50.0001	20.0004	119.8904	124.7640	239.2678	104.2990	178.9790	25.0558	176.5970
5	61.0675	58.3209	0	124.9159	139.7358	273.6890	94.2244	119.7487	174.6065	40.0449	223.3538	85.0589	98.4727	176.7610
6	68.3906	53.7998	45.3094	215.9834	229.4193	125.1702	20.0000	120.2536	124.7198	289.1639	222.1683	134.2248	25.0000	126.3967
7	80.8140	67.2851	43.3817	134.0935	319.2095	274.4587	94.2960	119.6850	173.8420	189.0789	104.2134	134.6693	97.8724	117.1004
8	52.6940	52.8663	0	187.4420	229.7633	349.2578	94.6387	69.7966	324.1460	287.1512	104.1468	84.6620	98.1583	75.2771
9	88.5164	77.8345	42.3013	227.0123	318.9880	348.6034	20.0000	69.8373	124.7022	189.6397	222.7823	134.9166	98.5611	126.3049
10	94.5742	52.2096	44.1260	227.7515	229.2607	347.6756	20.1319	69.9257	224.2217	239.2966	222.9305	35.0367	98.4181	174.4411
11	75.5537	87.5986	41.4255	259.1608	319.4205	199.4831	94.8218	119.7352	323.0090	40.0006	281.7792	84.8624	98.1757	74.9741
12	75.6297	73.5535	35.9179	284.1861	229.4701	124.5714	20.0058	119.6885	373.3563	239.2792	104.1592	183.7503	159.9221	126.5099
13	88.9545	51.5721	26.9853	229.1679	139.6887	423.1678	94.6534	69.6805	423.9153	139.5681	163.5473	35.0051	97.4705	126.6236
14	81.8635	80.8717	47.4727	255.1393	229.2460	348.7871	94.8599	20.0255	274.1660	139.6729	222.7474	84.0564	25.0013	126.0903
15	54.7486	75.1676	48.7010	264.1232	139.9014	423.6967	94.6401	119.7889	174.8115	40.0294	103.9937	184.3588	159.9997	126.0392
16	89.6371	65.3307	12.0227	297.4801	229.8796	124.8048	94.7917	119.7629	25.0400	189.4061	341.1465	134.6513	160.0000	176.0465
17	98.3834	82.2172	49.6345	285.8024	140.0193	199.3870	20.4951	20.1612	124.7868	339.3083	282.0454	234.4866	98.2815	74.9913
18	90.1868	53.2709	47.0367	257.1652	229.4313	423.9930	94.7168	69.9551	323.7187	139.9808	104.1276	135.3306	25.0005	126.0858
19	64.5535	68.2912	51.4123	300.8917	409.0538	199.8691	20.0001	69.5723	74.5428	239.4277	163.5398	234.6874	98.1449	76.0135
20	81.9364	46.6343	55.7243	285.0431	50.0000	200.0078	94.3709	119.8313	324.0908	40.0000	281.1232	134.4220	159.9998	176.8164
21	54.7444	60.4544	55.5549	302.2867	229.7679	274.3812	94.8104	20.0633	274.5393	89.9110	45.0000	184.5704	98.1656	125.7504
22	80.5452	81.5119	58.4872	233.7478	319.2161	349.1525	20.0583	69.7106	25.0000	40.0004	223.1170	134.7023	98.4035	126.3471
23	94.5605	68.7179	46.3529	297.0912	139.8009	199.6968	94.3613	20.1141	74.6949	415.5009	163.1718	35.0003	25.0000	175.9365
24	59.3956	57.2693	58.2317	291.4354	319.2163	274.2234	91.0358	69.5051	124.7541	139.4959	45.0011	35.0009	159.9996	75.4360

Table 8.9: Comparison of performance for Test system 2

Techniques	MEP	DE
Best cost ($)	170344.24	170964.15
Average cost ($)	170403.51	-
Worst cost ($)	170578.40	-
CPU time (s)	157.06	-

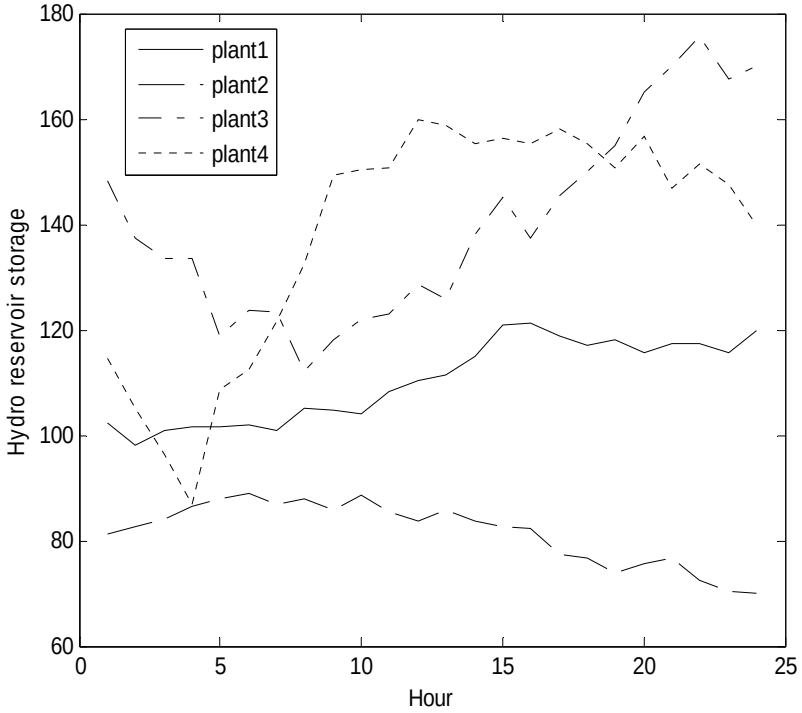

Fig. 8.5. Hydro reservoir storage volumes for Case 1 of Test system 2

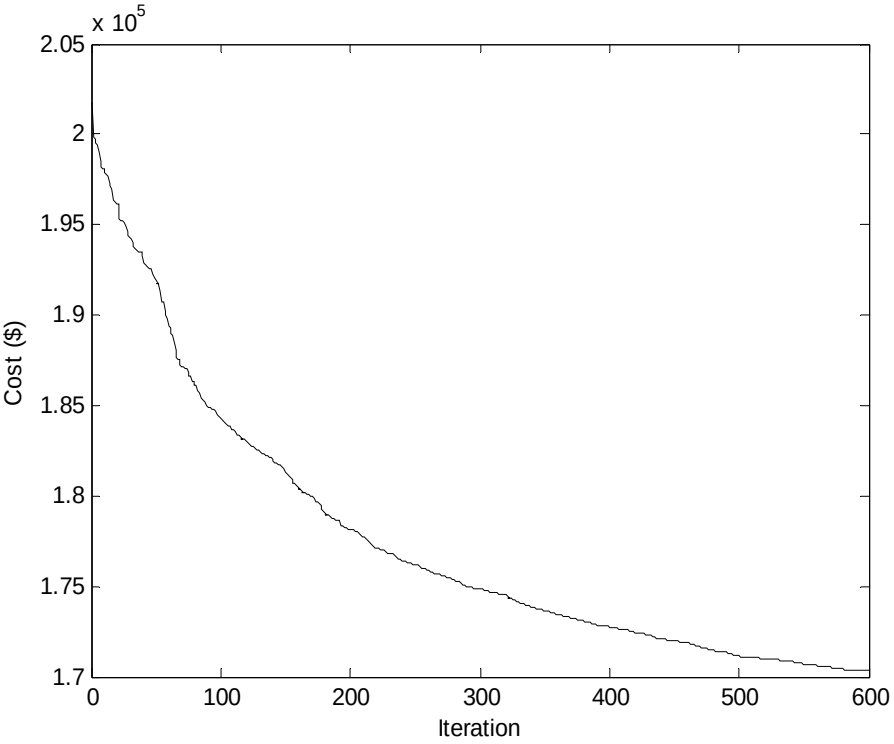

Fig. 8.6. Cost convergence characteristics for Case 1 of Test system 2

8.4. Conclusion

In this paper, MEP has been developed and applied to solve the two test problems and two hydrothermal multi-reservoir cascaded hydroelectric test systems having prohibited operating zones and thermal units with valve point loading. It has been observed that MEP method has the ability to converge to a better quality solution and robustness. MEP has both good exploration and exploitation ability. It is clear from the results obtained by different trials that the proposed MEP method can avoid the shortcoming of premature convergence.

8.5. Application of GSO method

Three hydrothermal test systems are investigated and the computational results have been used to compare the performance of the proposed GSO method with that of other evolutionary methods. The algorithm used in this paper is implemented by using MATLAB 7.0 on a PC (Pentium-IV, 80 GB, 3.0 GHz).

Three hydrothermal test systems are considered to inspect and verify the proposed GSO method.

8.5.1. Test System 1: This test system considers a multi-chain cascade of four reservoir hydro plants and an equivalent thermal plant. The entire scheduling period is 1 day and divided into 24 intervals. Here, two cases are considered.

Case 1: Here fuel cost is considered as a quadratic function of the power from the composite thermal plant. The detailed parameters for this case come from [108].

The problem is solved by using GSO. Here, the population size (N_P) and maximum iteration number have been selected 100 and 200 respectively for this case.

The optimal hourly discharges and hydrothermal generation obtained by the proposed GSO method are provided in Table 8.10 and Table 8.11 respectively. Figure 8.7 depicts the reservoir storage volumes of four hydro plants obtained from GSO. The best, average and the worst cost and average CPU time among 100 runs of solutions obtained from the proposed GSO are summarized in Table 8.12. The cost obtained from modified differential evolution (MDE) [123], improved particle swarm optimization (IPSO) [125], teaching learning based optimization (TLBO) [114], improved fast evolutionary programming (IFEP) [108] and genetic algorithm

(GA) [106] methods are also shown in Table 8.12. The cost convergence characteristic in case of GSO is shown in Fig. 8.8.

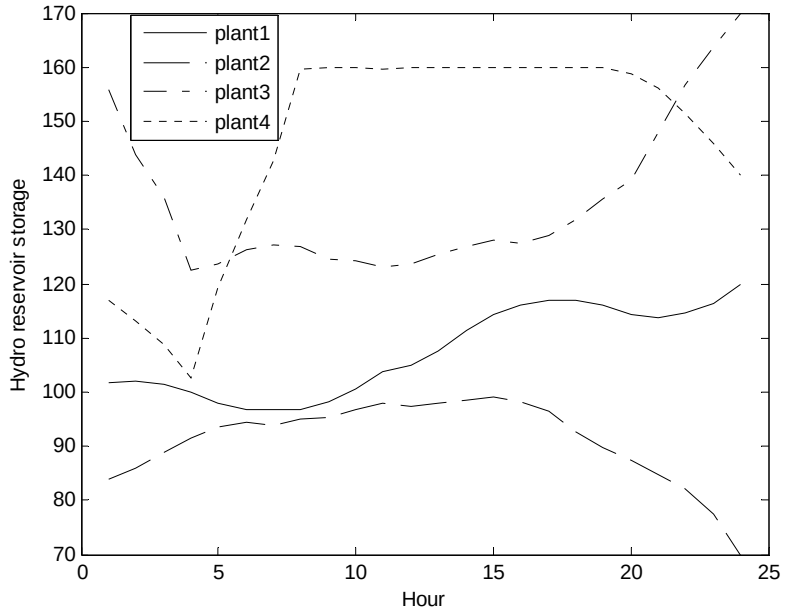

Fig. 8.7. Hydro reservoir storage volumes for Case 1 of Test system 1

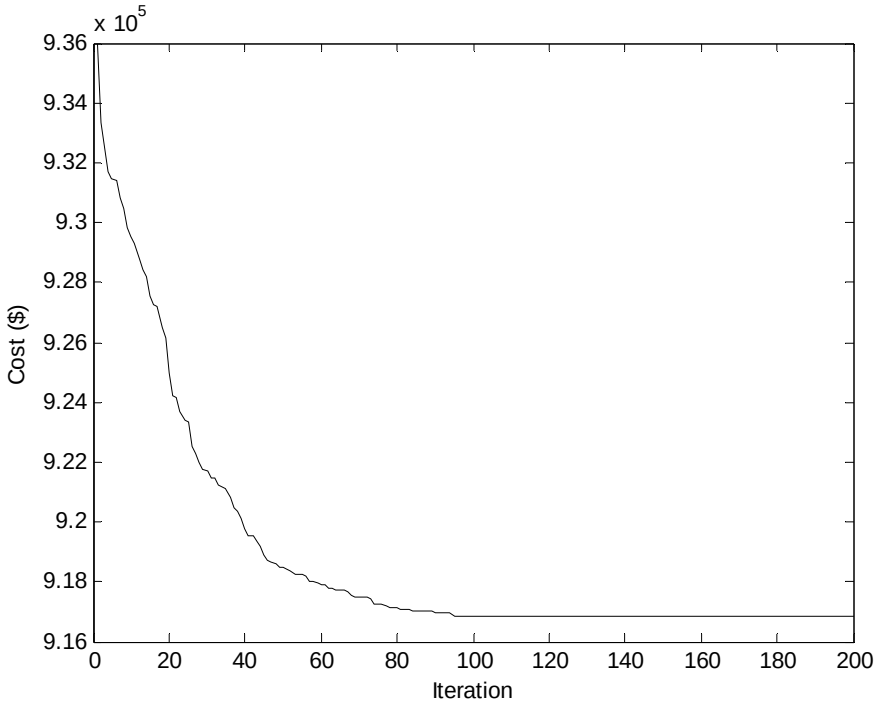

Fig. 8.8. Cost convergence characteristics for Case 1 of Test system 1

Table 8.10: Optimal Hydro Discharge ($\times 10^4 m^3$) for Case 1 of Test System 1

Hour	Q_{h1}	Q_{h2}	Q_{h3}	Q_{h4}
1	9.3207	6.0007	29.8079	6.0000
2	8.1025	6.1972	30.0000	6.0000
3	8.1651	6.0036	17.4038	6.0824
4	8.6098	6.0000	16.3785	6.2337
5	8.2380	6.0274	16.5929	6.4178
6	7.1368	6.0297	16.2300	6.9001
7	8.9886	6.0720	16.7684	10.2395
8	8.7364	6.8314	16.6709	13.6340
9	8.7740	7.3950	16.2860	15.8907
10	8.8471	7.7045	16.0385	16.9213
11	8.5867	7.6832	15.7894	16.7272
12	8.3218	7.7423	16.6544	16.0383
13	8.0765	7.7875	19.0441	16.6773
14	8.1759	8.8526	19.3577	16.0927
15	8.4697	8.2522	19.0018	17.0796
16	8.9454	8.7810	18.6988	17.1725
17	7.6274	8.8878	16.5303	18.1705
18	7.5446	9.5904	16.8461	18.4444
19	7.9694	10.7311	14.3550	19.1983
20	7.6817	11.2308	13.7930	20.0000
21	8.2990	10.9637	10.3630	20.0000
22	7.2589	11.6870	10.9224	19.4549
23	6.7623	12.5093	11.7597	20.0000
24	6.3617	13.0396	13.6474	19.6723

Table 8.11: Optimal Hydrothermal generation (MW) for Case 1 of Test system 1

Hour	P_{h1}	P_{h2}	P_{h3}	P_{h4}	P_s
1	82.681	49.005	0	131.88	1106.4
2	75.963	52.696	0	129.03	1132.3
3	76.616	52.315	39.644	126.84	1064.6
4	79.234	53.882	41.024	124.62	991.24
5	76.530	55.604	40.342	120.91	996.62
6	68.693	56.583	41.596	149.02	1094.1
7	80.042	57.354	41.077	209.98	1261.5
8	78.317	62.673	41.527	252.43	1565.1
9	78.618	66.505	41.969	275.42	1777.5
10	79.446	68.783	42.476	284.45	1844.8
11	78.685	69.278	42.966	282.27	1756.8
12	78.128	70.280	41.118	276.71	1843.8
13	77.049	70.687	33.496	282.50	1766.3
14	78.408	77.162	32.679	277.38	1734.4
15	81.124	73.722	34.038	285.24	1655.9
16	84.550	77.185	35.186	284.72	1588.4
17	76.191	77.417	42.049	291.50	1642.8
18	75.809	80.288	42.236	294.26	1647.4
19	78.850	83.882	48.143	300.15	1729.0
20	76.707	83.878	49.736	304.88	1764.8
21	80.591	80.816	50.222	303.54	1724.8
22	73.201	82.464	53.076	296.68	1614.6
23	69.578	83.560	55.877	297.14	1343.8
24	66.684	82.021	57.991	289.15	1094.2

Table 8.12: Comparison of performance for Case 1 of Test System 1

Techniques	GSO	TLBO	IPSO	MDE	IFEP	GA
Best cost ($)	916869.96	922373.39	922553.49	922556.44	930129.82	926707.00
Average cost ($)	917001.20	922462.24	-	-	930290.13	-
Worst cost ($)	917022.33	922873.81	-	-	930881.92	-
CPU time (s)	354.2781	-	-	-	1033.20	-

Case 2: Here prohibited operating zones of hydro plants and valve point loading of thermal generator are considered. The detailed parameters for this case come from [108].

The problem is solved by using GSO.Here, the population size (N_P) and maximum iteration number have been selected 100 and 200 ,respectively for this case.

The optimal hourly discharges and hydrothermal generation obtained by the proposed GSO method are provided in Table 8.13 and Table 8.14 respectively. Figure 8.9 shows the reservoir storage volumes of four hydro plants obtained from GSO. The best, average and worst cost and average CPU time among 100 runs of solutions obtained from the proposed GSO are summarized in Table 8.15. The cost obtained from improved fast evolutionary programming (IFEP) [108], improved particle swarm optimization (IPSO) [125] and teaching learning based optimization (TLBO) [114] method are also shown in Table 8.15. The cost convergence characteristic in case of GSO is depicted in Fig. 8.10.

Table 8.15: Comparison of performance for Case 2 of Test system 1

Techniques	GSO	TLBO	IPSO	IFEP
Best cost ($)	922838.19	924550.78	925978.84	933949.25
Average cost ($)	922882.64	924702.43	-	938508.87
Worst cost ($)	922966.62	925149.06	-	942593.02
CPU time (s)	381.5471	-	-	1450.90

Table 8.13: Optimal Hydro Discharge ($\times 10^4 m^3$) for Case 2 of Test system 1

Hour	Q_{h1}	Q_{h2}	Q_{h3}	Q_{h4}
1	7.4898	6.9473	19.5968	6.7572
2	10.4231	6.5828	21.9846	6.0889
3	11.3134	6.1767	20.0759	6.0960
4	9.3925	8.6856	29.9608	6.0380
5	7.1830	6.0905	15.9483	8.4937
6	9.0076	9.3469	18.2507	6.2724
7	7.8955	6.9913	17.7056	11.0662
8	9.2724	8.9670	16.7099	13.4913
9	9.3371	6.5613	17.2705	15.7099
10	5.9732	6.0006	15.8547	14.4682
11	9.7379	6.3226	16.2620	18.0152
12	6.6540	6.0573	18.7716	15.9977
13	7.5780	6.9812	17.9492	18.6503
14	5.0727	10.7346	16.1525	18.8333
15	9.0183	8.1430	17.4240	13.7201
16	12.0758	10.2880	21.9906	19.8576
17	7.6567	8.3800	14.2722	18.4646
18	9.3625	11.4929	14.7963	15.9875
19	6.7271	8.2192	16.0289	19.9939
20	6.1177	10.9451	15.7040	19.4079
21	7.0894	8.7609	11.2012	18.5244
22	5.0784	9.0879	10.2714	20.0000
23	6.5126	12.9916	13.8940	20.0000
24	9.4855	10.9554	10.2551	18.9738

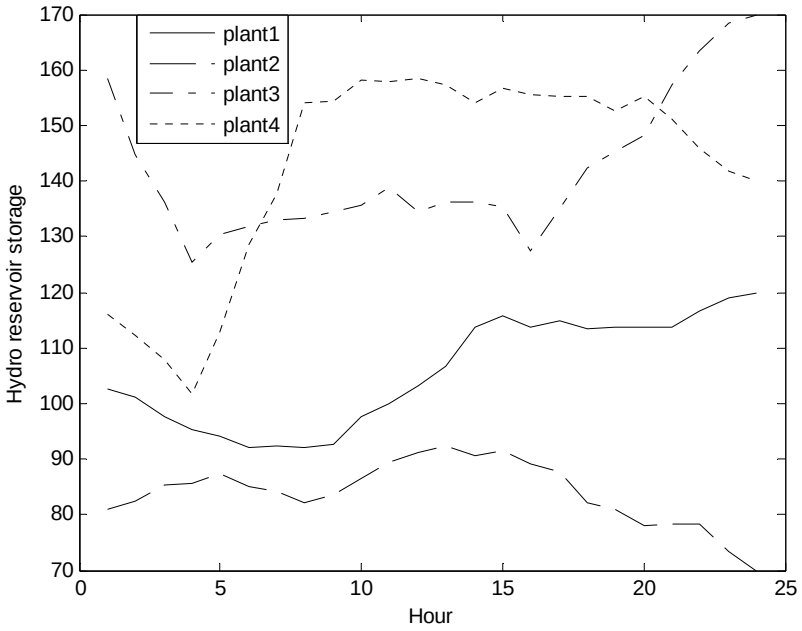

Fig. 8.9. Hydro reservoir storage volumes for Case 2 of Test system 1

Table 8.14: Optimal Hydrothermal generation (MW) for Case 2 of Test system 1

Hour	P_{h1}	P_{h2}	P_{h3}	P_{h4}	P_s
1	71.807	55.457	46.472	141.94	1054.3
2	88.780	53.662	31.683	129.53	1086.3
3	91.746	51.685	36.266	126.24	1054.1
4	82.269	69.128	0	121.23	1017.4
5	68.347	52.830	43.273	145.42	980.13
6	78.964	73.989	38.319	129.10	1089.6
7	71.885	58.764	40.704	200.99	1277.7
8	79.576	70.007	44.089	233.96	1572.4
9	79.786	54.195	42.644	269.47	1793.9
10	58.692	51.105	46.617	258.75	1904.8
11	83.938	55.038	46.185	291.22	1753.6
12	65.901	54.569	39.518	275.34	1874.7
13	73.303	61.985	40.914	296.01	1757.8
14	54.377	83.410	46.642	295.84	1719.7
15	84.813	68.958	43.192	251.55	1681.5
16	99.319	80.874	22.682	301.79	1565.3
17	76.073	69.574	46.957	291.85	1645.5
18	87.047	83.915	48.728	272.73	1647.6
19	69.223	64.661	48.892	301.09	1756.1
20	64.376	77.455	50.454	294.91	1792.8
21	72.002	65.093	53.597	291.91	1757.4
22	55.301	66.987	54.389	296.63	1646.7
23	67.925	82.738	57.433	290.96	1350.9
24	88.558	72.147	56.295	280.62	1092.4

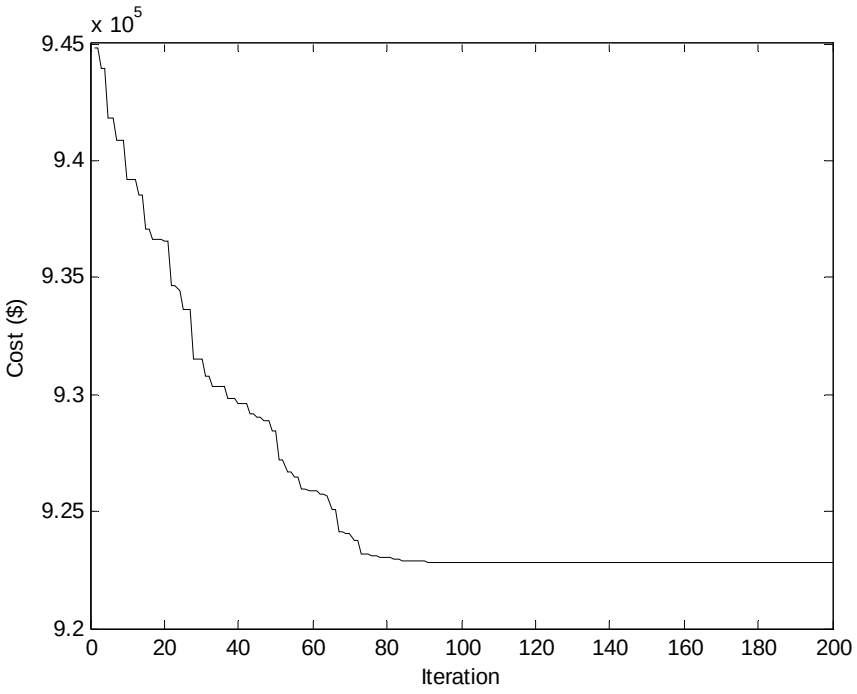

Fig. 8.10. Cost convergence characteristics for Case 2 of Test system 1

8.5.2. Test System 2: This system considers a multi-chain cascade of four reservoir hydro plants and three thermal plants. The entire scheduling period is 1 day and divided into 24 intervals. The effect of valve point loading is considered. Transmission loss is also considered. Here, two cases are considered.

Case 1: Here prohibited operating zones of hydro plants and ramp rate limits of thermal generators are not considered. The detailed parameters for this case are taken from [110].

The problem is solved by using GSO. Here, the population size (N_P) and maximum iteration number have been selected 100 and 200 respectively for this case.

The optimal hourly discharges and hydrothermal generation obtained by the proposed GSO method are provided in Table 8.16 and Table 8.17 respectively. Figure 8.11 shows the reservoir storage volumes of four hydro plants obtained from GSO. The best, average and worst cost and average CPU time among 100 runs of solutions obtained from the proposed GSO are shown in Table 8.18. The cost obtained from modified differential evolution (MDE) [123], clonal selection algorithm (CSA) [113] and teaching learning based optimization (TLBO) [114] are also shown in Table 8.18. The cost convergence characteristic in case of GSO is depicted in Fig. 8.12.

Table 8.18: Comparison of performance for Case 1 of Test system 2

Techniques	GSO	TLBO	CSA	MDE
Best cost ($)	42316.39	42385.88	42440.574	43435.41
Average cost ($)	42339.35	42407.23	-	-
Worst cost ($)	42379.18	42441.36	-	-
CPU time (s)	617.36	-	-	-

Table 8.16: Optimal Hydro Discharge ($\times 10^4\, m^3$) for Case 1 of Test system 2

Hour	Q_{h1}	Q_{h2}	Q_{h3}	Q_{h4}
1	11.7993	7.1449	30.0000	7.6659
2	5.9325	6.8499	29.9757	6.5549
3	11.4742	9.3709	29.7421	10.3072
4	5.0019	6.2129	20.4887	9.6863
5	8.5132	6.0097	10.0000	8.4503
6	9.1282	6.7017	17.6091	10.4643
7	6.8646	7.4826	10.0568	14.9192
8	7.8009	6.0002	17.6538	12.3589
9	10.0992	6.3307	14.0775	17.9668
10	5.6734	10.2662	18.8554	11.8789
11	10.2460	7.0654	20.2200	11.4409
12	5.2613	6.0093	13.6258	11.8636
13	11.8242	6.0103	15.9895	19.8410
14	6.1295	12.9566	16.3355	19.8356
15	6.8119	14.0000	10.0000	16.4685
16	9.8751	6.1626	17.9912	16.4937
17	5.5286	9.5098	29.2693	10.8819
18	10.9777	11.7961	14.1740	18.8395
19	5.8392	8.1255	14.5868	19.9943
20	5.2688	11.2726	10.7198	16.9838
21	5.7397	7.9265	12.5406	19.5902
22	9.7474	7.3261	13.5104	18.8458
23	8.6849	8.7383	10.8830	17.7032
24	10.7782	12.7314	12.7362	19.1362

Table 8.17: Optimal Hydrothermal generation (MW) for Case 1 of Test system 2

Hour	P_{h1}	P_{h2}	P_{h3}	P_{h4}	P_{s1}	P_{s2}	P_{s3}
1	92.9170	56.7357	0	153.5424	20.0859	294.3998	138.7168
2	59.8990	55.3298	0	134.8516	20.0018	124.6736	408.5219
3	92.3743	70.7927	0	175.1130	102.5884	40.0044	228.9469
4	52.0329	51.4571	20.5900	159.1629	20.0047	125.1561	229.8831
5	78.1663	51.5997	40.5012	134.8991	104.5505	40.0160	229.9579
6	80.7310	57.5201	35.6610	180.0767	102.5262	40.3496	319.1720
7	66.0599	62.7948	44.5356	242.5705	20.2328	294.5374	230.0391
8	72.7030	51.9763	38.9242	232.8835	102.3008	294.8682	229.7055
9	85.5131	54.8651	46.7771	289.3656	102.7033	294.8192	229.6595
10	57.6052	78.7446	34.4928	227.9884	174.5848	295.0858	229.3351
11	88.0720	60.0656	27.3119	228.0775	102.5632	294.4701	319.1498
12	55.6598	53.8275	45.4523	231.5432	174.7684	293.5248	319.1802
13	96.4554	54.8569	41.6027	303.7958	102.6171	294.5824	229.9690
14	63.6529	91.9548	43.9481	297.7683	20.0009	294.5678	229.3138
15	69.9805	92.4030	47.3566	273.6624	102.4510	294.4136	139.3255
16	90.5602	52.2215	42.6548	277.4700	174.9796	209.3063	228.9159
17	59.7794	73.5932	0	220.6096	101.6658	295.0208	319.0892
18	96.6357	82.0140	47.4006	296.7394	174.9860	209.6134	228.9350
19	62.5461	60.9118	50.6503	301.3292	172.5992	208.6725	229.3000
20	57.5274	75.3514	50.6731	271.1026	174.7675	294.6420	139.8677
21	61.8007	56.8489	54.3700	289.3822	20.0223	294.2171	140.3575
22	90.5670	53.9499	55.9288	294.9577	20.1260	124.1832	229.6206
23	84.0251	63.2512	55.3422	282.4407	20.0032	124.5925	229.5589
24	95.4774	79.4479	58.0089	288.7071	20.0000	40.0046	227.4394

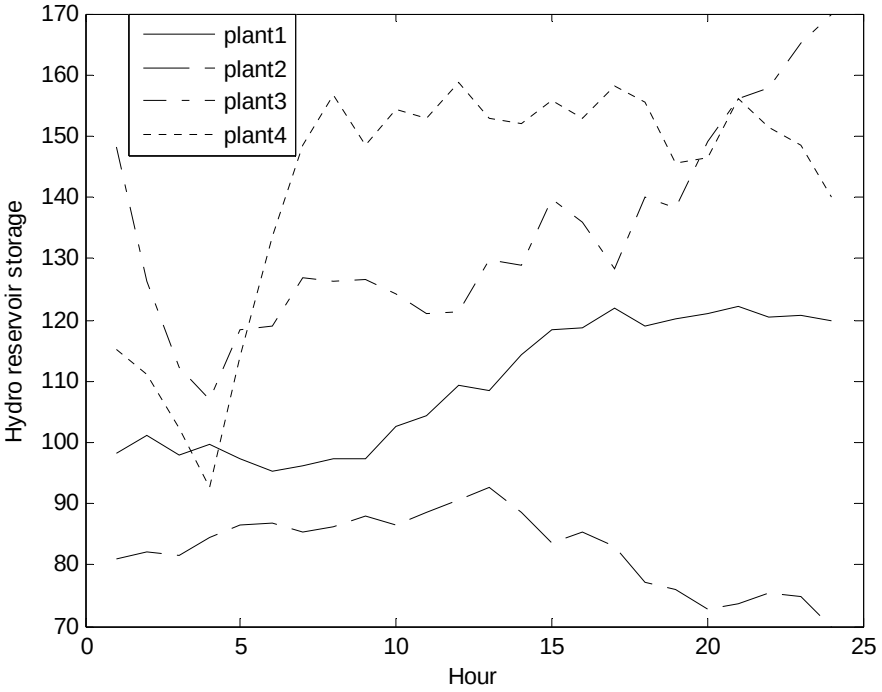

Fig. 8.11. Hydro reservoir storage volumes for Case 1 of test system 2

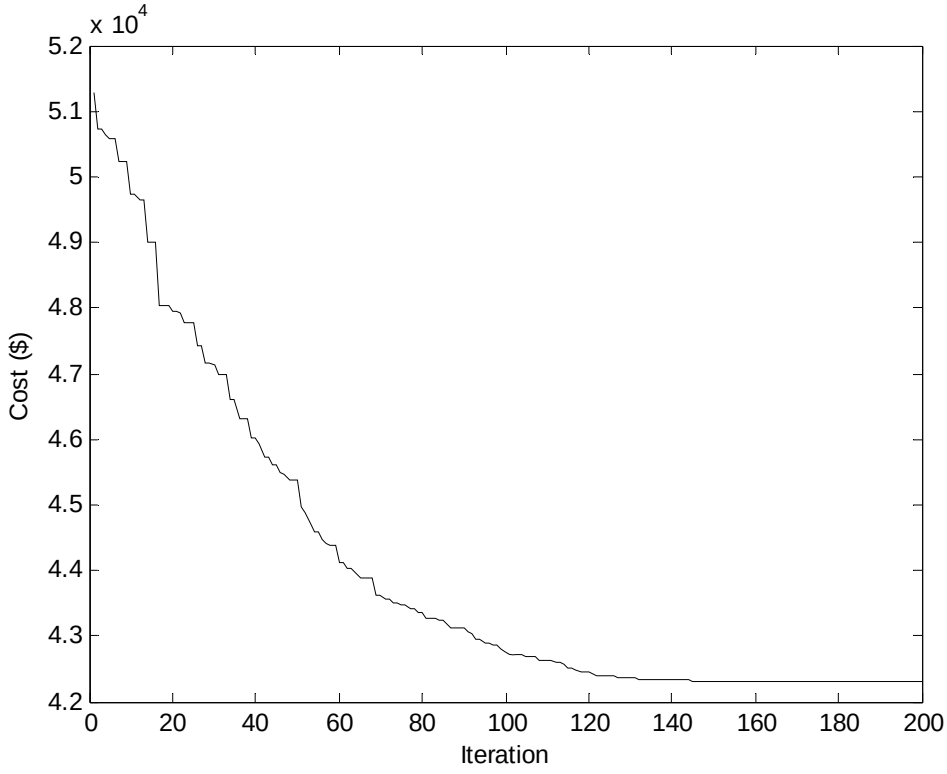

Fig. 8.12. Cost convergence characteristics for Case 1 of Test system 2

Case 2: Here prohibited operating zones of hydro plants and ramp rate limits of thermal generators are considered. Hydro plants data is taken from [108]. The data of thermal plants considered here is same as in [110] except the following modifications in Table 8.19. The other parameters for this case are taken from [110].

The problem is solved by using GSO. Here, the population size (N_P) and maximum iteration number have been selected 100 and 200 respectively for this case.

The optimal hourly discharges and hydrothermal generation obtained by the proposed GSO method are provided in Table 8.20 and Table 8.21 respectively. Figure 8.13 shows the reservoir storage volumes of four hydro plants obtained from GSO. The best, average and the worst cost and average CPU time among 100 runs of solutions obtained from proposed GSO are shown in Table 8.22. The cost convergence characteristic in case of GSO is depicted in Fig. 8.14.

Table 8.19: Ramp-rate limits of thermal generators for Case 2 of Test system 2

Unit	1	2	3
UR (MW/h)	80	90	100
DR (MW/h)	80	90	100

Table 8.22: Cost and CPU time for Case 2 of Test system 2

Techniques	GSO
Best cost ($)	43774.75
Average cost ($)	43781.16
Worst cost ($)	43799.08
CPU time (s)	692.56

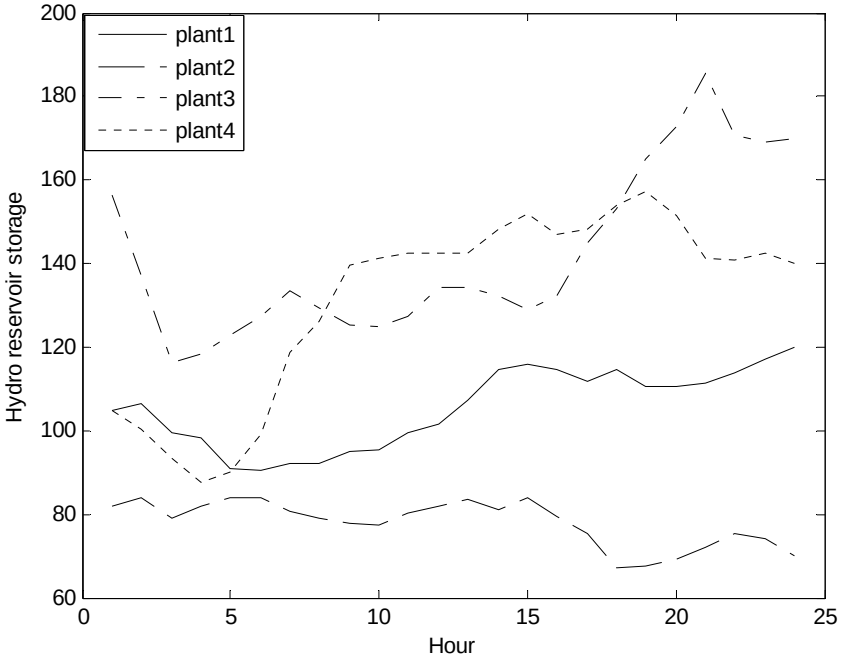

Fig. 8.13 Hydro reservoir storage volumes for Case 2 of Test system 2

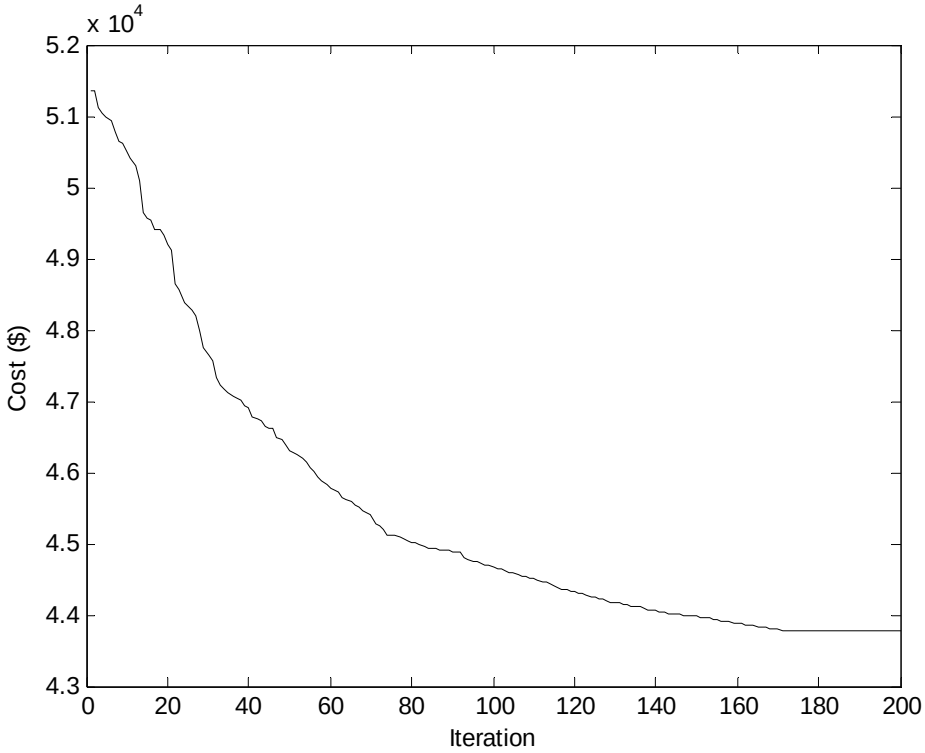

Fig. 8.14. Cost convergence characteristics for Case 2 of Test system 2

Table 8.20: Optimal Hydro Discharge ($\times 10^4\, m^3$) for Case 2 of Test system 2

Hour	Q_{h1}	Q_{h2}	Q_{h3}	Q_{h4}
1	5.0022	6.0000	21.8889	18.0744
2	7.6741	6.0000	27.3248	6.7778
3	14.9422	14.0000	29.7236	8.4532
4	7.9967	6.0595	13.5291	6.0000
5	13.5833	6.0064	19.5864	19.2826
6	7.2906	6.8220	21.5786	18.1877
7	6.2453	9.3678	16.3958	10.2862
8	9.0029	8.7083	19.2798	6.1596
9	7.3276	9.3516	18.3507	6.0005
10	10.4621	9.2971	19.6994	19.7656
11	7.9773	6.0000	14.8063	15.3276
12	7.8944	6.4903	14.8618	19.1044
13	5.1299	6.5289	21.0918	18.4728
14	5.0234	11.2937	18.9006	14.1483
15	9.5472	6.0006	18.1416	11.1422
16	11.2730	12.4542	10.0000	19.7209
17	11.8342	11.3973	10.0816	20.0000
18	5.2603	13.9985	11.1896	13.0295
19	10.8954	6.8402	13.4471	14.9644
20	6.2619	6.2340	10.0003	15.7475
21	6.0023	6.0000	14.1569	20.0000
22	5.6803	6.0001	29.9249	11.9390
23	5.7410	9.0908	14.9247	11.4638
24	6.9523	12.0588	10.5727	12.6300

Table 8.21: Optimal Hydrothermal generation (MW) for Case 2 of Test system 2

Hour	P_{h1}	P_{h2}	P_{h3}	P_{h4}	P_{s1}	P_{s2}	P_{s3}
1	52.5198	49.0000	36.0076	249.9305	20.0000	121.8730	229.3679
2	74.3746	50.1642	0	127.7152	99.9957	209.8170	229.5065
3	101.5216	89.3760	0	143.3878	20.0000	124.8957	229.4525
4	74.9124	48.8266	43.8749	106.3947	29.8837	124.9499	229.5217
5	96.3242	50.1756	27.8428	213.2713	22.3687	124.8622	139.7530
6	67.5342	56.9413	19.5322	211.7184	102.3605	209.7682	139.7393
7	60.0816	72.0747	42.8313	162.1264	102.0268	294.7090	229.2949
8	78.1917	66.4954	35.4813	132.8511	102.6692	294.7107	319.2485
9	68.2906	68.8056	37.5856	137.1086	102.6636	294.6694	409.0199
10	86.0345	67.6461	30.2632	282.7028	102.6528	209.7789	319.2740
11	73.5362	47.4312	45.3048	253.9524	174.9994	124.9056	408.9281
12	74.3013	52.6395	46.0040	282.1173	102.7070	209.8180	408.9789
13	53.9676	53.7910	27.1335	278.3916	102.6098	294.6888	319.2202
14	54.0458	80.3876	37.3269	244.8019	102.6426	294.7446	229.4708
15	87.9594	49.6335	39.4027	219.5364	102.6870	294.6769	229.4714
16	96.4449	85.0593	47.3212	295.7992	22.7066	209.7730	319.3186
17	98.1964	78.3257	48.3967	292.1468	20.0002	294.7109	229.5504
18	56.7472	83.1132	52.8259	239.2710	99.6411	288.4889	319.2301
19	94.5174	46.4018	55.2527	262.8101	99.9742	209.8106	319.2742
20	65.0969	42.5200	55.2920	272.5335	20.0011	209.7822	409.0589
21	62.9371	42.1274	59.2242	296.9141	20.0022	124.8878	319.2493
22	60.3696	44.1224	0	222.1697	20.0000	209.8192	319.2826
23	61.1830	64.8979	58.1670	216.4727	20.0009	124.8946	319.2746
24	71.4254	76.8184	56.8657	230.3650	20.0221	40.0002	319.2846

8.5.3. Test System 3: This system considers a multi-chain cascade of four reservoir hydro plants and ten thermal plants. The entire scheduling period is 1 day and divided into 24 intervals. The effect of valve point loading is taken into account. Here transmission loss is not considered. The prohibited operating zones of hydro plants and ramp rate limits of thermal generators are not considered. The detailed data for this system is taken from [110].

The problem is solved by using GSO. Here, the population size (N_P) and maximum iteration number have been selected 100 and 600, respectively for this case.

The optimal hourly discharges and hydrothermal generation obtained by the proposed GSO method are provided in Table 8.23 and Table 8.24 respectively. Figure 8.15 shows the reservoir storage volumes of four hydro plants obtained from GSO. The best, average and the worst cost and average CPU time among 100 runs of solutions obtained from the proposed GSO are summarized in Table 8.25. The cost obtained from differential evolution (DE) [110] method are also shown in Table 8.25. The cost convergence characteristic in case of GSO is shown in Fig. 8.16.

Table 8.23: Optimal Hydro Discharge ($\times 10^4 m^3$) for Test system 3

Hour	Q_{h1}	Q_{h2}	Q_{h3}	Q_{h4}
1	7.5577	8.0585	22.8612	6.0000
2	6.4444	8.5873	21.5338	12.3138
3	5.0002	6.0007	18.6591	6.1247
4	6.6913	10.6902	14.8013	7.3935
5	10.6590	6.0000	10.0052	10.9356
6	6.3560	6.0000	29.9996	10.2606
7	10.2523	8.4295	21.3387	14.2211
8	8.4169	7.7590	19.7126	19.9994
9	5.0734	12.2299	19.7473	18.2140
10	8.9442	6.0000	23.2289	13.9644
11	14.9999	10.0815	20.0240	6.0000
12	5.5153	6.3749	17.0962	16.9200
13	9.9712	6.6623	25.6696	18.6404
14	7.7850	8.5880	15.0575	18.3978
15	8.6514	6.3156	11.7309	17.7684
16	5.0002	13.8791	19.0578	17.8808
17	9.1944	6.0027	10.0147	18.2795
18	12.9994	11.4764	18.7304	19.9999
19	5.0010	6.0101	10.0000	10.9960
20	7.3047	10.0714	11.3912	13.8901
21	5.0063	6.0086	12.5867	14.6602
22	6.0075	6.3902	10.0001	15.2083
23	8.8456	10.8083	10.0000	19.5912
24	13.3228	13.5758	13.1107	19.8000

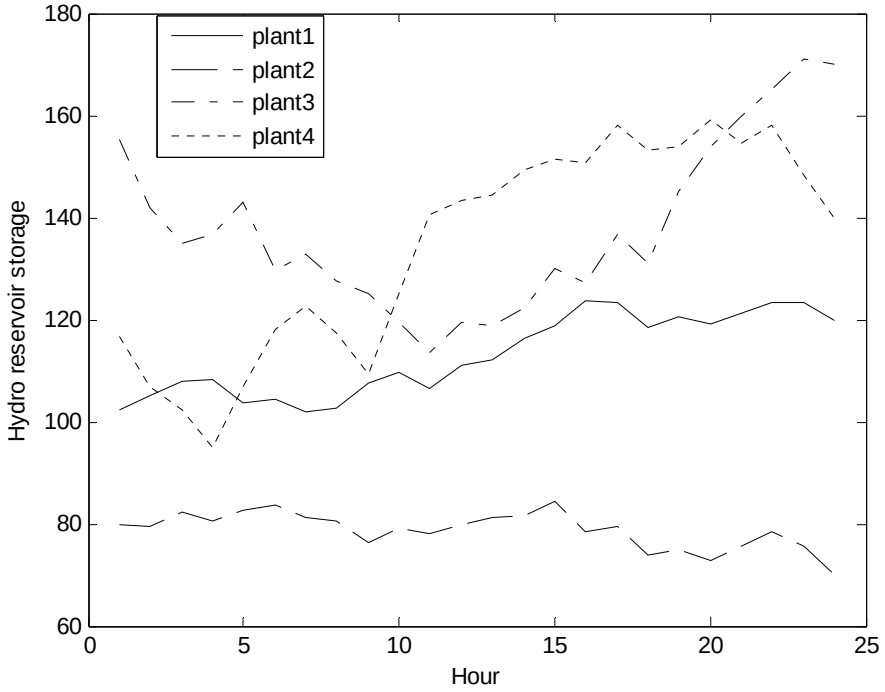

Fig. 8.15. Hydro reservoir storage volumes for Test system 3

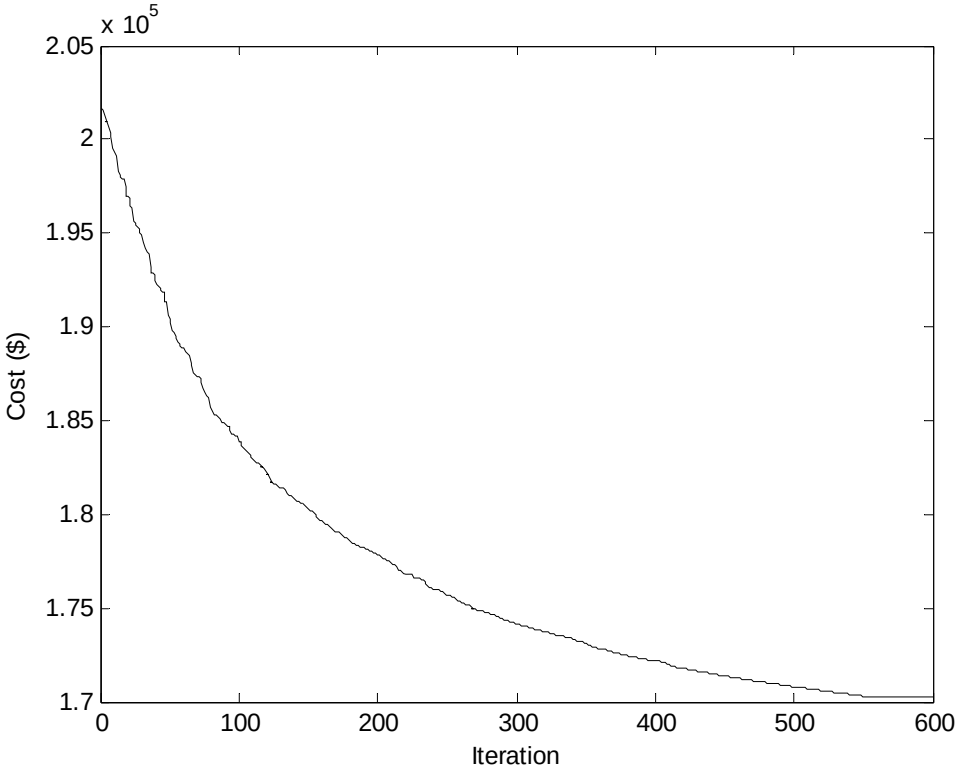

Fig. 8.16. Cost convergence characteristics for Test system 3

Table 8.24: Optimal Hydrothermal generation (MW) for Test system 3

Hour	P_{h1}	P_{h2}	P_{h3}	P_{h4}	P_{s1}	P_{s2}	P_{s3}	P_{s4}	P_{s5}	P_{s6}	P_{s7}	P_{s8}	P_{s9}	P_{s10}
1	72.2601	62.3442	30.6161	131.8801	319.3551	50.0109	94.9296	119.6769	174.7456	189.5279	45.0000	184.5191	98.0315	177.1027
2	64.9278	65.3247	32.9477	201.4856	139.7063	423.8989	94.8070	20.0003	174.7278	139.6300	163.2579	35.0004	98.0943	126.1913
3	53.4467	48.6219	41.0743	121.4353	139.6312	124.9215	94.6318	69.8439	74.9719	239.5347	282.0520	134.7605	98.0828	176.9914
4	67.9989	77.2332	48.6841	132.9646	318.9741	50.0058	20.0003	20.1742	224.4839	139.8490	163.4484	184.4845	25.0003	176.6987
5	91.7137	49.3896	49.3821	163.7640	139.7657	274.3774	94.7265	69.8314	224.4709	40.0001	163.3234	84.8241	98.0541	126.3770
6	64.5189	50.5430	0	170.2728	229.5086	124.8692	94.5753	20.0000	224.4086	339.0431	222.9347	35.0207	98.0502	126.2549
7	88.6340	66.7197	23.9621	220.0439	229.4893	50.0000	94.3835	119.7408	222.9151	139.7808	222.7886	134.7395	159.9630	176.8398
8	78.2847	61.3151	33.3120	263.6588	408.9686	124.7360	20.0000	129.9994	174.5873	189.2430	104.2007	84.6737	159.9548	177.0660
9	53.6710	81.9124	30.9598	247.6043	319.5553	349.1525	20.0058	69.8129	124.7554	89.7646	281.9429	134.9208	160.0000	125.9423
10	82.9143	46.7281	10.2562	207.6945	229.5166	274.3251	20.0230	69.8238	274.2518	289.2822	104.1828	134.0206	159.9999	176.9811
11	103.0109	72.4873	26.2456	136.4138	408.7956	199.5924	94.5593	20.0000	124.7086	438.9464	104.0969	84.8143	159.9993	126.3296
12	58.2287	50.5122	35.2667	265.4916	409.0818	50.0091	94.7881	119.7262	373.6642	189.5478	45.0000	234.4624	97.9500	126.2714
13	89.3332	53.4438	0	280.1900	409.0638	274.5701	94.6998	119.8329	124.7295	189.6488	104.2496	134.6591	160.0000	75.5795
14	76.6911	66.0687	42.5896	279.8282	139.7277	349.1097	94.0867	119.4470	274.2975	239.4445	163.3329	84.7565	25.0000	75.6198
15	83.1311	52.1162	46.6587	280.6343	319.3016	274.2278	20.0000	69.7605	469.9900	40.0000	45.0095	84.8819	98.0588	126.2295
16	54.9590	89.2367	34.9740	283.7200	139.7005	274.3465	94.8615	20.0375	324.2143	239.4445	45.0000	184.5966	97.8885	177.0205
17	87.6191	48.0309	46.9321	285.6586	229.5316	274.3415	94.6829	69.7073	174.5832	40.0000	340.7829	184.5322	98.0492	75.5485
18	104.2707	78.4404	38.8418	304.1160	139.8034	124.8011	94.9481	119.6707	124.4632	139.6831	341.4470	234.4153	97.9888	177.1104
19	54.9565	45.3003	47.9668	222.1599	229.5208	274.3298	94.7433	69.7420	274.3045	189.5576	163.4458	134.6431	97.7758	171.5538
20	74.5065	69.4777	53.0071	252.9794	229.4922	274.3338	94.6885	119.7096	224.4505	239.5236	104.2217	35.0895	152.3784	126.1415
21	55.0419	44.5934	55.5466	264.7787	319.2777	124.7947	20.0001	69.8404	224.2817	139.7319	222.1884	84.5163	160.0000	125.4081
22	64.1434	49.1351	54.3869	265.5061	319.1151	124.6251	94.7981	20.0000	274.3385	189.2662	45.0003	84.8897	97.8277	176.9678
23	85.4137	75.1225	55.2928	301.4979	229.4050	274.3244	94.8180	129.2892	25.0001	289.2480	104.2107	35.0062	25.0068	126.3647
24	105.0841	82.3791	59.2108	292.6400	50.0238	199.5332	94.8087	69.9823	25.0000	239.4523	222.7865	134.4310	98.4056	126.2627

Table 8.25: Comparison of performance for Test system 3

Techniques	GSO	DE
Best cost ($)	170302.86	170964.15
Average cost ($)	170350.19	-
Worst cost ($)	170411.26	-
CPU time (s)	652.35	-

Table 8.24: Optimal Hydrothermal generation (MW) for Test system 3

Hour	P_{h1}	P_{h2}	P_{h3}	P_{h4}	P_{s1}	P_{s2}	P_{s3}	P_{s4}	P_{s5}	P_{s6}	P_{s7}	P_{s8}	P_{s9}	P_{s10}
1	72.2601	62.3442	30.6161	131.8801	319.3551	50.0109	94.9296	119.6769	174.7456	189.5279	45.0000	184.5191	98.0315	177.1027
2	64.9278	65.3247	32.9477	201.4856	139.7063	423.8989	94.8070	20.0003	174.7278	139.6300	163.2579	35.0004	98.0943	126.1913
3	53.4467	48.6219	41.0743	121.4353	139.6312	124.9215	94.6318	69.8439	74.9719	239.5347	282.0520	134.7605	98.0828	176.9914
4	67.9989	77.2332	48.6841	132.9646	318.9741	50.0058	20.0003	20.1742	224.4839	139.8490	163.4484	184.4845	25.0003	176.6987
5	91.7137	49.3896	49.3821	163.7640	139.7657	274.3774	94.7265	69.8314	224.4709	40.0001	163.3234	84.8241	98.0541	126.3770
6	64.5189	50.5430	0	170.2728	229.5086	124.8692	94.5753	20.0000	224.4086	339.0431	222.9347	35.0207	98.0502	126.2549
7	88.6340	66.7197	23.9621	220.0439	229.4893	50.0000	94.3835	119.7408	222.9151	139.7808	222.7886	134.7395	159.9630	176.8398
8	78.2847	61.3151	33.3120	263.6588	408.9686	124.7360	20.0000	129.9994	174.5873	189.2430	104.2007	84.6737	159.9548	177.0660
9	53.6710	81.9124	30.9598	247.6043	319.5553	349.1525	20.0058	69.8129	124.7554	89.7646	281.9429	134.9208	160.0000	125.9423
10	82.9143	46.7281	10.2562	207.6945	229.5166	274.3251	20.0230	69.8238	274.2518	289.2822	104.1828	134.0206	159.9999	176.9811
11	103.0109	72.4873	26.2456	136.4138	408.7956	199.5924	94.5593	20.0000	124.7086	438.9464	104.0969	84.8143	159.9993	126.3296
12	58.2287	50.5122	35.2667	265.4916	409.0818	50.0091	94.7881	119.7262	373.6642	189.5478	45.0000	234.4624	97.9500	126.2714
13	89.3332	53.4438	0	280.1900	409.0638	274.5701	94.6998	119.8329	124.7295	189.6488	104.2496	134.6591	160.0000	75.5795
14	76.6911	66.0687	42.5896	279.8282	139.7277	349.1097	94.0867	119.4470	274.2975	239.4445	163.3329	84.7565	25.0000	75.6198
15	83.1311	52.1162	46.6587	280.6343	319.3016	274.2278	20.0000	69.7605	469.9900	40.0000	45.0095	84.8819	98.0588	126.2295
16	54.9590	89.2367	34.9740	283.7200	139.7005	274.3465	94.8615	20.0375	324.2143	239.4445	45.0000	184.5966	97.8885	177.0205
17	87.6191	48.0309	46.9321	285.6586	229.5316	274.3415	94.6829	69.7073	174.5832	40.0000	340.7829	184.5322	98.0492	75.5485
18	104.2707	78.4404	38.8418	304.1160	139.8034	124.8011	94.9481	119.6707	124.4632	139.6831	341.4470	234.4153	97.9888	177.1104
19	54.9565	45.3003	47.9668	222.1599	229.5208	274.3298	94.7433	69.7420	274.3045	189.5576	163.4458	134.6431	97.7758	171.5538
20	74.5065	69.4777	53.0071	252.9794	229.4922	274.3338	94.6885	119.7096	224.4505	239.5236	104.2217	35.0895	152.3784	126.1415
21	55.0419	44.5934	55.5466	264.7787	319.2777	124.7947	20.0001	69.8404	224.2817	139.7319	222.1884	84.5163	160.0000	125.4081
22	64.1434	49.1351	54.3869	265.5061	319.1151	124.6251	94.7981	20.0000	274.3385	189.2662	45.0003	84.8897	97.8277	176.9678
23	85.4137	75.1225	55.2928	301.4979	229.4050	274.3244	94.8180	129.2892	25.0001	289.2480	104.2107	35.0062	25.0068	126.3647
24	105.0841	82.3791	59.2108	292.6400	50.0238	199.5332	94.8087	69.9823	25.0000	239.4523	222.7865	134.4310	98.4056	126.2627

Table 8.25: Comparison of performance for Test system 3

Techniques	GSO	DE
Best cost ($)	170302.86	170964.15
Average cost ($)	170350.19	-
Worst cost ($)	170411.26	-
CPU time (s)	652.35	-

8.6. Conclusion

A novel approach based on group search optimization has been presented to solve the three hydrothermal test systems. The results have been compared with those obtained by other evolutionary algorithms reported in the literature. It is seen from the comparisons that the proposed group search optimization method performs better than other evolutionary algorithms reported in the literature.

CHAPTER 9

Short-term Scheduling of Fixed Head Hydrothermal Power system

9.1. Introduction

Optimal scheduling of power plant generation is of great importance to electric utility systems. Because of insignificant marginal cost of hydroelectric power, the problem of minimizing the operational cost of hydrothermal system essentially reduces to minimizing the fuel cost of thermal plants.

Here, group search optimization (GSO), opposition-based group search optimization (OGSO) and opposition-based differential evolution (ODE) have been proposed for optimal scheduling of generation in a fixed head hydrothermal system. Here, system with fixed head hydro plants whose water discharge rate curves are modeled as quadratic functions of the hydropower generations and thermal units with nonsmooth fuel cost function are considered. Here, scheduling period is divided into a number of subintervals each having a constant load demand. The proposed methods are validated by testing on two test systems. The test results are compared with those obtained by using of differential evolution (DE), particle swarm optimization (PSO) and evolutionary programming (EP) techniques.

9.2. Problem Formulation

Hydrothermal scheduling problem with N_h hydro units and N_s thermal units over M time subintervals is described as follows:

The fuel cost function of each thermal generator, considering valve-point effect, is expressed as a sum of quadratic and sinusoidal functions. The superimposed sine components represent rippling effect produced by steam admission valve opening. The problem minimizes following total fuel cost given by 9.1.

$$f = \sum_{m=1}^{\mathrm{M}} \sum_{i=1}^{\mathrm{N}_s} t_m \left[a_{si} + b_{si} \mathrm{P}_{sim} + c_{si} \mathrm{P}_{sim}^2 + d_{si} \times \sin\left\{ e_{si} \times \left(\mathrm{P}_{si}^{\min} - \mathrm{P}_{sim} \right) \right\} \right] \qquad (9.1)$$

where a_{si}, b_{si}, c_{si}, d_{si}, and e_{si} are cost coefficients of i th thermal generator ; P_{sim} is real power output of i th thermal generator during subinterval m; $\mathrm{P}_{si}^{\min}$ is lower limit of generation of i th thermal generator ; t_m is the duration of subinterval m.

subject to

(i) Power balance constraints:

$$\sum_{i=1}^{\mathrm{N}_s} \mathrm{P}_{sim} + \sum_{j=1}^{\mathrm{N}_h} \mathrm{P}_{hjm} - \mathrm{P}_{Dm} - \mathrm{P}_{Lm} = 0 \qquad m \in \mathrm{M} \qquad (9.2)$$

and

$$\mathrm{P}_{Lm} = \sum_{l=1}^{\mathrm{N}_h + \mathrm{N}_s} \sum_{r=1}^{\mathrm{N}_h + \mathrm{N}_s} \mathrm{P}_{lm} \mathrm{B}_{lr} \mathrm{P}_{rm} \qquad m \in \mathrm{M} \qquad (9.3)$$

where P_{hjm} is real power output of j th hydro unit during subinterval m ; P_{Dm} is load demand during subinterval m; P_{Lm} is transmission loss during subinterval m; B_{lr} is loss formula coefficients.

(ii) Water availability constraints:

$$\sum_{m=1}^{\mathrm{M}} \left[t_m \left(a_{0hj} + a_{1hj} \mathrm{P}_{hjm} + a_{2hj} \mathrm{P}_{hjm}^2 \right) \right] - W_{hj} = 0 \qquad j \in \mathrm{N}_h \qquad (9.4)$$

where a_{0hj}, a_{1hj}, and a_{2hj} are coefficients for water discharge rate function of j th hydro generator. W_{hj} ; is prespecified volume of water available for generation by j th hydro unit during the scheduling period.

(iii) Generation limits:

$$\mathrm{P}_{hj}^{\min} \le \mathrm{P}_{hjm} \le \mathrm{P}_{hj}^{\max} \qquad j \in \mathrm{N}_h,\ m \in \mathrm{M} \qquad (9.5)$$

and

$$P_{si}^{\min} \le P_{sim} \le P_{si}^{\max} \qquad i \in N_s,\ m \in M \qquad (9.6)$$

where $P_{hj}^{\min}$ and $P_{hj}^{\max}$ are lower and upper generation limits of j th hydro unit ; $P_{si}^{\max}$ is upper limit of generation of i th thermal generator.

Determination of Generation Level of Slack Generator

Thermal generators and hydro generators deliver their power outputs subject to the power balance constraint (9.2), water availability constraint (9.4) and respective capacity constraints (9.5) and (9.6). Assuming the power loading of N_h and first $(N_s - 1)$ generators are known, the power level of the N_s th generator (i.e. the slack generator) is given by

$$P_{N_s m} = P_{Dm} + P_{Lm} - \sum_{l=1}^{N_h+N_s-1} P_{lm} \qquad m \in M \qquad (9.7)$$

The transmission loss P_{Lm} is a function of all the generators including the slack generator and it is given by

$$P_{Lm} = \sum_{l=1}^{N_h+N_s-1} \sum_{r=1}^{N_h+N_s-1} P_{lm} B_{lr} P_{rm} + 2P_{N_s m}\left(\sum_{l=1}^{N_h+N_s-1} B_{N_s l} P_{lm}\right) + B_{N_s N_s} P_{N_s m}^2 \qquad m \in M \qquad (9.8)$$

Expanding and rearranging, (7) becomes

$$B_{N_s N_s} P_{N_s m}^2 + \left(2\sum_{l=1}^{N_h+N_s-1} B_{N_s l} P_{lm} - 1\right) P_{N_s m} + P_{Dm} + \sum_{l=1}^{N_h+N_s-1} \sum_{r=1}^{N_h+N_s-1} P_{lm} B_{lr} P_{rm} - \sum_{l=1}^{N_h+N_s-1} P_{lm} = 0$$

$$m \in M \qquad (9.9)$$

The loading of the slack generator (i.e. N_s th) can then be found by solving equation (9.9) using standard algebraic method.

9.3. Application of GSO method

The proposed GSO algorithm has been applied to two test systems. In order to show the effectiveness of the proposed GSO algorithm, DE, PSO and EP have been applied to solve these two test systems. The algorithms used in this paper have been implemented by using MATLAB 7.0 on a PC (Pentium-IV, 80 GB, 3.0 GHz).

9.3.1. Test System 1

Test system 1 consists of two hydro plants and two thermal plants whose characteristics and load demands are given in Appendix-18,19. Transmission loss formula coefficients are also given in the appendix-1. Hydro plant data are taken from [115].

The problem is solved by using GSO. Here, the population size (N_P) and the maximum iteration number (N_{max}) have been selected as 100 and 100, respectively for this test system. Results obtained by using the proposed GSO algorithm, are shown in Table 9.1.

To validate the proposed GSO based approach, the same test system is solved by using DE, PSO and EP. In case of DE, the population size (N_P), scaling factor (F) and crossover constant (C_R) have been selected as 300, 0.35 and 1.0, respectively. The population size (N_P) and scaling factor (F) are taken 100 and 0.01 respectively in case of EP. In case of PSO parameters are taken as $N_P = 100, w_{max} = 0.9, w_{min} = 0.4$, $c_1 = 1$ and $c_2 = 1$. Maximum number of iterations has been selected 100 for DE, PSO and EP.

Tables 9.2, 9.3 and 9.4 summarize the generation schedules and total costs obtained from DE, PSO and EP, respectively. From tables 9.1, 9.2, 9.3 and 9.4 it is seen that the proposed GSO-based approach achieves the lowest cost. Figure 9.1 shows the cost convergence obtained from GSO, DE, PSO and EP.

Table 9.1: Results obtained from group search optimization for Test system 1

Subin-terval	P_{h1} (MW)	P_{h2} (MW)	P_{s1} (MW)	P_{s2} (MW)	Cost ($)
1	243.4698	92.0913	179.8065	424.3732	
2	306.0539	164.2677	227.7667	571.4884	66031
3	287.8832	137.0735	211.6398	522.2039	

Table 9.2: Results obtained from differential evolution for Test system 1

Subin-terval	P_{h1} (MW)	P_{h2} (MW)	P_{s1} (MW)	P_{s2} (MW)	Cost ($)
1	244.5113	90.1677	185.4240	419.7421	
2	307.8611	162.4868	226.8048	572.5680	66036
3	284.9912	140.7026	204.3000	528.5755	

Table 9.3: Results obtained from particle swarm optimization for Test system 1

Subin-terval	P_{h1} (MW)	P_{h2} (MW)	P_{s1} (MW)	P_{s2} (MW)	Cost ($)
1	248.2268	88.6941	183.2422	419.7770	
2	297.8146	173.8526	231.1074	566.0421	66050
3	291.6767	130.3988	191.4772	545.8811	

Table 9.4: Results obtained from evolutionary programming for Test system 1

Subin-terval	P_{h1} (MW)	P_{h2} (MW)	P_{s1} (MW)	P_{s2} (MW)	Cost ($)
1	237.6474	97.7308	183.3124	420.6857	
2	310.2027	170.4667	226.3238	562.0064	66054
3	289.1620	124.9021	212.3097	533.4285	

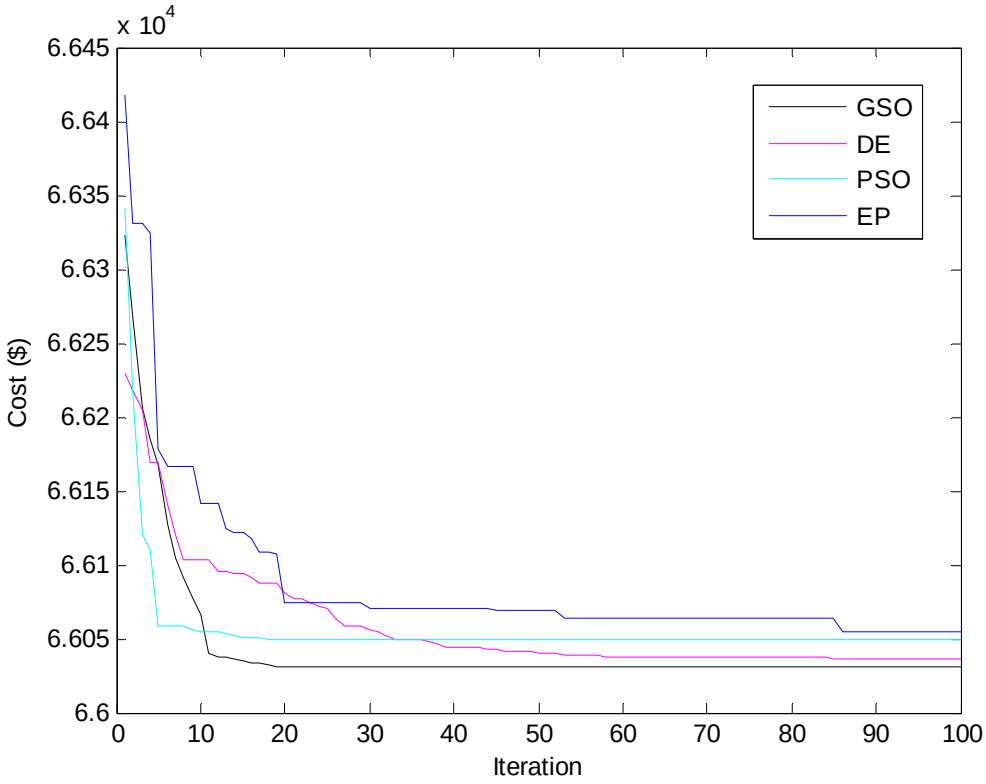

Fig. 9.1. Cost convergence curves of GSO,DE,PSO & EP for Test system 1

9.3.2. Test System 2

Test system 2 comprises of two hydro plants and four thermal plants whose characteristics and load demands are given in Appendix-21,22. Transmission loss formula coefficients are also given in the Appendix-20.

The problem is solved by using GSO. Here, the population size (N_P) and the maximum iteration number (N_{max}) have been selected as 100 and 200, respectively for this test system. Results obtained by using the proposed GSO algorithm, are shown in Table 9.5.

To validate the proposed GSO based approach, the same test system is solved by using DE, PSO and EP. In case of DE, population size (N_P), scaling factor (F) and crossover constant (C_R) have been selected as 300, 0.35 and 1.0. PSO control parameters are $c_1 = 1$, $c_2 = 1$, $W_{max} = 0.9$, $W_{min} = 0.4$ and $N_P = 100$. In case of EP, scaling factor (β) is 0.04 and population size (N_P) is 100. Maximum number of iterations (N_{max}) has been selected 200 for DE, PSO and EP.

Results obtained from DE, PSO and EP have been presented in Table 9.6, Table 9.7 and Table 9.8 ,respectively. From tables 9.5, 9.6, 9.7 and 9.8 it is seen that proposed GSO-based approach achieves the lowest cost. Figure 9.2 depicts the cost convergence obtained from GSO, DE, PSO and EP.

Table 9.5: Results obtained from group search optimization for Test system 2

Subin-terval	P_{h1} (MW)	P_{h2} (MW)	P_{s1} (MW)	P_{s2} (MW)	P_{s3} (MW)	P_{s4} (MW)	Cost ($)
1	180.8024	310.0646	90.2007	174.9568	112.3003	50.1058	
2	242.2065	413.9211	124.9257	174.9033	122.4442	50.0762	82454
3	203.9131	356.4540	117.1073	174.9483	120.5008	50.0395	
4	249.6967	499.8905	125.0000	174.9823	135.2275	50.2552	

Table 9.6: Results obtained from differential evolution for Test system 2

Subin-terval	P_{h1} (MW)	P_{h2} (MW)	P_{s1} (MW)	P_{s2} (MW)	P_{s3} (MW)	P_{s4} (MW)	Cost ($)
1	182.8655	301.6497	95.7823	175.0000	111.8177	51.1751	
2	244.5562	415.5654	125.0000	175.0000	117.8218	50.5832	82644
3	200.6844	362.6198	109.3270	175.0000	123.7448	51.6890	
4	248.5012	499.8208	124.8401	175.0000	135.4351	51.4319	

Table 9.7: Results obtained from particle swarm optimization for Test system 2

Subin-terval	P_{h1} (MW)	P_{h2} (MW)	P_{s1} (MW)	P_{s2} (MW)	P_{s3} (MW)	P_{s4} (MW)	Cost ($)
1	214.5427	332.7399	83.1521	139.9089	98.6144	50.0000	
2	220.5221	430.6452	125.0000	174.9998	127.4662	50.0000	84767
3	212.0450	373.1574	90.2184	175.0000	122.2852	50.7310	
4	231.7915	450.6662	125.0000	175.0000	196.9212	54.4280	

Table 9.8: Results obtained from evolutionary programming for Test system 2

Subin-terval	P_{h1} (MW)	P_{h2} (MW)	P_{s1} (MW)	P_{s2} (MW)	P_{s3} (MW)	P_{s4} (MW)	Cost ($)
1	167.3948	313.3530	100.5135	174.2207	112.5857	50.2814	
2	242.1179	413.6478	123.3193	174.6693	123.6975	51.0171	82663
3	217.9242	354.6699	109.4371	174.8655	115.8588	50.3171	
4	248.5116	499.0005	123.0134	174.9305	137.8363	51.7244	

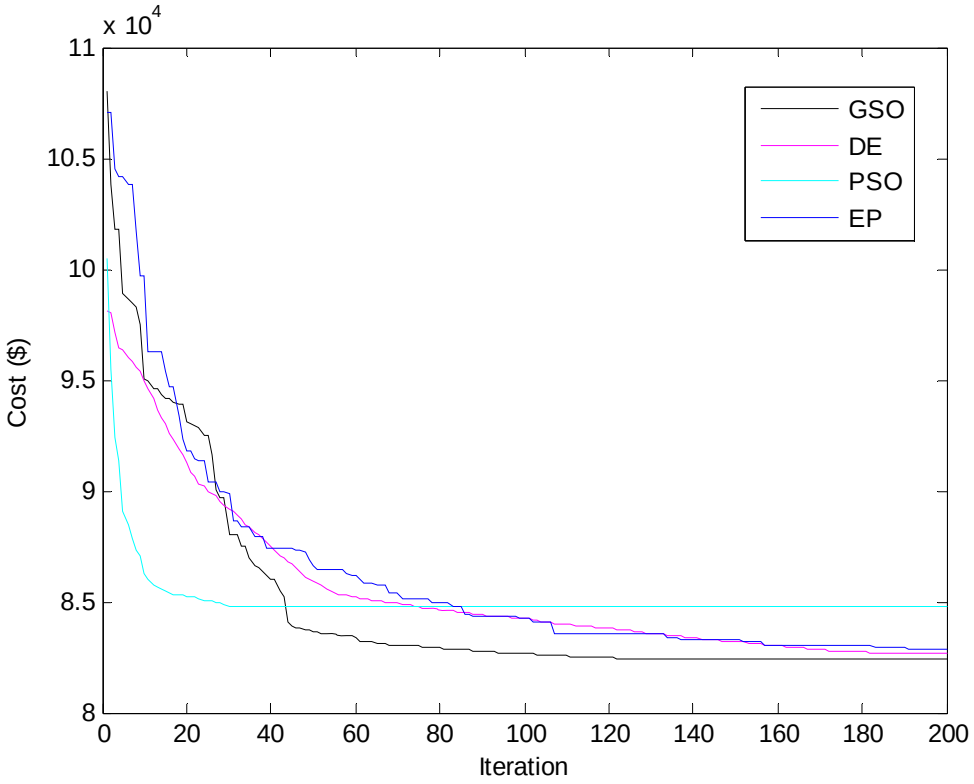

Fig. 9.2. Cost convergence curves of GSO,DE,PSO & EP for Test system 2

9.4. Conclusion

A novel approach based on group search optimization has been presented to solve the fixed head hydrothermal scheduling problem. The results have been compared with those obtained by differential evolution, particle swarm optimization and evolutionary programming technique. It is seen from the comparisons that the proposed group search optimization method performs better than differential evolution, particle swarm optimization and evolutionary programming technique.

9.5. Application of OGSO method

Two test systems are investigated and the computational results have been used to compare the performance of the proposed OGSO method with other evolutionary methods. The proposed OGSO algorithm and GSO algorithms used in this paper are implemented by using MATLAB 7.0 on a PC (Pentium-IV, 80 GB, 3.0 GHz).

9.5.1. Test System 1

This system consists of two hydro plants and two thermal plants whose characteristics and load demands are given in Appendix-18,19. Transmission loss formula coefficients are also given in the Appendix. Hydro plant data is taken from [115].

The problem is solved by using both OGSO and GSO. Here, the population size (N_P) and the maximum iteration number (N_{max}) have been selected as 100 and 100,respectively for this test system.

The optimal hydrothermal generation obtained by the proposed OGSO method and GSO method are provided in Table 9.9 and Table 9.10, respectively. The best, average and the worst costs and average CPU time among 100 runs of solutions obtained from the proposed OGSO method and GSO method are summarized in Table 9.11. The costs obtained from artificial immune system (AIS), particle swarm optimization (PSO) and evolutionary programming (EP) are also shown in Table 9.11. The cost convergence characteristics obtained from the proposed OGSO and GSO are shown in Fig. 9.3.

Table 9.9: Results obtained from OGSO for Test system 1

Subin-terval	P_{h1} (MW)	P_{h2} (MW)	P_{s1} (MW)	P_{s2} (MW)
1	244.9386	90.7338	179.2973	424.8595
2	306.6517	163.7245	228.0283	571.2122
3	285.8694	138.9314	211.6712	522.1936

Table 9.10: Results obtained from GSO for Test system 1

Subin-terval	P_{h1} (MW)	P_{h2} (MW)	P_{s1} (MW)	P_{s2} (MW)
1	233.1555	83.3467	166.3713	460.6468
2	315.3488	170.9049	225.9303	556.7394
3	290.8319	138.5059	221.8515	507.4179

Table 9.11: Comparison of performance for Test System 1

Techniques	Best cost ($)	Average cost ($)	Worst cost ($)	CPU time (s)
OGSO	66030.75	66031.41	66033.52	42.61
GSO	66065.44	66066.01	66069.04	37.95
AIS	66117	-	-	53.43
PSO	66166	-	-	71.62
EP	66198	-	-	75.48

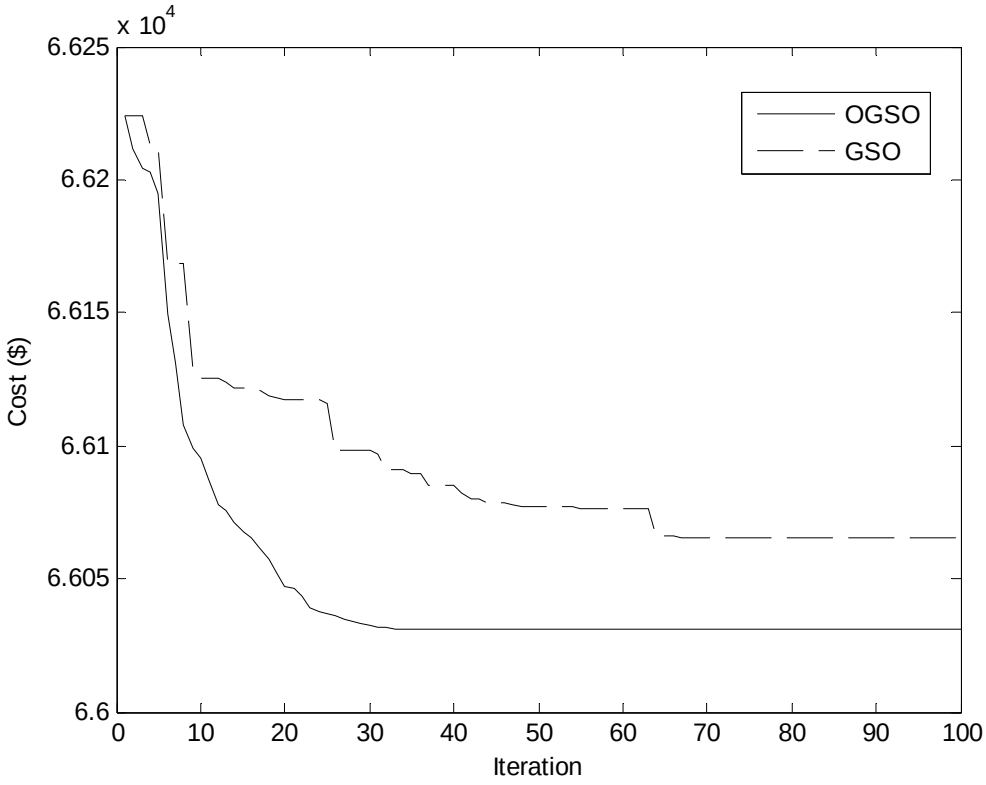

Fig. 9.3. Cost convergence curves of OGSO & GSO for Test system 1

9.5.2. Test System 2

This system comprises of two hydro plants and four thermal plants whose characteristics and load demands are given in Appendix-21,22. Transmission loss formula coefficients are also given in the Appendix-20.

The problem is solved by using both OGSO and GSO. Here, the population size (N_P) and the maximum iteration number (N_{max}) have been selected as 100 and 200 ,respectively for this test system.

The optimal hydrothermal generation obtained by the proposed OGSO method and GSO method are provided in Table 9.12 and Table 9.13 respectively. The best, average and the worst cost and average CPU time among 100 runs of solutions obtained from proposed OGSO method and GSO method are summarized in Table 9.14. The cost obtained from artificial immune system (AIS), particle swarm optimization (PSO) and evolutionary programming (EP) are also shown in Table 9.14. The cost convergence characteristic obtained from proposed OGSO and GSO is depicted in Fig. 9.4.

Table 9.12: Results obtained from OGSO for Test system 2

Subin-terval	P_{h1} (MW)	P_{h2} (MW)	P_{s1} (MW)	P_{s2} (MW)	P_{s3} (MW)	P_{s4} (MW)
1	178.2594	309.8640	90.1466	174.9133	115.1804	50.0487
2	244.1894	414.8758	122.9172	174.5022	121.8108	50.2252
3	203.9455	355.5239	119.0391	174.7680	119.5966	50.0658
4	249.9875	499.9671	119.0391	174.9214	220.0110	70.3489

Table 9.13: Results obtained from GSO for Test system 2

Subin-terval	P_{h1} (MW)	P_{h2} (MW)	P_{s1} (MW)	P_{s2} (MW)	P_{s3} (MW)	P_{s4} (MW)
1	186.9940	304.6033	87.9787	174.6272	114.0842	50.1157
2	248.4656	407.9398	122.2465	174.2861	124.7968	50.6900
3	192.1784	367.8174	112.5050	174.1396	125.3678	51.0776
4	248.7385	499.9457	125.0000	174.9793	227.3411	64.1132

Table 9.14: Comparison of performance for Test System 2

Techniques	Best cost ($)	Average cost ($)	Worst cost ($)	CPU time (s)
OGSO	92798.04	92800.22	92803.38	48.97
GSO	93061.96	93065.32	93071.02	43.03
AIS	93950	-	-	59.14
PSO	94126	-	-	83.54
EP	94250	-	-	67.82

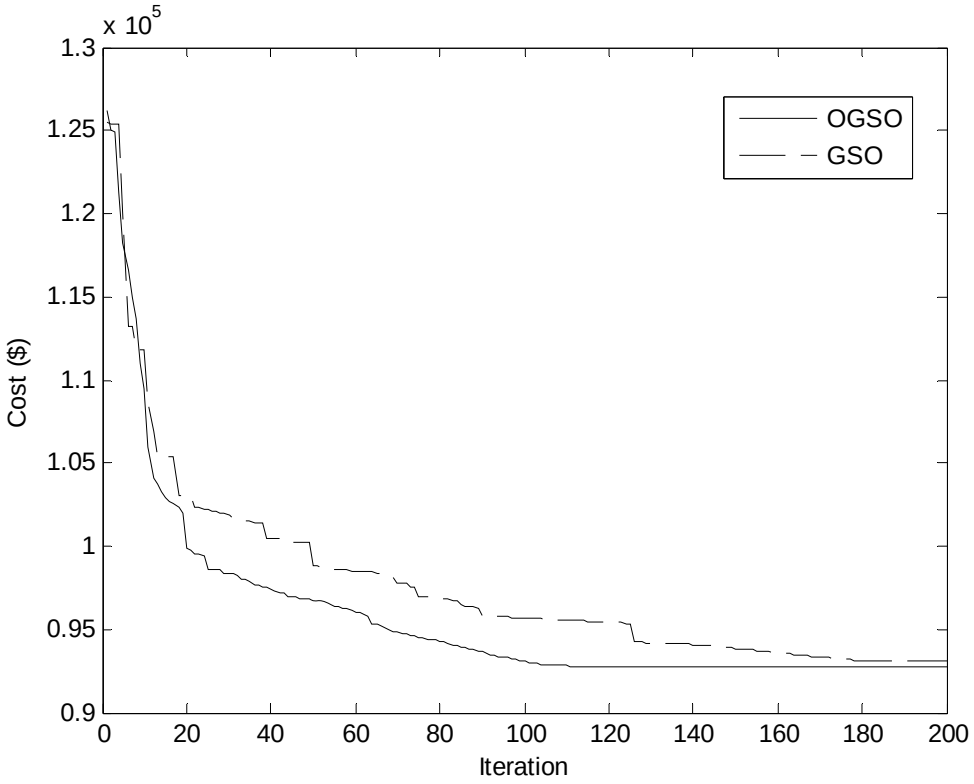

Fig. 9.4. Cost convergence curves of GSO & OGSO for Test system 2

9.6. Conclusion

Here, opposition-based group search optimization has been has been developed and applied to solve five test problems and two fixed head hydrothermal scheduling problems. The results have been compared with those obtained by other evolutionary algorithms reported in the literature. It is seen from the comparisons that the proposed opposition-based group search optimization method provides better solution. Due to this property, opposition-based group search optimization method can be tried for the solution of complex power system optimization problems in future.

9.7. Application of ODE method

Two fixed head hydrothermal systems are investigated. The computational results have been used to compare the performance of the proposed ODE method with other evolutionary methods.

The proposed ODE algorithm and DE algorithm used in this paper are implemented by using MATLAB 7.0 on a PC (Pentium-IV, 80 GB, 3.0 GHz).

9.7.1. Test System 1

This system consists of two hydro plants and two thermal plants whose characteristics and load demands are taken from [12].

The problem is solved by using both the proposed ODE and DE. Here, the population size (N_P), scaling factor (F), crossover rate (C_R) and the maximum iteration number (N_{max}) have been selected as 100, 1.0, 1.0 and 100, respectively for the test system under consideration.

The optimal hydrothermal generation obtained by the proposed ODE and DE are provided in Table 9.15 and Table 9.16, respectively. The best, average and the worst costs and average CPU time among 100 runs of solutions obtained from the proposed ODE and DE method are summarized in Table 9.17. The costs obtained from artificial immune system (AIS), particle swarm optimization (PSO) and evolutionary programming (EP) are also shown in Table 9.17. The cost convergence characteristics obtained from the proposed ODE and DE is shown in Fig. 9.5. It is seen from Table 9.17 that the cost found by using ODE is the lowest among all other methods.

Table 9.15: Results obtained from ODE of Test system 1

Sub-interval	P_{h1} (MW)	P_{h2} (MW)	P_{s1} (MW)	P_{s2} (MW)
1	244.5860	90.7689	179.4953	424.9773
2	307.3581	163.3383	228.7850	570.1572
3	285.4852	139.2931	211.2739	522.5895

Table 9.16: Results obtained from DE for Test system 1

Sub-interval	P_{h1} (MW)	P_{h2} (MW)	P_{s1} (MW)	P_{s2} (MW)
1	240.3807	85.6583	206.3934	407.6673
2	310.1176	167.5754	206.3934	585.2895
3	286.6845	139.7912	206.3934	525.7479

Table 9.17: Comparison of performance for Test System 1

Techniques	Best cost ($)	Average cost ($)	Worst cost ($)	CPU time (s)
ODE	66030.85	66031.68	66032.46	40.31
DE	66060.74	66061.44	66064.14	36.01
AIS	66117	-	-	53.43
PSO	66166	-	-	71.62
EP	66198	-	-	75.48

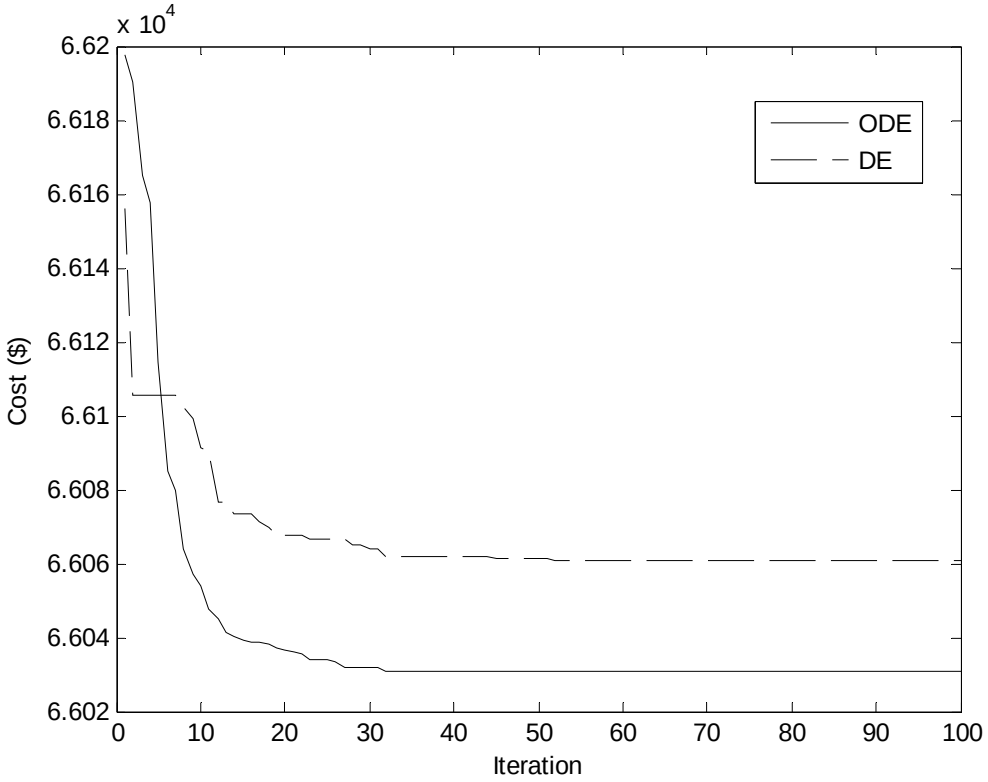

Fig. 9.5. Cost convergence curves of DE & ODE for Test system 1

9.7.2. Test System 2

This system comprises of two hydro plants and four thermal plants whose characteristics and load demands are taken from [12].

The problem is solved by using both the proposed ODE and DE. Here, the population size (N_P), scaling factor (F), crossover rate (C_R) and the maximum iteration number (N_{max}) have been selected as 100, 1.0, 1.0 and 200, respectively for the test system under consideration.

The optimal hydrothermal generation obtained by the proposed ODE and DE are provided in Table 9.18 and Table 9.19 respectively. The best, average and the worst costs and average CPU time among 100 runs of solutions obtained from the proposed ODE and DE are summarized in Table 9.20. The cost obtained from artificial immune system (AIS), particle swarm optimization (PSO) and evolutionary programming (EP) are also shown in Table 9.20. The cost convergence characteristics obtained from the proposed ODE and DE is depicted in Fig. 9.6. It is seen from Table 9.20 that the cost found by using ODE is the lowest among all other methods.

Table 9.18: Results obtained from ODE of Test system 2

Subin-terval	P_{h1} (MW)	P_{h2} (MW)	P_{s1} (MW)	P_{s2} (MW)	P_{s3} (MW)	P_{s4} (MW)
1	172.6478	317.8272	93.6207	174.7438	109.2596	50.3779
2	243.8370	411.3216	124.8716	174.6929	123.6025	50.1150
3	209.7780	351.8750	116.1764	174.7282	120.3243	50.0519
4	249.8641	499.8741	124.8642	174.9127	222.4536	68.0992

Table 9.19: Results obtained from DE of Test system 2

Subin-terval	P_{h1} (MW)	P_{h2} (MW)	P_{s1} (MW)	P_{s2} (MW)	P_{s3} (MW)	P_{s4} (MW)
1	184.4627	303.6346	88.3611	174.7233	116.2664	50.9170
2	241.0344	419.5791	117.4402	174.8712	124.7407	50.9397
3	201.9931	357.2371	123.3403	173.9739	115.3547	51.0280
4	249.3076	499.1428	124.0676	174.7184	221.4260	71.3501

Table 9.20: Comparison of performance for Test System 2

Techniques	Best cost ($)	Average cost ($)	Worst cost ($)	CPU time (s)
ODE	92817.01	92819.81	92822.68	46.09
DE	93107.34	93110.45	93114.07	41.53
AIS	93950	-	-	59.14
PSO	94126	-	-	83.54
EP	94250	-	-	67.82

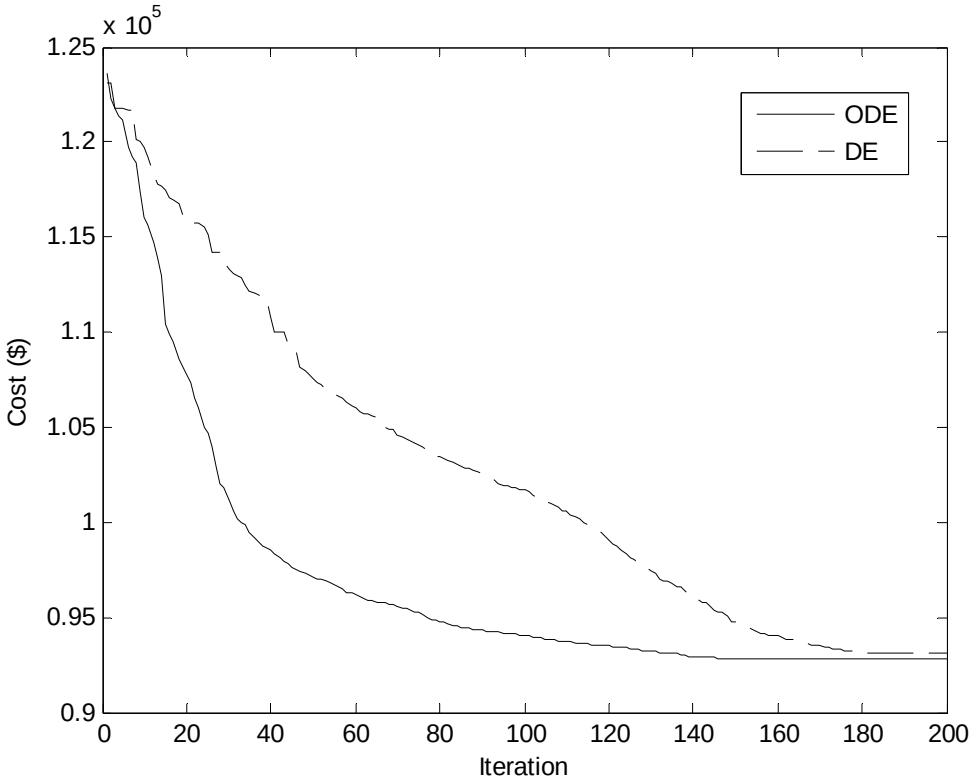

Fig. 9.6. Cost convergence curves of DE & ODE for Test system 2

9.8. Conclusion

Here, opposition-based differential evolution is demonstrated and presented to solve the fixed head hydrothermal scheduling problem. Test results have been compared with those obtained by other evolutionary algorithms reported in the literature. It is seen from the comparisons that the proposed opposition-based differential evolution method performs better than other evolutionary algorithms in the literature.

CHAPTER 10

(a) Overall Conclusion

In this thesis nature-inspired meta-heuristics techniques like Differential evolution with Gaussian mutation, Improved differential evolution, Group search optimization, Modified evolutionary algorithm, Opposition–based group search optimization, Opposition-based differential evolution, have been applied to solve different complex power system optimization problems such as economic dispatch, combined heat and power economic dispatch, multi area economic dispatch, short-term hydrothermal scheduling problem of fixed head and variable head hydrothermal power systems.

Also multi-objective optimization techniques have been applied for multi-area economic environmental dispatch problem and fuel constrained economic environmental dispatch problem.

Results obtained from all the techniques were compared with the results obtained from other computation intelligent technique from the literature. It was found that here the results are competitive and quite encouraging.

Chapter wise conclusion has been presented below.

Chapter-3

The DEGM method has been developed and successfully implemented to solve the non-smooth /non-convex economic dispatch problem with the generator constraints. It has been observed that DEGM method has the ability to converge to a better quality solution and possesses good convergence characteristics and robustness.

Chapter-4

Here, DEGM & IDE method has been implemented to solve the complex non-smooth /non-convex combined heat and power economic dispatch problem.It is seen from the comparisons that the proposed DEGM & IDE method performs better than other evolutionary algorithms in the literature. It is clear from the results obtained by different trials that the proposed DEGM can

avoid the shortcoming of premature convergence. Due to these properties, in future DEGM can be tried for solution of complex power system optimization problems.

It has also been observed that IDE algorithm has the ability to converge to a better quality solution and exhibit more robustness. It is clear from the results obtained by different trials that the proposed IDE algorithm can avoid the shortcoming of premature convergence. Due to these properties, the IDE algorithm in future can be tried for solution of complex power system optimization problems.

Chapter-5

Here, IDE algorithm has been successfully implemented to solve MAED problems. It has been observed from the comparison that the proposed IDE has the ability to converge to a better quality solution and exhibit more robustness than DE, EP and RCGA. It is also clear from the results obtained by different trials that the proposed IDE algorithm can avoid the shortcoming of premature convergence. Due to these properties, the IDE algorithm in future can be tried for the solution of complex power system optimization problems.

Here, GSO has also been successfully implemented to solve MAED problems. The effectiveness of the proposed method is illustrated by using three different test systems and the test results are compared with those obtained from DE, EP and RCGA. It has been observed from the comparison that the proposed GSO has the ability to converge to a better quality solution than DE, EP and RCGA. Due to this property, the GSO method in future can be tried for the solution of complex power system optimization problems.

Chapter -6

Here, multi-objective differential evolution has been implemented to solve multi-area economic environmental dispatch problem. Results obtained from the proposed approach have been compared to those obtained from strength pareto evolutionary algorithm 2. The proposed multi-objective differential evolution is simple, robust and efficient. It does not impose any limitation on the number of objectives and can be extended to include more objectives.

Chapter-7

Here, the usefulness of the multi-objective differential evolution is examined for solving fuel constrained economic emission dispatch problem of thermal generating units. The results show that fuel consumption can be adequately controlled to satisfy constraints imposed by suppliers using the proposed method. Optimum economic emission dispatch is not achieved always, but this is generally much less than the penalty that could be imposed for violating the fuel system constraints.

Chapter-8

In this paper, MEP has been developed and applied to solve the two test problems and two hydrothermal multi-reservoir cascaded hydroelectric test systems having prohibited operating zones and thermal units with valve point loading. It has been observed that MEP method has the ability to converge to a better quality solution and robustness. MEP has both good exploration and exploitation ability. It is clear from the results obtained by different trials that the proposed MEP method can avoid the shortcoming of premature convergence.

A novel approach based on GSO has been presented to solve the three hydrothermal test systems. The results have been compared with those obtained by other evolutionary algorithms reported in the literature. It is seen from the comparisons that the proposed group search optimization method performs better than other evolutionary algorithms reported in the literature.

Chapter-9

A novel approach based on GSO has been presented to solve the fixed head hydrothermal scheduling problem. The results have been compared with those obtained by DE, PSO and EA technique. It is seen from the comparisons that the proposed GSO method performs better than DE, PSO and EA technique.

Here, OGSO has been has been developed and applied to solve fixed head hydrothermal scheduling problems. The results have been compared with those obtained by other EA's

reported in the literature. It is seen from the comparisons that the proposed OGSO method provides better solution. Due to this property, opposition-based group search optimization method can be tried for the solution of complex power system optimization problems in future.

Here, ODE is demonstrated and presented to solve the fixed head hydrothermal scheduling problem. Test results have been compared with those obtained by other EA ‘s reported in the literature. It is seen from the comparisons that the proposed ODE method performs better than other evolutionary algorithms in the literature.

(b) Future Scope

DE GM can avoid the shortcoming of premature convergence. Due to these properties, in future DEGM can be tried for solution of complex power system optimization problems.

IDE algorithm can avoid the shortcoming of premature convergence. Due to these properties, the IDE algorithm in future can be tried for solution of complex power system optimization problems.

GSO has the ability to converge to a better quality solution than. Due to this property, the GSO method in future can be tried for the solution of complex power system optimization problems.

The proposed multi-objective differential evolution is simple, robust and efficient. It does not impose any limitation on the number of objectives and can be extended to include more objectives.

MEP has both good exploration and exploitation ability. MEP method can avoid the shortcoming of premature convergence. So, it can be be tried for solution of complex power system optimization problems.

OGSO method provides better solution. Due to this property, this method can be tried for the solution of complex power system optimization problems in future

References

[1] L. J. Fogel, A. J. Owens, M. J. Walsh, “Artificial Intelligence Through simulated Evolution”, John Wiley, 1966.

[2] J. H. Holland, “Adaptation in Natural and Artificial Systems”, Ann Arbor: University of Michigan Press, 1975.

[3] D. E. Goldberg, “Genetic Algorithms in Search, Optimization, and Machine Learing, Addison-Wesley, 1989.

[4] D. B. Fogel, “An introduction to simulated evolutionary optimization”, IEEE Trans. Neural Networks, vol. 5, pp. 3-14, January 1994.

[5] D. B. Fogel, Evolutionary Computation: towards a new philosophy of machine intelligence. IEEE Press, New York, NY, 1995.

[6] K. Deb and R. B. Agrawal, “Simulated binary crossover for continuous search space”, Complex Systems, vol. 9, no. 2, pp. 115-148, 1995.

[7] F. Herrera, M. Lozano, and J. L. Verdegay, “Tackling real-coded genetic algorithms: Operators and tools for behavioral analysis”, Artif. Intell. Rev., vol.12, no. 4, pp. 265-319, 1998.

[8] R. Storn and K. V. Price, “Differential evolution- a simple and efficient heuristic for global optimization over continuous spaces”, J. Global Optimization, Vol. 11, No. 4, pp. 341-359, December 1997.

[9] K. V. Price, R. Storn and J. Lampinen. Differential Evolution: A Practical Approach to Global Optimization. Springer-Verlag, Berlin, 2005.

[10] J. Kennedy and R. C. Eberhart, “Particle swarm optimization”, Proc. IEEE Int Conf. Neural Networks, vol. IV, pp. 1942-1948,1995.

[11] Y. Shi and R. C. Eberhart, “Empirical study of particle swarm optimization”, in Proc. IEEE Int. Congr. Evolutionary Computation, 1999, vol. 3, pp. 94-97.

[12] R. C. Eberhart and Y. Shi, “Tracking and optimizing dynamic systems with particle swarms”, in Proc. IEEE Congr. Evolutionary computation, 2001, pp. 94-97.

[13] S. He, Q. H. Wu, and J. R. Saunders. “Group search optimizer: an optimization algorithm inspired by animal searching behavior”, IEEE Transactions on Evolutionary Computation, vol. 13, no. 5 (2009): 973- 990.

[14] H. Shen, Y. Zhu, W. Zou, Z. Zhu, Group search optimizer algorithm for constrained optimization, Comput. Sci. Environ. Eng. EcoInf. (2011).

[15] D. Mustard, "Numerical integration over the n-dimensional spherical shell" Mathematics of Computation 18, no. 88 (1964): 578-589.

[16] L. A. Giraldeau and L. Lefebvre, “Exchangeable producer and scrounger roles in a captive flock of feral pigeons- a case for the skill pool effect”, Animal Behavior, vo. 34, no. 3, pp. 797-803, June 1986.

[17] C. A. C. Coello, “A comprehensive survey of evolutionary-based multiobjective optimization techniques”, Knowledge and Information Systems, vol. 1, no. 3, pp. 269-308, 1999.

[18] D. A. V. Veldhuizen and G. B. Lamont, “Multiobjective evolutionary algorithms: Analyzing the state-of-the-art”, IEEE Trans. on Evol. Comput., vol. 8, no. 2, pp. 125-147, 2000.

[19] E. Zitzler, and L. Thiele, “An Evolutionary Algorithm for Multiobjective Optimization: The Strength Pareto Approach”, Swiss Federal Institute of Technology (ETH), Zurich, Switzerland, Technical report TIK-Report 43, May 1998.

[20] E. Zitzler, M. Laumanns, and L. Thiele, “SPEA2: Improving the Strength Pareto Evolutionary Algorithm”, Swiss Federal Institute of Technology (ETH), Zurich, Switzerland, Technical report TIK-Report 103, May 2001.

[21] K. Deb, A. Pratap, S Agarwal, and T. Meyarivan, “A fast and elitist multiobjective genetic algorithm: NSGA-II”, IEEE Trans. on Evol. Comput., vol. 6, no. 2, pp. 182-197, April 2002.

[22] K. Deb, “Multi-Objective Optimization using Evolutionary Algorithms,” John Wiley & Sons, Ltd., 2002.

[23] Babu, B.V. and B. Anbarasu, “Multi-Objective Differential Evolution (MODE): An Evolutionary Algorithm for Multi-Objective Optimization Problems (MOOPs)”, Proceedings of The Third International Conference on Computational Intelligence, Robotics, and Autonomous Systems (CIRAS-2005), Singapore, December 13-16, 2005.

[24] B.V. Babu: ‘Process Plant Simulation’, Oxford University Press, New Delhi, January, 2006.

[25] H. R. Tizhoosh, “Opposition-based learning: a new scheme for machine intelligence”, In: Proc int conf comput intell modeling control and autom, vol. 1, 2005, pp. 695-701.

[26] H. R. Tizhoosh, “Reinforcement learning based on actions and opposite actions”, In Proc. ICGST int conf artif intell mach learn, Cairo, Egypt, 2005.

[27] H. R. Tizhoosh, “Opposition-based reinforcement learning”, J. Adv. Comput. Intell. Intelligent Inform 2006, 10(3), pp. 578-585.

[28] M. Ventresca, H. R. Tizhoosh., “Improving the convergence of back propagation by opposite transfer functions”, In Proc IEEE world congr. comput. intell., Vancouver, BC, Canada, 2006, pp. 9527–9534.

[29] S. Rahnamayan, H. R. Tizhoosh., M. M. A. Salama., “Opposition-based differential evolution”, IEEE Transactions on Evolutionary Computation, 12(1), 2008, pp.64–79.

[30] Z-L Gaing, “Particle Swarm Optimization to Solving the Economic Dispatch Considering the Generator Constraints”, IEEE Trans. on Power Syst., vol. 18**,** no.3**,** pp. 1187-1195, August 2003.

[31] Whei-Min Lin, Fu-Sheng Cheng and Ming-Tong Tsay, “An improved Tabu search for economic dispatch with multiple minima”, IEEE Trans. on Power Syst., vol. 17**,** no.1**,** pp. 108-112, February 2002.

[32] D. C. Walter and G. B. Sheble, “Genetic algorithm solution of economic dispatch with valve point loading”, IEEE Trans. on Power Syst., vol.8, pp. 1325-1332, August 1993.

[33] P. H. Cheng and H. C. Chang, “Large scale economic dispatch by genetic algorithm”, IEEE Trans. on Power Syst., vol.10, No. 4, pp. 1919-1926, November 1995.

[34] C.-L. Chiang, “Improved genetic algorithm for power economic dispatch of units with valve-point effects and multiple fuels,” IEEE Trans. Power Syst., vol. 20, no. 4, pp. 1690–1699, Nov. 2005.

[35] A. Pereira-Neto, C. Unsihuary and O. R. Saavedra, “Efficient evolutionary strategy optimization procedure to solve the nonconvex economic dispatch problem with generator constraints”, IEE Proc. Gen., Trans., Distrib,, 2005, vol. 152, No. 5, pp. 653-660.

[36] Z. X. Liang and J. D. Glover, “A zoom feature for a dynamic programming solution to economic dispatch including transmission losses”, IEEE Trans. on Power Syst., vol. 7**,** pp. 544-549, May 1992.

[37] C. T. Su and C.-T. Lin, “New approach with a Hopfield modeling framework to economic dispatch”, IEEE Trans. Power Syst., vol. 15,no. 2, p. 541, May 2000.

[38] K. P. Wong and C. C. Fung, “Simulated annealing based economic dispatch algorithm”, IEE Proc. Gen., Trans., Distrib., vol. 140, no. 6, pp. 509–515, Nov. 1993.

[39] K. P. Wong and Y. W. Wong, “Thermal generator scheduling using hybrid genetic/simulated-annealing approach”, IEE Proc. Gen., Trans., Distrib., vol. 142, no. 4, pp. 372–380, 1995.

[40] H. T. Yang, P. C. Yang and C. L. Huang, “Evolutionary programming based economic dispatch for units with nonsmooth fuel cost functions”, IEEE Transactions on Power Systems, vol. 11**,** pp. 112-118, Feb.1996.

[41] N. Sinha, R. Chakrabarti, and P. K. Chattopadhyay, “Evolutionary programming techniques for economic load dispatch”, IEEE Trans. Evol. Comput., vol. 7, no. 1, pp. 83–94, Feb. 2003.

[42] A. I. Selvakumar and K. Thanushkodi, “A new particle swarm optimization solution to nonconvex economic dispatch problems”, IEEE Trans.Power Syst., vol. 22, no. 1, pp. 42–51, Feb. 2007.

[43] K. T. Chaturvedi, M. Pandit, and L. Srivastava, “Self-organizing hierarchical particle swarm optimization for nonconvex economic dispatch”, IEEE Trans. Power Syst., vol. 23, no. 3, p. 1079, Aug. 2008.

[44] Y. H. Hou, Y. W. Wu, L. J. Lu, and X. Y. Xiong, “Generalized ant colony optimization for economic dispatch of power systems”, in Proc. Int. Conf. Power System Technology, Power-Con 2002, Oct. 13–17, 2002, vol. 1, pp. 225–229.

[45] N. Nomana and H. Iba, “Differential evolution for economic load dispatch problems,” Elect. Power Syst. Res., vol. 78, no. 3, pp. 1322–1331, 2008.

[46] S. K. Wang, J. P. Chiou, C. W. Liu, “Non-smooth/non-convex economic dispatch by a novel hybrid differential evolution algorithm”, IET Generation, transmission and Distribution (1) (5) (2007) 793-803.

[47] B. K. Panigrahi, S. R. Yadav, S. Agrawal, and M. K. Tiwari, “A clonal algorithm to solve economic load dispatch,” Elect. Power Syst. Res.,vol. 77, no. 10, pp. 1381–1389, 2007.

[48] B. K. Panigrahi and V. R. Pandi, “Bacterial foraging optimization: Nelder-Mead hybrid algorithm for economic load dispatch”, IET Gen., Transm., Distrib., vol. 2, no. 4, pp. 556–565, 2008.

[49] A. Bhattacharya and P. K. Chattopadhyay, “Biogeography-Based Optimization for Different Economic Load Dispatch Problems”, IEEE Trans. Power Syst., vol. 25, no. 2, pp. 1064-1077, May 2010.

[50] F. J. Rooijers, R.A.M. van Amerongen, “Static economic dispatch for co-generation systems”, IEEE Transactions on Power Systems 9 (3) (1994) 1392-1398.

[51] Tao Guo, M.I. Henwood, M. van Ooijen, An algorithm for heat and power dispatch, IEEE Transactions on Power Systems 11 (4) (1996) 1778-1784.

[52] Y. H. Song, C. S. Chou, T. J. Stonham, “Combined heat and power dispatch by improved ant colony search algorithm”, Electric Power System Research (52) (1999) 115-121.

[53] K. P. Wong , C. Algie, “Evolutionary programming approach for combined heat and power dispatch”, Electric Power Systems Research (61) (2002) 227–232.

[54] C. T. Su, C. L. Chiang, “An incorporated algorithm for combined heat and power economic dispatch”, Electric Power System Research 2004, 69 (2-3) 187-195.

[55] A. Vasebi, M. Fesanghary, S. M. T. Bathaee, “Combined heat and power economic dispatch by harmony search algorithm”, Electric Power and Energy Systems, (29) (2007) 713–719.

[56] L. Wang, C. Singh, “Stochastic combined heat and power dispatch based on multi-objective particle swarm optimization”, Electric Power and Energy Systems (30) (2008) 226–234.

[57] P. Subbaraj, R. Rengaraj, S. Salivahanan, “Enhancement of combined heat and power economic dispatch using self adaptive real-coded genetic algorithm”, Applied Energy 86 (2009) 915–921.

[58] V. Ramesh, T. Jayabaratchi, N. Shrivastava, A. Baska, “A novel selective particle swarm optimization approach for combined heat and power economic dispatch”, Electric Power Components and Systems 37 (2009) 1231–1240.

[59] S. S. Sadat Hosseini, A. Jafarnejad, A. H. Behrooz, A. H. Gandomi, “Combined heat and power economic dispatch by mesh adaptive direct search algorithm”, Expert Systems with Applications 38 (2011) 6556–6564.

[60] A. M. Jubril, A. O. Adediji, O. A. Olaniyan, “Solving the combined heat and power dispatch problem: A semi-definite programming approach”, Electric Power Components and Systems, Volume 40, 2012, pp. 1362 - 1376.

[61] H. Karami, M. J. Sanjari, A, Tavakoli, G. B. Gharehpetian, “Optimal scheduling of residential energy system including combined heat and power system and storage device”, Electric Power Components and Systems, Volume 41, 2013, pp. 765 – 781.

[62] Behnam Mohammadi-Ivatloo, Mohammad Moradi-Dalvand and Abbas Rabiee, “Combined heat and power economic dispatch problem solution using particle swarm optimization with time varying acceleration coefficients”, Electric Power System Research 2013, 95 9-18.

[63] P. K. Roy, C. Paul and S. Sultana, “Oppositional teaching learning based optimization approach for combined heat and power dispatch”, Electric Power and Energy Systems, (57) (2014) 392–403.

[64] B. H. Chowdhury and S. Rahman, “A review of recent advances in economic dispatch”, IEEE Transactions on Power Systems, vol.5, no. 4, pp. 1248-1259, Nov. 1990.

[65] R. R. Shoults, S. K. Chang, S. Helmick and W. M. Grady, “A practical approach to unit commitment, economic dispatch and savings allocation for multiple-area pool operation with import/export constraints”, IEEE Trans Power Apparatus Syst. Vol. 99, no. 2, pp. 625-635, 1980.

[66] R. Romano, V. H. Quintana, R. Lopez and V. Valadez, “Constrained economic dispatch of multi-area systems using the Dantzig–Wolfe decomposition principle”, IEEE Trans. Power Apparatus Syst., vol. 100, no. 4, pp. 2127-2137, 1981.

[67] K. W. Doty and P. L. McEntire, “An analysis of electric power brokerage systems”, IEEE Trans Power Apparatus Syst. Vol. 101, no. 2, pp. 389-396, 1982.

[68] A. L. Desell, E. C. McClelland, K. Tammar and P. R.Van Horne, “Transmission constrained production cost analysis in power system planning”, IEEE Trans Power Apparatus Syst., vol. 103, no. 8, pp. 2192-2198, 1984.

[69] S. D. Helmick and R. R. Shoults, “A practical approach to an interim multi-area economic dispatch using limited computer resources”, IEEE Trans Power Apparatus Syst., vol. 104, no. 6, pp. 1400-1404, 1985.

[70] Z. Ouyang, S. M. Shahidehpour, “Heuristic multi-area unit commitment with economic dispatch”, IEE Proceedings-C, vol. 138, no. 3, pp. 242-252, 1991.

[71] C. Wang and S. M. Shahidehpour, “A decomposition approach to non-linear multi area generation scheduling with tie-line constraints using expert systems”, IEEE Trans Power Syst., vol. 7, no. 4, pp. 1409-1418, 1992.

[72] D. Streiffert, “Multi-area economic dispatch with tie line constraints”, IEEE Trans. Power Syst. Vol. 10, no. 4, pp. 1946-1951, 1995.

[73] J. Wernerus and L. Soder, “Area price based multi-area economic dispatch with tie line losses and constraints”, In: IEEE/KTH Stockholm power tech conference, Sweden,. pp. 710–715, 1995.

[74] T. Yalcinoz and M. J. Short, “Neural networks approach for solving economic dispatch problem with transmission capacity constraints”, IEEE Trans Power Syst., vol. 13, no. 2, pp. 307-313, 1998.

[75] T. Jayabarathi, G. Sadasivam and V. Ramachandran, “Evolutionary programming based multi-area economic dispatch with tie line constraints”, Electric Machine and Power System, vol. 28, pp. 1165-1176, 2000.

[76] C. L. Chen and N. Chen, “Direct Search Method for solving Economic Dispatch Problem Considering Transmission Capacity Constraints”, IEEE Trans. Power Syst., Vol. 16, no. 4, pp. 764-769, Nov. 2001.

[77] P.S. Manoharan, P.S. Kannan, S. Baskar, M. Willjuice Iruthayarajan, “Evolutionary algorithm solution and KKT based optimality verification to multi-area economic dispatch”, International Journal of Electrical Power & Energy Systems, Volume 31, Issues 7–8, September 2009, Pages 365-373.

[78] Lingfeng Wang, Chanan Singh, “Reserve-constrained multiarea environmental/ economic dispatch based on particle swarm optimization with local search”, Engineering Applications of Artificial Intelligence, Volume 22, Issue 2, March 2009, Pages 298-307.

[79] Manisha Sharma, Manjaree Pandit, Laxmi Srivastava, “Reserve constrained multi-area economic dispatch employing differential evolution with time-varying mutation”, International Journal of Electrical Power & Energy Systems, Volume 33, Issue 3, March 2011,Pages753-766.

[80] Kalpana Jain, Manjaree Pandit, Discussion of “Reserve constrained multi-area economic dispatch employing differential evolution with time-varying mutation” by Manisha Sharma et al. “International Journal of Electrical Power and Energy Systems”, 33 March (2011)

753–766, International Journal of Electrical Power & Energy Systems, Volume 39, Issue 1, July 2012, Pages 68-69.

[81] N. Sinha, R. Chakrabarti, and P. K. Chattopadhyay, “Evolutionary programming techniques for economic load dispatch”, IEEE Trans. Evol. Comput., vol. 7, no. 1, pp. 83–94, Feb. 2003.

[82] IEEE Current Operating Problems Working Group, Potential impacts of clean air regulations on system operations, IEEE Trans. on Power Syst., vol. 10, pp. 647-653, 1995.

[83] J. H. Talaq, F. El-Hawary, and M. E. El-Hawary, “A summary of environmental/economic dispatch algorithms”, IEEE Trans. on Power Syst., vol. 9, pp. 1508-1516, Aug. 1994.

[84] Nanda J, Kothari DP, Linga Murthy KS, “Economic emission load dispatch through goal programming techniques”, IEEE Trans Energy Convers, vol. 3, no. 1, pp.26–32. 1988.

[85] J. S. Dhillon, S. C. Parti, and D. P. Kothari, “Stochastic economic emission load dispatch”, Electric Power Syst. Res., vol. 26, pp. 186-197, 1993.

[86] D. Srinivasan, C.S. Chang, and A.C. Liew: ‘Multiobjective generation scheduling using fuzzy optimal search technique’, IEE Proc.-C, vol. 141, no. 3, pp. 233-242, 1994.

[87] A. Farag, S. Al-Baiyat, and T. C. Cheng, “Economic load dispatch multiobjective optimization procedures using linear programming techniques”, IEEE Trans. on Power Syst., vol. 10, pp. 731-738, May 1995**.**

[88] C. M. Huang, H. T. Yang, C. L. Huang, “Bi-objective power dispatch using fuzzy satisfaction-maximizing decision approach”, IEEE Trans Power Syst. Vol. 12, no. 4, pp. 1715-1721, 1997.

[89] D. B. Das and C. Patvardhan, “New multi-objective stochastic search technique for economic load dispatch”, IEE Proc. -C, vol. 145, no. 6, pp. 747-752, 1998.

[90] M. A. Abido, “Environmental / economic power dispatch using multoobjective evolutionary algorithm”, IEEE Trans Power Syst. Vol. 18, no. 4, pp. 1529-1537, 2003.

[91] T. F. Robert, A. H. King, C. S. Harry, Rughooputh, and K. Deb, “Evolutionary multiobjective environmental / economic dispatch: Stochastic versus deterministic approaches”, KanGAL, Rep. 2004019, 2004, pp. 1-15.

[92] L. Wang and C. Singh, “Stochastic economic emission load dispatch through a modified particle swarm optimization algorithm” Electric Power Syst Res . vol. 78, pp. 1466–1476, 2008.

[93] S. Agrawal, B. K. Panigrahi, M. K. Tiwari, “Multiobjective particle swarm algorithm with fuzzy clustering for electrical power dispatch. IEEE Trans. Evol. Comput. vol. 12, no. 5, pp.529–541, 2008.

[94] F. J. Trefny, K. Y. Lee, “Economic fuel dispatch”, IEEE Trans. Power Apparatus and Systems, PAS-100, Vol. 7, pp. 3468-3477, 1981.

[95] S. Vemuri, A. B. R. Kumar, D. F. Hackett, J. T. Eisenhauer, R. Lugtu, “Fuel resource scheduling, Part-I- overview of an energy management problem”, IEEE Trans. Power Apparatus and Systems, PAS-103, Vol. 7, pp. 1542-1548, 1984.

[96] A. B. R. Kumar, S. Vemuri, “Fuel resource scheduling, Part-II- contrained economic dispatch”, IEEE Trans. Power Apparatus and Systems, PAS-103, Vol. 7, pp. 1549-1555, 1984.

[97] A. B. R. Kumar, S. Vemuri, L. A. Gibbs, D. F. Hackett, J. T. Eisenhauer, “Fuel resource scheduling, Part-III- the short-term problem”, IEEE Trans. Power Apparatus and Systems, PAS-103, Vol. 7, pp. 1556-1561, 1984.

[98] Pereira M. V. F. and Pinto L. M. V. G., “A decomposition approach to the economic dispatch of the hydrothermal systems”, IEEE Transactions on PAS, Vol. 101, No. 10, 1982, pp. 3851-3860.

[99] Xia Q., Xiang N., Wang S., Zhang B. and Huang M., “Optimal daily scheduling of Cascaded plants using a new algorithm of non-linear minimum cost network flow”, IEEE Transactions on PWRS, Vol. 3, No. 3, 1988, pp. 929-935.

[100] Chang S., Chen C., Fong I. and Luh P. B., “Hydroelectric generation scheduling with an effective differential programming”, IEEE Transaction on PWRS, Vol. 5, No. 3, 1990, pp. 737-743.

[101] Carneiro A. A. F. M., Soares S. and Bond P. S., “ A large scale of an optimal deterministic hydrothermal scheduling algorithm”, IEEE Transactions on PWRS, Vol. 5, No. 1, Feb. 1990, pp. 204-211.

[102] Salam M. S., Nor K. M., and Hamdam A.R., “Hydrothermal scheduling based Lagrangian relaxation approach to hydrothermal coordination”, IEEE Transactions on PWRS, Vol. 13, No. 1, Feb. 1998, pp. 226-235.

[103] Sifuentes W. S. and Vargas A., “Hydrothermal Scheduling Using Benders Decomposition: Accelerating Techniques”, IEEE Trans. on PWRS, Vol. 22, No. 3, Aug. 2007, pp. 1351-1359.

[104] Wong K. P. and Wong Y. W., “Short-term hydrothermal scheduling part 1: simulated annealing approach”, IEE Proceedings Generation, Transmission and Distribution, 1994, Vol. 141, No.5, pp. 497-501.

[105] Yang P. C., Yang H. T. and Huang C. L., “Scheduling short-term hydrothermal generation using evolutionary Programming techniques”, IEE Proceedings Generation Transmission and Distribution, vol. 143, No. 4, July 1996, pp. 371-376.

[106] Orero S. O. and Irving M. R., “A genetic algorithm modeling framework and solution technique for short term optimal hydrothermal scheduling”, IEEE Trans. on PWRS, Vol. 13, No. 2, May 1998.

[107] Gil E., Bustos J. and Rudnick H., “Short-term hydrothermal generation scheduling model using a genetic algorithm”, IEEE Trans. on PWRS, Vol. 18, No. 4, Nov. 2003, pp. 1256-1264.

[108] Sinha N., Chakrabarti R. and Chattopadhyay P. K., “Fast evolutionary programming techniques for short-term hydrothermal scheduling”, IEEE Trans. on PWRS, Vol. 18, No. 1, Feb. 2003, pp. 214-220.

[109] Lakshminarasimman L. and Subramanian S., “Short-term scheduling of hydrothermal power system with cascaded reservoirs by using modified differential evolution”, IEE Proceedings – Generation, Transmission and Distribution, Volume 153, No. 6, November 2006, pp.693-700.

[110] M. Basu, "Improved differential evolution for short-term hydrothermal scheduling", International Journal of Electrical Power & Energy Systems, Volume 58, June 2014, Pages 91-100.

[111] Yuan X., Cao B., Yang B., Yuan, Y., “Hydrothermal scheduling using chaotic hybrid differential evolution”, Energy Conversion and Management, 49 (12), 3627–33, 2008.

[112] Hota P. K., Barisal A. K. and Chakrabarti R., “An improved PSO technique for short-term optimal hydrothermal scheduling”, Electric Power System Research, vol. 79, no. 7, pp. 1047-1053, July 2009.

[113] Swain R.K., Barisal A.K., Hota P.K., Chakrabarti, R., “Short-term hydrothermal scheduling using clonal selection algorithm”, Int J Electr Power Energy Syst. 33, 647–56, 2011.

[114] Roy, P. K., “Teaching learning based optimization for short-term hydrothermal scheduling problem considering valve point effect and prohibited discharge constraint”, Int J Electr Power Energ Syst, Vol.-53, pp. 10-19, 2013.

[115] M.F. Zaghlool, F. C. Trutt, “Efficient methods for optimal scheduling of fixed head hydrothermal power systems”, IEEE Transactions on Power Systems, vol.3, no. 1, 1988.

[116] A. H. A. Rashid and K. M. Nor, “An efficient method for optimal scheduling of fixed head hydro and thermal plants”, IEEE Transactions on Power Systems, Vol. 6, No. 2, pp. 632-636, May 1991.

[117] O. Nilsson, D. Sjelvgren, “Mixed-integer programming applied to short-term planning of a hydro-thermal system”, Proceedings of the 1995, IEEE PICA, Salt Lake City, UT, USA, May 1995, pp. 158-163.

[118] L. Engles, R. E. Larson, J. Peschon, K. N. Stanton, “Dynamic programming applied to hydro and thermal generation scheduling”, IEEE tutorial course text, 76CH1107-2-PWR, IEEE, New York, 1976.

[119] K. P. Wong and Y. W. Wong, “Short-term hydrothermal scheduling part 1: simulated annealing approach”, IEE Proceedings Generation, Transmission and Distribution, 1994, Vol. 141, No.5, pp. 497-501.

[120] P. C. Yang, H. T. Yang and C. L. Huang, “Scheduling short-term hydrothermal generation using evolutionary Programming techniques”, IEE Proceedings Generation Transmission and Distribution, vol. 143, No. 4, July 1996, pp. 371-376.

[121] S. O. Orero and M. R. Irving, “A genetic algorithm modeling framework and solution technique for short term optimal hydrothermal scheduling”, IEEE Trans. on PWRS, Vol. 13, No. 2, May 1998.

[122] E. Gil, J. Bustos and H. Rudnick, “Short-term hydrothermal generation scheduling model using a genetic algorithm”, IEEE Trans. on PWRS, Vol. 18, No. 4, Nov. 2003, pp. 1256-1264.

[123] L. Lakshminarasimman and S. Subramanian, “Short-term scheduling of hydrothermal power system with cascaded reservoirs by using modified differential evolution”, IEE

Proceedings – Generation, Transmission and Distribution, Volume 153, No. 6, November 2006, pp.693-700.

[124] X. Yuan, B. Cao, B. Yang, Y. Yuan, “Hydrothermal scheduling using chaotic hybrid differential evolution”, Energy Conversion and Management, 49 (12), 3627–33, 2008.

[125] P. K. Hota, A. K. Barisal and R. Chakrabarti, “An improved PSO technique for short-term optimal hydrothermal scheduling”, Electric Power System Research, vol. 79, no. 7, pp. 1047-1053, July 2009.

[126] R. K. Swain, A. K. Barisal, P. K. Hota, R. Chakrabarti, “Short-term hydrothermal scheduling using clonal selection algorithm”, Int J Electr Power Energy Syst. 33, 647–56, 2011.

[127] X. Yao, Y. Liu, and G. Lin, “Evolutionary Programming Made Faster”, IEEE Trans. Evol. Comput., vol. 3, no. 2, pp. 82–102, July 1999.

[128] A. J. Wood and B. F. Wollenberg, Power Generation, Operation and Control, John Willey, New York, 1996.

.

Appendices

Table A.1: Prohibited zones of conventional thermal generator for test system 1

Unit	Zone 1, MW	Zone 2, MW	Zone 3, MW
1	[30, 40]	[70, 80]	[110, 120]

Table A.2: Prohibited zones of conventional thermal generators for test system 2

Unit	Zone 1, MW	Zone 2, MW
1	[20, 30]	[50, 60]
2	[40, 50]	[90, 100]
3	[50, 70]	[120, 140]
4	[70, 90]	[180, 200]

Table A.3: Prohibited zones of zones of conventional thermal generators for test system 3

Unit	Zone 1, MW	Zone 2, MW	Zone 3, MW
1	[180, 200]	[260, 335]	[390, 420]
2	[30, 40]	[180, 220]	[305, 335]
3	[30, 40]	[180, 220]	[305, 335]
10	[45, 55]	[65, 75]	-
11	[45, 55]	[65, 75]	-

Table A.4: Prohibited zones of zones of conventional thermal generators for test system 4

Unit	Zone 1, MW	Zone 2, MW	Zone 3, MW
1	[180, 200]	[260, 335]	[390, 420]
2	[30, 40]	[180, 220]	[305, 335]
3	[30, 40]	[180, 220]	[305, 335]
10	[45, 55]	[65, 75]	-
11	[45, 55]	[65, 75]	-
14	[180, 200]	[260, 335]	[390, 420]
15	[30, 40]	[180, 220]	[305, 335]
16	[30, 40]	[180, 220]	[305, 335]
23	[45, 55]	[65, 75]	-
24	[45, 55]	[65, 75]	-

Table A.5: Data for 2 area system

Generator ij	a_{ij}	b_{ij}	c_{ij}	P_{ij}^{min}	P_{ij}^{max}	Prohibited zones
	\$/h	\$/MWh	\$/(MW)^{2}h	MW	MW	MW
$G_{1,1}$	550	8.10	0.00028	100	500	[210 240] [350 380]
$G_{1,2}$	350	7.50	0.00056	50	200	[90 110] [140 160]
$G_{1,3}$	310	8.10	0.00056	50	150	[80 90] [110 120]
$G_{2,1}$	240	7.74	0.00324	80	300	[150 170] [210 240]
$G_{2,2}$	200	8.00	0.00254	50	200	[90 110] [140 150]
$G_{2,3}$	126	8.60	0.00284	50	120	[75 85] [100 105]

The transmission loss formula coefficients of two-area system are:

$$B_1 = \begin{bmatrix} 17 & 12 & 7 \\ 12 & 14 & 9 \\ 7 & 9 & 31 \end{bmatrix} X10^{-6}$$

$$B_{01} = \begin{bmatrix} -0.3908 & -0.1297 & 0.7047 \end{bmatrix} X10^{-3}$$

$$B_{001} = 0.045$$

$$B_2 = \begin{bmatrix} 24 & -6 & -8 \\ -6 & 129 & -2 \\ -8 & -2 & 150 \end{bmatrix} X10^{-6}$$

$$B_{02} = \begin{bmatrix} 0.0591 & 0.2161 & -0.6635 \end{bmatrix} X10^{-3}$$

$$B_{002} = 0.056$$

The transmission loss formula coefficients of three-area system are:

$$B_1 = \begin{bmatrix} 8.70 & 0.43 & -4.61 & 0.36 \\ 0.43 & 8.30 & -0.97 & 0.22 \\ -4.61 & -0.97 & 9.00 & -2.00 \\ 0.36 & 0.22 & -2.00 & 5.30 \end{bmatrix} X10^{-5}$$

$$B_{01} = \begin{bmatrix} -0.3908 & -0.1297 & 0.7047 & 0.0591 \end{bmatrix} X10^{-3}$$

$B_{001} = 0.056$

$$B_2 = \begin{bmatrix} 8.60 & -0.80 & 0.37 \\ -0.80 & 9.08 & -4.90 \\ 0.37 & -4.90 & 8.24 \end{bmatrix} X10^{-5}$$

$$B_{02} = \begin{bmatrix} 0.2161 & -0.6635 & 0.5034 \end{bmatrix} X10^{-3}$$

$B_{002} = 0.045$

$$B_3 = \begin{bmatrix} 1.20 & -0.96 & 0.56 \\ -0.96 & 4.93 & -0.30 \\ 0.56 & -0.30 & 5.99 \end{bmatrix} X10^{-5}$$

$$B_{03} = \begin{bmatrix} -0.3216 & 0.4635 & 0.3503 \end{bmatrix} X10^{-3}$$

$B_{003} = 0.055$

Table A.6: Generator characteristics

Generator ij	P_{ij}^{min} MW	P_{ij}^{max} MW	a_{ij} \$/h	b_{ij} \$/MWh	c_{ij} \$/(MW)^{2}h	d_{ij} \$/h	e_{ij} rad/MW	α_{ij} *lb*/h	β_{ij} *lb*/MWh	γ_{ij} *lb*/(MW)^{2}h	η_{ij} *lb*/h	δ_{ij} 1/MW
G_{11}	0.05	14	0	38.53900	0.15247	100	0.084	13.85932	0.32767	0.004190	1.310000	0.056900
G_{12}	0.05	10	0	46.15916	0.10587	150	0.063	13.85932	0.32767	0.004190	0.914200	0.045400
G_{13}	0.05	13	0	40.39655	0.02803	120	0.077	40.26690	-0.54551	0.006830	0.993600	0.040600
G_{14}	0.05	12	0	38.30553	0.03546	200	0.042	40.26690	-0.54551	0.006830	0.655000	0.028460
G_{21}	0.05	25	0	36.32782	0.02111	300	0.035	42.89553	-0.51116	0.004610	0.503500	0.020750
G_{22}	0.05	12	0	38.27041	0.01799	150	0.063	42.89553	-0.51116	0.004610	0.914200	0.045400
G_{23}	0.05	20	0	2.0000	0.00375	18.0	0.037	40.91000	-0.05554	0.006490	0.000200	0.002857
G_{24}	0.05	18	0	1.7500	0.01750	16.0	0.038	2.54300	-0.06047	0.005638	0.000500	0.003333
G_{31}	0.05	30	0	3.0000	0.02500	13.5	0.041	6.13100	-0.05555	0.005151	0.000010	0.006667
G_{32}	0.05	30	0	2.0000	0.00375	18.0	0.037	3.49100	-0.05754	0.006390	0.000300	0.002657
G_{33}	0.05	30	0	1.0000	0.06250	14.0	0.040	4.25800	-0.05094	0.004586	0.000001	0.008000
G_{34}	0.05	30	0	1.7500	0.01950	15.0	0.039	2.75400	-0.05847	0.005238	0.000400	0.002875
G_{41}	0.05	11	0	3.2500	0.00834	12.0	0.045	5.32600	-0.03550	0.003380	0.002000	0.002000
G_{42}	0.05	20	0	3.2500	0.00834	12.0	0.045	5.32600	-0.03550	0.003380	0.002000	0.002000
G_{43}	0.05	30	0	1.7500	0.01950	15.0	0.039	2.75400	-0.05847	0.005238	0.000400	0.002875
G_{44}	0.05	30	0	1.0000	0.06250	14.0	0.040	4.25800	-0.05094	0.004586	0.000001	0.008000

Table A.6: Generator characteristics

Generator ij	P_{ij}^{min} MW	P_{ij}^{max} MW	a_{ij} \$/h	b_{ij} \$/MWh	c_{ij} \$/(MW)^{2}h	d_{ij} \$/h	e_{ij} rad/MW	α_{ij} *lb* /h	β_{ij} *lb* /MWh	γ_{ij} *lb* /(MW)^{2}h	η_{ij} *lb* /h	δ_{ij} 1/MW
G_{11}	0.05	14	0	38.53900	0.15247	100	0.084	13.85932	0.32767	0.004190	1.310000	0.056900
G_{12}	0.05	10	0	46.15916	0.10587	150	0.063	13.85932	0.32767	0.004190	0.914200	0.045400
G_{13}	0.05	13	0	40.39655	0.02803	120	0.077	40.26690	-0.54551	0.006830	0.993600	0.040600
G_{14}	0.05	12	0	38.30553	0.03546	200	0.042	40.26690	-0.54551	0.006830	0.655000	0.028460
G_{21}	0.05	25	0	36.32782	0.02111	300	0.035	42.89553	-0.51116	0.004610	0.503500	0.020750
G_{22}	0.05	12	0	38.27041	0.01799	150	0.063	42.89553	-0.51116	0.004610	0.914200	0.045400
G_{23}	0.05	20	0	2.0000	0.00375	18.0	0.037	40.91000	-0.05554	0.006490	0.000200	0.002857
G_{24}	0.05	18	0	1.7500	0.01750	16.0	0.038	2.54300	-0.06047	0.005638	0.000500	0.003333
G_{31}	0.05	30	0	3.0000	0.02500	13.5	0.041	6.13100	-0.05555	0.005151	0.000010	0.006667
G_{32}	0.05	30	0	2.0000	0.00375	18.0	0.037	3.49100	-0.05754	0.006390	0.000300	0.002657
G_{33}	0.05	30	0	1.0000	0.06250	14.0	0.040	4.25800	-0.05094	0.004586	0.000001	0.008000
G_{34}	0.05	30	0	1.7500	0.01950	15.0	0.039	2.75400	-0.05847	0.005238	0.000400	0.002875
G_{41}	0.05	11	0	3.2500	0.00834	12.0	0.045	5.32600	-0.03550	0.003380	0.002000	0.002000
G_{42}	0.05	20	0	3.2500	0.00834	12.0	0.045	5.32600	-0.03550	0.003380	0.002000	0.002000
G_{43}	0.05	30	0	1.7500	0.01950	15.0	0.039	2.75400	-0.05847	0.005238	0.000400	0.002875
G_{44}	0.05	30	0	1.0000	0.06250	14.0	0.040	4.25800	-0.05094	0.004586	0.000001	0.008000

Table A.7: Tie-line transfer limits

Tie line *ik*	$-T_{ik}^{max}$ (MW)	T_{ik}^{max} (MW)
T_{12}	-6.0	6.0
T_{13}	-4.0	4.0
T_{14}	-2.0	2.0
T_{23}	-3.5	3.5
T_{24}	-5.5	5.5
T_{34}	-0.9	0.9

Table A.8. LOAD DEMAND AND FUEL DELIVERED DURING SCHEDULING PERIOD

Inter-val	Duration (h)	Load demand P_D (MW)	Fuel delivered F_D (ton)
1	168	700	7000
2	168	800	7000
3	168	650	7000

Table A.9. GENERATOR CHARACTERISTICS

Unit	P_i^{min}	P_i^{max}	a_i	b_i	c_i	d_i	e_i	α_i	β_i	γ_i	σ_i	θ_i	η_i	δ_i	μ_i	F_i^{min}	F_i^{max}	V_i^{min}	V_i^{max}
	MW	MW	$/h	$/MWh	$/(MW)^{2}h	$/h	rad/MW	*lb* /h	*lb* /MWh	*lb* /(MW)^{2}h	*lb* /h	1/MW	ton/h	ton/MWh	ton/(MW)^{2}h	ton	ton	ton	ton
1	20	75	25	2.0	0.0080	10	0.012	80	-0.805	0.0180	0.008	0.0735	0.83612	0.066889	0.00026756	0	1000	0	10000
2	20	125	60	1.8	0.0030	20	0.010	50	-0.555	0.0150	0.009	0.0655	2.00669	0.060200	0.00010033	0	1000	0	10000
3	30	175	100	2.1	0.0012	30	0.009	70	-0.955	0.0115	0.010	0.0504	3.34448	0.070230	0.00004013	0	2000	0	20000
4	40	250	120	2.2	0.0040	40	0.008	45	-0.600	0.0080	0.015	0.0340	4.01338	0.073578	0.00013378	0	3000	0	30000
5	50	300	40	1.8	0.0015	50	0.007	30	-0.555	0.0120	0.017	0.0285	1.33779	0.060200	0.00005017	0	3000	0	30000

Table A.9. GENERATOR CHARACTERISTICS

Unit	P_i^{min}	P_i^{max}	a_i	b_i	c_i	d_i	e_i	α_i	β_i	γ_i	σ_i	θ_i	η_i	δ_i	μ_i	F_i^{min}	F_i^{max}	V_i^{min}	V_i^{max}
	MW	MW	$/h	$/MWh	$/(MW)^{2}h	$/h	rad/MW	*lb* /h	*lb* /MWh	*lb* /(MW)^{2}h	*lb* /h	1/MW	ton/h	ton/MWh	ton/(MW)^{2}h	ton	ton	ton	ton
1	20	75	25	2.0	0.0080	10	0.012	80	-0.805	0.0180	0.008	0.0735	0.83612	0.066889	0.00026756	0	1000	0	10000
2	20	125	60	1.8	0.0030	20	0.010	50	-0.555	0.0150	0.009	0.0655	2.00669	0.060200	0.00010033	0	1000	0	10000
3	30	175	100	2.1	0.0012	30	0.009	70	-0.955	0.0115	0.010	0.0504	3.34448	0.070230	0.00004013	0	2000	0	20000
4	40	250	120	2.2	0.0040	40	0.008	45	-0.600	0.0080	0.015	0.0340	4.01338	0.073578	0.00013378	0	3000	0	30000
5	50	300	40	1.8	0.0015	50	0.007	30	-0.555	0.0120	0.017	0.0285	1.33779	0.060200	0.00005017	0	3000	0	30000

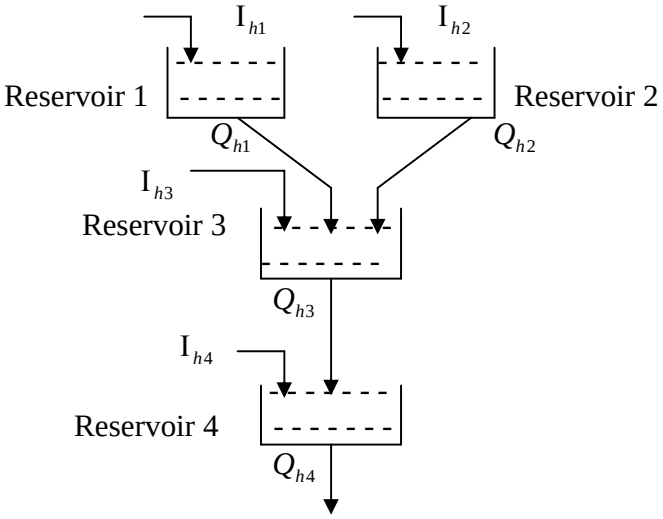

where:

I_{hj} : natural inflow to reservoir j

Q_{hj} : discharge of plant j

Table A.10: Hydraulic system network

Plant	1	2	3	4
R_u	0	0	2	1
t_d	2	3	4	0

R_u : no of upstream plants

t_d : time delay to immediate downstream plant

Table A.11: Load demand for Test system 1

Hour	P_D(MW)	Hour	P_D(MW)	Hour	P_D(MW)
1	750	9	1090	17	1050
2	780	10	1080	18	1120
3	700	11	1100	19	1070
4	650	12	1150	20	1050
5	670	13	1110	21	910
6	800	14	1030	22	860
7	950	15	1010	23	850
8	1010	16	1060	24	800

Table A.12: Hydro power generation coefficients

Plant	C_1	C_2	C_3	C_4	C_5	C_6
1	-0.0042	-0.42	0.030	0.90	10.0	-50
2	-0.0040	-0.30	0.015	1.14	9.5	-70
3	-0.0016	-0.30	0.014	0.55	5.5	-40
4	-0.0030	-0.31	0.027	1.44	14.0	-90

Table A.13: Reservoir inflows ($\times 10^4 m^3$)

Hour	Reservoir				Hour	Reservoir				Hour	Reservoir			
	1	2	3	4		1	2	3	4		1	2	3	4
1	10	8	8.1	2.8	9	10	8	1	0	17	9	7	2	0
2	9	8	8.2	2.4	10	11	9	1	0	18	8	6	2	0
3	8	9	4	1.6	11	12	9	1	0	19	7	7	1	0
4	7	9	2	0	12	10	8	2	0	20	6	8	1	0
5	6	8	3	0	13	11	8	4	0	21	7	9	2	0
6	7	7	4	0	14	12	9	3	0	22	8	9	2	0
7	8	6	3	0	15	11	9	3	0	23	9	8	1	0
8	9	7	2	0	16	10	8	2	0	24	10	8	0	0

Table A.14: Reservoir storage capacity limits, plant discharge limits, reservoir end conditions ($\times 10^4 m^3$) and plant generation limits (MW)

Plant	$V^{\min}$	$V^{\max}$	V_{ini}	V_{end}	$Q^{\min}$	$Q^{\max}$	$P_h^{\min}$	$P_h^{\max}$
1	80	150	100	120	5	15	0	500
2	60	120	80	70	6	15	0	500
3	100	240	170	170	10	30	0	500
4	70	160	120	140	6	20	0	500

Table A.15: Cost curve coefficients and operating limits of thermal generators for Test system 1

Unit	a_s	b_s	c_s	d_s	e_s	$P_s^{\min}$	$P_s^{\max}$
	\$/h	\$/MWh	\$/(MW)^{2}h	\$/h	rad/MW	MW	MW
1	100	2.45	0.0012	160	0.038	20	175
2	120	2.32	0.0010	180	0.037	40	300
3	150	2.10	0.0015	200	0.035	50	500

Transmission loss coefficients for test system 1 are given as below:

$$B = 10^{-4} \times \begin{bmatrix} 0.34 & 0.13 & 0.09 & -0.01 & -0.08 & -0.01 & -0.02 \\ 0.13 & 0.14 & 0.10 & 0.01 & -0.05 & -0.02 & -0.01 \\ 0.09 & 0.10 & 0.31 & 0.00 & -0.11 & -0.07 & -0.05 \\ -0.01 & 0.01 & 0.00 & 0.24 & -0.08 & -0.04 & -0.07 \\ -0.08 & -0.05 & -0.11 & -0.08 & 1.92 & 0.27 & -0.02 \\ -0.01 & -0.02 & -0.07 & -0.04 & 0.27 & 0.32 & 0.00 \\ -0.02 & -0.01 & -0.05 & -0.07 & -0.02 & 0.00 & 1.35 \end{bmatrix} \text{ per MW}$$

$$B0 = 10^{-6} \times [-0.7500 \quad -0.0600 \quad 0.7000 \quad -0.0300 \quad 0.2700 \quad -0.7700 \quad -0.0100]$$

$B00 = 0.55$ MW

Table A.16: Cost curve coefficients and operating limits of thermal generators for Test system 2

Unit	P_s^{min} MW	P_s^{max} MW	a_s \$/h	b_s \$/MWh	c_s \$/(MW)^{2}h	d_s \$/h	e_s rad/MW
1	50	455	150	1.89	0.0050	300	0.035
2	50	450	115	2.00	0.0055	200	0.042
3	20	130	40	3.50	0.0060	200	0.042
4	20	130	122	3.15	0.0050	150	0.063
5	25	470	125	3.05	0.0050	150	0.063
6	40	460	120	2.75	0.0070	150	0.063
7	45	465	70	3.45	0.0070	200	0.053
8	25	160	130	2.45	0.0050	180	0.043
9	25	180	130	2.45	0.0050	100	0.062
10	35	300	70	3.45	0.0070	150	0.063

Table A.17: Load demand for Test system 2

Hour	P_D (MW)	Hour	P_D (MW)	Hour	P_D (MW)
1	1750	9	2090	17	2050
2	1780	10	2080	18	2120
3	1700	11	2100	19	2070
4	1650	12	2150	20	2050
5	1670	13	2110	21	1910
6	1800	14	2030	22	1860
7	1950	15	2010	23	1850
8	2010	16	2060	24	1800

Table A.18: Fixed Head Hydro system data of Test system 1

Unit	a_{0h}	a_{1h}	a_{2h}	W_h	P_h^{min}	P_h^{max}
	MCF/h	MCF/MWh	MCF/(MW)^{2}h	MCF	MW	MW
1	1.980	0.306	0.000216	2500	0	400
2	0.936	0.612	0.000360	2100	0	300

Table A.19: Thermal generator data of Test system 1

Unit	P_s^{min}	P_s^{max}	a_s	b_s	c_s	d_s	e_s
	MW	MW	$/h	$/MWh	$/(MW)^{2}h	$/h	1/MW
1	50	300	25	3.2	0.0025	0	0
2	50	700	30	3.4	0.0008	0	0

Table A.20: Load demands of Test system 1

Sub-interval	Duration (hr)	P_D (MW)
1	8	900
2	8	1200
3	8	1100

The transmission loss formula coefficients of test system 1 are

$$B = \begin{bmatrix} 0.000140 & 0.000010 & 0.000015 & 0.000015 \\ 0.000010 & 0.000060 & 0.000010 & 0.000013 \\ 0.000015 & 0.000010 & 0.000068 & 0.000065 \\ 0.000015 & 0.000013 & 0.000065 & 0.000070 \end{bmatrix}$$

Table A.21: Hydro system data of Test system 2

Unit	a_{0h}	a_{1h}	a_{2h}	W_h	P_h^{min}	P_h^{max}
	acre-ft/h	acre-ft/MWh	acre-ft/(MW)^{2}h	acre-ft	MW	MW
1	260	8.5	0.00986	125000	0	250
2	250	9.8	0.01140	286000	0	500

Table A.22: Thermal generator data of Test system 2

Unit	P_s^{min}	P_s^{max}	a_s	b_s	c_s	d_s	e_s
	MW	MW	$/h	$/MWh	$/(MW)^{2}h	$/h	rad/MW
3	20	125	10	3.25	0.0083	12	0.0450
4	30	175	10	2.00	0.0037	18	0.0370
5	40	250	20	1.75	0.0175	16	0.0380
6	50	300	20	1.00	0.0625	14	0.0400

Table A.23: Load demands of Test system 2

Sub-interval	Duration (hr)	P_D (MW)
1	12	900
2	12	1100
3	12	1000
4	12	1200

The transmission loss formula coefficients are of Test system 2

$$B = \begin{bmatrix} 0.000049 & 0.000014 & 0.000015 & 0.000015 & 0.000020 & 0.000017 \\ 0.000014 & 0.000045 & 0.000016 & 0.000020 & 0.000018 & 0.000015 \\ 0.000015 & 0.000016 & 0.000039 & 0.000010 & 0.000012 & 0.000012 \\ 0.000015 & 0.000020 & 0.000010 & 0.000040 & 0.000014 & 0.000010 \\ 0.000020 & 0.000018 & 0.000012 & 0.000014 & 0.000035 & 0.000011 \\ 0.000017 & 0.000015 & 0.000012 & 0.000010 & 0.000011 & 0.000036 \end{bmatrix} \text{ per MW}$$